Oxidative Medicine and Cellular Longevity

Exposomic Fingerprint in the Development of Diseases: the Role of Free Radicals and Multi-Omics

Lead Guest Editor: Gordana Kocic
Guest Editors: Andrej Veljkovic, Dusan Sokolovic, and Nataša Poklar Ulrih

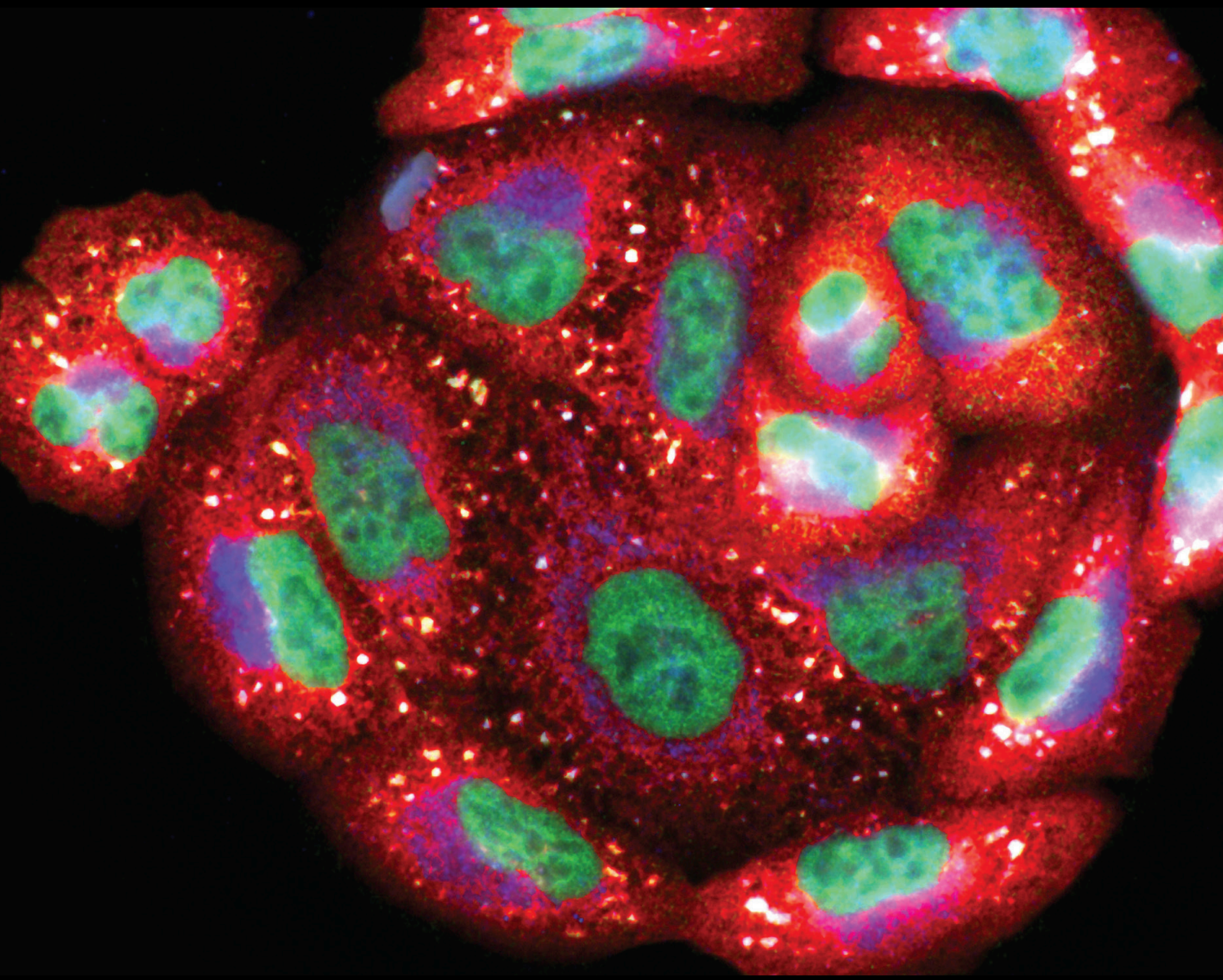

Exposomic Fingerprint in the Development of Diseases: the Role of Free Radicals and Multi-Omics

Oxidative Medicine and Cellular Longevity

Exposomic Fingerprint in the Development of Diseases: the Role of Free Radicals and Multi-Omics

Lead Guest Editor: Gordana Kocic
Guest Editors: Andrej Veljkovic, Dusan Sokolovic, and Nataša Poklar Ulrih

Copyright © 2022 Hindawi Limited. All rights reserved.

This is a special issue published in “Oxidative Medicine and Cellular Longevity.” All articles are open access articles distributed under the Creative Commons Attribution License, which permits unrestricted use, distribution, and reproduction in any medium, provided the original work is properly cited.

Chief Editor

Jeannette Vasquez-Vivar, USA

Editorial Board

Ivanov Alexander, Russia
Fabio Altieri, Italy
Silvia Alvarez, Argentina
Fernanda Amicarelli, Italy
José P. Andrade, Portugal
Cristina Angeloni, Italy
Daniel Arcanjo, Brazil
Sandro Argüelles, Spain
Antonio Ayala, Spain
Elena Azzini, Italy
Peter Backx, Canada
Damian Bailey, United Kingdom
Jiaolin Bao, China
George E. Barreto, Colombia
Sander Bekeschus, Germany
Ji C. Bihl, USA
Consuelo Borrás, Spain
Nady Braidy, Australia
Ralf Braun, Austria
Laura Bravo, Spain
Matt Brody, USA
Amadou Camara, USA
Gianluca Carnevale, Italy
Roberto Carnevale, Italy
Marcio Carocho, Portugal
Angel Catalá, Argentina
Peter Celec, Slovakia
Giulio Ceolotto, Italy
Shao-Yu Chen, USA
Deepak Chhangani, USA
Ferdinando Chiaradonna, Italy
Zhao Zhong Chong, USA
Xinxin Ci, China
Fabio Ciccarone, Italy
Alin Ciobica, Romania
Ana Cipak Gasparovic, Croatia
Giuseppe Cirillo, Italy
Maria R. Ciriolo, Italy
Massimo Collino, Italy
Graziamaria Corbi, Italy
Manuela Corte-Real, Portugal
Mark Crabtree, United Kingdom
Manuela Curcio, Italy
Andreas Daiber, Germany
Felipe Dal Pizzol, Brazil
Francesca Danesi, Italy
Domenico D'Arca, Italy
Sergio Davinelli, Italy
Claudio de Lucia, Italy
Damião de Sousa, Brazil
Enrico Desideri, Italy
Francesca Diomede, Italy
Cinzia Domenicotti, Italy
Raul Dominguez-Perles, Spain
Dimitrios Draganidis, Greece
Joël R. Drevet, France
Grégory Durand, France
Alessandra Durazzo, Italy
Anne Eckert, Switzerland
Javier Egea, Spain
Pablo A. Evelson, Argentina
Stefano Falone, Italy
Ioannis G. Fatouros, Greece
Qingping Feng, Canada
Gianna Ferretti, Italy
Giuseppe Filomeni, Italy
Pasquale Fino, Italy
Omidreza Firuzi, Iran
Swaran J. S. Flora, India
Teresa I. Fortoul, Mexico
Anna Fracassi, USA
Rodrigo Franco, USA
Joaquin Gadea, Spain
Juan Gambini, Spain
José Luís García-Giménez, Spain
Gerardo García-Rivas, Mexico
Janusz Gebicki, Australia
Alexandros Georgakilas, Greece
Husam Ghanim, USA
Jayeeta Ghose, USA
Rajeshwary Ghosh, USA
Lucia Gimeno-Mallench, Spain
Eloisa Gitto, Italy
Anna M. Giudetti, Italy
Daniela Giustarini, Italy
José Rodrigo Godoy, USA
Saeid Golbidi, Canada
Aldrin V. Gomes, USA

Arantxa González, Spain
Tilman Grune, Germany
Chi Gu, China, China
Nicoletta Guaragnella, Italy
Solomon Habtemariam, United Kingdom
Ying Han, China
Eva-Maria Hanschmann, Germany
Md Saquib Hasnain, India
Md Hassan, India
Tim Hofer, Norway
John D. Horowitz, Australia
Silvana Hrelia, Italy
Dragan Hrncic, Serbia
Juan Huang, China
Zebo Huang, China
Tarique Hussain, Pakistan
Stephan Immenschuh, Germany
Maria Isaguliants, Latvia
Luigi Iuliano, Italy
FRANCO J. L, Brazil
Vladimir Jakovljevic, Serbia
Jason Karch, USA
Peeter Karihtala, Finland
Kum Kum Khanna, Australia
Neelam Khaper, Canada
Thomas Kietzmann, Finland
Ramoji Kosuru, USA
Demetrios Kouretas, Greece
Andrey V. Kozlov, Austria
Esra Küpeli Akkol, Turkey
Daniele La Russa, Italy
Jean-Claude Lavoie, Canada
Wing-Kee Lee, Germany
Simon Lees, Canada
Xin-Feng Li, China
Qiangqiang Li, China
Gaocai Li, China
Jialiang Liang, China
Christopher Horst Lillig, Germany
Paloma B. Liton, USA
Ana Lloret, Spain
Lorenzo Loffredo, Italy
Camilo López-Alarcón, Chile
Daniel Lopez-Malo, Spain
Antonello Lorenzini, Italy
Massimo Lucarini, Italy
Hai-Chun Ma, China
Mateusz Maciejczyk, Poland
Nageswara Madamanchi, USA
Kenneth Maiese, USA
Marco Malaguti, Italy
Tullia Maraldi, Italy
Reiko Matsui, USA
Juan C. Mayo, Spain
Steven McAnulty, USA
Antonio Desmond McCarthy, Argentina
Sonia Medina-Escudero, Spain
Pedro Mena, Italy
Víctor M. Mendoza-Núñez, Mexico
Lidija Milkovic, Croatia
Alexandra Miller, USA
Sanjay Misra, USA
Premysl Mladenka, Czech Republic
Raffaella Molteni, Italy
Maria U. Moreno, Spain
Sandra Moreno, Italy
Trevor A. Mori, Australia
Ryuichi Morishita, Japan
Fabiana Morroni, Italy
Ange Mouithys-Mickalad, Belgium
Iordanis Mourouzis, Greece
Danina Muntean, Romania
Colin Murdoch, United Kingdom
Ryoji Nagai, Japan
Amit Kumar Nayak, India
David Nieman, USA
Cristina Nocella, Italy
Susana Novella, Spain
Hassan Obied, Australia
Julio J. Ochoa, Spain
Pál Pacher, USA
Pasquale Pagliaro, Italy
DR DILIPKUMAR PAL, India
Valentina Pallottini, Italy
Rosalba Parenti, Italy
Mayur Parmar, USA
Vassilis Paschalis, Greece
Visweswara Rao Pasupuleti, Malaysia
Daniela Pellegrino, Italy
Ilaria Peluso, Italy
Claudia Penna, Italy
Serafina Perrone, Italy
Tiziana Persichini, Italy
Shazib Pervaiz, Singapore

Vincent Pialoux, France
Alessandro Poggi, Italy
Ada Popolo, Italy
Aijuan Qu, China
José L. Quiles, Spain
Walid Rachidi, France
Zsolt Radak, Hungary
Sachchida Rai, India
Namakkal Soorappan Rajasekaran, USA
Dario C. Ramirez, Argentina
Erika Ramos-Tovar, Mexico
Abdur Rauf Rauf, Pakistan
Sid D. Ray, USA
Muneeb Rehman, Saudi Arabia
Hamid Reza Rezvani, France
Alessandra Ricelli, Italy
Francisco J. Romero, Spain
Mariana G. Rosca, USA
Joan Roselló-Catafau, Spain
Esther Roselló-Lletí, Spain
Subhadeep Roy, India
Josep V. Rubert, The Netherlands
H. P. Vasantha Rupasinghe, Canada
Sumbal Saba, Brazil
Kunihiro Sakuma, Japan
Gabriele Saretzki, United Kingdom
Ajinkya S. Sase, USA
Luciano Saso, Italy
Nadja Schroder, Brazil
Sebastiano Sciarretta, Italy
Ratanesh K. Seth, USA
Anwen Shao, China
Xiaolei Shi, China
Cinzia Signorini, Italy
Mithun Sinha, USA
Giulia Sita, Italy
Eduardo Sobarzo-Sánchez, Chile
Adrian Sturza, Romania
Yi-Rui Sun, China
Eisa Tahmasbpour Marzouni, Iran
Carla Tatone, Italy
Shane Thomas, Australia
Carlo Gabriele Tocchetti, Italy
Angela Trovato Salinaro, Italy
Paolo Tucci, Italy
Rosa Tundis, Italy
Giuseppe Valacchi, Italy
Daniele Vergara, Italy
Victor M. Victor, Spain
László Virág, Hungary
Kai Wang, China
Min-qi Wang, China
Natalie Ward, Australia
Grzegorz Wegrzyn, Poland
Philip Wenzel, Germany
Qiongming Xu, China
Sho-ichi Yamagishi, Japan
Liang-Jun Yan, USA
Guillermo Zalba, Spain
Junmin Zhang, China
Ziwei Zhang, China
Jia Zhang, First Affiliated Hospital of Xi'an Jiaotong University, Xi'an, Shaanxi Province, China, China
Chen-he Zhou, China
Yong Zhou, China
Mario Zoratti, Italy

Contents

Hindawi
Oxidative Medicine and Cellular Longevity
Volume 2022, Article ID 9851253, 5 pages
https://doi.org/10.1155/2022/9851253

Editorial

Exposomic Fingerprint in the Development of Diseases: The Role of Free Radicals and Multiomics

Gordana Kocić,[1] **Andrej Veljković**,[1] **Dušan Sokolović**,[1] **and Nataša Poklar Ulrih**[2,3]

[1]*Faculty of Medicine, University of Nis, 18000 Nis, Serbia*
[2]*Department of Food Science and Technology, Biotechnical Faculty, University of Ljubljana, Jamnikarjeva 101, SI-1000 Ljubljana, Slovenia*
[3]*The Centre of Excellence for Integrated Approaches in Chemistry and Biology of Proteins (CipKeBiP), Slovenia*

Correspondence should be addressed to Gordana Kocić; kocicrg@yahoo.co.uk

Received 6 December 2021; Accepted 6 December 2021; Published 20 March 2022

Copyright © 2022 Gordana Kocić et al. This is an open access article distributed under the Creative Commons Attribution License, which permits unrestricted use, distribution, and reproduction in any medium, provided the original work is properly cited.

The concept of the exposome refers to the totality of environmental exposures, including general or specific external, internal, and psychosocial factors, affecting the body from the embryonic period to the old age. The importance of exposome for the development of chronic diseases and multiorgan failure may account for about 70 to 90% of disease risks. It has been documented that the majority of important chronic diseases are likely to result from the combination of environmental exposures to infective, chemical, and physical stressors and their interaction with the human genome [1–4]. Most often, a number of different exposomic risk factors may act simultaneously and exert cumulative effect.

When trying to understand the factors responsible for the individual sensitivity to the development of malignant and chronic diseases, the emphasis has been placed on individual genetic variations due to single-nucleotide polymorphism (SNP) and their proteome-related response. They can be defined as genetic exposure susceptibility to disease development. Polymorphic variants in oxidative stress enzymes may explain the interindividual variability in response to chronic disease, tumor development, and tumor therapy.

Among specific external exposures, the infectious agents, especially viruses, environmental pollutants, drugs, diet, lifestyle factors (smoking, alcohol abuse), and medical interventions (supplemental oxygen ventilation and high flow oxygen therapy of critically ill patients), may affect cell and tissue systems, due to a deregulated free radical production and their neutralization [5]. The balance between the exposome and endogenous circulating hormones, body composition, aging, inflammation, wider social, economic, and psychological influences may affect the host individual response and the disease outcome.

The objective of the special issue is to provide molecular mechanisms related to how specific environmental factors provoke reactive oxygen species (ROS) production, and how ROS, as a part of environmental exposure or internal production, can affect human health. It includes articles related to the role of free radicals and multiomics in describing exposomic marker and other biomarkers of a disease. The originality lies in the ability to distinguish and recognize the earliest and innovative exposomic biomarkers accurately, the earliest genetic predisposition markers, and new therapeutic influences in disease diagnostics, prevention, and treatment. The articles may be clustered concerning specific type(s) of diseases and to specific environmental factors. All of the abovementioned exposomic factors are shown in Figure 1.

Devastating effects of viral infections, particularly the COVID-19 (SARS-CoV-2) pandemic and HCV infection, may belong to the most important external exposures at the moment. Four of eight published articles refer to viral infections. They are related to a deeper explanation of molecular mechanisms associated with late consequences and serious organ damage. The authors Zdravković M et al. and Popadić et al. in their collaborating studies nested

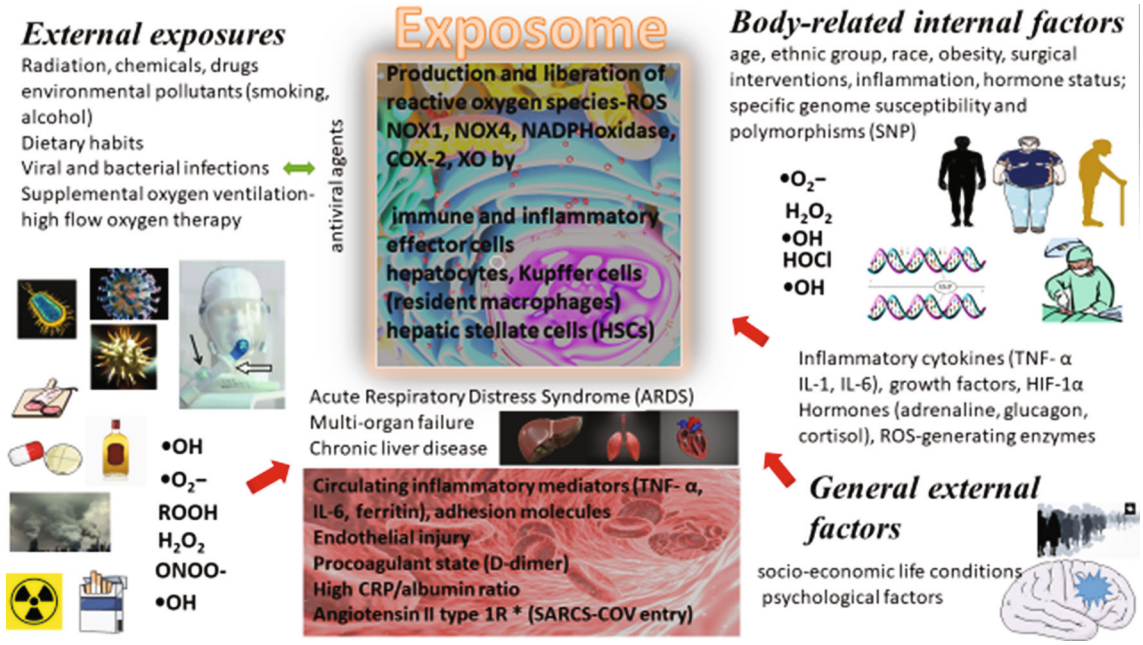

Figure 1: The concept of the exposome and its relation to cell injury and laboratory markers.

from more than 1000 COVID-19 patients per month. They emphasized the importance of the appropriate risk stratification in 460 COVID-19 patients with a higher risk of poor clinical outcomes at admission to the ICU, under the specific (prooxidative) conditions demanding high oxygen flow. The clinical outcome of the disease includes acute respiratory distress syndrome, superinfection, shock, acute heart, liver, and kidney injury, evaluated also by specific laboratory biomarkers. The use of AIDA score has been defined as a reliable tool for delivering the appropriate therapy on time. It was developed by combining significant variables from the multivariate logistic regression analysis including serum albumin, interleukin-6, and D-dimer, accompanied by age. They also developed and validated a multivariable predictive model for mortality of COVID-19 patients at admission to ICU, in relation to respiratory status (development of acute respiratory distress syndrome ARDS) as the most important clinical outcome. The appearance of ARDS was considered in relation to invasive or noninvasive mechanical ventilation and high flow oxygen therapy. In the final multivariate analysis, serum albumin (below 33 g/L), interleukin-6 (above 72 pg/mL), and D-dimer, accompanied by age and CT severity score as parts of univariate analysis, were marked as independent predictors of mortality. These predictors have been referred to the three most probable pathophysiological mechanisms of a lethal outcome, septic infections associated with septic shock, procoagulable state, procoagulant state associated with micro- and macrothrombosis, and cytokine storm proceeded to multiorgan failure. The COVID-19 research-related articles were followed by a research of Cekerevac et al. This is the first study where it documented the level of circulating oxidative stress parameters as predictors in the disease severity and mortality. In their prospective cross-sectional study, they reported novel information about potential molecular mechanisms during the different degree of COVID-19 in adult patients, due to the infiltration of neutrophils, a marked elevation of proinflammatory cytokines, and cytokine storm association with elevated levels of superoxide anion radicals. They may act as significant contributors to the disease progress, severity, and mortality. Moreover, by using a linear regression model, they documented that hypertension, anosmia, ageusia, the O_2^-level, and the duration at the ICU may be predictors of severity of COVID-19 (SARS-CoV-2) disease in a group of 127 patients. In order to evaluate the influence of severity of the disease, all patients were divided into a group with a mild form of COVID-19 (mild symptoms up to mild pneumonia, with moderate COVID-19 form (dyspnea, hypoxia, or less than 50% lung involvement on imaging) and a group of patients with a severe COVID-19 (severe respiratory failure, high flow oxygen therapy, mechanical ventilation, sepsis, or multiorgan system dysfunction). Besides the evaluation of standard laboratory markers, the concentration of prooxidative markers (superoxide anion radical (O_2^-), hydrogen peroxide (H_2O_2), nitric oxide (NO^-), and lipid peroxidation (TBARS)) and antioxidative markers (catalase (CAT), superoxide dismutase (SOD), and reduced glutathione GSH) were determined in blood plasma and lysate.

The association of chronic HCV infection-specific genotype and viral load association with increased oxidative stress has been emphasized by a comprehensive study by Đorđevic et al. The intensity of oxidative stress may be a detrimental factor in liver injury and may determine the severity of the disease. In their case-control study, which involved 52 HCV patients and 50 control healthy patients, they demonstrated the intensity of oxidative stress (level of lipid peroxidation TBARS and protein oxidative modification AOPP) and decreased antioxidative defense (catalase activity) as a detrimental factor in liver injury and severity of the disease. The cells responsible for ROS production and

liberation are hepatocytes, Kupffer cells (resident macrophages), inflammatory cells, hepatic stellate cells (HSCs), and other immune effector cells. The values of oxidative stress parameters (TBARS and AOPP) and catalase activity in patients infected with different HCV genotypes revealed that HCV1b patients were more likely to have a higher TBARS compared to others, HCV 3 patients were more likely to have a higher AOPP level, while patients infected with HCV1a were more likely to have a low catalase activity. A positive correlation was found between virus genome copy concentration and AOPP, while a high level of HCV viral load was more likely to have a higher TBARS. In a gender-based comparison, a significantly higher level of AOPP was reported in female patients. The results obtained confirmed the existence of imbalance between the ROS production and antioxidative defense system in HCV-infected patients. Since oxidative stress may have a profound influence on disease progression, fibrosis, and carcinogenesis, our results may meet the aspirations of mandatory introduction of antioxidants as early HCV therapy to counteract ROS consequences.

In in the cohort of 292 participants of adult population, Klisic et al. highlighted the role of internal exposome as potential factors specific to the individual physiology, age, and body morphology and their relation to oxidative stress markers. They examined a prooxidant-antioxidant balance (PAB)) and the marker of antioxidant defense capacity (total sulphydryl groups (tSHG)), their ratio (PAB/tSHG) and their relationship with different cardiometabolic risk factors (waist-to-height ratio, body mass index, visceral adiposity index, and lipid accumulation products). They reported tSHG and PAB/tSHG correlation with lipid parameters (HDL-c and TG) and lipid indices (VAI and LAP); HDL-c showed negative and TG, VAI, and LAP positive independent associations and predictions. To assess the associations of clinical markers with tSHG, PAB levels and PAB/tSHG index univariate and multivariate ordinal regression analyses were applied. By using principal component analysis (PCA), various cardiometabolic risk parameters produced scores for significant factors, which were used in the subsequent binary logistic regression analysis to estimate the predictive potency of the factors towards the highest PAB and tSHG values. In that way, obesity-renal function-related factor predicted both high PAB and low tSHG, while obesity-dyslipidemia-related factor predicted significantly high tSHG values. The authors concluded that unfavorable cardiometabolic profile was associated with higher tSHG values.

Durand et al. addressed the importance of oxidative stress as a pathogenetic key for development of nonalcoholic fatty liver disease (NAFLD). The severity of hepatic damage depends on whether simple fat accumulation (steatosis), nonalcoholic steatohepatitis (NASH), and hepatic fibrosis are developed. The lipid composition of mitochondrial membranes, presumably the composition of PE and CL is of crucial importance in maintaining mitochondrial structure and function in the assembly and activity of respiratory chain complexes III and IV and supercomplex formation. Accordingly, in the transport of electrons from complex I to ubiquinone, the oxidized state of coenzyme Q (CoQ) depends on the composition of lipophilic environment, i.e., cardiolipins (CLs). Their experimental model of NAFLD has been developed to integrate specific "omics" signature (lipidomics) and oxidative stress markers specifically adapted for mitochondrial liver cell fraction. Moreover, the mRNA expression levels for the key transcription factors for lipid synthesis, sterol regulatory element-binding transcription factor 1 (*Srebf1*), nuclear receptor peroxisome proliferator-activated receptor α (*Ppar*α) and inflammation, Toll-like receptor 9 (*Tlr9*), and tumor necrosis factor (*Tnf-*α) were evaluated. The cardiolipin and CoQ antioxidant function impairment precede fibrosis, emphasizing a causal relationship with NAFLD development and progression. The optimal structure of mitochondrial lipids may represent a new therapeutic intervention in nonalcoholic fatty liver disease (NAFLD) prevention strategy.

It was documented that cancer develops from a combination of exposomic factors influencing specific susceptibility genes and family history. Among exposomic factors, there are specific external exposures and body-related internal exposome (Figure 1). The clear-cell renal cell carcinoma (ccRCC) belongs to types of carcinomas associated with Keap1/Nrf2 (Kelch-like ECH-associated protein 1/nuclear factor (erythroid-derived 2)-like2) pathway alterations. The authors Mihailovic et al. highlighted the relation between the reactive oxygen species and electrophiles and the activation of specific adaptive cytoprotective response, including changes in the Keap1/Nrf2 pathway. The enzymes encoded by Nrf2 target genes are glutathione S-transferases (GST), superoxide dismutase (SOD2), and glutathione peroxidase (GPX). The interaction between GSTP1: JNK1 may reveal the functional link between the upregulated GSTP1 and malignant phenotype. At the same time, the reaction catalyzed by mitochondrial SOD2 releases H_2O_2, which may act as the signaling molecule in cell proliferation, differentiation, and migration. It may also induce the activation of AMP-activated kinase activating glycolysis, where the energy production is essential for malignant cell survival. The antioxidant enzyme, glutathione peroxidase (GPX), catalyzes the reduction of H_2O_2. The single-nucleotide polymorphisms of Nrf2 gene and genes encoding GSTP1, SOD2, and GPX1 may change the expression of specific protein or affect the activity of synthesized proteins. The authors investigated the effect of specific *Nrf2*, *SOD2*, and *GPX1* gene variants and *GSTP1ABCD* haplotype on ccRCC risk and the prognosis in 223 ccRCC patients and 336 matched controls by PCR-CTTP and qPCR. Haplotype analysis revealed a significant risk of ccRCC development in carriers of the *GSTP1C* haplotype, while GSTP1 variant affected the overall survival in ccRCC patients. The increased ccRCC susceptibility was observed among carriers of individual variant genotypes of *SOD2* and *GSTP1* and *Nrf2*. Moreover, the analysis of *GSTP1ABCD* haplotype revealed significant risk of ccRCC development and the overall survival in patients with ccRCC. This interaction is summarized in Figure 2.

Jerotic Dj et al. reported in an experimental study a nowel mechanism of glutathione S-transferase M1 (GSTM1) downregulation influence on increased oxidative stress and

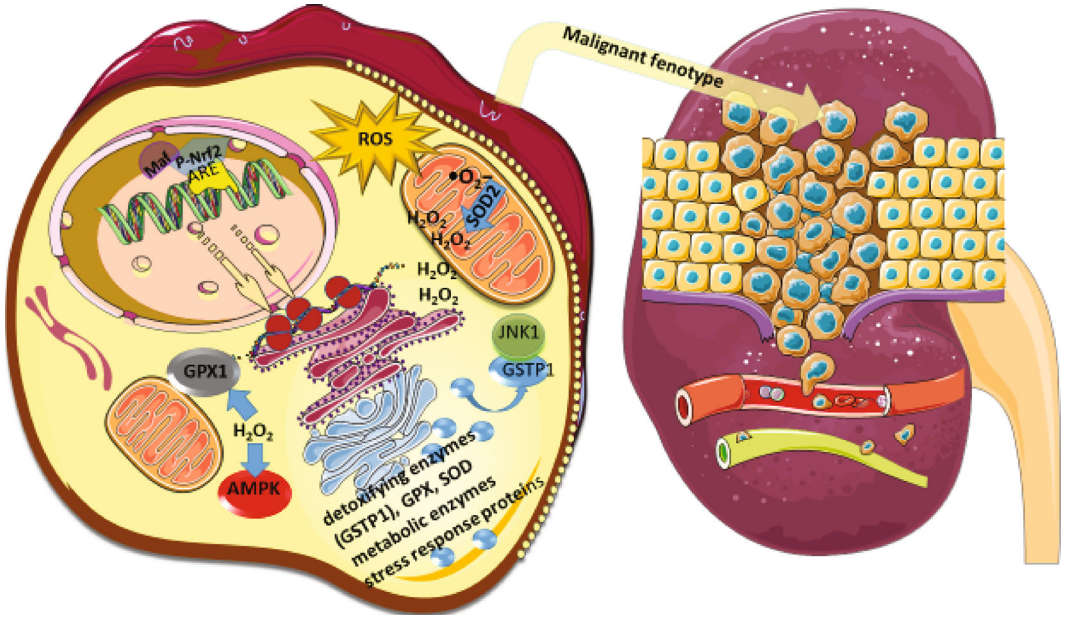

Figure 2: Relation between p-Nrf2 and expression pattern of detoxifying enzymes (created according to the results referred by Mihailovic et al.).

inflammation in endothelial cells in uremic conditions. The also reported that the deletion polymorphism of glutathione S-transferase M1 (GSTM1), a phase II detoxification and antioxidant enzyme, increased susceptibility to end-stage renal disease (ESRD), as well as the development of cardiovascular diseases (CVD) among ESRD patients and their shorter cardiovascular survival. When human umbilical vein endothelial cells (HUVECs) were exposed to uremic serum, they exhibited impaired redox balance, associated with enhanced lipid peroxidation and decreased antioxidant enzyme activities, expression of a series of inflammatory cytokines including retinol-binding protein 4 (RBP4), regulated upon activation, normal T cell expressed and secreted (RANTES), C-reactive protein (CRP), angiogenin, dickkopf-1 (Dkk-1), and platelet factor 4 (PF4). In order to obtain *GSTM1-null* genotype, with no GSTM1 protein expression, HUVECs were transfected with GSTM1 small interfering RNA (siRNA). The authors documented that *GSTM1-null* genotype exposed to uremic serum led to the upregulation of monocyte chemoattractant protein-1 (MCP-1), intracellular and vascular cell adhesion molecules (ICAM-1 and VCAM-1). Very interesting was the finding on the increased levels of serum ICAM-1 and VCAM-1 (sICAM-1 and sVCAM-1) in ESRD patients lacking GSTM1, in comparison with patients with the *GSTM1-active* genotype. A novel function of endothelial GSTM1 in the regulation of monocyte migration and adhesion, through its role in the upregulation of MCP-1, might be relevant as a potential therapy target.

In summary, this special issue is compatible and consistent with the research topic requirements, delineated in the aim and description proposed for this special issue:

(i) to perform translational studies focused on specific external exposures (viruses COVID-19 and HCV), by using human blood samples

(ii) to create *in vivo* experimental animal models for the examination of the role of free radical-induced chronic diseases in relation to proteome and lipidome signature (NAFLD)

(iii) to perform *in vitro* cell culture models to explore a role of free radicals in chronic diseases (HUVEC)

(iv) to identify and characterize potential cell signaling pathways sensing specific external exposures and body-related internal exposome in chronic disease and tumor development (ccRCC and cardiometabolic syndrome)

(v) to identify and characterize the novel regulatory pathways connecting redox-sensitive signaling enzymes to cell transcriptome and proteome and small interfering RNA silencing connection with redox enzymes (*GSTM1-null* genotype)

Conflicts of Interest

The authors declare that they have no conflicts of interests regarding the publication of this Special Issue.

Acknowledgments

The Editors wish to thank the authors for their valuable contribution enriching this issue with novel scientific methods, based on profound *scientific* experience, modern and conscientious scientific approach, and future research agenda.

Gordana Kocić
Andrej Veljković
Dušan Sokolović
Natasa Poklar Ulrih

References

[1] C. P. Wild, "Complementing the genome with an "exposome": the outstanding challenge of environmental exposure measurement in molecular epidemiology," *Cancer Epidemiology, Biomarkers & Prevention*, vol. 14, no. 8, pp. 1847–1850, 2005.

[2] S. M. Rappaport and M. T. Smith, "Epidemiology. Environment and disease risks," *Science*, vol. 330, no. 6003, pp. 460-461, 2010.

[3] W. C. Willett, "Balancing life-style and genomics research for disease prevention," *Science*, vol. 296, no. 5568, pp. 695–698, 2002.

[4] D. G. DeBord, T. Carreón, T. J. Lentz, P. J. Middendorf, M. D. Hoover, and P. A. Schulte, "Use of the "exposome" in the practice of epidemiology: a primer on -omic technologies," *American Journal of Epidemiology*, vol. 184, no. 4, pp. 302–314, 2016.

[5] G. R. S. Budinger and G. M. Mutlu, "Balancing the risks and benefits of oxygen therapy in critically III adults," *Chest*, vol. 143, no. 4, pp. 1151–1162, 2013.

Hindawi
Oxidative Medicine and Cellular Longevity
Volume 2021, Article ID 6654388, 6 pages
https://doi.org/10.1155/2021/6654388

Research Article

Development and Validation of a Multivariable Predictive Model for Mortality of COVID-19 Patients Demanding High Oxygen Flow at Admission to ICU: AIDA Score

Marija Zdravkovic[1,2] **Viseslav Popadic**[1] **Slobodan Klasnja**[1] **Vedrana Pavlovic**[3] **Aleksandra Aleksic**[1] **Marija Milenkovic**[2,4] **Bogdan Crnokrak**[1,2] **Bela Balint**[5,6] **Milena Todorovic-Balint**[2,7] **Davor Mrda**[1] **Darko Zdravkovic**[1,2] **Borislav Toskovic**[1,2] **Marija Brankovic**[1,2] **Olivera Markovic**[1,2] **Jelica Bjekic-Macut**[1,2] **Predrag Djuran**[1] **Lidija Memon**[1] **Ana Stojanovic**[1] **Milica Brajkovic**[1] **Zoran Todorovic**[1,2] **Jovan Hadzi-Djokic**[2,6] **Igor Jovanovic**[1] **Dejan Nikolic**[1,2] **Dane Cvijanovic**[8] **and Natasa Milic**[3,9]

[1]*University Clinical Hospital Center, Bezanijska kosa, Belgrade, Serbia*
[2]*Faculty of Medicine, University of Belgrade, Belgrade, Serbia*
[3]*Institute for Medical Statistics and Informatics, Faculty of Medicine University of Belgrade, Belgrade, Serbia*
[4]*Clinical Center of Serbia, Belgrade, Serbia*
[5]*Institute of Cardiovascular Diseases "Dedinje", Belgrade, Serbia*
[6]*Department of Medical Sciences, Serbian Academy of Sciences and Arts, Serbia*
[7]*Clinic for Hematology, Clinical Center of Serbia, Belgrade, Serbia*
[8]*University Clinical Center Zvezdara, Belgrade, Serbia*
[9]*Department of Internal Medicine, Division of Nephrology and Hypertension, Mayo Clinic, Rochester, USA*

Correspondence should be addressed to Marija Zdravkovic; sekcija.kardioloska@gmail.com

Received 17 March 2021; Accepted 29 May 2021; Published 30 June 2021

Academic Editor: Gordana Kocic

Copyright © 2021 Marija Zdravkovic et al. This is an open access article distributed under the Creative Commons Attribution License, which permits unrestricted use, distribution, and reproduction in any medium, provided the original work is properly cited.

Introduction. Risk stratification is an important aspect of COVID-19 management, especially in patients admitted to ICU as it can provide more useful consumption of health resources, as well as prioritize critical care services in situations of overwhelming number of patients. *Materials and Methods*. A multivariable predictive model for mortality was developed using data solely from a derivation cohort of 160 COVID-19 patients with moderate to severe ARDS admitted to ICU. The regression coefficients from the final multivariate model of the derivation study were used to assign points for the risk model, consisted of all significant variables from the multivariate analysis and age as a known risk factor for COVID-19 patient mortality. The newly developed AIDA score was arrived at by assigning 5 points for serum albumin and 1 point for IL-6, D dimer, and age. The score was further validated on a cohort of 304 patients admitted to ICU due to the severe form of COVID-19. *Results*. The study population included 160 COVID-19 patients admitted to ICU in the derivation and 304 in the validation cohort. The mean patient age was 66.7 years (range, 20–93 years), with 68.1% men and 31.9% women. Most patients (76.8%) had comorbidities with hypertension (67.7%), diabetes (31.7), and coronary artery disease (19.3) as the most frequent. A total of 316 patients (68.3%) were treated with mechanical ventilation. Ninety-six (60.0%) in the derivation cohort and 221 (72.7%) patients in the validation cohort had a lethal outcome. The population was divided into the following risk categories for mortality based on the risk model score: low risk (score 0–1) and at-risk (score > 1). In addition, patients were considered at high risk with a risk score > 2. By applying the risk model to the validation cohort ($n = 304$), the positive predictive value was 78.8% (95% CI 75.5% to 81.8%); the negative predictive value was 46.6% (95% CI 37.3% to 56.2%); the sensitivity was 82.4% (95% CI 76.7% to 87.1%), and the specificity was 41.0% (95% CI 30.3% to 52.3%). The *C* statistic was 0.863 (95% CI 0.805-0.921) and 0.665 (95% CI

0.598-0.732) in the derivation and validation cohorts, respectively, indicating a high discriminative value of the proposed score. *Conclusion*. In the present study, AIDA score showed a valuable significance in estimating the mortality risk in patients with the severe form of COVID-19 disease at admission to ICU. Further external validation on a larger group of patients is needed to provide more insights into the utility of this score in everyday practice.

1. Introduction

COVID-19 infection represents a highly contagious infective disease with a wide array of clinical presentations and a massive burden for the health systems worldwide [1–4]. Symptoms at disease onset are relatively mild, and a significant group of patients does not show apparent symptoms before the development of respiratory failure, which makes it more difficult to identify patients at risk [5–7]. Different prediction models were developed based on various demographic, radiographic, and laboratory parameters but only a few of them focusing on clinical risk, ICU care, and in-hospital mortality [8–10]. Patients with the severe form of the disease were more likely to be older, associated with multiple comorbidities, severe lung involvement, and immune response [11, 12].

Risk stratification is a very important part of the management of COVID-19 mostly due to the need to prioritize critical care services in situations of an overwhelming number of patients. A proper risk stratification could provide more useful consumption of health resources, as well as to reorient more attention to the patients most likely to develop a severe form of the disease [13–15]. In certain studies, it is shown that predictive models using laboratory parameters had stronger discriminatory power compared to the clinical models [16]. Careful monitoring of laboratory and clinical parameters followed by a purposeful risk stratification of patients admitted to ICU could allow a forehand reaction in case of disease progression, reducing further deterioration and overall mortality.

In this multicenter study, we aimed to develop and validate a multivariable predictive model for mortality of COVID-19 patients admitted to ICU.

2. Materials and Methods

The AIDA score was developed according to the results and methodology of the previous study by Popadic et al. [17], combining all significant variables from the multivariate logistic regression analysis including serum albumin, interleukin-6, and D-dimer, accompanied by age.

2.1. Study Population and Risk Factors. The derivation group consisted of 160 COVID-19 patients with moderate to severe ARDS admitted to the Respiratory Intensive Care Unit between June 23, 2020, and October 2, 2020, in University Clinical Hospital Center Bezanijska kosa, Belgrade, Serbia, while further analysis and validation were performed on additional consecutive 318 patients admitted to ICU between October 2, 2020, and January 14, 2021, in University Clinical Hospital Center Bezanijska kosa, Belgrade, Serbia (160 patients), and University Clinical Hospital Center Zvezdara, Belgrade, Serbia (158 patients). The patients in both groups were treated by the National Protocol of the Republic of Serbia for the treatment of COVID-19 infection, as explained in Materials and Methods of the development study by Popadic et al. [17].

The Institutional Review Boards of the University Clinical Hospital Center Bezanijska kosa and University Clinical Hospital Center Zvezdara approved the conducting of the study.

2.2. Predictive Model Development. The predictive model was developed using data completely from a development cohort, which consisted of 160 patients. Patient characteristics were first assessed by univariate logistic regression analysis, following with the final model being developed using a stepwise multivariate logistic regression analysis. The characteristics pool for stepwise-regression modeling was defined based on characteristics known relevance or correlation with increased mortality risk (p value < 0.10 in univariate analysis). The variance inflation factor (VIF) was used to examine covariates for colinearity. The risk prediction score was developed using coefficients from the final regression multivariate model with the addition of age from univariate analysis. Missing data was rare (<5%) among characteristics considered for the final model development, and no imputations were performed. Patients who had their data missing for an outcome (14 patients in total) were excluded from the analysis. Wilson procedure, including continuity correction, was used to evaluate differences between characteristics frequency in the development and validation cohorts, shown with a 95% confidence intervals (CI). Patients were divided into 2 risk groups according to the risk score once the final model had been defined.

2.3. Model Validation. The validation cohort (304 patients) was used to assess the final model. Definitions, measurements, and outcomes used in the validation study were the same as the ones used in the development study. Model discrimination performance was tested by means of sensitivity, specificity, positive, and negative predictive values. *C* statistic, representing the area under the receiver operating characteristic curve, was used for overall assessment of the predictive model. Larger values of *C* statistics indicated improved discrimination. For the statistical analysis, the SPSS version 25 statistical software (Chicago, USA) was used.

3. Results

3.1. Patient Characteristics. The study population included 160 COVID-19 patients admitted to ICU in the derivation and 304 in the validation cohort. The two cohorts were well balanced concerning the most assessed patient characteristics (Table 1). The mean patient age was 66.7 years (range, 20–93 years), with 68.1% men and 31.9% women. Most patients (76.8%) had comorbidities with hypertension (67.7%), diabetes (31.7), and coronary artery disease (19.3) as the most

Table 1: Characteristics of patients in both development and validation cohorts.

Patient characteristics	Development cohort ($n = 160$)	Validation cohort ($n = 304$)	Difference	95% CI for the difference
Gender, n (%)				
Male	110 (68.8)	206 (67.8)	-0.010	-0.100 to 0.080
Female	50 (31.3)	98 (32.2)		
Age, mean ± sd	65.6 ± 14.0	67.2 ± 12.6	-1.559	-4.067 to 0.949
CT score, mean ± sd	19.0 ± 4.9	17.6 ± 6.0	1.394	0.009 to 2.778
Mechanic ventilation, *n* (%)	107 (66.9)	209 (69.0)	-0.021	-0.111 to 0.069
Comorbidities, n (%)				
Hypertension	109 (69.4)	203 (66.8)	0.027	-0.064 to 0.117
Diabetes	52 (33.1)	94 (31.0)	0.021	-0.069 to 0.111
Obesity	14 (8.9)	62 (20.4)	-0.115	-0.168 to -0.044
HOBP	8 (5.1)	13 (4.3)	0.008	-0.032 to 0.049
Asthma	6 (3.8)	14 (4.6)	-0.008	-0.047 to 0.032
Coronary disease	28 (17.8)	61 (20.1)	-0.022	-0.099 to 0.054
Cardiomyopathy	14 (8.9)	24 (7.9)	0.010	-0.043 to 0.063
Total number of patients with comorbidities, *n* (%)	120 (75.9)	235 (77.3)	-0.014	-0.095 to 0.068
Total number of patients with 2+ comorbidities, *n* (%)	72 (45.6)	137 (45.1)	0.005	-0.091 to 0.101
Tocilizumab, *n* (%)	38 (23.8)	51 (16.8)	0.070	-0.006 to 0.145

frequent. Obesity was present in 16.5% of patients and was more prevalent in the validation cohort. A total of 316 patients (68.3%) were treated with mechanical ventilation, and 89 (19.2%) received Tocilizumab. Ninety-six (60.0%) in the derivation cohort and 221 (72.7%) patients in the validation cohort had a lethal outcome.

3.2. Risk Assessment Model. In the derivation cohort, the following variables were associated with the mortality of patients admitted to ICU due to COVID-19-related pneumonia in univariate logistic regression analysis: age (RR = 3.495, 95% CI 1.801–6.779), albumin (RR = 22.286, 95% CI 9.319–53.294), D-dimer (RR = 2.111, 95% CI 1.091–4.085), IL-6 at admission to ICU (RR = 6.100, 95% CI 2.857–13.023), and CT score (RR = 2.362, 95% CI 1.120–4.980). In the multivariate analysis, serum albumin (RR = 25.740, 95% CI 7.491–88.443), IL-6 (RR = 6.245, 95% CI 1.937–20.129), and D-dimer at admission to ICU (RR = 4.574, 95% CI 1.375–15.212) were independently associated with mortality [17]. Subsequently, the regression coefficients from the final multivariate model were used to assign points for the risk model. The newly developed AIDA score included all significant patient characteristics from the multivariate analysis and age as a known risk factor for COVID-19 patient mortality. The AIDA score was arrived at by assigning 5 points for serum albumin and 1 point for IL-6, D dimer, and age (Table 2). Finally, based on the risk prediction score, the population consisted of the following division risk categories for mortality: low risk (score 0–1) and at risk (score > 1). In addition, patients were considered at high risk with a risk score > 2.

3.3. Accuracy and Validation of AIDA Risk Model. In the development cohort, for patients classified as at risk (score > 1), the AIDA risk model produced a positive predictive value (probability of a lethal outcome in patient designated at risk) of 73.8% (95% CI 68.9% to 78.2%) and a negative predictive value (probability of recovering in patients designated low risk) of 91.2% (95% CI 76.7% to 97.0%). The sensitivity (probability of being classified as at risk in patients with the lethal outcome) was 96.9% (95% CI 91.1% to 99.4%), and the specificity (probability of being classified as low risk in patients recovered) was 48.4% (95% CI 35.8% to 61.3%). A high-risk AIDA score > 2 had a positive predictive value (probability of a lethal outcome in patient designated at high risk) of 81.2% (95% CI 74.6% to 86.4%) and a negative predictive value (probability of recovering in patients designated as not being at high risk) of 76.3% (95% CI 65.9% to 84.3%). The sensitivity (probability of being classified as at high risk in patients with the lethal outcome) was 85.4% (95% CI 76.7% to 91.8%), and the specificity (probability of being classified as not at high risk in patients recovered) was 70.3% (95% CI 57.6% to 81.1%).

The AIDA risk model was then tested for accuracy in the validation cohort ($n = 304$), where the positive predictive value was 78.8% (95% CI 75.5% to 81.8%); the negative predictive value was 46.6% (95% CI 37.3% to 56.2%); the sensitivity was 82.4% (95% CI 76.7% to 87.1%), and the specificity was 41.0% (95% CI 30.3% to 52.3%). The *C* statistic was 0.863 (95% CI 0.805-0.921) and 0.665 (95% CI 0.598-0.732) in the development (Figure 1) and validation cohorts (Figure 2), respectively. Both cohorts were similar according to AIDA score accuracy, as well as the frequency of patients classified into each risk category.

4. Discussion

The clinical setting of COVID-19 infection could be diverse, affecting multiple organs and provoking various symptoms

Table 2: Predictive model for mortality in patientss admitted to ICU due to COVID-19-related pneumonia.

Variable	Assigned score
Albumin, serum < 33 g/L	5
IL6 > 72 pg/mL	1
D dimer > 1000 ng/mL	1
Age ≥ 65 years	1

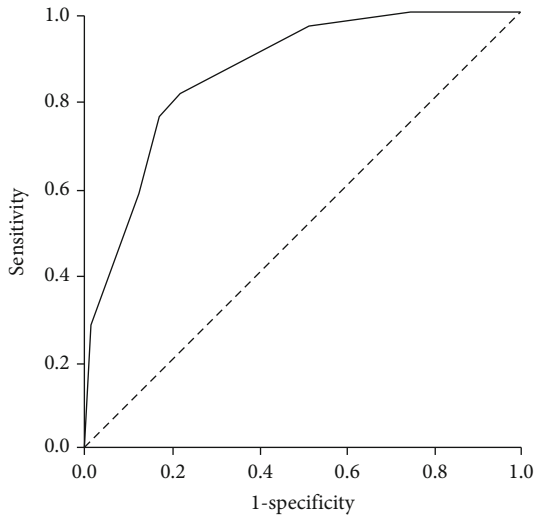

Figure 1: ROC curve in development cohort.

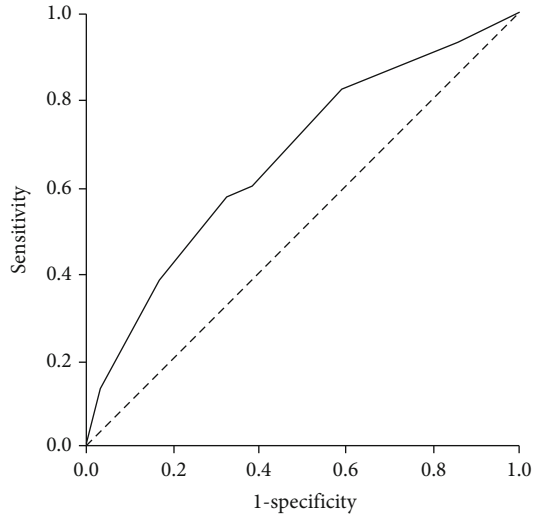

Figure 2: ROC curve in validation cohort.

and signs, making it more difficult to enable an appropriate risk stratification of these patients [18]. Also, the clinical course of the disease in terms of different pathophysiological mechanisms and complications, including acute respiratory distress syndrome, superinfection, shock, acute heart, liver, and kidney injury, is unpredictable and is leaving a limited timespan to bring the right treatment decision in a real clinical scenario [19, 20].

In the present study, we reported a process of development and validation of a multivariable predictive model for mortality of COVID-19 patients demanding high oxygen flow at admission to ICU.

In order to develop a simple but highly predictable risk score, we have started by identifying credible predictors of mortality in a group of patients with the worst possible clinical condition, considering respiratory status as the most important aspect. This is why the derivation group consisted only of patients with moderate to severe ARDS and on invasive, noninvasive mechanical ventilation and high flow oxygen therapy. The main aim of the following analysis was to extract only those clinical and laboratory parameters which are most likely to be linked with the poor clinical outcome. In the final multivariate analysis, serum albumin, interleukin-6, and D-dimer, accompanied by age and CT severity score as parts of univariate analysis, were marked as independent predictors of mortality. It is important to underline that these predictors are reflecting the three most probable pathophysiological mechanisms of a lethal outcome, infection with sepsis and shock, procoagulable state provoking micro and macrothrombosis, and cytokine storm as a potential trigger of multiorgan failure [21]. Different risk scores have been developed to stratify hospitalized COVID-19 patients, with very few being applicable in patients admitted to ICU. AIDA score primarily relies on the high sensitivity (being 82.4% (95% CI 76.7% to 87.1%) in the validation group) and positive predictive value (78.8% (95% CI 75.5% to 81.8%)), as the most important part of the risk stratification in COVID-19 patients was to identify patients at risk, but not to eliminate the subgroup of low-risk patients, as that would be a two-edged sword, considering the unpredictability of the disease and rapid progression of certain clinical forms. One of the most important advantages of this score is a quite respectable sample size in both derivation and validation groups, encompassing more than 460 patients admitted to ICU with a severe form of the disease. The validation group consisted of patients from two different hospital centers but treated according to the same therapy protocol, while the baseline characteristics between the derivation and validation group did not differ significantly (Table 1). The score is easy to use, as it includes usual laboratory parameters for every COVID-19 patient. Also, the significance of CT severity score was already marked as an important part of risk stratification, although it was not statistically analyzed in our study, due to the lack of data in the external validation group. However, it can be helpful as an additional factor considering the results of the univariate logistic regression model where values of CT severity score above 20 were highly predictable for poor clinical outcome among patients admitted to ICU.

Interleukin-6 values above 72 pg/mL were significant for predicting poor clinical outcomes, which may be helpful in the decision-making process, as immunomodulatory therapy should be administrated earlier in the clinical course. According to the results, the interleukin-6 receptor antagonists might be effective in patients with elevated values of interleukin-6 (but below 72 pg/mL), and before the clinical deterioration in terms of respiratory failure and need for mechanical ventilation, as positive results in terms of lower

mortality rate among this subset of patients are still to be demonstrated [22]. As presented in our derivation study, the mortality rates did not differ between the groups that received and did not receive Tocilizumab in ICU, although the baseline characteristics were not significantly different.

It is of great importance to note that a low value of serum albumin, below 33 g/L, is already highly significant as a predictor of mortality and is a sufficient parameter to stratify patients into a high-risk group. Following the worsening of the patient's condition, the values of interleukin-6 and D-dimer were usually already elevated above their significant values, while the value of serum albumin was preserved a certain amount of time before further clinical worsening. In patients with a severe form of COVID-19, hypoalbuminemia should be considered the most pertinent marker of an advanced clinical condition and is usually followed by the further rising of proinflammatory parameters and D-dimer, indicating a coupling of progressed shock and an increased procoagulable state [23]. This is meaningful as it can point out that various important regulatory mechanisms are already expended, initiating an irreversible condition refractory to a wide specter of different therapeutic modalities [24]. The potential therapeutical benefit of albumins in patients with COVID-19 is yet to be established [25].

The main limitation of the study is a lack of a more comprehensive external validation in a condition of different therapy protocols being used. It is still unknown if different therapeutic modalities in the earlier phase of the disease can significantly affect the credibility of the score, although this score is primarily intended for the risk stratification of patients admitted to ICU. The score could be developed further by implementing different ICU scoring systems to encompass a wider image of the patient's current condition.

5. Conclusion

Risk stratification of patients with COVID-19 is an important aspect of everyday practice, having in mind the unpredictability of clinical course and possible complications of the disease. AIDA score could be a reliable tool capable of identifying patients with a higher risk of poor clinical outcomes at admission to the ICU, providing more space to deliver an appropriate therapy on time. Further validation on a larger group of patients will provide more insights into the utility and definitive clinical significance of this score.

Abbreviations

COVID-19: Coronavirus disease 19
ICU: Intensive care unit
ARDS: Acute respiratory distress syndrome
CT: Computerized tomography
IL-6: Interleukin-6.

Data Availability

The data that support the findings of this study are available from the corresponding author (MZ) upon reasonable request.

Disclosure

The authors state that no relationship with industry exists. The funders had no role in preparation of the manuscript or the decision to publish.

Conflicts of Interest

The authors declare that there is no conflict of interest regarding the publication of this paper.

Authors' Contributions

Collaborator details are as follows: Nina Rajovic[3] MD; Jasna GACIC[1, 2] MD, PhD; Ljiljana Denic Markovic[1, 2] MD, PhD; Aleksandra Petrovic[1] MD; Natasa Stanisavljevic[1] MD, PhD; Igor Nadj[1] MD; Uros Marjanovic[1] MD; Aleksandra Dumic[1] MD; Simona Petricevic[1] MD; Maja Popovic[1] MD; Filip Lukic[1] MD; Zdravko Kalaba[1] MD; Aleksandar Davidovic[8, 10] MD, PhD; Natasa Markovic Nikolic[2, 8] MD, PhD; Gordana Mihajlovic[2, 8] MD, PhD; Miljanka Vuksanovic[2, 8] MD, PhD; Milica Marjanovic Petkovic[2, 8] MD, PhD; Natasa Petrovic Stanojevic[8, 10] MD, PhD. [1]University Clinical Hospital Center, Bezanijska kosa, Belgrade, Serbia. [2]Faculty of Medicine, University of Belgrade, Belgrade, Serbia. [3]Institute for Medical Statistics and Informatics, Faculty of Medicine University of Belgrade, Belgrade, Serbia. [4]Clinical Center of Serbia, Belgrade, Serbia. [5]Institute of Cardiovascular Diseases "Dedinje," Belgrade, Serbia. [6]Department of Medical Sciences, Serbian Academy of Sciences and Arts. [7]Clinic for Hematology, Clinical Center of Serbia, Belgrade, Serbia. [8]University Clinical Center Zvezdara, Belgrade, Serbia. [10]Faculty of Stomatology, University of Belgrade, Belgrade, Serbia.

Acknowledgments

The authors would like to acknowledge all healthcare professionals which are in the first line against COVID-19 disease in the Republic of Serbia and worldwide.

References

[1] A. Sarkesh, A. Daei Sorkhabi, E. Sheykhsaran et al., "Extrapulmonary clinical manifestations in COVID-19 patients," *The American Journal of Tropical Medicine and Hygiene*, vol. 103, no. 5, pp. 1783–1796, 2020.

[2] D. Bandyopadhyay, T. Akhtar, A. Hajra et al., "COVID-19 pandemic: cardiovascular complications and future implications," *American Journal of Cardiovascular Drugs*, vol. 20, no. 4, pp. 311–324, 2020.

[3] C. C. Lai, W. C. Ko, P. I. Lee, S. S. Jean, and P. R. Hsueh, "Extra-respiratory manifestations of COVID-19," *International Journal of Antimicrobial Agents*, vol. 56, no. 2, article 106024, 2020.

[4] E. Kordzadeh-Kermani, H. Khalili, and I. Karimzadeh, "Pathogenesis, clinical manifestations and complications of coronavirus disease 2019 (COVID-19)," *Future Microbiology*, vol. 15, no. 13, pp. 1287–1305, 2020.

[5] P. M. George, S. L. Barratt, R. Condliffe et al., "Respiratory follow-up of patients with COVID-19 pneumonia," *Thorax*, vol. 75, no. 11, pp. 1009–1016, 2020.

[6] W. Ottestad and S. Søvik, "COVID-19 patients with respiratory failure: what can we learn from aviation medicine?," *British Journal of Anaesthesia*, vol. 125, no. 3, pp. e280–e281, 2020.

[7] R. B. Serafim, P. Póvoa, V. Souza-Dantas, A. C. Kalil, and J. I. F. Salluh, "Clinical course and outcomes of critically ill patients with COVID-19 infection: a systematic review," *Clinical Microbiology and Infection*, vol. 27, no. 1, pp. 47–54, 2021.

[8] L. Wynants, B. van Calster, G. S. Collins et al., "Prediction models for diagnosis and prognosis of COVID-19: systematic review and critical appraisal," *BMJ*, vol. 369, article m1328, 2020.

[9] M. Parohan, S. Yaghoubi, A. Seraji, M. H. Javanbakht, P. Sarraf, and M. Djalali, "Risk factors for mortality in patients with coronavirus disease 2019 (COVID-19) infection: a systematic review and meta-analysis of observational studies," *The Aging Male*, vol. 23, no. 5, pp. 1416–1424, 2020.

[10] A. M. Leeuwenberg and E. Schuit, "Prediction models for COVID-19 clinical decision making," *The Lancet Digital Health*, vol. 2, no. 10, pp. e496–e497, 2020.

[11] R. A. Armstrong, A. D. Kane, and T. M. Cook, "Outcomes from intensive care in patients with COVID-19: a systematic review and meta-analysis of observational studies," *Anaesthesia*, vol. 75, no. 10, pp. 1340–1349, 2020.

[12] M. Mudatsir, J. K. Fajar, L. Wulandari et al., "Predictors of COVID-19 severity: a systematic review and meta-analysis," *F1000Research*, vol. 9, article 1107, 2020.

[13] R. Cherian, "Clinical risk stratification in COVID-19: the need for a revised approach?," *Pulmonary Circulation*, vol. 11, no. 1, article 204589402098863, 2021.

[14] N. R. Smilowitz, V. Nguy, Y. Aphinyanaphongs et al., "Multiple biomarker approach to risk stratification in COVID-19," *Circulation*, vol. 143, no. 13, pp. 1338–1340, 2021.

[15] R. Xu, K. Hou, K. Zhang et al., "Performance of two risk-stratification models in hospitalized patients with coronavirus disease," *Frontiers in Medicine*, vol. 7, p. 518, 2020.

[16] B. M. Henry, M. H. De Oliveira, S. Benoit, M. Plebani, and G. Lippi, "Hematologic, biochemical and immune biomarker abnormalities associated with severe illness and mortality in coronavirus disease 2019 (COVID-19): a meta-analysis," *Clinical Chemistry and Laboratory Medicine*, vol. 58, no. 7, pp. 1021–1028, 2020.

[17] V. Popadic, S. Klasnja, N. Milic et al., "Predictors of mortality in critically ill COVID-19 patients demanding high oxygen flow: a thin line between inflammation, cytokine storm, and coagulopathy," *Oxidative Medicine and Cellular Longevity*, vol. 2021, 9 pages, 2021.

[18] R. da Rosa Mesquita, L. C. Francelino Silva Junior, F. M. Santos Santana et al., "Clinical manifestations of COVID-19 in the general population: systematic review," *Wiener Klinische Wochenschrift*, vol. 133, no. 7-8, pp. 377–382, 2021.

[19] Z. Wang, H. Deng, C. Ou et al., "Clinical symptoms, comorbidities and complications in severe and non-severe patients with COVID-19: a systematic review and meta-analysis without cases duplication," *Medicine (Baltimore)*, vol. 99, no. 48, article e23327, 2020.

[20] K. Vakili, M. Fathi, A. Pezeshgi et al., "Critical complications of COVID-19: a descriptive meta-analysis study," *Reviews in Cardiovascular Medicine*, vol. 21, no. 3, pp. 433–442, 2020.

[21] J. R. Jose and A. Manuel, "COVID-19 cytokine storm: the interplay between inflammation and coagulation," *The Lancet Respiratory Medicine*, vol. 8, no. 6, pp. e46–e47, 2020.

[22] P. Du, J. Geng, F. Wang, X. Chen, Z. Huang, and Y. Wang, "Role of IL-6 inhibitor in treatment of COVID-19-related cytokine release syndrome," *International Journal of Medical Sciences*, vol. 18, no. 6, pp. 1356–1362, 2021.

[23] G. Ramadori, "Hypoalbuminemia: an underestimated, vital characteristic of hospitalized COVID-19 positive patients?," *Hepatoma Research*, vol. 2020, p. 28, 2020.

[24] C. Lee and W. J. Choi, "Overview of COVID-19 inflammatory pathogenesis from the therapeutic perspective," *Archives of Pharmacal Research*, vol. 44, no. 1, pp. 99–116, 2021.

[25] F. Violi, G. Ceccarelli, L. Loffredo et al., "Albumin supplementation dampens hypercoagulability in COVID-19: a preliminary report," *Thrombosis and Haemostasis*, vol. 121, no. 1, pp. 102–105, 2021.

Hindawi
Oxidative Medicine and Cellular Longevity
Volume 2021, Article ID 9986299, 9 pages
https://doi.org/10.1155/2021/9986299

Research Article

Changes in Key Mitochondrial Lipids Accompany Mitochondrial Dysfunction and Oxidative Stress in NAFLD

Manon Durand,[1] Marine Coué,[2] Mikaël Croyal,[1,3,4] Thomas Moyon,[2] Angela Tesse,[1] Florian Atger,[1] Khadija Ouguerram,[2] and David Jacobi[1]

[1]*Université de Nantes, CHU Nantes, CNRS, INSERM, L'institut du Thorax, F-44000 Nantes, France*
[2]*Université de Nantes, CHU Nantes, INRAE, UMR1280, Physiopathologie des Adaptations Nutritionnelles (PhAN), Institut des Maladies de l'Appareil Digestif (IMAD), Centre de Recherche en Nutrition Humaine Ouest (CRNH-O), F-44093 Nantes, France*
[3]*Université de Nantes, CHU Nantes, Inserm, CNRS, SFR Santé, Inserm UMS 016, CNRS UMS 3556, F-44000 Nantes, France*
[4]*Centre de Recherche en Nutrition Humaine Ouest (CRNH-O) Mass Spectrometry Core Facility, F-44000 Nantes, France*

Correspondence should be addressed to David Jacobi; david.jacobi@univ-nantes.fr

Manon Durand and Marine Coué contributed equally to this work.

Received 7 March 2021; Accepted 6 May 2021; Published 28 June 2021

Academic Editor: Gordana Kocic

Copyright © 2021 Manon Durand et al. This is an open access article distributed under the Creative Commons Attribution License, which permits unrestricted use, distribution, and reproduction in any medium, provided the original work is properly cited.

Nonalcoholic fatty liver disease (NAFLD) is a dysmetabolic hepatic damage of increasing severity: simple fat accumulation (steatosis), nonalcoholic steatohepatitis (NASH), and hepatic fibrosis. Oxidative stress is considered an important factor in producing hepatocyte injury associated with NAFLD progression. Studies also suggest a link between the accumulation of specific hepatic lipid species, mitochondrial dysfunction, and the progression of NAFLD. However, it is unclear whether mitochondrial lipid modifications are involved in NAFLD progression. To gain insight into the relationship between mitochondrial lipids and disease progression through different stages of NAFLD, we performed lipidomic analyses on mouse livers at different stages of western diet-induced NAFLD, with or without hepatic fibrosis. After organelle separation, we studied separately the mitochondrial and the "nonmitochondrial" hepatic lipidomes. We identified 719 lipid species from 16 lipid families. Remarkably, the western diet triggered time-dependent changes in the mitochondrial lipidome, whereas the "nonmitochondrial" lipidome showed little difference with levels of hepatic steatosis or the presence of fibrosis. In mitochondria, the changes in the lipidome preceded hepatic fibrosis. In particular, two critical phospholipids, phosphatidic acid (PA) and cardiolipin (CL), displayed opposite responses in mitochondria. Decrease in CL and increase in PA were concurrent with an increase of coenzyme Q. Electron paramagnetic resonance spectroscopy superoxide spin trapping and Cu^{2+} measurement showed the progressive increase in oxidative stress in the liver. Overall, these results suggest mitochondrial lipid modifications could act as an early event in mitochondrial dysfunction and NAFLD progression.

1. Introduction

Nonalcoholic fatty liver disease (NAFLD) is reaching epidemic proportions, affecting a quarter of the world's adult population [1]. NAFLD begins with an accumulation of cellular fat (steatosis), progresses to hepatocellular injury with inflammation (nonalcoholic steatohepatitis (NASH)), and culminates in hepatic fibrosis, a cause of liver cirrhosis and hepatocellular carcinoma [2]. The current mechanistic view of the progression of simple steatosis into NASH proposes that exceeding the elimination capacity of free fatty acids in hepatocytes contributes to the formation of lipotoxic species, endoplasmic reticulum (ER) stress, and maladaptive responses of mitochondria (mitochondrial dysfunction) [3–5].

As the power house of hepatocytes, mitochondria play a major role in oxidative metabolism and normal function of the liver. In the early stages of NAFLD, namely, simple steatosis, mitochondrial respiration increases to adapt to the higher substrate availability and increased ATP demand.

No defects were observed in the respiratory function of liver mitochondria isolated from *ob*/*ob* mice with hepatic steatosis [6]. The capacity of isolated liver mitochondria to oxidize fatty acids was even increased in *ob*/*ob* mice [6]. Humans with simple steatosis and insulin resistance show elevated mitochondrial hepatic fatty acid oxidation and respiratory function when measured noninvasively by metabolite labeling *in vivo* [7, 8] and even *ex vivo* after isolating mitochondria from liver biopsies [9]. As hepatocytes store more lipids and reach full storage capacity, free fatty acid-mediated toxicity damages mitochondria. In the transition to NASH, mitochondrial respiration is decreased and reactive oxygen species (ROS) are increased. The adaptation of hepatic mitochondrial function in humans to simple steatosis is lost in steatohepatitis [7].

The lipid composition of mitochondrial membranes is pivotal to maintain mitochondrial structure and function [10]. The proximity of mitochondrial phospholipids known as cardiolipins (CLs) to the electron transport chain (ETC) provides the lipophilic environment necessary for oxidative phosphorylation [11]. CLs maintain supercomplexes [12] and regulate the transport of electrons from complex I to ubiquinone, the oxidized state of coenzyme Q (CoQ) [13]. Notably, in NAFLD, changes in CL [14] and CoQ [15, 16] contribute to the altered activity of respiratory chain complexes and oxidative stress. Accumulation of hepatic CL and CoQ in NAFLD patients has been interpreted as an early adaptive mechanism to preserve mitochondrial function [17].

Despite all this recent progress, it is still unclear whether mitochondrial dysfunction is involved in NAFLD progression or whether it is a consequence of cellular stress or fibrosis. Preclinical models for NAFLD are increasingly evaluated on the basis of "omics" features, rather than on histology alone [2]. Hepatic mitochondrial lipidome is accessible [18], and its physiological changes can be assessed [19]. However, the hepatic mitochondrial lipidome alterations during NAFLD progression are unknown. We hypothesized that hepatic mitochondria undergo specific alterations during NAFLD evolution that could be causative of mitochondrial dysfunction. In this respect, we aimed to study the evolution of liver mitochondrial lipidome and oxidative stress in a diet-induced NAFLD mouse model.

2. Materials and Methods

2.1. Animals. The local ethics committee approved the care and use of experimental animals (Pays de la Loire, France, project APAFIS#6697, compliant with directive 2010/63/EU). We studied five-week-old male C57Bl/6J mice fed *ad libitum* with either a control chow diet (A04; Safe Diets, France: 8.4% of energy from fat, no cholesterol) or a western diet (WD) for 8, 16, or 25 weeks. The WD associated a high-fat diet (U8958v250, Safe Diets, France: 45% of energy from fat and 2% cholesterol) with 42 g/L fructose (61252 from Safe Diets) in drinking water. Mice were housed five per cage under 12 h : 12 h light : dark conditions. Mice were euthanized by exsanguination under isoflurane anesthesia.

2.2. Liver Steatosis and Fibrosis Quantification. A slice of the liver was fixed in 4% paraformaldehyde for 24 h before paraffin embedding. Then, 5-micron thick sections were stained with hematoxylin-eosin-saffron (HES) or 0.1% picrosirius red (area of steatosis and fibrosis) solution. The entire stained specimen was analyzed by an automatic thresholding technique using an algorithm developed in HIFIH laboratory (EA 3859, Angers, France) as previously described [20].

2.3. Isolation of Liver Mitochondria. For mitochondria isolation, the differential centrifugation method was used, as described previously [21], with minor modifications. All steps were on ice or at 4°C. Caudate liver lobes (≈100 mg) were rinsed, chopped with scissors, and homogenized with a Dounce tissue grinder in 1.5 mL mitochondria isolation buffer (70 mM sucrose, 210 mM mannitol, 5 mM HEPES, 1 mM EGTA, and 0.2% fatty acid BSA, pH 7.2). The homogenate was spun 8 min at 800 g. The filtered supernatants (70 μM cell strainer) were spun 8 min at 8.000 g. The resulting pellet was rinsed and spun 5 min at 8000 g. The final pellet represented the mitochondria-enriched fraction. The first pellet was pooled with the supernatants of the last two centrifugations to make the "nonmitochondrial fraction."

2.4. Lipidome Analysis

2.4.1. Preparation of Samples. The nonmitochondrial fraction was evaporated to dryness under a nitrogen stream. The mitochondrial-enriched and nonmitochondrial pellets were resuspended in PBS. The samples were diluted at 10 mg protein/mL.

2.4.2. Nontargeted Lipidomic Analysis by Mass Spectrometry. The lipids were extracted with a methanol/chloroform method [18] and MTBE [22] method. For the methanol/-chloroform method, 30 μL of "extracted solution" was mixed consecutively with 200 μL of methanol, 400 μL of dichloromethane, and 120 μL of water. After 10 minutes of incubation at room temperature (RT), the mix was spun 10 min at 8000 g at 10°C, and 370 μL of the lower phase was sampled. For MTBE, 50 μL of "extracted solution" was successively mixed with 450 μL of ice-cold methyl-*tert*-butyl-ether (MTBE, Biosolve, Netherlands), 1500 μL of ice-cold methanol (Biosolve, Netherlands), and 375 μL of water. The mixes were centrifuged 10 min at 10,000 g at 4°C, and 800 μL of the supernatant was sampled. For the two methods, the samples were dried under a nitrogen stream. Samples were finally resuspended in 150 μL acetonitrile/isopropanol/water (65/30/5, *v*/*v*/*v*) for liquid chromatography–high-resolution mass spectrometry (LC-HRMS). A quality control (QC) was prepared by pooling 20 μL of each. Samples and QC were loaded in the analytical system consisting of a SYNAPT G2 HRMS Q-TOF mass spectrometer, equipped with an electrospray ionization (ESI) interface operating in positive and negative mode, and a AQUITY UPLC H-Class System (Waters Corporation, Milford, MA, USA). Five microliters of each sample was randomly injected onto a reverse-phase CSH C18 (2.1 × 100 mm; 1.7 μM) column (Waters Corporation) as described previously [23]. The data was acquired and

normalized using MassLynx and MarkerLynx software, respectively (version 4.1, Waters Corporation).

2.4.3. Apolipoprotein E (ApoE) Measurements. ApoE was measured by liquid chromatography–tandem mass spectrometry (LC–MS/MS) as described previously [24].

2.4.4. Targeted Lipidomic Analysis. Data points with zero values or with a coefficient of variation for QC ≥ 30% were excluded from the analysis. Lipid markers were extracted from variables using both LipidMaps (http://www.lipidmaps.org) and an in-house database containing reference lipid standards. All lipid markers were checked for their exact mass-to-charge ratio (m/z), their elemental compositions with a mass error of ±5 ppm, their retention time (±30 s), and their fragmentation patterns obtained by tandem mass spectrometry (Supplementary Table S1).

2.5. Total RNA Extraction and RT-qPCR. Pieces of the liver (≈50 mg) were homogenized in 750 μL of NucleoZOL (Macherey-Nagel, Germany) and spun 5 min at 12,000 g. The supernatant was mixed with 300 μL of RNase-free H_2O, incubated 15 min, and spun 15 min at 12,000 g. For phase separation, 3.75 μL of 4-bromoanisole was added to 800 μL of the supernatant and incubated 5 min. After spinning 10 min at 12,000 g, the supernatant was mixed with isopropanol (1 : 1, v/v), incubated 10 min, and spun 10 min at 12,000 g. The final pellet was washed twice with 750 μL of 75% ethanol and spun 3 min at 10,000 g. The RNA pellet was dried and resuspended in water.

Following reverse transcription (High-Capacity cDNA Reverse Transcription Kit, Applied Biosystems, CA, USA), we performed real-time quantitative PCR (qPCR) with PowerUp SYBR Green Master Mix (Applied Biosystems, CA, USA) on a 7900 HT Fast Real-Time PCR system (Applied Biosystems, CA, USA). The primer sequences are listed in Supplementary Table S2. The mRNA expression levels are presented as the ratio of the gene of interest and a housekeeping gene (glyceraldehyde-3-phosphate dehydrogenase (GAPDH)).

2.6. Electron Paramagnetic Resonance (EPR). Pieces of the same liver lobe were used for Cu^{2+}, $O_2^{\cdot-}$, and semiquinone radical detection on a MiniScope MS 5000 spectrometer (Freiberg Instruments, Germany).

For Cu^{2+} measurements, a pale yellow-brown opalescent colloid Fe-$(DETC)_2$ was obtained by separately dissolving 15 mM of Na-DETC (Sigma-Aldrich) and 8 mM of $FeSO_4$-$7H_20$ (Sigma-Aldrich) in ice-cold Krebs-HEPES buffer under nitrogen gas bubbling and mixing the two solutions immediately. The tissue was incubated for 45 min at 37°C in colloid Fe-$(DETC)_2$ solution as a spin trap. Then, the samples were frozen in liquid nitrogen before spectrometry (microwave power: 10 mW, amplitude modulation: 1 mT, modulation frequency: 100 kHz, sweep time: 150 s, 3 scans). The spectra were used to detect the peak corresponding to the oxidized Copper (Cu^{2+}) linked to DETC [25].

We measured $O_2^{\cdot-}$ levels in tissues as described previously [26]. The tissue was incubated for 45 min at 37°C in a Krebs-HEPES solution containing 1-hydroxy-3-methoxycarbonyl-2,2,5,5-tetramethylpyrrolidine (CMH, 500 mM, Noxygen; Denzlingen, Germany) as spin probe, deferoxamine (25 mM, Sigma-Aldrich), and diethyldithiocarbamate (DETC, 5 mM, Sigma-Aldrich). The sample was analyzed in liquid nitrogen (microwave power: 10 mW, amplitude modulation: 0.4 mT, modulation frequency: 100 kHz, sweep time: 60 s, 3 scans).

For semiquinone radical detection, the tissue was frozen and analyzed in liquid nitrogen (microwave power: 10 mW, amplitude modulation: 0.7 mT, modulation frequency: 100 kHz, sweep time: 180 s, 3 scans) [27].

Signals were quantified from the amplitude peaks of the spectra after baseline correction (ESR Studio software, Freiberg Instruments, Germany). All values were expressed in arbitrary units (a.u.)/CL (a.u.).

2.7. Statistical Analysis. First, the unsupervised analyses, principal component analysis (PCA), were performed to assess the separation of the experiment. Then, the supervised partial least square regression analyses (PLS-DA) were performed to maximize the discrimination of the groups.

All multivariate analyses were computed under R version 3.6.0 (R Development Core Team, R Foundation for Statistical Computing, Vienna, Austria; http://www.R-project.org), with Factominer and pls packages for multivariate analysis.

For quantitative data depending on diet group and duration of diet, we used a two-way analysis of variance (ANOVA) test with a subsequent Bonferroni post hoc test, and when the equal variance test failed, a two-way ANOVA on rank test with the subsequent Tukey post hoc test was used. All statistical analyses were realized with GraphPad Prism 6 and SigmaStat 4.0 software. N represents the number of mice used for each time point and condition; $^*p < 0.05$ was considered statistically significant.

3. Results

3.1. Metabolic Phenotyping of Mice on the Western Diet. Mice with WD developed obesity, increased liver weight normalized to body weight, hepatic steatosis, ASAT, ALAT, and liver fibrosis. Notably, fibrosis was delayed, appearing at week 25 only as opposed to steatosis that was present from week 8 (Figures 1(a)–1(f)). mRNA expression of the key transcription factor for lipid synthesis, Sterol Regulatory Element-Binding Transcription Factor 1 (*Srebf1*), was increased, while that of the nuclear receptor peroxisome proliferator-activated receptor α (*Ppar*α) was decreased. There was also an increase of mRNA levels of inflammatory pathway genes toll-like receptor 9 (*Tlr9*) and tumor necrosis factor (*Tnf-*α) with steatosis (Figure 1(g)).

CL 72 : 8 and 70 : 7, used as references for the CL family, were more extracted using MTBE method than the methanol/chloroform method (Supplementary Figure 1a). Thus, we used the MTBE method. We verified that the diet type or duration did not affect the isolation process. Based on CL retrieval, the mitochondrial fraction contained over 70% of the total mitochondria. Based on ApoE content, cytosolic contamination was below 5% (Supplementary Figure 1b).

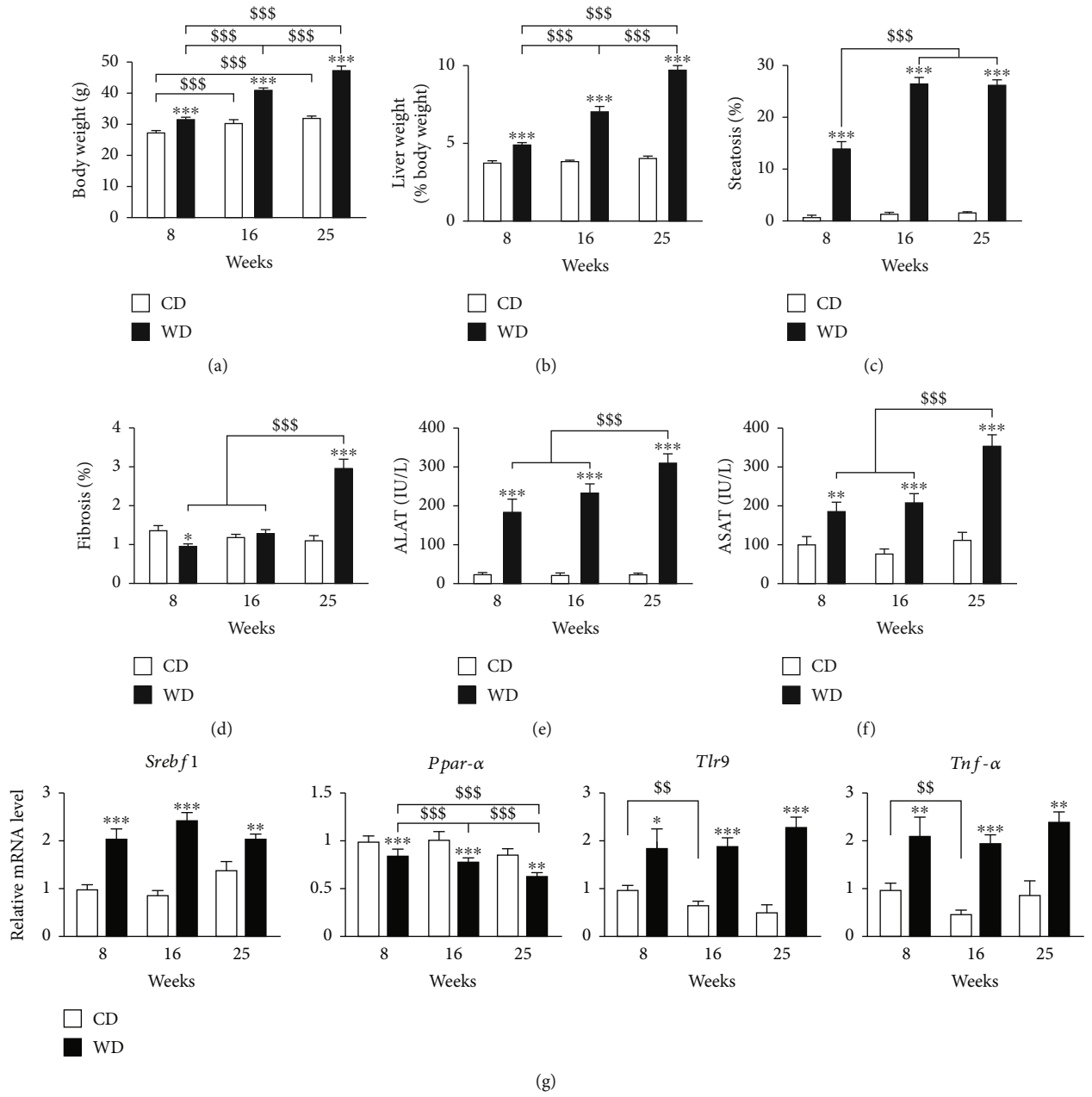

Figure 1: Course of metabolic phenotype under the western diet regimen. CD: control diet; WD: western diet. (a) Body weight. (b) Liver weight. (c) Hepatic steatosis. (d) Hepatic fibrosis. (e) ALAT. (f) ASAT. (g) mRNA expression of genes involved in lipid metabolism (*Srebf1*, *Pparα*) and inflammation (*Tlr9*, *Tnf-α*), from left to right. Data are expressed as mean + / − SEM; 2-way ANOVA with a subsequent Bonferroni post hoc test or 2-way ANOVA with rank with Tukey post hoc test; $^{*}p < 0.05$, $^{**}p < 0.01$, and $^{***}p < 0.001$ versus control diet; $^{\$\$\$}p < 0.001$ versus weeks of diet. $n = 9 - 10$ mice per time point and condition.

3.2. NAFLD Alters the Hepatic Mitochondrial Lipidome. The complete raw MS results and the corresponding identified lipid species are presented in Supplementary Table 1. We identified 719 lipids from 16 different lipid families in the liver samples (Figure 2(a)). Five families (phosphatidic acid (PA), phosphatidylcholine (PC), phosphatidylethanolamine (PE), diacylglycerol (DAG), and triacylglycerol (TAG)) represented over 80% of the number of detected lipid species. For all fractions, over 90% of the lipid species were detected in the positive mode.

The PCA discriminated the CD and WD groups and showed an evolution over time for the mitochondria-enriched fractions in the WD condition (Supplementary Figure 2). The PLS-DA (a supervised method, contrary to the PCA) discriminated the CD and WD groups both for the mitochondrial and nonmitochondrial fractions (Figure 2(b)). Notably, for the mitochondrial fraction, PLS-DA showed an evolution over time only for the WD condition (Figure 2(b)), in the positive mode. This pattern was not seen in the nonmitochondrial fraction

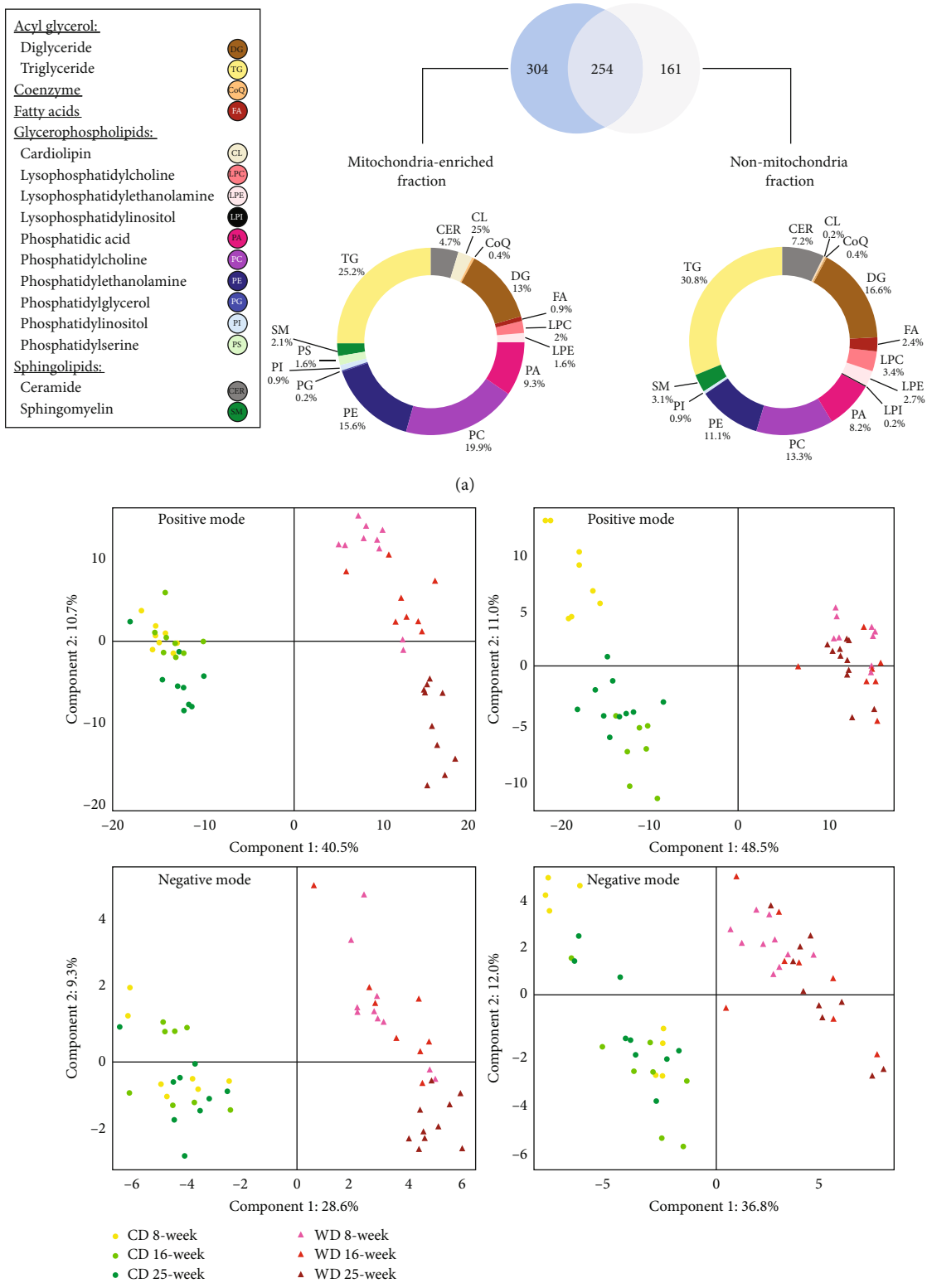

Figure 2: The western diet triggers time-dependent changes in the hepatic mitochondrial lipidome. (a) Venn diagram of the 719 lipid species detected in the mitochondria-enriched fraction and the nonmitochondrial fraction. The analyses were pooled for all animals included in the study. The individual species are grouped within 16 lipid families. (b) Partial least square regression analysis of lipids in the liver. Left panels: from the mitochondria-enriched fractions in positive mode (505 lipid species, top panel) and negative mode (53 lipid species, bottom panel). Right panels: from the non-mitochondria fractions in positive mode (356 lipid species, top panel) and negative mode (59 lipid species, bottom panel).

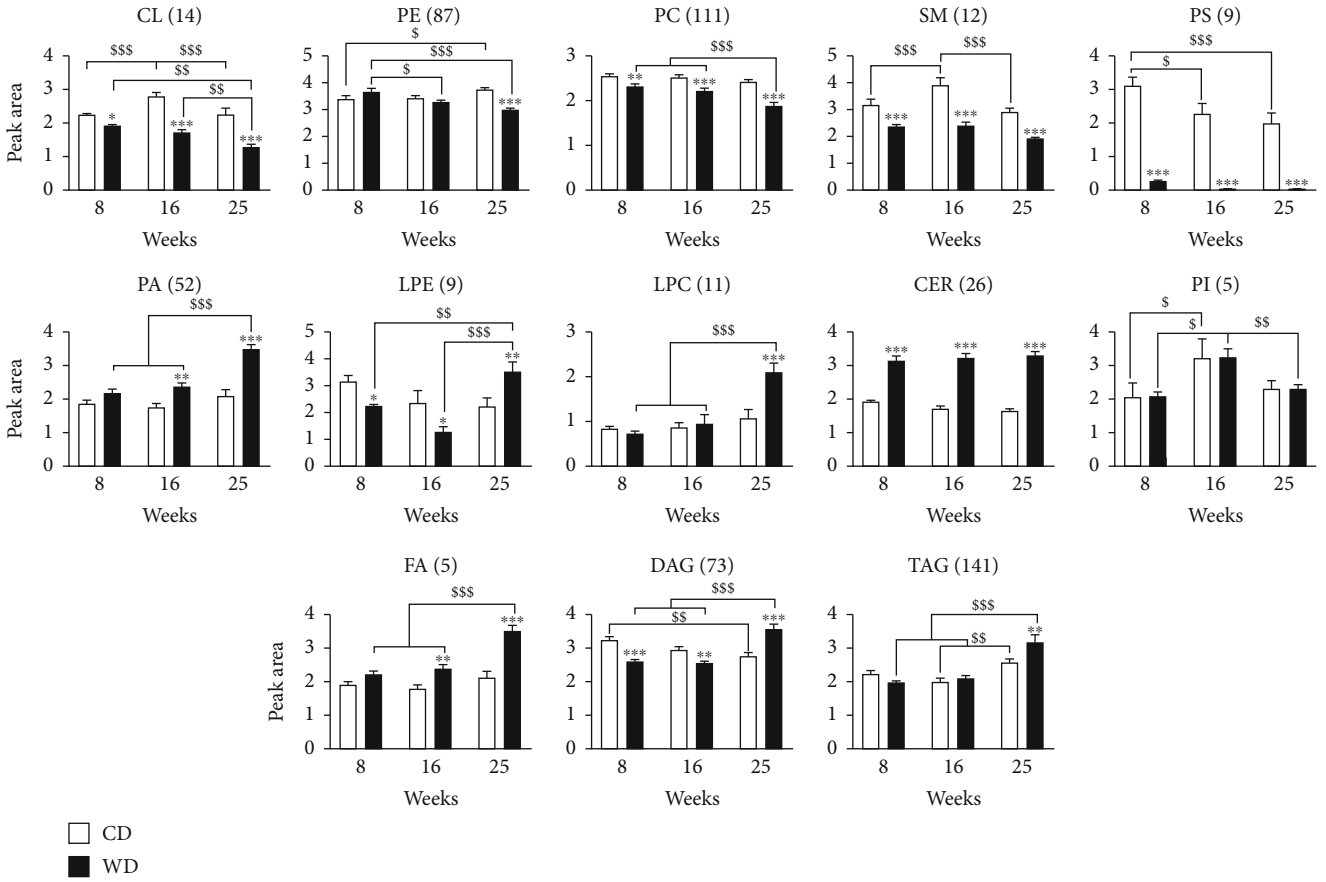

Figure 3: NAFLD alters mitochondrial lipid species. LC-HRMS semiquantification analysis of lipids extracted from the mitochondria-enriched fraction of the liver. After identification of the individual lipid signatures, lipids were grouped in families by adding the individual peak areas. The number of lipid species is indicated between brackets. Peak area values are arbitrary. CL: cardiolipins; PE: phosphatidylethanolamine; PC: phosphatidylcholine; SM: sphingomyelin; PS: phosphatidylserine; PA: phosphatidic acid; LPE: lysophosphoethanolamine; LPC: lysophosphatidylcholine; CER: ceramide; PI: phosphatidylinositol; FA: fatty acids; DAG: diacylglycerol; TAG: triacylglycerol. (a, b) Data are expressed as mean + / − SEM; 2-way ANOVA with subsequent Bonferroni or 2-way ANOVA with rank with Tukey *post hoc* test; $^{*}p < 0.05$, $^{**}p < 0.01$, and $^{***}p < 0.001$ versus control diet; $^{\$}p < 0.05$, $^{\$\$}p < 0.01$, and $^{\$\$\$}p < 0.001$ versus weeks of diet. $n = 7 - 10$ mice per time point and condition.

(Figure 2(b)), indicating that WD specifically affected the mitochondrial lipidome over time.

3.3. NAFLD Specifically Decreases Mitochondrial Cardiolipin. We performed a semiquantification of the lipid families to determine the evolution of mitochondrial lipids under WD (Figure 3). CLs, PEs, and PCs significantly decreased over time, while PAs, lysophosphatidylcholines (LPC), fatty acids (FA), DAGs, and TAGs increased. SM and PS were decreased at all time points while ceramides (CER) were increased at all time points. In contrast, phosphatidylinositol (PI) was unchanged by WD over time.

3.4. Liver Steatosis Increases Hepatic Oxidative Stress. To investigate whether the alteration of mitochondrial lipids was associated with oxidative stress, we analyzed ROS levels by EPR in the whole liver. Free Cu^{2+} and O_2^- levels were similar at week 8 between groups. Cu^{2+} (Figure 4(a)) and O_2^- (Figure 4(b)) increased in the WD group at weeks 16 and 25 compared to the controls. For O_2^-, there was an increase

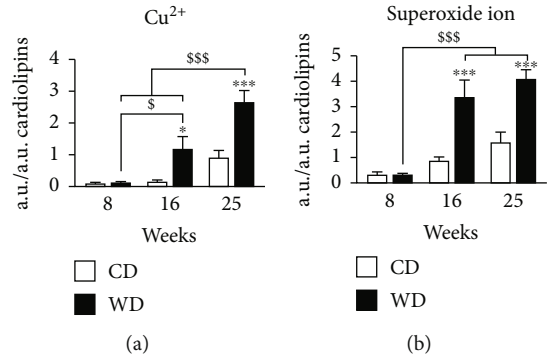

Figure 4: Western diet progressively increases oxidative stress in the liver. EPR was applied to a piece of the liver for the detection of (a) oxidized state of copper (Cu^{2+}) and (b) superoxide ion. All values were expressed in arbitrary units (a.u.)/a.u. of cardiolipin. Data are expressed as mean + / − SEM; 2-way ANOVA with (b) subsequent Bonferroni or 2-way ANOVA on rank with (a) Tukey post hoc test; $^{*}p < 0.05$ and $^{***}p < 0.001$ versus control diet; $^{\$}p < 0.05$ and $^{\$\$\$}p < 0.001$ versus weeks of diet. $n = 4 - 5$ mice per time point and condition.

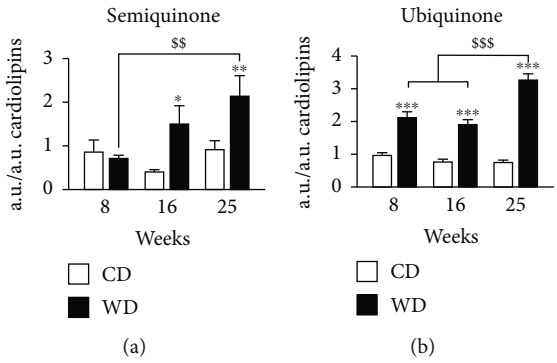

FIGURE 5: Western diet increases semiquinone and ubiquinone levels in mitochondria. (a) Semiquinone from EPR spectrometry applied to a piece of the liver. (b) LC-MS ubiquinone semiquantification analysis was performed on the lipids extracted from the mitochondria-enriched fraction of the liver. Peak area values are arbitrary. (a, b) Data are expressed as mean + / − SEM; 2-way ANOVA on rank with Tukey post hoc test; $^{*}p < 0.05$, $^{**}p < 0.01$, and $^{***}p < 0.001$ versus control diet; $^{\$\$}p < 0.01$ and $^{\$\$\$}p < 0.001$ versus weeks of diet. $n = 7 - 10$ mice per time point per condition.

over time in mice under CD that quadrupled between week 8 and week 25. The increase in $O_2^{\cdot-}$ was significantly higher in mice with WD.

3.5. Liver Steatosis Increases Semiquinone and Ubiquinone Levels in Mitochondria. To determine the consequences of steatosis on mitochondrial function, we performed a semiquantification of semiquinone by EPR and ubiquinone by LC-HRMS (Figure 5). Semiquinone is the intermediate molecule between the fully oxidized (ubiquinone) and the fully reduced states (ubiquinol) of coenzyme Q and participates to modulate ROS production during the electron traffic from complexes I and II to complex III of the ETC [28]. EPR analysis showed a significant increase after 25 weeks of WD for semiquinone (Figure 5(a)). In contrast to its intermediate form, ubiquinone sharply increased already from week 8 of WD (Figure 5(b)).

4. Discussion

We used a murine dietary model of NAFLD to demonstrate for the first time the presence of a specific evolution of the hepatic mitochondrial lipidome during NAFLD progression. The most notable modifications are a progressive decrease in CL, PE, and PC and a progressive increase in PA and CoQ (ubiquinone and semiquinone). These alterations accompany steatosis and oxidative stress but precede hepatic fibrosis.

WD induces steatosis in the short time of eight weeks [29]. The C57BL/6 mouse strain is prompt to develop hepatic steatosis [30]. However, further stages of NAFLD are not triggered with a high-fat diet (HFD) and fructose supplementation in drinking water is necessary [31]. Our nontargeted LC-HRMS profiling method with the Q-TOF mass spectrometer identified 719 species from 16 different lipid families. Previous lipidomic studies using LTQ-Orbitrap for mass spectrometry in liver mitochondria identified 217 species in mice fed 2 weeks [19] and 381 species in rats fed 8 weeks [18].

Mitochondrial membranes are composed of 80% of PE and PC, as well as 10-15% of CL, a component exclusive to mitochondria. Mice fed a WD for 6 to 24 weeks (45% fat and fructose in drinking water) showed an alteration of the mitochondrial lipidome with monounsaturated fatty acids [32].

Dietary-induced obesity studies in mice show changes in hepatic lipid composition, with an increase of TAG, FA, and LPC and a decrease in PE [33]. CER are typically increased and have been linked to the pathogenicity of NAFLD in association with inflammation [34]. DAG [35], CER [36, 37], and LPC [38, 39] are candidate lipotoxic species in NAFLD.

We showed that the increase of ROS was associated with lipidome alteration. The increase of ROS in NAFLD is involved in fibrosis development [15]. Interestingly, free copper was increased as well. Copper in the oxidized (Cu^{2+}) state assists oxidative tissue injury through a free radical-mediated pathway [40]. In this context, Cu^{2+} may also participate in CL decrease by catalyzing its fragmentation as was demonstrated in the *Atp7b*$^{-/-}$ mouse model of Wilson's disease [41]. ROS would be aggravating the mitochondrial dysfunction itself by damaging lipids and complexes of the respiratory chain [42]. Here, a vicious circle developing between the ROS and mitochondrial lipidome changes is possible. Alteration of the oxidative phosphorylation process is a key factor in pathological ROS production [28]. The modification of mitochondrial lipidome, furthermore, among several factors involved in increasing steatosis, was highlighted as a factor for the alteration of mitochondrial structure and complex I of the respiratory chain [32].

Phospholipids such as PE and CL have a specific role in the assembly and activity of respiratory chain complexes, especially complexes III and IV, and supercomplex formation [43]. The modification of membrane lipids leads to a deficiency of respiratory complex proteins causing oxidative stress, mitochondrial damage, and insulin resistance [44]. In the context of steatosis progression, we found a significant increase in oxidative stress, associated with a decrease of CL and PE. A possibility is that the alteration of phospholipid nature, in particular CL, could be due to an overproduction of ROS. This is suggested by studies on mitochondrial dysfunction in NAFLD that showed complex I and III alterations [45] and fat accumulation [46]. We also observed that the decrease of CL is associated with an increase in ubiquinone, which could reflect an alteration of the respiratory chain. The close association between CL and ubiquinone has been previously shown to facilitate the efficiency of the electron transporter chain [13]. In a study on NAFLD in humans, an increase of CL and ubiquinone was interpreted as a compensatory mechanism [17], and our results suggest that the relationship may be more complex, depending on the stage of disease.

5. Conclusions

Our results show that a specific evolution of the hepatic mitochondrial lipidome typifies NAFLD natural history. Changes

such as cardiolipin and CoQ antioxidant function impairment precede fibrosis, raising the possibility of a causal relationship with NAFLD progression. This specific lipid signature allows the identification of new lipid candidates in the genesis of NAFLD mitochondrial dysfunction. It could pave the way for association studies with oxidative stress or even therapeutic interventions to delay mitochondrial dysfunction. Exploration of specific mitochondrial composition alterations may offer new intervention points to treat NAFLD.

Data Availability

The lipidomic data used to support the findings of this study are included within the supplementary information files.

Conflicts of Interest

The authors declare that there is no conflict of interest regarding the publication of this paper.

Authors' Contributions

Manon Durand and Marine Coué contributed equally to this work.

Acknowledgments

Manon Durand is supported by a scholarship from INSERM and the French Regional Council of Pays de la Loire (2017-08542). Florian Atger is supported by a scholarship "*Allocation de Recherche SFD jeune chercheur Francophone 2018*" from the *Société Francophone du Diabète*. This work was funded by grants from INSERM ATIP-Avenir (R16067NS-RSE17002NSA) (David Jacobi) and the French Regional Council of Pays de la Loire (2017-02946/02947) (David Jacobi) and the Fondation Genavie (David Jacobi). Additional financial support was provided by the Biogenouest Corsaire core facility. We thank Lionel Fizanne, Julien Chaigneau, and Jérôme Boursier (EA 3859, hémodynamique, interaction, fibrose, l'invasivité tumorale hépatique et digestive, Angers, France) for help with the histological studies.

Supplementary Materials

Supplementary Table 1: details of the in-house database for lipid identification in positive and negative mode. Supplementary Table 2: list of primers for RT-qPCR. Supplementary Table 3: raw mass spectrometry data. Theoretical *m*/*z*, experimental *m*/*z*, retention time, raw lipid formula, and lipid species name. Supplementary Figure 1: quality control of mitochondria enrichment. Supplementary Figure 2: principal component analysis (PCA) of lipids in the liver. *(Supplementary Materials)*

References

[1] Z. M. Younossi, A. B. Koenig, D. Abdelatif, Y. Fazel, L. Henry, and M. Wymer, "Global epidemiology of nonalcoholic fatty liver disease-Meta-analytic assessment of prevalence, incidence, and outcomes," *Hepatology*, vol. 64, no. 1, pp. 73–84, 2016.

[2] S. L. Friedman, B. A. Neuschwander-Tetri, M. Rinella, and A. J. Sanyal, "Mechanisms of NAFLD development and therapeutic strategies," *Nature Medicine*, vol. 24, no. 7, pp. 908–922, 2018.

[3] C. Peng, A. G. Stewart, O. L. Woodman, R. H. Ritchie, and C. X. Qin, "Non-alcoholic steatohepatitis: a review of its mechanism, models and medical treatments," *Frontiers in Pharmacology*, vol. 11, article 603926, 2020.

[4] J. C. Bournat and C. W. Brown, *Mitochondrial dysfunction in obesity*, vol. 14, Frontiers Media, Lausanne, 2016.

[5] J. Tumova, M. Andel, and J. Trnka, "Excess of free fatty acids as a cause of metabolic dysfunction in skeletal muscle," *Physiological Research*, vol. 65, no. 2, pp. 193–207, 2016.

[6] L. J. Brady, P. S. Brady, D. R. Romsos, and C. L. Hoppel, "Elevated hepatic mitochondrial and peroxisomal oxidative capacities in fed and starved adult obese (ob/ob) mice," *The Biochemical Journal*, vol. 231, no. 2, pp. 439–444, 1985.

[7] C. Koliaki, J. Szendroedi, K. Kaul et al., "Adaptation of hepatic mitochondrial function in humans with non-alcoholic fatty liver is lost in steatohepatitis," *Cell Metabolism*, vol. 21, no. 5, pp. 739–746, 2015.

[8] N. E. Sunny, E. J. Parks, J. D. Browning, and S. C. Burgess, "Excessive hepatic mitochondrial TCA cycle and gluconeogenesis in humans with nonalcoholic fatty liver disease," *Cell Metabolism*, vol. 14, no. 6, pp. 804–810, 2011.

[9] P. Iozzo, M. Bucci, A. Roivainen et al., "Fatty acid metabolism in the liver, measured by positron emission tomography, is increased in obese individuals," *Gastroenterology*, vol. 139, no. 3, pp. 846–856.e6, 2010.

[10] C. U. Mårtensson, K. N. Doan, and T. Becker, "Effects of lipids on mitochondrial functions," *Biochim Biophys Acta BBA - Mol Cell Biol Lipids*, vol. 1862, no. 1, pp. 102–113, 2017.

[11] J. Dudek, "Role of cardiolipin in mitochondrial signaling pathways," *Frontiers in Cell and Development Biology*, vol. 5, p. 90, 2017.

[12] J. A. Enriquez and G. Lenaz, "Coenzyme Q and the respiratory chain: coenzyme Q pool and mitochondrial supercomplexes," *Mol Syndromol*, vol. 5, no. 3-4, pp. 119–140, 2014.

[13] M. Vos, A. Geens, C. Böhm et al., "Cardiolipin promotes electron transport between ubiquinone and complex I to rescue *PINK1* deficiency," *The Journal of Cell Biology*, vol. 216, no. 3, pp. 695–708, 2017.

[14] G. Paradies, V. Paradies, F. M. Ruggiero, and G. Petrosillo, "Oxidative stress, cardiolipin and mitochondrial dysfunction in nonalcoholic fatty liver disease," *World journal of gastroenterology: WJG*, vol. 20, no. 39, pp. 14205–14218, 2014.

[15] K. M. Botham, M. Napolitano, and E. Bravo, "The emerging role of disturbed CoQ metabolism in nonalcoholic fatty liver disease development and progression," *Nutrients*, vol. 7, no. 12, pp. 9834–9846, 2015.

[16] Z. Yesilova, H. Yaman, C. Oktenli et al., "Systemic markers of lipid peroxidation and antioxidants in patients with nonalcoholic fatty liver disease," *The American Journal of Gastroenterology*, vol. 100, no. 4, pp. 850–855, 2005.

[17] K.-Y. Peng, M. J. Watt, S. Rensen et al., "Mitochondrial dysfunction-related lipid changes occur in nonalcoholic fatty liver disease progression," *Journal of Lipid Research*, vol. 59, no. 10, pp. 1977–1986, 2018.

[18] S. S. Bird, V. R. Marur, I. G. Stavrovskaya, and B. S. Kristal, "Qualitative characterization of the rat liver mitochondrial lipidome using LC–MS profiling and high energy collisional dissociation (HCD) all ion fragmentation," *Metabolomics*, vol. 9, no. S1, pp. 67–83, 2013.

[19] R. Aviram, G. Manella, N. Kopelman et al., "Lipidomics analyses reveal temporal and spatial lipid organization and uncover daily oscillations in intracellular organelles," *Molecular Cell*, vol. 62, no. 4, pp. 636–648, 2016.

[20] Multicentre group ANRS HC EP23 FIBROSTAR, J. Boursier, V. de Ledinghen et al., "Precise evaluation of liver histology by computerized morphometry shows that steatosis influences liver stiffness measured by transient elastography in chronic hepatitis C," *Gastroenterologia Japonica Supplement*, vol. 49, no. 3, pp. 527–537, 2014.

[21] D. Jacobi, S. Liu, K. Burkewitz et al., "Hepatic Bmal1 regulates rhythmic mitochondrial dynamics and promotes metabolic fitness," *Cell Metabolism*, vol. 22, no. 4, pp. 709–720, 2015.

[22] Z. Kaabia, J. Poirier, M. Moughaizel et al., "Plasma lipidomic analysis reveals strong similarities between lipid fingerprints in human, hamster and mouse compared to other animal species," *Scientific Reports*, vol. 8, no. 1, pp. 15893–15899, 2018.

[23] M. Croyal, Z. Kaabia, L. León et al., "Fenofibrate decreases plasma ceramide in type 2 diabetes patients: a novel marker of CVD?," *Diabetes & Metabolism*, vol. 44, no. 2, pp. 143–149, 2018.

[24] V. Blanchard, D. Garçon, C. Jaunet et al., "A high-throughput mass spectrometry-based assay for large-scale profiling of circulating human apolipoproteins[S]," *Journal of Lipid Research*, vol. 61, no. 7, pp. 1128–1139, 2020.

[25] M. P. Koeners, E. E. van Faassen, S. Wesseling et al., "Maternal supplementation with citrulline increases renal nitric oxide in young spontaneously hypertensive rats and has long-term antihypertensive effects," *Hypertension*, vol. 50, no. 6, pp. 1077–1084, 2007.

[26] M. Coué, A. Tesse, J. Falewée et al., "Spirulina liquid extract protects against fibrosis related to non-alcoholic steatohepatitis and increases ursodeoxycholic acid," *Nutrients*, vol. 11, no. 1, p. 194, 2019.

[27] A. Kozlov, "Intracellular free iron in liver tissue and liver homogenate: studies with electron paramagnetic resonance on the formation of paramagnetic complexes with desferal and nitric oxide," *Free Radical Biology & Medicine*, vol. 13, no. 1, pp. 9–16, 1992.

[28] V. Larosa and C. Remacle, "Insights into the respiratory chain and oxidative stress," *Bioscience Reports*, vol. 38, no. 5, 2018.

[29] A. Asgharpour, S. C. Cazanave, T. Pacana et al., "A diet-induced animal model of non-alcoholic fatty liver disease and hepatocellular cancer," *Journal of Hepatology*, vol. 65, no. 3, pp. 579–588, 2016.

[30] V. H. I. Fengler, T. Macheiner, S. M. Kessler et al., "Susceptibility of different mouse wild type strains to develop diet-induced NAFLD/AFLD-associated liver disease," *PLoS One*, vol. 11, no. 5, article e0155163, 2016.

[31] M. Van Herck, L. Vonghia, and S. Francque, "Animal models of nonalcoholic fatty liver disease—a starter's guide," *Nutrients*, vol. 9, no. 10, p. 1072, 2017.

[32] C. Einer, S. Hohenester, R. Wimmer et al., "Mitochondrial adaptation in steatotic mice," *Mitochondrion*, vol. 40, pp. 1–12, 2018.

[33] K. Eisinger, S. Krautbauer, T. Hebel et al., "Lipidomic analysis of the liver from high-fat diet induced obese mice identifies changes in multiple lipid classes," *Experimental and Molecular Pathology*, vol. 97, no. 1, pp. 37–43, 2014.

[34] M. Pagadala, T. Kasumov, A. J. McCullough, N. N. Zein, and J. P. Kirwan, "Role of ceramides in nonalcoholic fatty liver disease," *Trends in Endocrinology and Metabolism: TEM*, vol. 23, no. 8, pp. 365–371, 2012.

[35] R. J. Perry, V. T. Samuel, K. F. Petersen, and G. I. Shulman, "The role of hepatic lipids in hepatic insulin resistance and type 2 diabetes," *Nature*, vol. 510, no. 7503, pp. 84–91, 2014.

[36] P. K. Luukkonen, Y. Zhou, S. Sädevirta et al., "Hepatic ceramides dissociate steatosis and insulin resistance in patients with non-alcoholic fatty liver disease," *Journal of Hepatology*, vol. 64, no. 5, pp. 1167–1175, 2016.

[37] A. S. Mauer, P. Hirsova, J. L. Maiers, V. H. Shah, and H. Malhi, "Inhibition of sphingosine 1-phosphate signaling ameliorates murine nonalcoholic steatohepatitis," *American Journal of Physiology. Gastrointestinal and Liver Physiology*, vol. 312, no. 3, pp. G300–G313, 2017.

[38] P. Hirsova, S. H. Ibrahim, G. J. Gores, and H. Malhi, "Lipotoxic lethal and sublethal stress signaling in hepatocytes: relevance to NASH pathogenesis[S]," *Journal of Lipid Research*, vol. 57, no. 10, pp. 1758–1770, 2016.

[39] M. S. Han, S. Y. Park, K. Shinzawa et al., "Lysophosphatidylcholine as a death effector in the lipoapoptosis of hepatocytes[S]," *Journal of Lipid Research*, vol. 49, no. 1, pp. 84–97, 2008.

[40] L. Antonucci, C. Porcu, G. Iannucci, C. Balsano, and B. Barbaro, "Non-alcoholic fatty liver disease and nutritional implications: special focus on copper," *Nutrients*, vol. 9, no. 10, p. 1137, 2017.

[41] I. L. Yurkova, J. Arnhold, G. Fitzl, and D. Huster, "Fragmentation of mitochondrial cardiolipin by copper ions in the Atp7b$^{-/-}$ mouse model of Wilson's disease," *Chemistry and Physics of Lipids*, vol. 164, no. 5, pp. 393–400, 2011.

[42] O. S. Ademowo, H. K. I. Dias, D. G. A. Burton, and H. R. Griffiths, "Lipid (per) oxidation in mitochondria: an emerging target in the ageing process?," *Biogerontology*, vol. 18, no. 6, pp. 859–879, 2017.

[43] W. Basu Ball, J. K. Neff, and V. M. Gohil, "The role of nonbilayer phospholipids in mitochondrial structure and function," *FEBS Letters*, vol. 592, no. 8, pp. 1273–1290, 2018.

[44] M. Kahle, A. Schäfer, A. Seelig et al., "High fat diet-induced modifications in membrane lipid and mitochondrial- membrane protein signatures precede the development of hepatic insulin resistance in mice," *Mol Metab*, vol. 4, no. 1, pp. 39–50, 2015.

[45] G. Petrosillo, P. Portincasa, I. Grattagliano et al., "Mitochondrial dysfunction in rat with nonalcoholic fatty liver: Involvement of complex I, reactive oxygen species and cardiolipin," *Biochim Biophys Acta BBA - Bioenerg*, vol. 1767, no. 10, pp. 1260–1267, 2007.

[46] K. Begriche, A. Igoudjil, D. Pessayre, and B. Fromenty, "Mitochondrial dysfunction in NASH: causes, consequences and possible means to prevent it," *Mitochondrion*, vol. 6, no. 1, pp. 1–28, 2006.

Hindawi
Oxidative Medicine and Cellular Longevity
Volume 2021, Article ID 6648199, 9 pages
https://doi.org/10.1155/2021/6648199

Research Article

Predictors of Mortality in Critically Ill COVID-19 Patients Demanding High Oxygen Flow: A Thin Line between Inflammation, Cytokine Storm, and Coagulopathy

Viseslav Popadic,[1] **Slobodan Klasnja**,[1] **Natasa Milic**,[2,3] **Nina Rajovic**,[2] **Aleksandra Aleksic**,[1] **Marija Milenkovic**,[4,5] **Bogdan Crnokrak**,[1] **Bela Balint**,[6,7] **Milena Todorovic-Balint**,[5,8] **Davor Mrda**,[1] **Darko Zdravkovic**,[1,5] **Borislav Toskovic**,[1,5] **Marija Brankovic**,[1,5] **Olivera Markovic**,[1,5] **Jelica Bjekic-Macut**,[1,5] **Predrag Djuran**,[1] **Lidija Memon**,[1] **Milica Brajkovic**,[1] **Zoran Todorovic**,[1,5] **Jovan Hadzi-Djokic**,[5,7] **Igor Jovanovic**,[1] **Dejan Nikolic**,[1,5] **and Marija Zdravkovic**[1,5]

[1]*University Hospital Medical Center, Bezanijska kosa, Belgrade, Serbia*
[2]*Institute for Medical Statistics and Informatics, Faculty of Medicine University of Belgrade, Belgrade, Serbia*
[3]*Department of Internal Medicine, Division of Nephrology and Hypertension, Mayo Clinic, Rochester, USA*
[4]*Clinical Center of Serbia, Belgrade, Serbia*
[5]*Faculty of Medicine, University of Belgrade, Belgrade, Serbia*
[6]*Institute of Cardiovascular Diseases "Dedinje", Belgrade, Serbia*
[7]*Department of Medical Sciences, Serbian Academy of Sciences and Arts, Serbia*
[8]*Clinic for Hematology, Clinical Center of Serbia, Belgrade, Serbia*

Correspondence should be addressed to Marija Zdravkovic; sekcija.kardioloska@gmail.com

Received 2 December 2020; Revised 21 December 2020; Accepted 6 March 2021; Published 21 April 2021

Academic Editor: Daniele Vergara

Copyright © 2021 Viseslav Popadic et al. This is an open access article distributed under the Creative Commons Attribution License, which permits unrestricted use, distribution, and reproduction in any medium, provided the original work is properly cited.

Introduction. Mortality among critically ill COVID-19 patients remains relatively high despite different potential therapeutic modalities being introduced recently. The treatment of critically ill patients is a challenging task, without identified credible predictors of mortality. *Methods*. We performed an analysis of 160 consecutive patients with confirmed COVID-19 infection admitted to the Respiratory Intensive Care Unit between June 23, 2020, and October 2, 2020, in University Hospital Center Bezanijska kosa, Belgrade, Serbia. Patients on invasive, noninvasive ventilation and high flow oxygen therapy with moderate to severe ARDS, according to the Berlin definition of ARDS, were selected for the study. Demographic data, past medical history, laboratory values, and CT severity score were analyzed to identify predictors of mortality. Univariate and multivariate logistic regression models were used to assess potential predictors of mortality in critically ill COVID-19 patients. *Results*. The mean patient age was 65.6 years (range, 29–92 years), predominantly men, 68.8%. 107 (66.9%) patients were on invasive mechanical ventilation, 31 (19.3%) on noninvasive, and 22 (13.8%) on high flow oxygen therapy machine. The median total number of ICU days was 10 (25^{th} to 75^{th} percentile: 6–18), while the median total number of hospital stay was 18 (25^{th} to 75^{th} percentile: 12–28). The mortality rate was 60% (96/160). Univariate logistic regression analysis confirmed the significance of age, CRP, and lymphocytes at admission to hospital, serum albumin, D-dimer, and IL-6 at admission to ICU, and CT score. Serum albumin, D-dimer, and IL-6 at admission to ICU were independently associated with mortality in the final multivariate analysis. *Conclusion*. In the present study of 160 consecutive critically ill COVID-19 patients with moderate to severe ARDS, IL-6, serum albumin, and D-dimer at admission to ICU, accompanied by chest CT severity score, were marked as independent predictors of mortality.

1. Introduction

COVID-19 infection is a pandemic disease that to this date affected more than 70 million people over the world with more than 1.6 million registered death cases [1]. Numerous studies over the last few months have shown a wide specter of clinical presentation of infection with SARS-CoV-2 virus. It is usually presented as bilateral pneumonia, but with multiple extrapulmonary manifestations that can lead to severe complications and death [2–5]. Rapid worsening of clinical status is a result of a combination of severe viral illness, increased demand on the heart, systemic inflammatory response, compounded by low oxygen levels due to pneumonia, and increased propensity for blood clot formation. Supportive oxygenation therapy, as well as mechanical ventilation, is still a key management strategy in treating patients. Although the overall intrahospital mortality is decreasing lately, the mortality rate of patients admitted to the Intensive Care Unit (ICU) remains relatively high [6]. Definitive predictors of poor clinical outcomes are still uncertain, mainly due to the unpredictability of the disease and multiple underlying pathophysiological mechanisms that can affect patient's condition and further prognosis [7–9]. It is shown so far that advanced age, male sex, the presence of comorbidities including hypertension, diabetes mellitus, malignancies, and cardiovascular and cerebrovascular diseases are associated with higher mortality rate [10–12]. Identifying credible predictors of mortality, especially in critically ill patients, is a challenging task considering the variety of different critical conditions, including acute respiratory distress syndrome, secondary infection, shock, acute heart, and kidney injury. Predictors of mortality among laboratory parameters are important as they can reflect possible mechanisms of disease progression and give important information on potentially useful therapeutic modalities [13].

In the present study, we analyzed patients admitted to ICU to evaluate potential independent predictors of mortality in critically ill COVID-19 patients with moderate to severe acute respiratory distress syndrome (ARDS).

2. Methods

In this single-center study, we included 160 consecutive patients with confirmed COVID-19 infection admitted to the Respiratory Intensive Care Unit of University Hospital Center Bezanijska kosa, Belgrade, Serbia, between June 23, 2020, and October 2, 2020. University Hospital Center Bezanijska kosa is a reference COVID-19 high-volume center, treating more than 1000 COVID-19 patients per month overall and more than 100 patients in ICU. Infection with SARS-CoV-2 virus was confirmed by real-time PCR assay from a nasopharyngeal swab sample. Chest X-ray was performed at hospital admission and onwards in terms of control if necessary. Chest CT was obligatory at admission, including the estimation of CT severity score. Typical COVID-19 pneumonia changes were evaluated including bilateral lung involvement with ground-glass opacities, consolidations, interlobular septal thickening, and crazy paving patterns, as well as pleural effusion and lymphadenopathy. According to the severity of the observed changes, every lobe was given 0-5 points (for upper, middle, and lower right lung lobe, and upper and lower left lung lobe, respectively) forming the maximum possible score of 25 points. Except scoring, the disease was classified into 4 stages (early, progressive, peak, and absorption). A follow-up chest CT was indicated in case of clinical deterioration and was usually performed right before or after the admission to ICU. Main clinical criteria for Respiratory Intensive Care Unit admission was radiographic or CT scan severity score progression, peripheral oxygen saturation (Sp02) below 93% despite maximal conventional supportive oxygen therapy (up to 15 L/min through a nasal cannula, conventional oxygen, or nonrebreather mask), laboratory test results, mainly an increase of inflammatory parameters after repeated controls and arterial blood gas test. Critically ill patients on invasive, noninvasive ventilation, and high flow oxygen therapy with moderate and severe ARDS were selected for the study according to the Berlin definition of ARDS [14]. Patients on conventional oxygen therapy being admitted to ICU due to gradual clinical deterioration were not included. During the hospitalization, patients were treated according to the adjusted National Protocol of the Republic of Serbia for the treatment of COVID-19 infection. Antiviral agents (favipiravir, remdesivir) were used in 5-7 days from symptom onset in patients on supportive oxygen therapy and with radiographically verified severe bilateral pneumonia. Favipiravir was administered orally, 3200 mg in two doses the first day, and 600 mg in two doses for the next 4 days. Remdesivir was administered intravenously, 200 mg the first day, and 100 mg for the next 4-9 days in consultation with an infectologist. Corticosteroids (prednisone 0.5 mg/kg in two doses, methylprednisolone 1-2 mg/kg, dexamethasone 6 mg/day) were used in patients with moderate to severe clinical image with signs of gradual clinical deterioration or in patients with incipient or developed acute respiratory distress syndrome (ARDS). Anticoagulant therapy was used in standard prophylactic dose of LMWH for patients with multiple risk factors and on conventional oxygen therapy. Therapeutical doses were used, according to the anti-Xa levels, for patients in intensive care unit requiring mechanical ventilation or hi-flow oxygen therapy, those on long-term anticoagulant therapy or in patients with suspectable or confirmed thrombosis. Antibiotics were used empirically or according to the antibiogram. The main criteria for tocilizumab administration was an increase in IL-6 values above 40 ng/L and CRP values above 50 mg/L or a threefold increase during the last 48 h in patients with clinical worsening with more than 25 resp/min, saturation below 93%, and p02 value bellow 8,66 kPa without supportive oxygen therapy. Tocilizumab was administered intravenously at 8 mg/kg body weight (up to a maximum of 800 mg) in two doses, 12 h apart. Convalescent plasma was used in patients with rapid worsening, positive PCR test for SARS-CoV-2 virus, the first two weeks from symptom onset. The recommended dose was 4-5 ml/kg or 200-500 ml per day in two doses. The indication was established according to the specific scoring system with different variables including patient's clinical status, form of the disease, time from symptom onset, respiratory status, radiographic findings,

Table 1: Characteristics of patients admitted to ICU with moderate to severe ARDS due to COVID-19-related pneumonia, overall and subpopulation analysis according to survival.

	Total ($n = 160$)	ICU patients		p
		Live ($n = 64$)	Dead ($n = 96$)	
Gender, *n* (%)				
Male	110 (68.8)	47 (73.4)	63 (65.6)	0.384
Female	50 (31.3)	17 (26.6)	33 (34.4)	
Age, mean ± sd	65.6 ± 14	58.8 ± 15.1	70.2 ± 11.1	**<0.001**
Laboratory at admission to hospital, median (IQR)				
CRP	81.2 (53.8–173.4)	74.7 (46.7–117.5)	105.2 (58.1–200.5)	**0.008**
Lymphocytes	0.74 (0.53–1.04)	0.84 (0.56–1.36)	0.66 (0.46–0.86)	**0.001**
D-dimer	881 (523–2660)	646 (372–1582)	1051 (650–3642)	**0.004**
Ferritin	875 (497–1482)	850 (516–1521)	891 (484–1482)	0.794
Thrombocytes	235 (177–329)	247 (200–345)	228 (159–302)	0.096
INR	1.13 (1.01–1.30)	1.12 (0.99–1.28)	1.14 (1.04–1.34)	0.130
PT	87 (69–100)	90 (72–103)	86 (68–99)	0.325
APTT	25.2 (21.9–29–8)	24.1 (21.4–28.0)	26.1 (22.7–30.2)	0.077
Fibrinogen	3.9 (3.4–4.9)	4.0 (3.5–4.8)	3.8 (3.2–4.9)	0.605
Laboratory at admission to ICU, median (IQR)				
CRP	87.8 (51.5–173.3)	78.4 (52.3–148.9)	95.1 (50.7–195.9)	0.166
Lymphocytes	0.63 (0.44–0.88)	0.7 (0.49–0.99)	0.61 (0.38–0.81)	**0.019**
D-dimer	1414 (701–5030)	1027 (566–2585)	1944 (860–7423)	**0.001**
Ferritin	1108 (485–1698)	1181 (625–1640)	1058 (454–1764)	0.947
Thrombocytes	191 (150–278)	191 (151–259)	195 (149–291)	0.668
Serum albumin	31 (29–34)	35 (33–37)	29 (27–31)	**<0.001**
INR	1.15 (1.05–1.29)	1.13 (1.01–1.28)	1.16 (1.08–1.35)	0.087
PT	89 (72–103)	96 (74–108)	86 (69–99)	0.115
APTT	25.9 (23.1–28.5)	25.4 (22.7–27.6)	26.1 (23.3–29.8)	0.272
Fibrinogen	4.3 (3.6–5.3)	4.4 (3.7–5.4)	4.2 (3.6–5.2)	0.744
IL6	91 (38.80–286.00)	50.42 (24.45–100.90)	133.80 (74.00–426.80)	**<0.001**
CT score	20 (16–23)	19 (16–22)	21 (19–23)	**0.017**
From beginning of symptoms to hospital admission (days), median (IQR)	7 (4–9)	7 (5–9)	7 (4–10)	0.844
From beginning of symptoms to IUC admission (days), median (IQR)	10 (8–12)	11 (8–13)	10 (7–12)	0.461
Mechanical ventilation, *n* (%)	107 (66.9)	13 (20.3)	94 (97.9)	**<0.001**
Tocilizumab, *n* (%)	38 (23.8)	13 (20.3)	25 (26)	0.452

comorbidities, and applied therapy. Among the inotropic agents, noradrenaline, dobutamine, vasopressin, and adrenaline were used. Outcomes were stratified as deceased or discharged from the hospital. All 160 patients were followed until their outcomes.

2.1. Data Collection. The data were collected through medical documentation and the hospital's health informational system (Heliant, v7.3, r48602). Demographic data (age, gender, and BMI), past medical history (hypertension, diabetes mellitus, COPD, coronary heart disease, heart failure, and chronic kidney disease), laboratory values (IL-6, CRP, PCT, ferritin, D-dimer, serum albumin, lymphocytes, thrombocytes, prothrombin time, activated partial thromboplastin time, and fibrinogen), and CT severity score were analyzed to identify predictors of mortality in critically ill COVID-19 patients. Clinical and laboratory parameters were followed upon admission to the hospital and Intensive Care Unit, with certain parameters being followed by their peak or lowest values (IL-6, CRP, PCT, D-dimer, serum albumin, lymphocytes, and CT severity score) during hospitalization. IL-6 values were followed in the period before the Tocilizumab administration. Reference values for evaluated laboratory parameters are presented in Supplemental Table 1.

3. Results

The study population included 160 consecutive patients admitted to ICU with moderate to severe ARDS due to COVID-19-related pneumonia. The mean patient age was 65.6 years (range, 29–92 years), predominantly men 68.8%. Laboratory values at admission to hospital and ICU are

Table 2: The presence of comorbidities in the study population.

Comorbidities, *n* (%)	Total (*n* = 160)	ICU patients		*p*
		Live (*n* = 64)	Dead (*n* = 96)	
Hypertension	109 (69.4)	40 (62.5)	69 (74.2)	0.158
Diabetes	52 (33.1)	26 (40.6)	26 (28.0)	0.121
Obesity	14 (8.9)	6 (9.5)	8 (8.5)	1.000
HOBP	8 (5.1)	1 (1.6)	7 (7.5)	0.095
Asthma	6 (3.8)	2 (3.1)	4 (4.3)	0.706
Coronary disease	28 (17.8)	10 (15.6)	18 (19.4)	0.672
Cardiomyopathy	14 (8.9)	6 (9.4)	8 (8.6)	1.000
Number of comorbidities				
None	37 (23.7%)	18 (28.6%)	19 (20.4%)	
1	48 (30.8%)	17 (27.0%)	31 (33.3%)	0.457
≥2	71 (45.5%)	28 (44.4%)	43 (46.2%)	
Total number of patients with comorbidities	120 (76.4%)	46 (71.9%)	74 (79.6%)	0.339

presented in Table 1. D-dimer, CRP, and ferritin levels were elevated, while the absolute number of lymphocytes was decreased. The median CT score was 20 (25^{th} to 75^{th} percentile: 16-23). 107 (66.9%) patients were on invasive mechanical ventilation, 31 (19.3%) on noninvasive, and 22 (13.8%) on high flow oxygen therapy machine. Median total number of ICU days was 10 (25^{th} to 75^{th} percentile: 6-18), while the median total number of hospital stay was 18 (25^{th} to 75^{th} percentile: 12-28). Detailed characteristics for the whole study population, as well as according to the survival groups, are presented in Table 1. The mortality rate was 60% (96/160). Patients who died were older and had higher CRP and D-dimer levels, and lower levels of lymphocytes at admission to hospital, higher CT score, as well as higher levels of D-dimer and IL-6 and lower levels of lymphocytes and serum albumin at admission to ICU, and they were significantly more on mechanical ventilation. There were no differences in the number of days from the beginning of symptoms to hospital admission or ICU admission between deceased and discharged patients. Tocilizumab was administered to 38 patients (23.8%). There were no differences in mortality between the groups according to Tocilizumab use. In addition, there were no significant baseline differences between the patients who received and did not receive Tocilizumab in the ICU, other than for age, i.e., patients who received Tocilizumab in the ICU were younger (see Supplemental Table 2).

The presence of comorbidities is presented in Table 2. There were 37 patients without comorbidities (23.7%) and 48 with one comorbidity (30.8%), while 71 patient had multiple comorbidities (45.5%). The total number of patients with comorbidities was 120 (76.4%). There were no significant differences in the presence of comorbidities according to the survival groups.

Univariate logistic regression analysis confirmed the significance of the following variables associated with the mortality of patients admitted to ICU due to COVID-19-related pneumonia: age, CRP, and lymphocytes at admission to hospital, albumin, D-dimer, and IL-6 at admission to ICU, and CT score Table 3.

Based on ROC curves (Figure 1) we determined cut-off points for significant continuous variables from the logistic regression analysis predicting mortality and used the categorical variables further in analysis to develop easy to use predictive model.

The following variables were independently associated with mortality in the final multivariate analysis: serum albumin, IL-6, and D-dimer at admission to ICU (Table 4).

4. Discussion

The present study on critically ill COVID-19 patients with moderate to severe ARDS showed a correlation of serum albumin, IL-6, and D-dimer all together at admission to ICU, accompanied by chest CT severity score, as independent predictors of mortality. These results are relying on the fact that cytokine storm and endothelial injury with induced procoagulable state have been marked as essential pathophysiological mechanisms of multiorgan failure and death in patients with severe COVID-19 infection [15–20].

It is important to point out that the results from univariate logistic regression analysis revealed age, CRP, and lymphocytes at admission to hospital as predictors of mortality in patients admitted to ICU, while serum albumin, D-dimer, IL-6, and CT severity score were significant predictors of mortality at admission to the ICU. Final multivariate analysis revealed serum albumin, IL-6, and D-dimer at admission to ICU as independently associated with mortality. These results are reflecting the unpredictability of the disease and its clinical course, aggravating the usage of appropriate therapy in a timely manner.

Hypoalbuminemia (serum albumin levels below 35 g/L) is more severe in critically ill patients and is associated with poor outcomes [21]. Its correlation with elevated D-dimer values in these patients, as in the study by Violi et al., has been linked to an enhanced risk of arterial and venous thrombosis [22]. Patients showed not only higher levels of D-dimer but also higher levels of CRP and creatinine, probably due to increased vascular permeability, kidney, or liver disease. Serum albumin is also a marker of severe oxidative

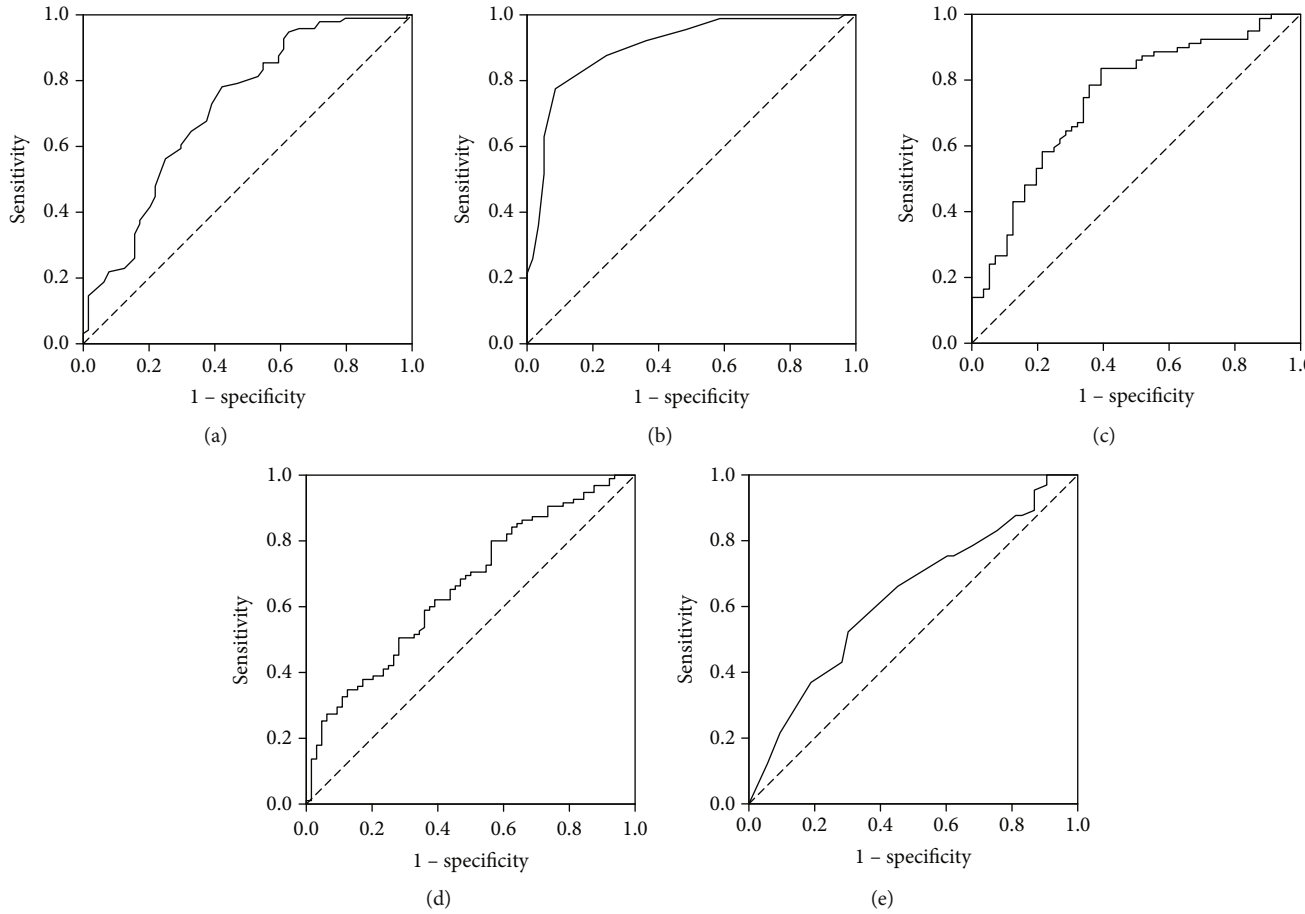

Figure 1: ROC curves for (a) age, (b) serum albumin, (c) IL-6, (d) D-dimer, and (e) CT score.

Table 3: Univariate logistic regression analysis for mortality of patients admitted to ICU due to COVID-19-related pneumonia, continuous variables used in the model.

Variable	p	RR	95% CI for RR
Age	<0.001	1.067	1.039–1.097
At admission to hospital			
CRP	0.013	1.005	1.001–1.009
Lymphocytes	0.003	0.341	0.168–0.690
D-dimer	0.585	1.000	1.000–1.000
At admission to ICU			
Lymphocytes	0.059	0.513	0.256–1.027
D-dimer	0.013	1.000	1.000–1.000
Serum albumin	<0.001	0.553	0.455–0.673
IL6	0.020	1.002	1.000–1.003
CT score	0.032	1.089	1.008–1.178
Mechanical ventilation	<0.001	184.385	40.037–849.161

stress and an acute phase reactant with antioxidant properties that may undergo irreversible oxidation [21]. It is a source of free thiols that can expel reactive oxidant species. Reactive oxidant species comprehend platelet and clotting activation, which is the reason why more patients with severe hypoalbuminemia are at greater risk of potential thrombotic events. Overall, synthesis in the liver is downregulated due to the effects of cytokines being released during the cytokine storm. Hypoalbuminemia followed by massive fluid loss due to severe infection is also responsible for hypovolemia and shock in these patients [23]. Correlation of albumin levels and severity of the infection is presented through the specific CRP/albumin ratio, already marked as an independent risk factor for severe COVID-19 infection [24, 25].

IL-6 induces oxidative stress and endothelial dysfunction by overexpression of the Angiotensin II type 1 receptor, which was presented 15 years ago in paperwork by Wassman et al. [26]. This also represents an important pathogenetic mechanism of the atherosclerotic process. Having in mind the cell entry mechanism of the SARS-CoV-2 virus through ACE2 receptors, the viral invasion is subsequently causing a dysregulation between ACE, Angiotensin II, and AT1 receptors, favoring the progression of inflammatory and thrombotic processes [27]. Lately, several studies have presented IL-6 as an independent predictor of patient outcomes in terms of the severity of the disease and survival [28, 29]. In our study, the values of IL-6 during hospitalization were followed before tocilizumab administration, as there was an elevation of IL-6 levels after usage due to disrupted clearance after drug saturation of the receptors. In a large study evaluating the role of different cytokines in COVID-19 infection,

Table 4: The univariate logistic regression analysis with categorical variables used and the full multivariate prognostic logistic model predicting mortality.

Variable	Univariate analysis			Multivariate analysis		
	p	RR	95% CI for RR	p	RR	95% CI for RR
Age > 65 yrs	<0.001	3.495	1.801–6.779	/	/	/
At admission to ICU						
Albumin < 33	<0.001	22.286	9.319–53.294	<0.001	25.740	7.491–88.443
IL – 6 > 72	<0.001	6.100	2.857–13.023	0.002	6.245	1.937–20.129
D – dimer > 1000	0.026	2.111	1.091–4.085	0.013	4.574	1.375–15.212
CT score ≥ 20	0.024	2.362	1.120–4.980	/	/	/

only IL-6 and TNF-α showed significant prognostic value [28]. Unlike other states where cytokine levels are increased, as in sepsis, the levels of IL-6 and TNF-α in patients with COVID-19 were sustained during days or even weeks, which makes the decision for administering the anticytokine treatment on time more difficult. Evaluating the levels of IL-6 early in disease onset can stratify patients at higher risk to develop a more severe form of the disease [30].

Increased levels of D-dimer, a fibrin degradation product, are associated with worse prognosis in patients with COVID-19, including an increased risk of ICU admission, mechanical ventilation, and death [31–33]. Severe endothelial dysfunction, subsequently caused by direct viral involvement and overproduction of cytokines, is causing a hypercoagulable state creating a suitable soil for intravascular thrombosis in both macro and microcirculation. The incidence of pulmonary embolism has been increased in patients with COVID-19 infection, estimated to be up to 9% of the cases, verified by CT pulmonary angiography [34]. In certain studies, venous thrombosis was found in up to 35% of the cases, mainly as deep vein thrombosis (DVT) [35]. Patients with ARDS within COVID-19 infection have a substantially increased rate of pulmonary embolism, estimated to be 11.8%, while patients diagnosed with thrombotic complications have more than a 5-fold increase in all-cause mortality [36]. The reported percentage of patients with increased D-dimer levels in ICU is going up to 81%, speaking in favor of a large portion of patients with microthrombosis as the main presentation of hypercoagulable state [37]. The overall coagulation status in patients with COVID-19 is extremely significant, as prolonged prothrombin time and activated partial thromboplastin time are also found to be associated with higher mortality from COVID-19 infection [38, 39].

Chest CT severity score is a useful imaging modality tool in evaluating the extensiveness of pulmonary involvement and stratifying patients not only numerically but also descriptively by estimating in which of the 4 stadiums of the disease the patient is (early, progressive, peak, or absorption) [40, 41]. In our study, the cut-off value of 20 points was related to poor clinical outcome, according to the prognostic logistic model. Previous studies on the importance of chest CT severity score are supporting this conclusion, with similar cut-off values being defined [42].

During the hospitalization, patients were strictly treated according to the protocol, as explained in the Methods section. Previously, the effects of anticoagulant therapy have been undisputedly proven to be connected with improved survival. In hospitalized COVID-19 patients receiving both prophylactic and therapeutical doses, there is a 30% lower chance of intubation and 50% higher chance of survival, especially in patients receiving low molecular weight heparin, as used in our study [43]. Although the anticoagulant therapy in COVID-19 patients has become almost mandatory in treatment protocols, the significant decrease in overall mortality of critically ill patients has not been noted yet, speaking in favor of multiple pathophysiological mechanisms being responsible for poor clinical outcomes.

The main difference between used therapeutic modalities in our study was the introduction of antiviral agents (remdesivir and favipiravir), although only 19 (11.8%) patients did not have it available during hospitalization. Considering the effects on outcomes, WHO recently recommended against the use of remdesivir, as evidence suggested no effects on mortality, need for mechanical ventilation, and other outcomes [44]. The positive effects, as presented by Beigel et al., are for now limited to evidence of shorter time to recovery, as this was the primary endpoint of the study [45]. Favipiravir promotes rapid viral clearance and a higher clinical recovery rate by shortening the disease course and reducing the need for oxygen requirement. However, the supportive data on resulting in lower rates of respiratory failure, ICU admissions, or all-cause mortality is missing [46]. Further studies will provide more insights into its clinical safety and efficacy.

Potential therapeutic effects of albumins must be considered, having in mind that serum albumin was the strongest independent predictor of mortality in our study. It is already shown that the administration of albumin in critically ill patients with acute respiratory distress syndrome might have its advantages. It improves oxygenation early after the treatment, probably by reducing the alveolar-capillary leakage, but without effects on the overall mortality rate [47]. Several limitations regarding the administration of albumin solutions are inevitable, including dosage, treatment length, possible effects on renal function, and the optimal moment of therapy initiation. However, the usefulness in critically ill COVID-19 patients is yet to be established in randomized controlled trials.

Speaking of novel therapeutic modalities, it is important to emphasize that in our results, there were no differences in mortality between the groups according to Tocilizumab use. To properly estimate the effectiveness of Tocilizumab and the possible role of IL-6 as an independent predictor of mortality, patients that received Tocilizumab before admission to ICU were not included in the study. Also, the baseline characteristics between the groups were not statistically significant, which is especially important to underline (Supplemental Table 2). After numerous trials investigating the potential benefits of this IL-6 receptor blocker, the definitive results are still controversial, probably due to an undetermined time frame of the best usability in correlation with clinical course [48, 49].

There are several limitations to the study. This is a single-center study. Although the sample size is quite satisfying, considering that these are critically ill patients, future multicenter, prospective studies will shed light on stronger correlations between different predictors of mortality in COVID-19 patients paving the way for potentially useful novel therapeutic modalities. ICU scoring systems (mainly SOFA and APACHE II scores) were not used as a part of the data considering their clinical utility has already been proven in several studies [50, 51].

5. Conclusion

In this single-center study of 160 consecutive critically ill COVID-19 patients with moderate to severe ARDS demanding high oxygen flow, serum albumin, IL-6, and D-dimer at admission to ICU, accompanied by a chest CT severity score, were marked as independent predictors of mortality. This conclusion supports previous studies on cytokine storm and diffuse microvascular thrombosis/thrombotic events as potential mechanisms of poor clinical outcomes. Further larger prospective multicenter studies are necessary to determine the exact correlation between different predictors of mortality in order to stratify patients with a significant chance of developing a severe form of the disease.

Abbreviations

COVID-19:	Coronavirus disease 19
ICU:	Intensive Care Unit
ARDS:	Acute Respiratory Distress Syndrome
CT:	Computerized tomography
CRP:	C-reactive protein
CAR:	CRP/albumin ratio
IL-6:	Interleukin-6
SARS-CoV-2:	Severe acute respiratory syndrome, coronavirus 2
PCR:	Polymerase chain reaction
LMWH:	Low-molecular-weight heparin
COPD:	Chronic obstructive pulmonary disease
PCT:	Procalcitonin
ACE-2:	Angiotensin-converting enzyme 2
TNF-α:	Tumor necrosis factor-α
APACHE-II:	Acute Physiology and Chronic Health Evaluation
SOFA:	Sequential Organ Failure Assessment.

Data Availability

The data that support the findings of this study are available from the corresponding author (MZ) upon reasonable request.

Disclosure

The authors state that no relationship with industry exists. The funders had no role in preparation of the manuscript or the decision to publish.

Conflicts of Interest

The authors declare that there is no conflict of interest regarding the publication of this paper.

Authors' Contributions

The following are the collaborators of this paper: Nebojsa Ladjevic, Ivana Milosevic, Goran Stevanovic, Milos Korac, Martina Glidzic-Pakenham, Jelena Velickovic, Jasna Gacic, Ana Sekulic, Ljiljana Denic Markovic, Aleksandra Petrovic, Ana Stojanovic, Igor Nadj, Natasa Stanisavljevic, Maja Popovic, Filip Lukic, and Zdravko Kalaba.

Acknowledgments

The authors would like to acknowledge all healthcare professionals which are in the first line against COVID-19 disease in the Republic of Serbia and worldwide.

Supplementary Materials

Supplemental Table 1: reference values of evaluated laboratory parameters. Supplemental Table 2: baseline differences between the patients who received and did not receive Tocilizumab in the ICU. *(Supplementary materials)*

References

[1] Coronavirus CasesRetrieved December 16, 2020, from https://www.worldometers.info/coronavirus/.

[2] C. C. Lai, W. C. Ko, P. I. Lee, S. S. Jean, and P. R. Hsueh, "Extra-respiratory manifestations of COVID-19," *International Journal of Antimicrobial Agents*, vol. 56, no. 2, p. 106024, 2020.

[3] D. Bandyopadhyay, T. Akhtar, A. Hajra et al., "COVID-19 pandemic: cardiovascular complications and future implications," *American Journal of Cardiovascular Drugs*, vol. 20, no. 4, pp. 311–324, 2020.

[4] A. A. Asadi-Pooya and L. Simani, "Central nervous system manifestations of COVID-19: a systematic review," *Journal of the Neurological Sciences*, vol. 413, article 116832, 2020.

[5] I. C. Lee, T. L. Huo, and Y. H. Huang, "Gastrointestinal and liver manifestations in patients with COVID-19," *Journal of the Chinese Medical Association*, vol. 83, no. 6, pp. 521–523, 2020.

[6] R. A. Armstrong, A. D. Kane, and T. M. Cook, "Outcomes from intensive care in patients with COVID-19: a systematic

review and meta-analysis of observational studies," *Anaesthesia*, vol. 75, no. 10, pp. 1340–1349, 2020.

[7] E. Mehraeen, A. Karimi, A. Barzegary et al., "Predictors of mortality in patients with COVID-19-a systematic review," *European Journal of Integrative Medicine*, vol. 40, p. 101226, 2020.

[8] B. M. Henry, M. H. S. de Oliveira, S. Benoit, M. Plebani, and G. Lippi, "Hematologic, biochemical and immune biomarker abnormalities associated with severe illness and mortality in coronavirus disease 2019 (COVID-19): a meta-analysis," *Clinical Chemistry and Laboratory Medicine*, vol. 58, no. 7, pp. 1021–1028, 2020.

[9] W. Tian, W. Jiang, J. Yao et al., "Predictors of mortality in hospitalized COVID-19 patients: a systematic review and meta-analysis," *Journal of Medical Virology*, vol. 92, no. 10, pp. 1875–1883, 2020.

[10] A. Hessami, A. Shamshirian, K. Heydari et al., "Cardiovascular diseases burden in COVID-19: Systematic review and meta-analysis," *European Journal of Integrative Medicine*, 2020.

[11] M. Parohan, S. Yaghoubi, A. Seraji, M. H. Javanbakht, P. Sarraf, and M. Djalali, "Risk factors for mortality in patients with coronavirus disease 2019 (COVID-19) infection: a systematic review and meta-analysis of observational studies," *The Aging Male*, vol. 23, pp. 1–9, 2020.

[12] A. E. Mesas, I. Cavero-Redondo, C. Álvarez-Bueno et al., "Predictors of in-hospital COVID-19 mortality: a comprehensive systematic review and meta-analysis exploring differences by age, sex and health conditions," *PLoS One*, vol. 15, no. 11, article e0241742, 2020.

[13] S. Kiss, N. Gede, P. Hegyi et al., "Early changes in laboratory parameters are predictors of mortality and ICU admission in patients with COVID-19: a systematic review and meta-analysis," *Medical Microbiology and Immunology*, vol. 210, no. 1, pp. 33–47, 2021.

[14] ARDS Definition Task Force, V. M. Ranieri, G. D. Rubenfeld et al., "Acute respiratory distress syndrome: the Berlin definition," *Journal of the American Medical Association*, vol. 307, no. 23, pp. 2526–2533, 2012.

[15] B. Hu, S. Huang, and L. Yin, "The cytokine storm and COVID-19," *Journal of Medical Virology*, vol. 93, no. 1, pp. 250–256, 2021.

[16] R. J. Jose and A. Manuel, "COVID-19 cytokine storm: the interplay between inflammation and coagulation," *The Lancet Respiratory Medicine*, vol. 8, no. 6, pp. e46–e47, 2020.

[17] P. Libby and T. Lüscher, "COVID-19 is, in the end, an endothelial disease," *European Heart Journal*, vol. 41, no. 32, pp. 3038–3044, 2020.

[18] R. Amraei and N. Rahimi, "COVID-19, renin-angiotensin system and endothelial dysfunction," *Cells*, vol. 9, no. 7, p. 1652, 2020.

[19] J. S. Rico-Mesa, D. Rosas, A. Ahmadian-Tehrani, A. White, A. S. Anderson, and R. Chilton, "The role of anticoagulation in COVID-19-induced hypercoagulability," *Current Cardiology Reports*, vol. 22, no. 7, p. 53, 2020.

[20] L. Spiezia, A. Boscolo, F. Poletto et al., "COVID-19-related severe hypercoagulability in patients admitted to intensive care unit for acute respiratory failure," *Thrombosis and Haemostasis*, vol. 120, no. 6, pp. 998–1000, 2020.

[21] J. Huang, A. Cheng, R. Kumar et al., "Hypoalbuminemia predicts the outcome of COVID-19 independent of age and co-morbidity," *Journal of Medical Virology*, vol. 92, no. 10, pp. 2152–2158, 2020.

[22] F. Violi, R. Cangemi, G. F. Romiti et al., "Is albumin predictor of mortality in COVID-19?," *Antioxidants & Redox Signaling*, 2020.

[23] G. Ramadori, "Hypoalbuminemia: an underestimated, vital characteristic of hospitalized COVID-19 positive patients?," *Hepatoma Research*, vol. 2020, p. 28, 2020.

[24] A. S. Bannaga, M. Tabuso, A. Farrugia et al., "C-reactive protein and albumin association with mortality of hospitalised SARS-CoV-2 patients: a tertiary hospital experience," *Clinical Medicine*, vol. 20, no. 5, pp. 463–467, 2020.

[25] G. M. Feketea and V. Vlacha, "The diagnostic significance of usual biochemical parameters in coronavirus disease 19 (COVID-19): albumin to globulin ratio and CRP to albumin ratio," *Frontiers in Medicine*, vol. 7, article 566591, 2020.

[26] S. Wassmann, M. Stumpf, K. Strehlow et al., "Interleukin-6 induces oxidative stress and endothelial dysfunction by overexpression of the angiotensin II type 1 receptor," *Circulation Research*, vol. 94, no. 4, pp. 534–541, 2004.

[27] P. Verdecchia, C. Cavallini, A. Spanevello, and F. Angeli, "The pivotal link between ACE2 deficiency and SARS-CoV-2 infection," *European Journal of Internal Medicine*, vol. 76, pp. 14–20, 2020.

[28] D. M. del Valle, S. Kim-Schulze, H. H. Huang et al., "An inflammatory cytokine signature predicts COVID-19 severity and survival," *Nature Medicine*, vol. 26, no. 10, pp. 1636–1643, 2020.

[29] R. Laguna-Goya, A. Utrero-Rico, P. Talayero et al., "IL-6-based mortality risk model for hospitalized patients with COVID-19," *Journal of Allergy and Clinical Immunology*, vol. 146, no. 4, pp. 799–807.e9, 2020.

[30] T. Herold, V. Jurinovic, C. Arnreich et al., "Elevated levels of IL-6 and CRP predict the need for mechanical ventilation in COVID-19," *Journal of Allergy and Clinical Immunology*, vol. 146, no. 1, pp. 128–136.e4, 2020.

[31] P. Paliogiannis, A. A. Mangoni, P. Dettori, G. K. Nasrallah, G. Pintus, and A. Zinellu, "D-dimer concentrations and COVID-19 severity: a systematic review and meta-analysis," *Frontiers in Public Health*, vol. 8, p. 432, 2020.

[32] J. S. Berger, D. Kunichoff, S. Adhikari et al., "Prevalence and outcomes of D-dimer elevation in hospitalized patients with COVID-19," *Arteriosclerosis, Thrombosis, and Vascular Biology*, vol. 40, no. 10, pp. 2539–2547, 2020.

[33] L. Zhang, X. Yan, Q. Fan et al., "D-dimer levels on admission to predict in-hospital mortality in patients with Covid-19," *Journal of Thrombosis and Haemostasis*, vol. 18, no. 6, pp. 1324–1329, 2020.

[34] Y. Sakr, M. Giovini, M. Leone et al., "Pulmonary embolism in patients with coronavirus disease-2019 (COVID-19) pneumonia: a narrative review," *Annals of Intensive Care*, vol. 10, no. 1, p. 124, 2020.

[35] Y. Yu, J. Tu, B. Lei et al., "Incidence and risk factors of deep vein thrombosis in hospitalized COVID-19 patients," *Clinical and Applied Thrombosis/Hemostasis*, vol. 26, p. 107602962095321, 2020.

[36] J. D. McFadyen, H. Stevens, and K. Peter, "The emerging threat of (micro)thrombosis in COVID-19 and its therapeutic implications," *Circulation Research*, vol. 127, no. 4, pp. 571–587, 2020.

[37] F. Zhou, T. Yu, and R. Du, "Clinical course and risk factors for mortality of adult inpatients with COVID-19 in Wuhan, China: a retrospective cohort study," *The Lancet*, vol. 395, pp. 1054–1062, 2020.

[38] H. Long, L. Nie, X. Xiang et al., "D-dimer and prothrombin time are the significant indicators of severe COVID-19 and poor prognosis," *BioMed Research International*, vol. 2020, Article ID 6159720, 10 pages, 2020.

[39] H. C. Luo, C. Y. You, S. W. Lu, and Y. Q. Fu, "Characteristics of coagulation alteration in patients with COVID-19," *Annals of Hematology*, vol. 100, no. 1, pp. 45–52, 2021.

[40] M. Francone, F. Iafrate, G. M. Masci et al., "Chest CT score in COVID-19 patients: correlation with disease severity and short-term prognosis," *European Radiology*, vol. 30, no. 12, pp. 6808–6817, 2020.

[41] B. Abbasi, R. Akhavan, A. Ghamari Khameneh et al., "Evaluation of the relationship between inpatient COVID-19 mortality and chest CT severity score," *American Journal of Emergency Medicine*, vol. S0735-6757, no. 20, pp. 30851-30852, 2020.

[42] R. Yang, X. Li, H. Liu et al., "Chest CT severity score: an imaging tool for assessing severe COVID-19," *Radiology: Cardiothoracic Imaging*, vol. 2, no. 2, article e200047, 2020.

[43] G. N. Nadkarni, A. Lala, E. Bagiella et al., "Anticoagulation, bleeding, mortality, and pathology in hospitalized patients with COVID-19," *Journal of the American College of Cardiology*, vol. 76, no. 16, pp. 1815–1826, 2020.

[44] WHO Solidarity Trial Consortium, "Repurposed antiviral drugs for COVID-19 - interim WHO Solidarity trial results," *The New England Journal of Medicine*, vol. 384, no. 6, pp. 497–511, 2020.

[45] J. H. Beigel, K. M. Tomashek, L. E. Dodd et al., "Remdesivir for the treatment of Covid-19 - final report," *The New England Journal of Medicine*, vol. 383, no. 19, pp. 1813–1826, 2020.

[46] S. Joshi, J. Parkar, A. Ansari et al., "Role of favipiravir in the treatment of COVID-19," *International Journal of Infectious Diseases.*, vol. 102, pp. 501–508, 2021.

[47] C. Uhlig, P. L. Silva, S. Deckert, J. Schmitt, and M. G. de Abreu, "Albumin versus crystalloid solutions in patients with the acute respiratory distress syndrome: a systematic review and meta-analysis," *Critical Care*, vol. 18, no. 1, p. R10, 2014.

[48] A. Cortegiani, M. Ippolito, M. Greco et al., "Rationale and evidence on the use of tocilizumab in COVID-19: a systematic review," *Pulmonology*, vol. S2531-0437, no. 20, pp. 30153–30157, 2021.

[49] J. H. Stone, M. J. Frigault, N. J. Serling-Boyd et al., "Efficacy of tocilizumab in patients hospitalized with Covid-19," *New England Journal of Medicine*, vol. 383, no. 24, pp. 2333–2344, 2020.

[50] S. Liu, N. Yao, Y. Qiu, and C. He, "Predictive performance of SOFA and qSOFA for in-hospital mortality in severe novel coronavirus disease," *The American Journal of Emergency Medicine*, vol. 38, no. 10, pp. 2074–2080, 2020.

[51] X. Zou, S. Li, M. Fang et al., "Acute physiology and chronic health evaluation II score as a predictor of hospital mortality in patients of coronavirus disease 2019," *Critical Care Medicine*, vol. 48, no. 8, pp. e657–e665, 2020.

Hindawi
Oxidative Medicine and Cellular Longevity
Volume 2021, Article ID 6617969, 15 pages
https://doi.org/10.1155/2021/6617969

Research Article

The Association of Polymorphisms in *Nrf2* and Genes Involved in Redox Homeostasis in the Development and Progression of Clear Cell Renal Cell Carcinoma

Smiljana Mihailovic,[1] **Vesna Coric**,[2,3] **Tanja Radic**,[4] **Ana Savic Radojevic**,[2,3] **Marija Matic**,[2,3] **Dejan Dragicevic**,[3,5] **Milica Djokic**,[6] **Vladimir Vasic**,[7] **Zoran Dzamic**,[3,5] **Tatjana Simic**,[2,3,8] **Jovan Hadzi-Djokic**,[8] **and Marija Pljesa Ercegovac**[2,3]

[1]*The Obstetrics and Gynaecology Clinic Narodni Front, 11000, Serbia*
[2]*Institute of Medical and Clinical Biochemistry, 11000, Serbia*
[3]*Faculty of Medicine, University of Belgrade, 11000, Serbia*
[4]*Institute of Mental Health Belgrade, 11000, Serbia*
[5]*Clinic of Urology, Clinical Center of Serbia, 11000, Serbia*
[6]*Institute for Oncology and Radiology of Serbia, 11000, Serbia*
[7]*Department of Urology, University Medical Center Zvezdara, 11000, Serbia*
[8]*Serbian Academy of Sciences and Arts, 11000, Serbia*

Correspondence should be addressed to Marija Pljesa Ercegovac; m.pljesa.ercegovac@gmail.com

Received 23 October 2020; Revised 28 November 2020; Accepted 3 April 2021; Published 17 April 2021

Academic Editor: Aldrin V. Gomes

Copyright © 2021 Smiljana Mihailovic et al. This is an open access article distributed under the Creative Commons Attribution License, which permits unrestricted use, distribution, and reproduction in any medium, provided the original work is properly cited.

Deleterious effects of SNPs found in genes encoding transcriptional factors, as well as antioxidant and detoxification enzymes, are disputable; however, their functional significance seems to modify the risk for clear cell renal cell carcinoma (ccRCC) development and progression. We investigated the effect of specific *Nrf2*, *SOD2*, *GPX1* gene variants and *GSTP1ABCD* haplotype on ccRCC risk and prognosis and evaluated the association between GSTP1 and regulatory (JNK1/2) and executor (caspase-3) apoptotic molecule expression in ccRCC tissue samples and the presence of GSTP1 : JNK1/2 protein : protein interactions. Genotyping was performed in 223 ccRCC patients and 336 matched controls by PCR-CTTP and qPCR. Protein expression was analyzed using immunoblot, while the existence of GSTP1 : JNK1 protein : protein interactions was investigated by immunoprecipitation experiments. An increased risk of ccRCC development was found among carriers of variant genotypes of both *SOD2* rs4880 and *GSTP1* rs1695 polymorphisms. *Nrf2* rs6721961 genetic polymorphism in combination with both rs4880 and rs1695 showed higher ccRCC risk as well. Haplotype analysis revealed significant risk of ccRCC development in carriers of the *GSTP1C* haplotype. Furthermore, GSTP1 variant forms seem to affect the overall survival in ccRCC patients, and the proposed molecular mechanism underlying the GSTP1 prognostic role might be the presence of GSTP1 : JNK1/2 protein : protein interactions.

1. Introduction

Cellular redox homeostasis is maintained by constant metabolic fluxes and redox feedback consisting of electrophilic molecules produced by all kinds of stressors that activate diverse mechanisms aimed at reestablishing nucleophilic environment [1]. Disturbance of this fine balance between reactive oxygen species (ROS) production and their disintegration leads to oxidative stress and cellular damage on multiple levels [2]. In order to adapt, a phenotypic switch has to take place [1]. Cells that have a high proliferation rate, such as cancer cells, demand constant energy production to maintain biosynthesis of macromolecules. In order to adapt and support their basic needs, both intrinsic and extrinsic

molecular mechanisms are involved in modifying cellular metabolism [3]. While constantly rapidly proliferating, cancer cells are, at the same time, exposed to increased ROS levels, which further upregulate antioxidant systems and create environment in which they are able to develop new redox balance and resistance to oxidative damage [3].

Clear cell renal cell carcinoma (ccRCC) remains one of the most frequent and the most aggressive adult renal malignancies, accounting for up to 90% of all kidney tumors [4, 5]. Since alterations in metabolism are among ccRCC hallmarks, it has been suggested that besides histological classification of RCC, certain molecular subtypes should also be identified [6, 7]. Precise classification is of utmost importance, since it might reveal types with more or less aggressive clinical features and therefore point out which patients should be more closely monitored and followed [8].

Clear cell RCC belongs to types of carcinomas associated with Keap1/Nrf2 (Kelch-like ECH-associated protein 1/nuclear factor (erythroid-derived 2)-like2) pathway alterations [8]. Namely, when cellular levels of reactive oxygen species and electrophiles are increased, specific adaptive cytoprotective response is activated, including changes in the Keap1/Nrf2 pathway [9, 10]. Induced allosteric changes in Keap1 lead to decreased proteasomal degradation of the transcriptional factor Nrf2 [10]. Once accumulated, Nrf2 enters the cell nucleus and binds to antioxidant response element (ARE) DNA sequences of Nrf2 target genes, further causing intensified transcription of numerous enzymes, including detoxifying enzymes, metabolic enzymes, and stress response proteins [8, 10, 11]. Although at first perceived as an anticancer molecule, some authors emphasize the role of Nrf2 in cancer cell survival and even suggest that it should be regarded as a possible target for future anticancer therapeutic approaches [9, 12, 13].

Among various enzymes encoded by Nrf2 target genes and regulated by their binding to AREs are glutathione S-transferases (GST). They represent a family of multifunctional enzymes involved in a number of catalytic and noncatalytic processes, still traditionally recognized as phase II cellular detoxification system enzymes [3, 14]. The liver, lung, and kidneys, as organs with intense metabolic activity, are known to have high expression of cytosolic GSTs, especially the pi (GSTP) form, whose gene activation is regulated by Nrf2 [14, 15]. GSTP1 also possesses binding activity toward macromolecules, as well as small molecules, and displays ability to participate in a large signal transduction pathway [14, 16]. Specifically, GSTP1 acts as a negative regulator of kinase-dependent apoptotic signaling pathways by forming protein : -protein complexes with regulatory mitogen-activated kinases such as JNK1 (c-Jun NH2-terminal kinase) [14, 17]. The particular GSTP1 : JNK1 interaction has gained attention as the new, functional link between the upregulated GSTP1 and malignant phenotype [3]. Additionally, GSTP1 has a potential to form a GSTP1/Nrf2 protein complex, suggesting a possibility that GSTP1 protein might help Nrf2 stabilization and its further actions [18]. When considering its role in cancer metabolism, in addition to detoxification of potential cancerogenic substances, GSTP1 is capable of increasing drug efflux from the cell thus contributing to chemoresistance [19].

Since cancer cells are energy-dependent, metabolic reprogramming is the basis of their sustenance [7]. In order to keep up with high energy demands and to defend themselves from many reactive molecules, tumor cells rely on enzymes that enable both processes [20, 21]. There are three isoenzymes of SOD, a major antioxidant enzyme [22]. In the reaction catalyzed by mitochondrial SOD2, H_2O_2, a well-known molecule with novel functions in cell proliferation, differentiation, and migration, is being produced. In addition to acting as a signaling molecule, H_2O_2 facilitates activation of AMP-activated kinase and promotes glycolysis which is a key change for cancer cells [20, 22]. Therefore, by controlling the H_2O_2 production, SOD2 plays an important role in numerous pathways.

And while SOD2 leads to H_2O_2 synthesis, another key antioxidant enzyme, glutathione peroxidase (GPX), leads to its further reduction and production of a neutral water molecule [23]. Eight members comprise the GPX family [24]. By helping cancer cells eliminate potentially harmful hydrogen peroxide, the role of GPX1 as the most abundant GPX form might be contradictory [25]. Namely, its increased activity protects normal cells from oxidative damage, while this could be helpful for cancer cells to escape ROS as well [25].

Both the Nrf2 gene and genes encoding GSTP1, SOD2, and GPX1 have functional polymorphisms, which either change the level of expression of specific protein or affect the activity of synthesized proteins. The widely analyzed *Nrf2* SNP polymorphism rs6721961 involves substitution of C to A, positioned at -617 of the proximal promoter [26]. Definite consequent functional changes are still unsolved, and it is discussed whether higher or lower transcriptional activity is associated with a variant-type genotype (-617AA) [27]. However, since this SNP is located in the ARE-like motif of the gene, importance for self-induction of the *Nrf2* is being emphasized throughout the literature [26, 28, 29]. In the case of *GSTP1* gene polymorphisms, two most commonly occurring SNPs are rs1695 and rs1138272 [30]. Substitution of A313G in the case of rs1695 causes change of isoleucine with valine at position 105 (Ile105Val) [31]. This *Val* allele variant represents a more potent c-Jun N-terminal kinase 1 (JNK1) inhibitor and has a stronger antiapoptotic effect [32]. The presence of T instead of C at position 341 results in coding of protein with valine instead of alanine (rs1138272, Ala114Val) [33]. It is assumed that the 341T variant of GSTP might have decreased activity or modified substrate specificity [34]. The haplotype *GSTP1ABCD* represents a combination of these two polymorphisms. When it comes to *SOD2* polymorphism, rs4880 corresponds to substitution of C>T in exon 2 leading to change from alanine to valine at position 16 [35]. Since there is a channel within the inner mitochondrial membrane that cannot import the Val16 variant of SOD2 as efficiently as Ala16, the Val16 variant remains trapped and later degraded by the proteasome [35]. The mostly studied SNP in the case of the *GPX1* gene is rs1050450 (Pro200Leu). Due to change of proline with leucine, secondary and tertiary structures of GPX1 are altered, leading to conformational change of the enzyme as a whole [36]. Proline is basically essential, because of its unsubstituted amino group on the α carbon atom which

enables formation of a specific kink; therefore, when absent, the whole structure is modified [36].

Considering the potential functional significance of polymorphisms in genes encoding the Nrf2 transcriptional factor, as well as antioxidant SOD2, GPX1, and detoxification GSTP1 enzymes in both the onset and prognosis of clear cell RCC, the aim of this study was to evaluate the effect of specific *Nrf2*, *SOD2*, and *GPX1* gene variants and *GSTP1ABCD* haplotype on the risk, development, and postoperative prognosis in patients with ccRCC. Furthermore, the aim was to evaluate the association between GSTP1 expression and expression of regulatory (JNK1/2) and executor (caspase-3) apoptotic molecules in human ccRCC tissue samples, as well as the presence of GSTP1 : JNK1/2 protein : protein interactions.

2. Materials and Methods

2.1. Participants. The case-control study included 223 patients with histologically confirmed clear cell renal cell carcinoma treated and followed at the Clinic of Urology of Clinical Center of Serbia, Belgrade. Incident cases were recruited at the time of diagnosis which included the presence of malignantly enhanced lesions detected by imaging techniques and confirmed by histological diagnosis. Obtained blood and tissue samples were assessed within the Biobank formed in the Laboratory for Functional Genetics and Proteomics at the Institute of Medical and Clinical Biochemistry of the Faculty of Medicine, University of Belgrade. The enrolled 336 controls were gender- and age-matched cancer-free subjects. These individuals with no previous history of cancer had undergone surgery for benign conditions at the same clinical center, unrelated to both nonmalignant and malignant urological conditions. Participants gave their informed consent for inclusion in the study. The study was conducted in accordance with the Declaration of Helsinki, and the protocol was approved by the Ethics Committee of the Faculty of Medicine, University of Belgrade (no. 29/X-3). Both cases and controls were interviewed using a standard epidemiological questionnaire in order to gain information about risk factors for ccRCC development. Smokers were defined as subjects who had a period of at least 60 days of consuming cigarettes prior to inclusion in the study. Pack-years was calculated by the formula pack-years = (cigarettes/day ÷ 20) × years of smoking. Overall survival was defined as time from nephrectomy to the date of death or last follow-up (November 2018).

2.2. DNA Isolation. Genomic DNA was isolated from 200 μl of the whole blood sample or from 25 mg of distant nontumor kidney tissue samples, using a QIAamp DNA mini kit (Qiagen, Chatsworth, CA, USA). Isolated DNA was stored at -20°C. The concentration, as well as purity of isolated DNA, was measured by spectrophotometry at 230, 260, 280, and 320 nm on GeneQuant pro (Biochrom, Cambridge, England).

2.3. Analysis of Examined Genotypes. The polymorphism rs6721961 for *Nrf2* was examined by the PCR-CTTP (polymerase chain reaction with confronting two-pair primers) method according to Shimoyama et al. [37]. Products of amplification were divided by electrophoresis with 2% agarose gel. Visualization of PCR products was enabled with SYBR® Safe DNA Gel Stain (Invitrogen Corporation, Carlsbad, California, USA) on a UV ChemiDoc camera (Bio-Rad, Hercules, California, USA). A lane containing 282 and 113 bp was considered a C/C genotype; a lane with 282, 205, and 113 bp, a heterozygous genotype; and a lane with 282 and 205 bp, a A/A genotype.

Genotyping of *GSTP1* (rs1695 and rs1138272), *SOD2* (rs4880), and *GPX1* (rs1050450) was done by applying quantitative polymerase chain reaction (qPCR) on Mastercycler ep realplex (Eppendorf, Hamburg, Germany) using appropriate assays of Applied Biosystems TaqMan Drug Metabolism Genotyping (Life Technologies, Applied Biosystems, Carlsbad, CA, USA). Assays C_3237198_20 in the case of *GSTP1* rs1695, C_1049615_20 for *GSTP1* rs1138272, and C_8709053_10 were used for *SOD2*. For the *GPX1* rs1050450 polymorphism, a custom-designed assay with sequences 5′ VIC-ACAGCT GGGCCCTT-MGB-3′ and 5′ FAM-ACAGCTGAGCCCTT-MGB-3′ was used.

2.4. Immunoblot Analysis. Cytosols were obtained from ccRCC tumor ($n = 20$) and respective nontumor kidney tissue samples. A pool of nontumor kidney tissue was made by mixing the equal parts of six different samples. 50 μg of total protein per sample was subjected to immunoblot analysis of JNK1/2, GSTP1, and cleaved caspase-3 expression [38, 39]. Membranes were blocked overnight and treated with primary antibodies against JNK1/2 (Sigma-Aldrich, St. Louis, Missouri, USA), GSTP1 (Abcam, Cambridge, UK), cleaved caspase-3 (Cell Signaling, Danvers, Massachusetts, USA), and housekeeping protein β-actin (Sigma-Aldrich, St. Louis, Missouri, USA). Afterwards, membranes were incubated with appropriate secondary antibodies, treated with a chemiluminescence detection substrate (Invitrogen Corporation, Carlsbad, CA, USA), and exposed to X-ray films (Amersham Hyperfilm ECL, GE Healthcare, Buckinghamshire, England). Densitometry analysis was performed using ImageJ (National Institutes of Health, Bethesda, USA). In order to obtain relative quantitation, the results were normalized using β-actin housekeeping protein.

In order to investigate the presence of GSTP1 : JNK1 protein : protein interactions in tumor ccRCC samples, immunoprecipitation experiments were performed using Catch and Release® v2.0 High Throughput (HT) Immunoprecipitation Assay Kit-96 well (Upstate Biotech Inc. for Merck Millipore, Darmstadt, Germany) according to the manufacturer's instructions. Namely, a 96-well filter plate was used for a precoating procedure with provided 20% w/v slurry resign and Affinity Ligand. Selected cytosols, containing 1 μg/μl of total cell proteins, previously quantified by using the Bicinchoninic Acid Protein Assay Kit (BCA-1, Sigma-Aldrich, St. Louis, Missouri, USA) were incubated with 2 μg of the primary antibody against GSTP1 (Cell Signaling, Danvers, Massachusetts, USA), followed by several washing steps. Finally, samples were resuspended in 30 μl of 2x Laemmli buffer (Bio-Rad, Hercules, CA, USA), denatured at 90°C for five minutes,

Table 1: Baseline characteristics of ccRCC patients and age- and gender-matched controls.

	ccRCC patients	Controls	OR (95% CI[a])	p
Age (years)[b]	58.95 ± 11.65	60.44 ± 10.84	/	0.125
Gender, n (%)				
Female	73 (33)	138 (41)	1.00[c]	
Male	147 (67)	198 (59)	1.467 (0.756-2.847)[d]	0.258
Obesity, n (%)[e]				
BMI < 25	65 (36)	110 (35)	1.00[c]	
BMI > 25	115 (64)	204 (65)	0.866 (0.494-1.518)[f]	0.616
BMI (kg/m^2)	26.61 ± 4.43	26.78 ± 4.08	/	0.677
Smoking, n (%)[e]				
Never	82 (44)	164 (49)	1.00[c]	
Ever[g]	106 (56)	171 (51)	1.289 (0.863-1.925)[h]	0.215
Pack-years[i]	31 (0.30-96.00)	30.00 (0.20-88.00)	/	0.131
Hypertension, n (%)[e]				
No	83 (45)	211 (65)	1.00[c]	
Yes	102 (55)	116 (35)	2.450 (1.375-4.435)[j]	0.002
Tumor grade, n (%)[k]				
Grade I, G1	28 (15)			
Grade II, G2	106 (55)			
Grade III, G3	49 (26)			
Grade IV, G4	8 (4)			
pT stage, n (%)[k]				
pT1	93 (45)			
pT2	23 (11)			
pT3	87 (42)			
pT4	5 (2)			

[a]CI: confidence interval; [b]mean ± SD; [c]reference group; [d]OR: odds ratio adjusted for age, BMI (body mass index), pack-years, and hypertension; [e]based on the data available; [f]OR adjusted for age, gender, pack-years, and hypertension; [g]minimum of a 60-day period any time prior to the study onset; [h]OR adjusted for age, gender, BMI, and hypertension; [i]median (Min–Max); [j]OR adjusted for age, gender, BMI, and pack-years; [k]data available on patients' tumor grade and pT stage, depending on the type of surgery and pathohistological diagnostics.

and collected by centrifugation at 1500 rpm for one minute. Supernatant fraction was further subjected to SDS-PAGE and Western blot analysis according to the previously described protocols.

2.5. Statistical Analysis. Calculations for this investigation were performed using the SPSS software version 17.0 (Chicago, IL, USA). Continuous variables were expressed as mean ± standard deviation (SD) or median (minimum–maximum). Frequency (n, %) counts were used for categorical variables. Distribution of different variables was tested by using the Kolmogorov-Smirnov test. For each examined polymorphism, the Hardy-Weinberg equilibrium was tested. The risk each genetic variant carries for ccRCC development was computed by odds ratios (OR) and 95% confidence intervals (CI) by logistic regression analysis. OR was adjusted for age, gender, and variables indicating recognized risk factors for ccRCC as potential confounders. Survival analysis was performed using the Kaplan-Meier method to estimate the cumulative survival probability. The log-rank test was performed for the assessment of differences in survival according to the different categories of variables. The association between GSTP1 and cleaved caspase-3 expression was analyzed using Spearman's coefficient of linear correlation.

3. Results and Discussion

3.1. Analysis of Genotypes. The analyzed sample included a total number of 223 ccRCC patients and 336 age- and gender-matched controls with the same geographic origin. The main demographic and clinical features of patients and controls are summarized in Table 1.

As presented, recognized risk factors for ccRCC, history of obesity, hypertension, and smoking status, were evaluated. While no significant difference among groups was found regarding obesity and smoking status, more than 50% of patients were presenting hypertension in comparison with 35% hypertensive controls. Additionally, subjects who had history of hypertension exhibited 2.45-fold increased risk for ccRCC development compared to normotensive subjects (95%CI = 1.375-4.435, $p < 0.05$). Grade II, according to the Fuhrman grading system, was the most prevalent among enrolled cases (106 patients—55%). When staged according

Table 2: *Nrf2*, *SOD2*, *GPX1*, and *GSTP1* genotypes in relation to the risk of ccRCC.

Genotypes	ccRCC patients, *n* (%)	Controls, *n* (%)	OR (95% CI)[a]	*p*
Nrf2 (rs6721961)				
C/C[c]	166 (77)	241 (72)	1.00[b]	
C/A and A/A[d]	50 (23)	95 (28)	0.692 (0.370-1.295)	0.250
SOD2 (rs4880)				
Ala/Ala[e]	45 (30)	111 (21)	1.00[b]	
Ala/Val and Val/Val[f]	175 (70)	225 (79)	4.521 (2.167-9.432)	<0.001
GPX1 (rs1050450)				
Pro/Pro[g]	109 (49)	142 (42)	1.00[b]	
Pro/Leu and Leu/Leu[h]	113 (51)	194 (58)	0.567 (0.323-0.994)	0.048
GSTP1 (rs1695)				
Ile/Ile[i]	55 (25)	159 (47)	1.00[b]	
Ile/Val+Val/Val[j]	168 (75)	177 (53)	3.714 (1.952-7.069)	<0.001
GSTP1 (rs1138272)				
Ala/Ala[k]	197 (89)	297 (89)	1.00[b]	
Ala/Val+Val/Val[l]	25 (11)	39 (11)	0.712 (0.309-1.642)	0.426
GSTP1 (rs1695 and rs1138272)				
(Ile/Ile) (Ala/Ala)[m]	54 (24)	144 (43)	1.00[b]	
(Ile/Ile) (Ala/Val+Val/Val)[n]	1 (1)	15 (4)	0.000 (NA[q])	0.999
(Ile/Val+Val/Val) (Ala/Ala)[o]	143 (64)	153 (46)	3.250 (1.668-6.331)	0.001
(Ile/Val+Val/Val) (Ala/Val+Val/Val)[p]	24 (11)	24 (7)	2.719 (0.970-7.624)	0.057

[a]OR: odds ratio adjusted for age, gender, BMI, pack-years, and hypertension; CI: confidence interval; [b]reference group; [c]C/C: carriers of both referent alleles; [d]C/A and A/A: carriers of at least one variant allele; [e]Ala/Ala: carriers of both referent alleles; [f]Ala/Val and Val/Val: carriers of at least one variant allele; [g]Pro/Pro: carriers of both referent alleles; [h]Pro/Leu and Leu/Leu: carriers of at least one variant allele; [i]Ile/Ile: carriers of both referent alleles; [j]Ile/Val and Val/Val: carriers of at least one variant allele; [k]Ala/Ala: carriers of both referent alleles; [l]Ala/Val and Val/Val: carriers of at least one variant allele; [m](Ile/Ile) (Ala/Ala): carriers of both referent alleles for rs1695 and rs1138272; [n](Ile/Ile) (Ala/Val+Val/Val): carriers of both referent alleles for rs1695 and at least one variant allele rs1138272; [o](Ile/Val+Val/Val) (Ala/Ala): carriers of at least one variant allele for rs1695 and both referent alleles for rs1138272; [p](Ile/Val+Val/Val) (Ala/Val+Val/Val): carriers of at least one variant allele for both rs1695 and rs1138272; [q]NA: not applicable.

to the TNM system, we found pT1 and pT3 to be the most numerous stages (93 pT1 cases and 87 pT3 cases).

The distribution of specific genotypes among ccRCC patients and controls is shown in Table 2.

No significant ccRCC risk was revealed for subjects carrying the C/A and A/A *Nrf2* genotype in comparison with carriers of the C/C genotype (OR = 0.692, 95%CI = 0.370–1.295, $p = 0.250$). On the contrary, the risk for ccRCC development was highly increased in individuals with at least one *SOD2* Val allele or precisely Ala/Val and Val/Val *SOD2* genotypes (OR = 4.521, 95%CI = 2.167–9.432, $p < 0.001$). Regarding *GPX1* polymorphism, the risk for ccRCC development was reduced in subjects carrying Pro/Leu and Leu/Leu genotypes when compared to individuals with the Pro/Pro genotype (OR = 0.567, 95%CI = 0.323–0.994, $p = 0.048$). *GSTP1* polymorphisms rs1695 and rs1138272 were studied individually and in combination, as well as the *GSTP1ABCD* haplotype. As presented, subjects with the Ile/Val and Val/Val rs1695 genotype combined with the Ala/Ala rs1138272 genotype had more than 3-fold increased risk for developing clear cell renal cell carcinoma in comparison with carriers of referent genotypes for both polymorphisms (OR = 3.250, 95%CI = 1.668–6.331, $p = 0.001$).

As a part of an immensely complex redox homeostasis maintenance system, the examined enzymes and their genetic polymorphisms were assessed in combination (Table 3). When observed altogether, subjects with the C/C *Nrf2* genotype who were, at the same time, carrying the Ala/Val or Val/Val *SOD2* genotype, exhibited three-fold increased ccRCC risk (OR 3.234, 95%CI = 1.436–7.280, $p = 0.005$), while subjects with C/A or A/A *Nrf2* in combination with the Ala/Val or Val/Val *SOD2* genotype had 2.9-fold increased risk for ccRCC development (OR = 2.918, 95%CI = 1.131–7.532, $p = 0.027$). Almost equally higher risk was found among carriers of combined C/C *Nrf2* and Ile/Val or Val/Val *GSTP1* rs1695 genotypes (OR = 3.211, 95% CI 1.516–6.814, $p = 0.002$). Logistic regression showed no substantial risk when *Nrf2* genotypes were analyzed in combination with *GPX1* and *GSTP1* rs1138272 genotypes.

The increased ccRCC risk was the most pronounced when *SOD2* and either *GSTP1* rs1695 or rs1138272 polymorphisms were examined. Ala/Val and Val/Val *SOD2* genotypes in combination with Ile/Val and Val/Val rs1695 genotypes were associated with almost 20-fold increased risk (OR = 19.724, 95%CI = 4.267–91.165, $p < 0.001$), while 4-fold increased risk for ccRCC development was observed when in combination with the Ala/Ala *GSTP1* rs1138272 genotype (OR = 4.374, 95%CI = 2.012–9.508, $p < 0.001$). Finally, the presence of the *GPX1* Pro/Pro genotype combined with either the Ala/Val or Val/Val *SOD2* genotype and Ile/Val or Val/Val *GSTP1* rs1695 genotype leads to significantly higher risk for this cancer (OR = 3.653, 95%

Table 3: Combined effect of *Nrf2*, *SOD2*, *GPX1*, and *GSTP1* genotypes in relation to the risk of ccRCC carriers of at least one variant allele.

Genotypes	*Nrf2* (rs6721961)		*SOD2* (rs4880)		*GSTP1* (rs1695)		*GSTP1* (rs1138272)	
	C/C[c]	C/A and A/A[d]	Ala/Ala[e]	Ala/Val and Val/Val[f]	Ile/Ile[i]	Ile/Val+Val/Val[j]	Ala/Ala[k]	Ala/Val+Val/Val[l]
Nrf2 (rs6721961) C/C[c]								
OR (95% CI)[a]	—	—	—	—	1.00[b]	3.211 (1.513-6.814)	1.00[b]	1.067 (0.41-2.779)
p	—	—	—	—	—	0.002	—	0.894
Nrf2 (rs6721961) C/A and A/A[d]								
OR (95% CI)[a]	—	—	—	—	0.385 (0.095-1.564)	2.731 (1.107-6.739)	0.835 (0.430-1.621)	0.162 (0.019-1.408)
p	—	—	—	—	0.182	0.029	0.594	0.099
SOD2 (rs4880) Ala/Ala[e]								
OR (95% CI)[a]	1.00[b]	0.308 (0.059-1.599)	—	—	1.00[b]	4.796 (0.927-24.81)	1.00[b]	0.594 (0.064-5.504)
p	—	0.161	—	—	—	0.062	—	0.646
SOD2 (rs4880) Ala/Val and Val/Val[f]								
OR (95% CI)[a]	3.234 (1.436-7.280)	2.918 (1.131-7.532)	—	—	5.875 (1.190-29.00)	19.724 (4.267-91.16)	4.374 (2.012-9.508)	3.290 (1.054-10.26)
p	0.005	0.027	—	—	0.030	<0.001	<0.001	0.040
GPX1 (rs1050450) Pro/Pro[g]								
OR (95% CI)[a]	1.00[b]	0.423 (0.158-1.133)	1.00[b]	3.653 (1.148-11.63)	1.00[b]	5.476 (2.127-14.10)	1.00[b]	0.826 (0.238-2.868)
p	—	0.087	—	0.028	—	*<0.001*	—	0.763
GPX1 (rs1050450) Pro/Leu and Leu/Leu[h]								
OR (95% CI)[a]	0.440 (0.223-0.868)	0.456 (0.188-1.057)	0.553 (0.144-2.120)	2.533 (0.793-8.094)	0.720 (0.239-2.165)	2.194 (0.912-5.287)	0.585 (0.322-1.063)	0.372 (0.115-1.199)
p	0.018	0.067	0.388	0.117	0.558	0.079	0.079	0.098

[a]OR: odds ratio adjusted for age, gender, BMI, pack-years, and hypertension; CI: confidence interval; [b]reference group; [c]C/C: carriers of both referent alleles; [d]C/A and A/A: carriers of both referent alleles; [e]Ala/Ala: carriers of both referent alleles; [f]Ala/Val and Val/Val: carriers of at least one variant allele; [g]Pro/Pro: carriers of both referent alleles; [h]Pro/Leu and Leu/Leu: carriers of at least one variant allele; [i]Ile/Ile: carriers of both referent alleles; [j]Ile/Val and Val/Val: carriers of at least one variant allele; [k]Ala/Ala: carriers of both referent alleles; [l]Ala/Val and Val/Val: carriers of at least one variant allele.

Table 4: Haplotype analysis of *GSTP1* rs1695 and rs1138272 polymorphisms in patients with ccRCC.

	Genotype		Haplotype frequencies			
	rs1695	rs1138272	ccRCC patients, %	Controls, %	OR (95% CI)[a]	*p* value
GSTP1A[d]	∗A	∗C	56	64	1.00[b]	
GSTP1B[e]	∗G	∗C	38	30	1.50 (1.10–2.05)	0.012
GSTP1C[f]	∗G	∗T	5	3	3.50 (1.49–8.22)	0.004
GSTP1D[g]	∗A	∗T	1	3	0.00 (N/A[c])	1.000
			Global haplotype association *p* value: <0.001			

[a]OR: odds ratio adjusted for age, gender, BMI, pack-years, and hypertension; CI: confidence interval; [b]reference group; [c]N/A: not applicable; [d]*GSTP1A* genotype consisting of Ile105 and Ala114; [e]*GSTP1B* genotype consisting of Val105 and Ala114; [f]*GSTP1C* genotype consisting of Val105 and Val114; [g]*GSTP1D* genotype consisting of Ile105 and Val114.

Table 5: *Nrf2*, *SOD2*, *GPX1*, and *GSTP1* genotype distribution among living and deceased ccRCC patients.

Genotype	Living patients, *n* (%)	Deceased patients, *n* (%)	*p* value
Nrf2 (rs6721961)			
C/C[a]	99 (76)	59 (75)	
C/A and A/A[b]	31 (24)	19 (25)	0.530
SOD2 (rs4880)			
Ala/Ala[c]	31 (24)	12 (15)	
Ala/Val and Val/Val[d]	101 (76)	68 (85)	0.093
GPX1 (rs1050450)			
Pro/Pro[e]	57 (43)	46 (57)	
Pro/Leu and Leu/Leu[f]	77 (57)	34 (43)	0.024
GSTP1 (rs1695 and rs1138272)			
(Ile/Ile) (Ala/Ala)[g]	41 (31)	12 (15)	
(Ala/Ala)(Pro/Leu+Leu/Leu) (Ala/Val+Val/Val)(Pro/Pro) (Ala/Val+Val/Val)(Pro/Leu+Leu/Leu)[h]	93 (69)	68 (85)	0.007

[a]C/C: carriers of both referent alleles; [b]C/A and A/A: carriers of at least one variant allele; [c]Ala/Ala: carriers of both referent alleles; [d]Ala/Val and Val/Val: carriers of at least one variant allele; [e]Pro/Pro: carriers of both referent alleles; [f] Pro/Leu and Leu/Leu: carriers of at least one variant allele; [g](Ile/Ile) (Ala/Ala): carriers of both referent alleles for rs1695 and rs1138272; [h]carriers of at least one variant allele for either rs1695 or rs1138272.

CI = 1.148–11.630, $p = 0.028$ and OR = 5.476, 95%CI = 2.127–14.102, $p < 0.001$, respectively).

In the next step, haplotype analysis of *GSTP1* rs1695 and rs1138272 polymorphisms was performed and is presented in Table 4. The *GSTP1A* genotype represents a combination of A313 and C114, meaning that the enzyme has isoleucine at position 105 and alanine at 114. The genotype with G313 and C114 or valine at 105 and alanine at 114 is *GSTP1B*. The presence of G313 and T114 or valine at both 105 and 114 represents *GSTP1C*, while the form consisting of isoleucine at position 105 and valine at 114 (A313 and T114) is *GSTP1D* [40]. The haplotype composed of wild-type alleles ∗A and ∗C was the most frequent among ccRCC patients (56%) and controls (64%). Regarding the effect of the GSTP1ABCD haplotype on ccRCC susceptibility, the haplotype consisting of variant alleles of both polymorphisms ∗G and ∗T was associated with 3.5-fold increased risk (OR = 3.50, 95%CI = 1.49–8.22, $p = 0.004$).

3.2. Follow-Up Analysis. Of 223 ccRCC cases, follow-up data were acquired for 215 (96%) patients in a period from 2005 to 2018. There were a total number of 80 deaths (37%) and 135 survivals during the mean follow-up period of 67.31 ± 37.68 months (ranging from 1 to 161 months). Table 5 presents Nrf2, SOD2, GPX1, and GSTP1 genotype distribution among living and deceased ccRCC patients.

Statistically significant difference in frequencies was observed among carriers of Pro/Leu and Leu/Leu genotypes of the examined *GPX1* polymorphism ($p = 0.024$). Regarding the *GSTP1ABCD* haplotype, statistically significant difference in frequencies was observed between carriers of at least one variant allele and carriers of a referent genotype of both *GSTP1* polymorphisms (Table 5).

Table 6 represents the analysis of different examined genotypes as potential predictors for overall mortality. The analysis was performed in two models, based on different adjustments. Although without reaching statistical significance, the *GSTP1-variant* genotype consisting of at least one Val105 allele in the case of rs1695, in combination with at least one Val114 allele in the case of rs1138272, expressed the highest hazard ratio in ccRCC patients (model 1 HR = 1.627, 95%CI = 0.664–3.986, $p = 0.287$; model 2 HR = 3.897,

Table 6: *Nrf2*, *SOD2*, *GPX1*, and *GSTP1* polymorphisms as predictors for overall mortality in patients with ccRCC.

Model 1[a]		Model 2[b]	
HR (95% CI)	*p* value	HR (95% CI)	*p* value
Risk for overall mortality comparing *Nrf2-variant*[c] genotype to *Nrf2-reference*[d]-type genotype carriers			
1.030 (0.579–1.833)	0.919	1.104 (0.456–2.674)	0.826
Risk for overall mortality comparing *SOD2-variant*[e] genotype to *SOD2-reference*[f]-type genotype carriers			
1.290 (0.676–2.461)	0.440	1.687 (0.494–5.755)	0.404
Risk for overall mortality comparing *GPX1-variant*[g] genotype to *GPX1-reference*[h]-type genotype carriers			
0.737 (0.462–1.177)	0.201	1.388 (0.654–2.946)	0.393
Risk for overall mortality comparing *GSTP1-variant*[i] genotype to *GSTP1-reference*[j]-type genotype carriers			
1.627 (0.664–3.986)	0.287	3.897 (0.681–22.304)	0.126

[a]Model 1 adjusted for age and gender; [b]model 2 adjusted for the covariates from model 1 and recognized risk factors for ccRCC development (pack-years, BMI, and hypertension); [c]*Nrf2-variant*-type genotype—C/A+A/A; [d]*Nrf2-reference* genotype—C/C; [e]*SOD2* variant-type genotype—Ala/Val+Val/Val; [f]*SOD2* reference genotype—Ala/Ala; [g]*GPX1-variant*-type genotype—Pro/Leu+Leu/Leu; [h]*GPX1-reference* genotype—Pro/Pro; [i]*GSTP1-variant*-type genotype—combination of genotypes of rs1695 and rs1138272 SNPs (Ile/Val+Val/Val) (Ala/Val+Val/Val); [j]*GSTP1-reference* genotype—combination of reference genotypes of both rs1695 and rs1138272 (Ile/Ile) (Ala/Ala); HR: hazard ratio; CI: confidence interval.

95%CI = 0.681–22.304, $p = 0.126$). On the other hand, none of the other investigated genotypes showed any predicting potential in terms of ccRCC overall mortality.

The Kaplan-Meier survival curves for overall mortality according to *Nrf2*, *GSTP1*, *SOD2*, and *GPX1* genes in ccRCC patients are presented in Figure 1. This analysis for overall survival did not show significantly shorter time of survival in patients carrying a specific *Nrf2*, *SOD2*, or *GPX1* genotype ($p > 0.05$, Figures 1(a), 1(c), and 1(d)). However, patients who were carrying any of variant *GSTP1* genotypes were recognized as patients with shorter overall survival (log-rank $p = 0.038$) (Figure 1(b)).

3.3. Analysis of Protein Expression. Since GSTP1 protein may negatively regulate JNK and therefore affect the apoptotic activity, especially within tumor tissue, we analyzed the GSTP1 protein expression both in a pool of nontumor kidney tissue samples and in ccRCC tissue samples, however independently of the *GSTP1* genotype. Moreover, the potential presence of GSTP1 : JNK1/2 complexes was assessed in specimens of tumor tissue obtained from 20 patients with ccRCC. Despite gradual increase in the expression across tumor grades (G1-G3), significant difference was not observed neither for GSTP1 protein levels in ccRCC tissue samples alone (Figure 2, $p > 0.05$) nor between the nontumor kidney tissue pool and ccRCC tissue samples ($p > 0.05$).

Although the JNK1/2 expressed was evidently higher in the nontumor kidney tissue pool in comparison with ccRCC tissue samples (Figure 3), the obtained results were not statistically significant ($p > 0.05$).

Still, the expression of executor cleaved caspase-3 gradually decreased across tumor grade (G1-G3), reaching the statistical significance only in G3, when compared to the pool of nontumor kidney tissue samples (Figure 4, $p < 0.05$).

However, a weak positive correlation (correlation coefficient, $r < 0.3$) was found only between GSTP1 and cleaved caspase-3 expression ($r = 0.024$, $p = 0.999$).

In order to investigate the presence of GSTP1 : JNK1 protein : protein interactions, tumor tissue samples were divided into three groups, according to the tumor's grade. Although the effect of *GSTP1* polymorphic expression was not assessed, the analyzed samples comprised all three GSTP genotypes. Namely, the *GSTP1 IleIle* genotype was present in 30%, *GSTP1 IleVal* in 40%, and *GSTP1 ValVal* in 30% samples. Protein immunoprecipitation, followed by Western blot analysis, showed the presence of JNK1/2/GSTP1 complexes in all assessed ccRCC samples (Figure 5).

4. Discussion

In recent years, attention has been raised toward genetic variants, often referred to as "quantitative trait loci" that could contribute to a small, but significant, risk not only for the development but also for the progression of complex disorder such as cancer [41]. Deleterious effects of SNP polymorphisms found in genes encoding transcriptional factors, as well as antioxidant and detoxification enzymes, are still disputable; however, their functional significance might seem to modify the risk for RCC development. Moreover, there is a growing body of evidence that glutathione transferases may participate in tumor progression and affect patients' survival by regulating a number of cellular processes via protein : protein interactions as endogenous negative regulators of protein kinases [16, 17, 42–45].

In this study, we examined the role of genetic polymorphisms of the transcriptional factor Nrf2 and genes coding SOD2 and GPX1, as well as GSTP1, in ccRCC development. We noticed an increased risk of ccRCC development among carriers of variant genotypes of both *SOD2* rs4880 and *GSTP1* rs1695 polymorphisms. *Nrf2* rs6721961 genetic polymorphism in combination with both rs4880 and rs1695 showed higher risk for this type of tumor as well. Since two examined SNPs of *GSTP1*, rs1695 and rs1138272, are close in their position, haplotype analysis was performed. It revealed that significant risk of ccRCC development is associated with a genotype consisting of variant forms of both polymorphisms, while the molecular mechanism underlying the role of GSTP1 forms in RCC progression might be explained by the presence of GSTP1 : JNK1/2 protein : protein interactions.

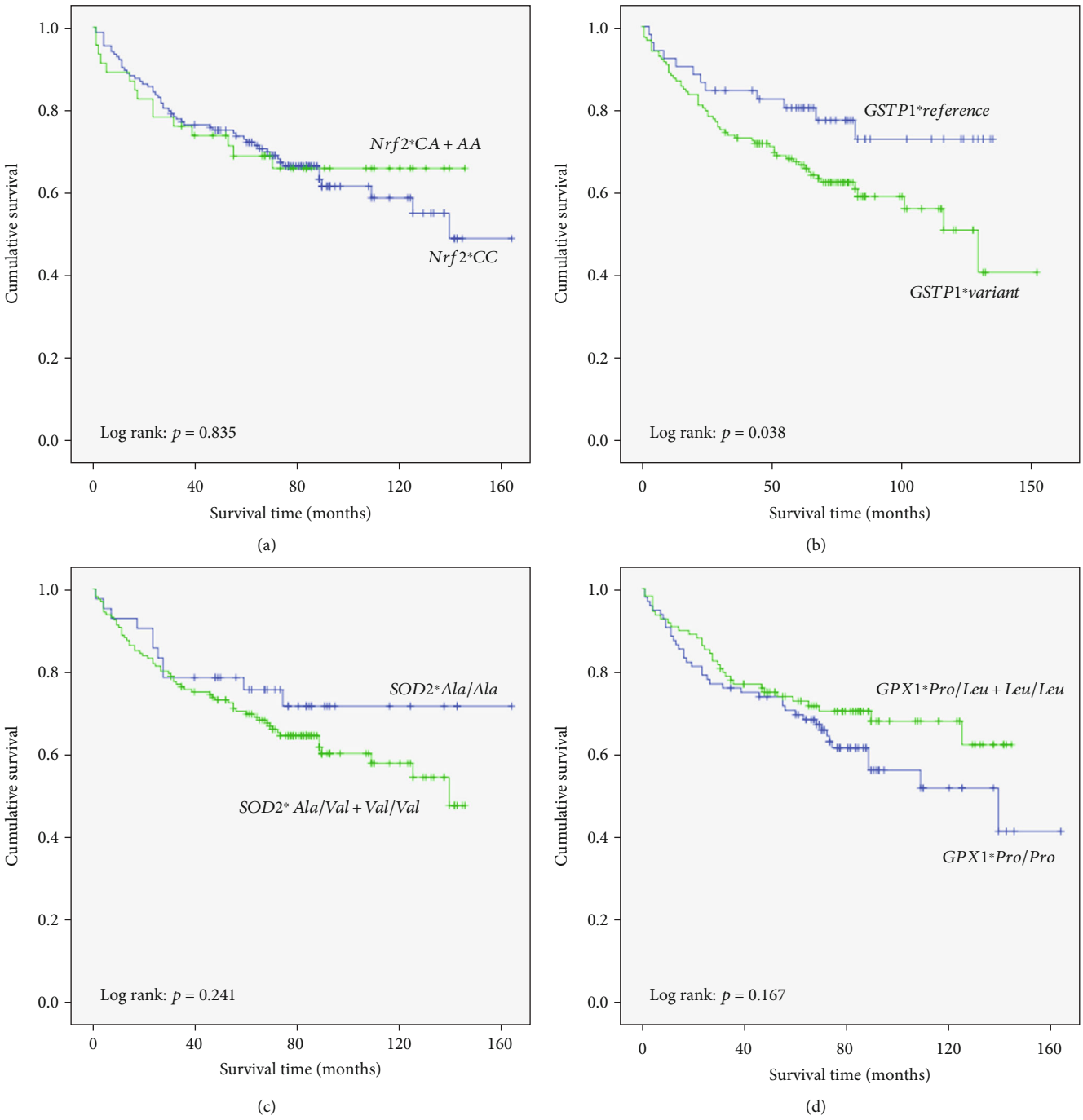

Figure 1: Kaplan-Meier survival curves for overall mortality according to (a) *Nrf2* polymorphism, (b) *GSTP1* polymorphisms rs1695 and rs1138272 in combination (*GSTP1* ∗ *reference* genotype—(Ile/Ile) (Ala/Ala); *GSTP1* ∗ *variant*-type genotypes—(Ile/Val+Val/Val)(Ala/Ala), (Ile/Ile)(Ala/Val+Val/Val), and (Ile/Val+Val/Val)(Ala/Val+Val/Val)), (c) *SOD2* polymorphism, and (d) *GPX1* polymorphism.

It has been shown that Nrf2 deficiency decreases the ability of tissue to properly react to exposure to oxidative and electrophilic stressors [46]. The importance of SNP rs6721961 for further Nrf2 activity has been shown, since this polymorphism is positioned in the middle of the ARE motif and affects the binding of Nrf2 to the ARE. Homozygous *A*/*A* subjects exhibit lower level of Nrf2 mRNA which further leads to lower protein activity [47]. Suzuki et al. demonstrated that smokers—carriers of the *A*/*ANrf2* genotype—had increased risk of lung cancer development [47], while at the same time, Okano et al. even suggested that this polymorphism should be considered a prognostic biomarker for assessing prognosis in lung adenocarcinoma patients [29]. What is more, women carrying this specific genotype have higher risk for breast cancer development and decreased protein expression in cancer tissue [48].

There are no studies of whether the *Nrf2*-617C/A polymorphism has impact on RCC development. When it comes

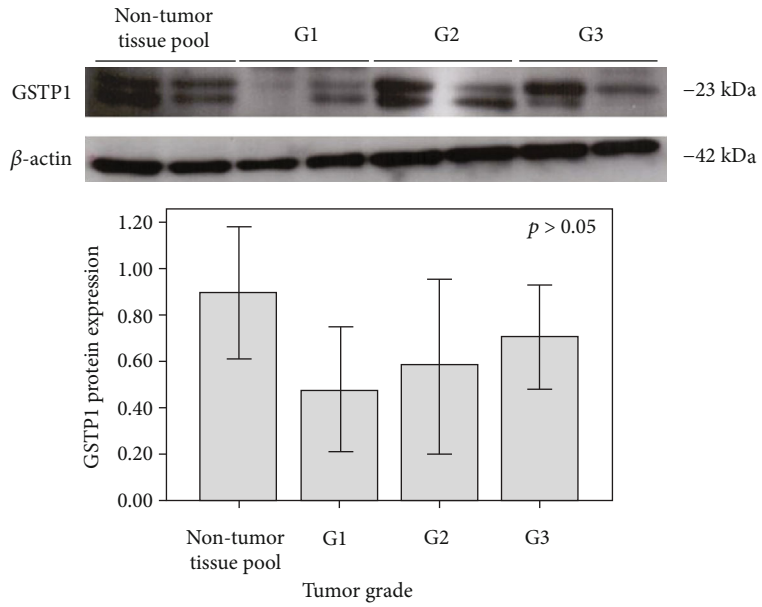

Figure 2: Expression of GSTP1 (23 kDa) protein analyzed by immunoblot in a pool of nontumor kidney tissue samples, as well as in ccRCC tissue samples (G1-G3). G1: tumor grade I; G2: tumor grade II; G3: tumor grade III. Expression of β-actin (42 kDa) protein in a pool of nontumor kidney tissue samples, as well as in ccRCC tissue samples (G1-G3), is used as a normalization control.

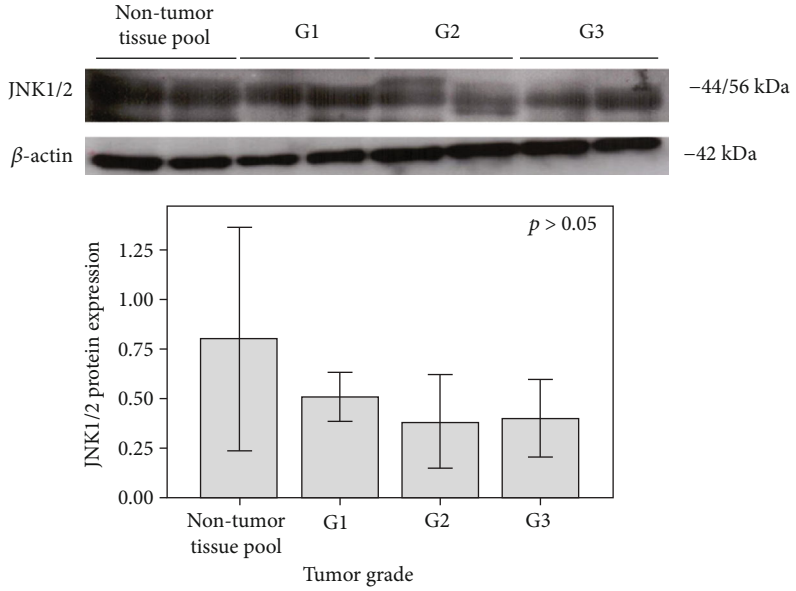

Figure 3: Expression of JNK1/2 (44/56 kDa) protein in a pool of nontumor kidney tissue samples, as well as in ccRCC tissue samples (G1-G3). G1: tumor grade I; G2: tumor grade II; G3: tumor grade III. Expression of β-actin (42 kDa) protein in a pool of nontumor kidney tissue samples, as well as in ccRCC tissue samples (G1-G3), is used as a normalization control.

to tumors of the urinary tract, Reszka et al. found no association between SNP rs6721961 and risk for urinary bladder cancer [27]. Similarly, our results did not show any significant difference in frequencies of different genotypes among ccRCC patients and corresponding controls. Still, in already developed renal cell carcinoma, higher expression of Nrf2 protein in carriers of the *C*/*C* genotype seems to point out the patients with poor prognosis and shorter overall survival [49]. Furthermore, when the expression of Nrf2 is elevated, RCC metastasis has inadequate and unsatisfying response to therapy which leads to unfavorable outcome [50]. According to our follow-up analysis, patients with the *C*/*C* genotype did have shorter overall survival compared to *C*/*A* and *A*/*A* carriers, although it was not statistically significant.

Many genes targeted by Nrf2 encode enzymes essential in antioxidative stress response which enables cellular adaptation to new conditions [47]. Glutathione S-transferases as enzymes regulated by Nrf2 activity take part in defense against stressors [51]. Although meta-analysis did not find association between *GSTP1* rs1695 polymorphism and RCC

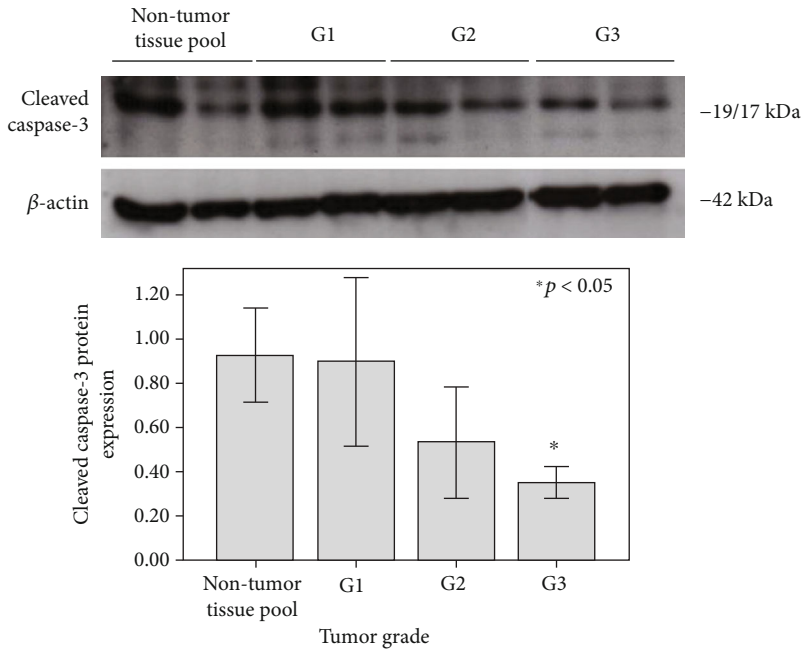

Figure 4: Expression of cleaved caspase-3 (19/17 kDa) protein in a pool of nontumor kidney tissue samples, as well as in ccRCC tissue samples (G1-G3) ($^*p < 0.05$). Expression of β-actin (42 kDa) protein in a pool of nontumor kidney tissue samples, as well as in ccRCC tissue samples (G1-G3), is used as a normalization control.

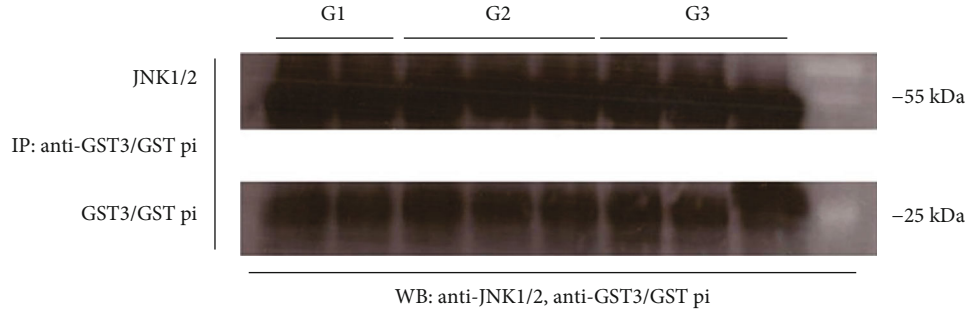

Figure 5: Cytosols obtained from ccRCC tissue homogenates were immunoprecipitated with an anti-GST3/GST pi antibody. The samples were subjected to SDS-PAGE on 10% gel, followed by incubation with the primary antibodies against GST3/GST pi and JNK1/2. G1: tumor grade I; G2: tumor grade II; G3: tumor grade III; IP: immunoprecipitation; WB: Western blot.

development [31, 52], the results of our previous studies on RCC patients indeed demonstrated a significantly increased risk for cancer development in patients carrying the *GSTP1-variant* (*Ile*/*Val*+*Val*/*Val*) genotype [16], which was in line with the results obtained on the subpopulation of ccRCC patients [53]. In addition to rs1695, in this study, we analyzed rs1138272 SNP as well. There was significant difference in distribution of the rs1695 genotype among patients and controls, but no association between ccRCC and rs1138272. Four haplotypes involving these two polymorphisms have been defined. Maniglia et al. found haplotypes *GSTP1A* and *GSTP1D* having higher frequency among cases of head and neck squamous cell carcinoma than among controls [54]. Since the overall functions of GSTs also include the regulation of cell signaling, the *GSTP1C* haplotype has been considered a better c-Jun N-terminal kinase 1 inhibitor than the reference *GSTP1A* haplotype [32]. In line with these results, our study showed higher risk for ccRCC for carriers of the *GSTP1C* haplotype.

Based on the established role of the GSTPi class in inhibition of JNK1 and its antiapoptotic effect [17, 45], we assessed the expression of GSTP1 and expression of regulatory (JNK1/2) and executor (caspase-3) apoptotic molecules in human ccRCC tissue samples, as well as the presence GSTP1 : JNK1/2 protein : protein interactions, however irrespective of the *GSTP1* genotype. At first, we noticed gradual increase in the GSTP1 protein across tumor grades, although without significant difference. Secondly, our results showed lower level of JNK1/2 expressed in tumor tissue in comparison with nontumor kidney tissue. Furthermore, the expression of cleaved caspase-3, one of the key executory enzymes leading to apoptosis, was statistically significantly decreased in grade 3 when compared to expression in nontumor tissue. In addition, we found a weak, yet positive, correlation

between GSTP1 and cleaved caspase-3 expression. Finally, by analyzing ccRCC tissue homogenates, we found GSTP1 : JNK1/2 complexes in all assessed samples. The particular interaction has been found in human leukemia, hepatic carcinoma, bladder cancer, and neuroblastoma cells [55]. Presumably, tumors with upregulated GSTP1, such as RCC, could have their kinase-dependent apoptotic signaling pathways suppressed, owning to negative regulation of JNK1. Thévenin et al. showed that protein produced in carriers of the Val105 and Val114 genotype acts as a better JNK inhibitor [32]. Indeed, our results have shown that carriers of *GSTP1-variant*-type genotypes—(*Ile*/*Val*+*Val*/*Val*) (*Ala*/*Val* +*Val*/*Val*)—exhibited poorer survival. It is important to note that the GSTP-JNK interaction is shown to be redox-dependent with possible formation of oligomeric forms of GSTP and other thiol-containing proteins, such as Prdx both 1 and 6 [56, 57]. Since Prdx6 seems to be responsible for substantial inhibition of GSTP1 heterodimerization, independently of allelic variations, while Prdx1, once released from the GSTP-JNK complex, maintains its peroxidase activity, it seems plausible that genetic variations in Prdx, both 1 and 6, might play a critical role in this context [57].

Another enzyme influenced by Nrf2 is manganese superoxide dismutase. Involvement of polymorphism rs4880 in cancer susceptibility has been extensively investigated. Comprehensive meta-analysis by Wang et al. showed *SOD2* rs4880 polymorphism to be connected with lung cancer [58]. Various meta-analyses found no association between this SNP and urinary bladder or breast cancer risk [21, 59]. Those studies that actually reported increased risk for breast cancer usually reported the Ala/Ala genotype to be the most frequent, although the carriers of the Val16 variant are expected to be at greater cancer risk [60]. Similarly, some authors found aggressive forms of prostate cancer to be associated with the *Ala*/*Ala* genotype [61]. Atilgan et al. found that risk for development of any kind of histologic subtypes of renal cell carcinoma is increased with *Ala*/*Val* and *Ala*/*Ala* genotypes [35]. In our study, when only clear cell carcinoma was observed, carriers of *Ala*/*Val* and *Val*/*Val* genotypes were exposed to significantly greater risk. When analyzed in combination with *Nrf2*, *GPX1*, and both rs1695 and rs1138272 *GSTP1* SNPs, significant risk was also noted. In addition, according to our results, overall survival was shorter among patients with *Ala*/*Val* and *Val*/*Val* genotypes still without statistical significance. It is suggested that the Val16 variant of SOD2 comprises parts of β-sheet structure and therefore is inefficiently transported into the mitochondrial cytosol which diminishes its function and further leads to inadequate superoxide anion neutralization [62]. However, Dasgupta et al. found that excessive H_2O_2 production leads to reduced sensitivity to tumor necrosis factor-α-mediated apoptosis [63]. Hence, it is still debated whether higher or lower SOD2 protein activity should be seen as a definite risk factor.

Glutathione peroxidase-1 is considered a gatekeeper able to stop detrimental damage caused by H_2O_2 produced by higher SOD2 activity [64]. In different stages of carcinogenesis, regulation of GPX1 levels is essential [65]. Many authors advocate SNP rs1050450 in the *GPX1* gene to contribute to susceptibility to various cancers [36, 66]. Namely, meta-analysis investigating the effect of this polymorphism revealed that variant genotypes (*Pro*/*Leu* and *Leu*/*Leu*) were associated with increased risk for lung cancer, bladder cancer, prostate cancer, head and neck cancer, and brain cancer [21, 67, 68]. However, Nikic et al. found no impact of *GPX1* polymorphism on overall survival in patients with metastatic urothelial bladder cancer [69]. Our results did not reveal increased risk for carriers of *Pro*/*Leu* and *Leu*/*Leu*; on the contrary, risk was reduced among these subjects. Follow-up analysis revealed that these variant allele carriers had shorter cumulative survival, but this was not statistically significant. This is not the first time to encounter that the Leu allele is associated with protection. Considering the fact that the variant GPX1 exhibits lower enzyme activity, the explanation of such phenomenon in ccRCC is challenging. However, as recently suggested, the roles of hydrogen peroxide in signal transduction and regulation of genes involved in longevity might have priority when compared to its potential to cause oxidative damage [70]. Further studies are needed to elucidate the mechanisms by which alteration in H_2O_2 reduction is associated with better survival and lower susceptibility to clear cell renal cell carcinoma.

Just recently, when expression of GPX1 protein was evaluated in RCC, high GPX1 level was in a positive correlation with tumor stage, distant metastasis, lymphatic metastasis, and shorter overall survival [24]. These contradictory results on the influence of *GPX1* polymorphism on both enzyme synthesis and activity should be further examined and revealed.

This study has several limitations that need to be addressed. The case-control study design and therefore selection bias, as well as the recall bias, regarding the recognized risk factors for ccRCC development might have influenced the results. Also, the control group was relatively small and comprised of hospital-based patients. Furthermore, the possible effect of ethnicity could not be evaluated as the study group consisted of Caucasians only.

5. Conclusions

Some important novel aspects regarding the role of SNPs in genes encoding the transcriptional factor Nrf2, mitochondrial SOD2, and GPX1 and *GSTP1ABCD* haplotype in pathophysiology of ccRCC are provided in this study. Namely, increased ccRCC susceptibility was observed among carriers of individual variant genotypes of both *SOD2* rs4880 and *GSTP1* rs1695 polymorphisms, as well as in combination with *Nrf2* rs6721961 genetic polymorphism. Furthermore, *GSTP1ABCD* haplotype analysis revealed significant risk of ccRCC development in carriers of the *GSTP1C* haplotype consisting of variant forms of both GSTP1 polymorphisms comprising this haplotype. Our study also provides evidence in favor of hypothesis that certain GST variant genotypes represent not only significant genetic risk factors for ccRCC development but also a significant prognostic factor. In this line, GSTP1 variant forms seem to affect the overall survival in patients with ccRCC and the proposed molecular mechanism underlying the role of GSTP1 forms in RCC progression

might be the presence of GSTP1 : JNK1/2 protein : protein interactions.

Data Availability

The data that support the findings of this study are available from the corresponding author (MPE) upon reasonable request.

Disclosure

A portion of the results presented in this paper (Western blot analysis) is a part of the PhD thesis from Vesna Coric, MD, conducted and defended at the Faculty of Medicine, University of Belgrade.

Conflicts of Interest

The authors declare that there is no conflict of interest regarding the publication of this paper.

Acknowledgments

We thank the patients for taking part in the study and clinical staff for facilitating the collections of the samples. This research was funded by the Ministry of Education, Science and Technological Development of Serbia (grant number 175052).

References

[1] F. Ursini, M. Maiorino, and H. J. Forman, "Redox homeostasis: the golden mean of healthy living," *Redox Biology*, vol. 8, pp. 205–215, 2016.

[2] S. Mena, A. Ortega, and J. M. Estrela, "Oxidative stress in environmental-induced carcinogenesis," *Mutation Research/-Genetic Toxicology and Environmental Mutagenesis*, vol. 674, no. 1-2, pp. 36–44, 2009.

[3] M. Pljesa-Ercegovac, A. Savic-Radojevic, V. Coric, T. Radic, and T. Simic, "Glutathione transferase genotypes may serve as determinants of risk and prognosis in renal cell carcinoma," *BioFactors*, vol. 46, no. 2, pp. 229–238, 2020.

[4] B. Ljungberg, L. Albiges, Y. Abu-Ghanem et al., "European Association of Urology guidelines on renal cell carcinoma: the 2019 update," *European Urology*, vol. 75, no. 5, pp. 799–810, 2019.

[5] C. Protzel, M. Maruschke, and O. W. Hakenberg, "Epidemiology, aetiology, and pathogenesis of renal cell carcinoma," *European Urology Supplements*, vol. 11, no. 3, pp. 52–59, 2012.

[6] F. Chen, Y. Zhang, Y. Şenbabaoğlu et al., "Multilevel genomics-based taxonomy of renal cell carcinoma," *Cell Reports*, vol. 14, no. 10, pp. 2476–2489, 2016.

[7] N. Pandey, V. Lanke, and P. K. Vinod, "Network-based metabolic characterization of renal cell carcinoma," *Scientific Reports*, vol. 10, no. 1, p. 5955, 2020.

[8] F. P. Fabrizio, M. Costantini, M. Copetti et al., "Keap1/Nrf2 pathway in kidney cancer: frequent methylation of Keap1 gene promoter in clear renal cell carcinoma," *Oncotarget*, vol. 8, pp. 11187–11198, 2016.

[9] P. Basak, P. Sadhukhan, P. Sarkar, and P. C. Sil, "Perspectives of the Nrf-2 signaling pathway in cancer progression and therapy," *Toxicology Reports*, vol. 4, pp. 306–318, 2017.

[10] D. V. Chartoumpekis, N. Wakabayashi, and T. W. Kensler, "Keap1/Nrf2 pathway in the frontiers of cancer and non-cancer cell metabolism," *Biochemical Society Transactions*, vol. 43, no. 4, pp. 639–644, 2015.

[11] V. Krajka-Kuźniak, J. Paluszczak, and W. Baer-Dubowska, "The Nrf2-ARE signaling pathway: an update on its regulation and possible role in cancer prevention and treatment," *Pharmacology Reports*, vol. 69, no. 3, pp. 393–402, 2017.

[12] M. B. Sporn and K. T. Liby, "NRF2 and cancer: the good, the bad and the importance of context," *Nature Reviews. Cancer*, vol. 12, no. 8, pp. 564–571, 2012.

[13] H. Y. Cho, J. Marzec, and S. R. Kleeberger, "Functional polymorphisms in Nrf2: implications for human disease," *Free Radical Biology & Medicine*, vol. 88, no. Part B, pp. 362–372, 2015.

[14] D. Bartolini and F. Galli, "The functional interactome of GSTP: a regulatory biomolecular network at the interface with the Nrf2 adaption response to oxidative stress," *Journal of Chromatography, B: Analytical Technologies in the Biomedical and Life Sciences*, vol. 1019, pp. 29–44, 2016.

[15] O. Vasieva, "The many faces of glutathione transferase pi," *Current Molecular Medicine*, vol. 11, no. 2, pp. 129–139, 2011.

[16] V. M. Coric, T. P. Simic, T. D. Pekmezovic et al., "GSTM1 genotype is an independent prognostic factor in clear cell renal cell carcinoma," *Urologic Oncology: Seminars and Original Investigations*, vol. 35, pp. 409–417, 2017.

[17] P. G. Board and D. Menon, "Glutathione transferases, regulators of cellular metabolism and physiology," *Biochimica et Biophysica Acta (BBA) - General Subjects*, vol. 1830, no. 5, pp. 3267–3288, 2013.

[18] D. Bartolini, J. Commodi, M. Piroddi et al., "Glutathione S-transferase pi expression regulates the Nrf2-dependent response to hormetic diselenides," *Free Radical Biology & Medicine*, vol. 88, no. Part B, pp. 466–480, 2015.

[19] M. Pljesa-Ercegovac, A. Savic-Radojevic, M. Matic et al., "Glutathione transferases: potential targets to overcome chemoresistance in solid tumors," *International Journal of Molecular Sciences*, vol. 19, no. 12, p. 3785, 2018.

[20] P. C. Hart, M. Mao, A. L. P. de Abreu et al., "MnSOD upregulation sustains the Warburg effect via mitochondrial ROS and AMPK-dependent signalling in cancer," *Nature Communications*, vol. 6, no. 1, 2015.

[21] M. Cao, X. Mu, C. Jiang, G. Yang, H. Chen, and W. Xue, "Single-nucleotide polymorphisms of GPX1 and MnSOD and susceptibility to bladder cancer: a systematic review and meta-analysis," *Tumor Biology*, vol. 35, no. 1, pp. 759–764, 2014.

[22] Y. Wang, R. Branicky, A. Noë, and S. Hekimi, "Superoxide dismutases: dual roles in controlling ROS damage and regulating ROS signaling," *The Journal of Cell Biology*, vol. 217, no. 6, pp. 1915–1928, 2018.

[23] H. Miess, B. Dankworth, A. M. Gouw et al., "The glutathione redox system is essential to prevent ferroptosis caused by impaired lipid metabolism in clear cell renal cell carcinoma," *Oncogene*, vol. 37, no. 40, pp. 5435–5450, 2018.

[24] Y. Cheng, T. Xu, S. Li, and H. Ruan, "GPX1, a biomarker for the diagnosis and prognosis of kidney cancer, promotes the progression of kidney cancer," *Aging (Albany NY)*, vol. 11, no. 24, pp. 12165–12176, 2019.

[25] E. Lubos, J. Loscalzo, and D. E. Handy, "Glutathione peroxidase-1 in health and disease: from molecular mechanisms to therapeutic opportunities," *Antioxidants & Redox Signaling*, vol. 15, no. 7, pp. 1957–1997, 2011.

[26] J. M. Marzec, J. D. Christie, S. P. Reddy et al., "Functional polymorphisms in the transcription factor NRF2 in humans increase the risk of acute lung injury," *The FASEB Journal*, vol. 21, no. 9, pp. 2237–2246, 2007.

[27] E. Reszka, Z. Jablonowski, E. Wieczorek et al., "Polymorphisms of NRF2 and NRF2 target genes in urinary bladder cancer patients," *Journal of Cancer Research and Clinical Oncology*, vol. 140, no. 10, pp. 1723–1731, 2014.

[28] T. Ishikawa, "Genetic polymorphism in the NRF2 gene as a prognosis marker for cancer chemotherapy," *Frontiers in Genetics*, vol. 5, 2014.

[29] Y. Okano, U. Nezu, Y. Enokida et al., "SNP (-617C>A) in ARE-like loci of the NRF2 gene: a new biomarker for prognosis of lung adenocarcinoma in Japanese non-smoking women," *PLoS One*, vol. 8, no. 9, article e73794, 2013.

[30] F. Ding, J. P. Li, Y. Zhang, G. H. Qi, Z. C. Song, and Y. H. Yu, "Comprehensive analysis of the association between the Rs1138272 polymorphism of the GSTP1 gene and cancer susceptibility," *Frontiers in Physiology*, vol. 9, 2019.

[31] X. Yang, S. Long, J. Deng, T. Deng, Z. Gong, and P. Hao, "Glutathione S-transferase polymorphisms (GSTM1, GSTT1 and GSTP1) and their susceptibility to renal cell carcinoma: an evidence-based meta-analysis," *PLoS One*, vol. 8, no. 5, article e63827, 2013.

[32] A. F. Thévenin, C. L. Zony, B. J. Bahnson, and R. F. Colman, "GST pi modulates JNK activity through a direct interaction with JNK substrate, ATF2," *Protein Science*, vol. 20, no. 5, pp. 834–848, 2011.

[33] A. M. Moyer, O. E. Salavaggione, T.-Y. Wu et al., "Glutathione S-transferase P1: gene sequence variation and functional genomic studies," *Cancer Research*, vol. 68, no. 12, pp. 4791–4801, 2008.

[34] D. Li, C. Dandara, and M. I. Parker, "The 341C/T polymorphism in the GSTP1 gene is associated with increased risk of oesophageal cancer," *BMC Genetics*, vol. 11, no. 1, p. 47, 2010.

[35] D. Atilgan, B. S. Parlaktas, N. Uluocak et al., "The relationship between ALA16VAL single gene polymorphism and renal cell carcinoma," *Advances in Urology*, vol. 2014, 5 pages, 2014.

[36] D. Ratnasinghe, J. A. Tangrea, M. R. Andersen et al., "Glutathione peroxidase codon 198 polymorphism variant increases lung cancer risk," *Cancer Research*, vol. 60, no. 22, pp. 6381–6383, 2000.

[37] Y. Shimoyama, Y. Mitsuda, Y. Tsuruta, N. Hamajima, and T. Niwa, "Polymorphism of Nrf2, an antioxidative gene, is associated with blood pressure and cardiovascular mortality in hemodialysis patients," *International Journal of Medical Sciences*, vol. 11, no. 7, pp. 726–731, 2014.

[38] H. Towbin, T. Staehelin, and J. Gordon, "Electrophoretic transfer of proteins from polyacrylamide gels to nitrocellulose sheets: procedure and some applications," *Proceedings of the National Academy of Sciences of the United States of America*, vol. 76, no. 9, pp. 4350–4354, 1979.

[39] U. K. Laemmli, "Cleavage of structural proteins during the assembly of the head of bacteriophage T4," *Nature*, vol. 227, no. 5259, pp. 680–685, 1970.

[40] I. Žuntar, S. Kalanj-Bognar, E. Topić, R. Petlevski, M. Štefanović, and V. Demarin, "The glutathione S-transferase polymorphisms in a control population and in Alzheimer's disease patients," *Clinical Chemistry and Laboratory Medicine*, vol. 42, no. 3, pp. 334–339, 2004.

[41] A. S. Foulkes, *Applied Statistical Genetics with R*, Springer, New York City, NY, USA, 2008.

[42] E. Laborde, "Glutathione transferases as mediators of signaling pathways involved in cell proliferation and cell death," *Cell Death and Differentiation*, vol. 17, no. 9, pp. 1373–1380, 2010.

[43] C. C. McIlwain, D. M. Townsend, and K. D. Tew, "Glutathione _S_ -transferase polymorphisms: cancer incidence and therapy," *Oncogene*, vol. 25, no. 11, pp. 1639–1648, 2006.

[44] J. Pajaud, S. Kumar, C. Rauch, F. Morel, and C. Aninat, "Regulation of signal transduction by glutathione transferases," *International Journal of Hepatology*, vol. 2012, 11 pages, 2012.

[45] K. D. Tew and D. M. Townsend, "Glutathione-S-transferases as determinants of cell survival and death," *Antioxidants & Redox Signaling*, vol. 17, no. 12, pp. 1728–1737, 2012.

[46] T. Ishii, K. Itoh, S. Takahashi et al., "Transcription factor Nrf2 coordinately regulates a group of oxidative stress-inducible genes in macrophages," *The Journal of Biological Chemistry*, vol. 275, no. 21, pp. 16023–16029, 2000.

[47] T. Suzuki, T. Shibata, K. Takaya et al., "Regulatory nexus of synthesis and degradation deciphers cellular Nrf2 expression levels," *Molecular and Cellular Biology*, vol. 33, no. 12, pp. 2402–2412, 2013.

[48] J. M. Hartikainen, M. Tengström, V. M. Kosma, V. L. Kinnula, A. Mannermaa, and Y. Soini, "Genetic polymorphisms and protein expression of NRF2 and sulfiredoxin predict survival outcomes in breast cancer," *Cancer Research*, vol. 72, no. 21, pp. 5537–5546, 2012.

[49] H. Yuki, T. Kamai, S. Murakami et al., "Increased Nrf2 expression by renal cell carcinoma is associated with postoperative chronic kidney disease and an unfavorable prognosis," *Oncotarget*, vol. 9, no. 47, pp. 28351–28363, 2018.

[50] Y. Yamaguchi, T. Kamai, S. Higashi et al., "Nrf2 gene mutation and single nucleotide polymorphism Rs6721961 of the Nrf2 promoter region in renal cell cancer," *BMC Cancer*, vol. 19, no. 1, p. 1137, 2019.

[51] S. I. Holley, A. A. Fryer, J. W. Haycock, S. E. W. Grubb, R. C. Strange, and P. R. Hoban, "Differential effects of glutathione S-transferase pi (GSTP1) haplotypes on cell proliferation and apoptosis," *Carcinogenesis*, vol. 28, no. 11, pp. 2268–2273, 2007.

[52] C. Y. Jia, Y. J. Liu, X. L. Cong et al., "Association of glutathione S-transferase M1, T1, and P1 polymorphisms with renal cell carcinoma: evidence from 11 studies," *Tumor Biology*, vol. 35, no. 4, pp. 3867–3873, 2014.

[53] V. M. Coric, T. P. Simic, T. D. Pekmezovic et al., "Combined GSTM1-null, GSTT1-active, GSTA1 low-activity and GSTP1-variant genotype is associated with increased risk of clear cell renal cell carcinoma," *PLoS One*, vol. 11, 2016.

[54] M. P. Maniglia, A. Russo, P. M. Biselli-Chicote et al., "Glutathione S-transferase polymorphisms in head and neck squamous cell carcinoma treated with chemotherapy and/or radiotherapy," *Asian Pacific Journal of Cancer Prevention*, vol. 21, pp. 1637–1644, 2020.

[55] M. Pljesa-Ercegovac, A. Savic-Radojevic, D. Dragicevic et al., "Enhanced GSTP1 expression in transitional cell carcinoma of urinary bladder is associated with altered apoptotic pathways," *Urologic Oncology: Seminars and Original Investigations*, vol. 29, no. 1, pp. 70–77, 2011.

[56] K. D. Tew, Y. Manevich, C. Grek, Y. Xiong, J. Uys, and D. M. Townsend, "The role of glutathione S-transferase P in

signaling pathways and S-glutathionylation in cancer," *Free Radical Biology & Medicine*, vol. 51, no. 2, pp. 299–313, 2011.

[57] Y. Manevich, S. Hutchens, K. D. Tew, and D. M. Townsend, "Allelic variants of glutathione S-transferase P1-1 differentially mediate the peroxidase function of peroxiredoxin VI and alter membrane lipid peroxidation," *Free Radical Biology & Medicine*, vol. 54, pp. 62–70, 2013.

[58] J. Wang, Q. Liu, S. Yuan et al., "Genetic predisposition to lung cancer: comprehensive literature integration, meta-analysis, and multiple evidence assessment of candidate-gene association studies," *Scientific Reports*, vol. 7, no. 1, p. 8371, 2017.

[59] X. Ma, C. Chen, H. Xiong et al., "No association between SOD2 Val16Ala polymorphism and breast cancer susceptibility: a meta-analysis based on 9, 710 cases and 11, 041 controls," *Breast Cancer Research and Treatment*, vol. 122, no. 2, pp. 509–514, 2010.

[60] A. Crawford, R. G. Fassett, D. P. Geraghty et al., "Relationships between single nucleotide polymorphisms of antioxidant enzymes and disease," *Gene*, vol. 501, no. 2, pp. 89–103, 2012.

[61] B. Mikhak, D. J. Hunter, D. Spiegelman et al., "Manganese superoxide dismutase (MnSOD) gene polymorphism, interactions with carotenoid levels and prostate cancer risk," *Carcinogenesis*, vol. 29, no. 12, pp. 2335–2340, 2008.

[62] A. Sutton, A. Imbert, A. Igoudjil et al., "The manganese superoxide dismutase Ala16Val dimorphism modulates both mitochondrial import and MRNA stability," *Pharmacogenetics and Genomics*, vol. 15, no. 5, pp. 311–319, 2005.

[63] J. Dasgupta, S. Subbaram, K. M. Connor et al., "Manganese superoxide dismutase protects from TNF-α-induced apoptosis by increasing the steady-state production of H2O2," *Antioxidants & Redox Signaling*, vol. 8, no. 7-8, pp. 1295–1305, 2006.

[64] D. N. Ekoue, C. He, A. M. Diamond, and M. G. Bonini, "Manganese superoxide dismutase and glutathione peroxidase-1 contribute to the rise and fall of mitochondrial reactive oxygen species which drive oncogenesis," *Biochimica et Biophysica Acta (BBA) - Bioenergetics*, vol. 1858, no. 8, pp. 628–632, 2017.

[65] R. Brigelius-Flohé and A. Kipp, "Glutathione peroxidases in different stages of carcinogenesis," *Biochimica et Biophysica Acta (BBA) - General Subjects*, vol. 1790, no. 11, pp. 1555–1568, 2009.

[66] Y. J. Hu and A. M. Diamond, "Role of glutathione peroxidase 1 in breast cancer: loss of heterozygosity and allelic differences in the response to selenium," *Cancer Research*, vol. 63, no. 12, pp. 3347–3351, 2003.

[67] J. Chen, Q. Cao, C. Qin et al., "GPx-1 polymorphism (Rs1050450) contributes to tumor susceptibility: evidence from meta-analysis," *Journal of Cancer Research and Clinical Oncology*, vol. 137, no. 10, pp. 1553–1561, 2011.

[68] C. Wang, R. Zhang, N. Chen et al., "Association between glutathione peroxidase-1 (GPX1) Rs1050450 polymorphisms and cancer risk," *International Journal of Clinical and Experimental Pathology*, vol. 10, no. 9, pp. 9527–9540, 2017.

[69] P. Nikic, D. Dragicevic, A. Savic-Radojevic et al., "Association between GPX1 and SOD2 genetic polymorphisms and overall survival in patients with metastatic urothelial bladder cancer: a single-center study in Serbia," *Journal of B.U.ON.*, vol. 23, no. 4, pp. 1130–1135, 2018.

[70] B. Dragicevic, S. Suvakov, D. Jerotic et al., "Association of SOD2 (Rs4880) and GPX1 (Rs1050450) gene polymorphisms with risk of Balkan endemic nephropathy and its related tumors," *Medicina*, vol. 55, no. 8, p. 435, 2019.

Hindawi
Oxidative Medicine and Cellular Longevity
Volume 2021, Article ID 6661940, 9 pages
https://doi.org/10.1155/2021/6661940

Research Article

Factorial Analysis of the Cardiometabolic Risk Influence on Redox Status Components in Adult Population

Aleksandra Klisic,[1] **Nebojsa Kavaric**,[1] **Sanja Vujcic**,[2] **Vesna Spasojevic-Kalimanovska**,[2] **Jelena Kotur-Stevuljevic**,[2] **and Ana Ninic**[2]

[1]*Primary Health Care Center, University of Montenegro-Faculty of Medicine, Podgorica, Montenegro*
[2]*Department for Medical Biochemistry, University of Belgrade-Faculty of Pharmacy, Belgrade, Serbia*

Correspondence should be addressed to Aleksandra Klisic; aleksandranklisic@gmail.com

Received 6 December 2020; Revised 15 December 2020; Accepted 16 January 2021; Published 15 April 2021

Academic Editor: Janusz Gebicki

Copyright © 2021 Aleksandra Klisic et al. This is an open access article distributed under the Creative Commons Attribution License, which permits unrestricted use, distribution, and reproduction in any medium, provided the original work is properly cited.

Different byproducts of oxidative stress do not always lead to the same conclusion regarding its relationship with cardiometabolic risk, since controversial results are reported so far. The aim of the current study was to examine prooxidant determinant ((prooxidant-antioxidant balance (PAB)) and the marker of antioxidant defence capacity (total sulphydryl groups (tSHG)), as well as their ratio (PAB/tSHG) in relation to different cardiometabolic risk factors in the cohort of adult population. Additionally, we aimed to examine the joint effect of various cardiometabolic parameters on these markers, since to our knowledge, there are no studies that investigated that issue. A total of 292 participants underwent anthropometric measurements and venipuncture procedure for cardiometabolic risk factors assessment. Waist-to-height ratio (WHtR), body mass index, visceral adiposity index (VAI), and lipid accumulation product (LAP) were calculated. Principal component analysis (PCA) grouped various cardiometabolic risk parameters into different factors. This analysis was used in the subsequent binary logistic regression analysis to estimate the predictive potency of the factors towards the highest PAB and tSHG values. Our results show that triglycerides, VAI, and LAP were positively and high density lipoprotein cholesterol (HDL-c) were negatively correlated with tSHG levels and vice versa with PAB/tSHG index, respectively. On the contrary, there were no independent correlations between each cardiometabolic risk factor and PAB. PCA revealed that obesity-renal function-related factor (i.e., higher WHtR, but lower urea and creatinine) predicts both high PAB (OR = 1.617, 95% CI (1.204-2.171), $P < 0.01$) and low tSHG values (OR = 0.443, 95% CI (0.317-0.618), $P < 0.001$), while obesity-dyslipidemia-related factor (i.e., lower HDL-c and higher triglycerides, VAI, and LAP) predicts high tSHG values (OR = 2.433, 95% CI (1.660-3.566), $P < 0.001$). In conclusion, unfavorable cardiometabolic profile was associated with higher tSHG values. Further studies are needed to examine whether increased antioxidative capacity might be regarded as a compensatory mechanism due to free radicals' harmful effects.

1. Introduction

A growing body of evidence revealed an enhanced prooxidant environment in a variety of cardiometabolic disorders. At the same time, the antioxidative potential of many enzymatic and nonenzymatic biomolecules is compromised in an attempt to cope with increased free radicals production [1–3].

Free radicals, if not properly and timely scavenged or decomposed by antioxidants, destroy cellular functionality and structures including lipid membranes, proteins, and nucleic acids and even lead to cellular death [1, 2, 4]. Since reactive oxygen/nitrogen species (ROS/RNS) are highly reactive and exhibit a short half-life, their measurement is difficult [4]. Therefore, oxidative stress secondary products are measured for such purposes. However, different byproducts of oxidative stress do not always reveal the same conclusion regarding its relationship with cardiometabolic risk. Hence, there is no universal index by which oxidative stress can be defined [5].

Prooxidant-antioxidant balance (PAB) represents the ratio of prooxidants to antioxidants concomitantly in one

assay, which is calibrated on the basis of different ratios of uric acid and hydrogen peroxide [6, 7]. High serum PAB values are assumed to be related to an increased production of ROS/RNS. It is presumed that PAB can be a better determinant of oxidative stress than each prooxidant measured separately [7].

Total protein sulphydryl groups (tSHG), a part of the antioxidant system also called thiols, are derived from amino acids, such as methionine and cysteine and their derivatives (i.e., homocysteine and glutathione), both in extracellular fluids and cells [8, 9]. In the state of increased ROS/RNS production, tSHG could be oxidized, and therefore, the antioxidant defence pool becomes diminished. Hence, the serum levels of tSHG directly represent the whole-body redox status, in terms that its decrease is indicative of increased oxidative stress, and vice versa its higher levels are attributed to cell repairment and detoxification of the harmful effects of ROS/RNS [2]. Namely, in case of increased prooxidant milieu, tSHG becomes oxidized and converted into disulphide bond structures. This process is reversible, and when prooxidant environment resolves, disulphide bonds shift into reduced thiol groups, therefore maintaining a thiol/disulphide and extracellular redox homeostasis [2, 8–10].

Although the majority of studies reported increased prooxidant byproducts and decreased antioxidative molecules and antioxidative enzyme activities [11–17] in many diseases, others reported the opposite, i.e., no changes or even increased antioxidative capacity [18–22].

As far as we know, there are no studies that investigated the joint effect of various cardiometabolic parameters on oxidative stress status. In the light of all these facts, the relationship between the antioxidant defence system and cardiometabolic disturbances still represents an open question. Therefore, in the current study, we aimed to examine PAB as a determinant of an increased prooxidant milieu and a marker of antioxidant defence capacity (tSHG), as well as their ratio (PAB/tSHG index) in relation to different cardiometabolic risk factors in the cohort of adult population. Moreover, to better understand the influence of different cardiometabolic risk factors on high PAB and tSHG, we aimed to group them into several factors in line with their common pathophysiological characteristics and further examine the direction of such potential relationships.

2. Patients and Methods

2.1. Subjects. A cohort of 292 patients participated in this cross-sectional study, which was approved by the Institutional Ethics Committee of the Primary Health Care Center, Podgorica, Montenegro. The patients were recruited consecutively in the period from May to July 2017. Each participant provided signed informed consent, with an attached filled questionnaire consisting of answers regarding demographic data, lifestyle habits, and acute/chronic diseases.

Blood pressure (systolic (SBP) and diastolic blood pressure (DBP)) and anthropometric indices (body weight (kg), height (cm), and waist circumference (WC)) were provided for each participant, whereas waist-to-height ratio (WHtR) and body mass index (BMI) were calculated. Lipid indices were calculated also [23].

Visceral adiposity index (VAI) was obtained as follows: $\{[\mathrm{WC}/36.58 + (1.89 \times \mathrm{BMI})] \times (\mathrm{TG}/0.81) \times (1.52/\mathrm{HDL} - \mathrm{c})\}$ for women, and $\{[\mathrm{WC}/39.68 + (1.88 \times \mathrm{BMI})] \times (\mathrm{TG}/1.03) \times (1.31/\mathrm{HDL} - \mathrm{c})\}$ for men, where WC is expressed in cm, BMI in kg/m^2, and triglycerides (TG) and high density lipoprotein cholesterol (HDL-c) in mmol/L.

Lipid accumulation product (LAP) was provided as follows: $[(\mathrm{WC} - 58) \times \mathrm{TG}]$ for women and $[(\mathrm{WC} - 65) \times \mathrm{TG}]$ for men, where WC is expressed in cm and TG in mmol/L.

In addition to lipid indices, we have also calculated siMS score, as a novel comprehensive approach for metabolic status quantification [24]. It was calculated as follows: siMS score = 2 x WC/height + glucose/5.6 + TG/1.70 + SBP/130 – HDL – c/1.02 or 1.28 (for males and females, respectively), where WC and height are expressed in cm, glucose, TG, and HDL-c in mmol/L and SBP in mmHg [24].

The inclusion criteria for the current study were participants older than 18 years and who were willing to enter the study. On the other hand, subjects that reported acute infection, endocrine disorders other than type 2 diabetes, malignant disease, severe anaemia, acute myocardial infarction or stroke in the previous 6 months, ethanol consumption >20 g/day, use of antibiotics, glucocorticoids and nonsteroidal anti-inflammatory medications, and pregnancy were excluded from the study. Additionally, patients with an estimated glomerular filtration rate ($\mathrm{eGFR}_{\mathrm{MDRD}}$) < 30 mL/min/1.73 m^2 and with high-sensitivity C-reactive protein (hsCRP) (>10 mg/L) were also excluded.

2.2. Methods. Two blood samples were obtained from each individual. The venipuncture was performed in the morning after a fast of at least 8 hours. The preanalytical processes of blood sampling and analyses have been described previously [12]. In brief, one blood sample was provided in the tube with serum separator and clot activator for determination of cardiometabolic and oxidative stress parameters, whereas the other one was collected in the tube with K_2EDTA for measurement of glycated haemoglobin (HbA1c) levels.

All biochemical parameters (i.e., fasting glucose, HbA1c, hsCRP, creatinine, urea, uric acid, gamma glutamyl transferase (GGT), total cholesterol, TG, HDL-c, and low-density lipoprotein cholesterol (LDL-c)) were analyzed using Roche Cobas c501 chemistry analyzer (Roche Diagnostics GmbH, Mannheim, Germany), using standard procedures.

Furthermore, tSHG groups were determined spectrophotometrically using 5,5'-dithiobis (2- nitro benzoic acid) [25], whereas PAB measurement was done spectrophotometrically using 3,3', 5,5'-tetramethylbenzidine as a chromo gen [6].

3. Statistical Analysis

Data distributions were tested by the Kolmogorov-Smirnov test. Normally distributed data were compared by Student's t-test and presented as arithmetic mean ± standard deviation. Skewed data were compared by the Mann–Whitney test and presented as median (interquartile range). Categorical variables were compared by Chi-square test for

Table 1: General data of participants according to gender.

	Men	Women	P
N	110	182	
Age, years	63 (56-68)	61 (56-69)	0.878
BMI, kg/m^2	29.2 (26.9-32.0)	28.2 (25.1-31.6)	0.082
WC, cm$^{\#}$	104.5 ± 9.8	95.4 ± 11.1	<0.001
WHtR	0.587 ± 0.054	0.582 ± 0.071	0.528
SBP, mmHg	134 (126-144)	133 (124-148)	0.642
DBP, mmHg	85 (78-90)	84 (77-94)	0.923
Diabetes, %	49.1	26.9	<0.001
Diabetes duration, years	6 (2-10)	4 (1-10)	0.251
Smokers, %	21.8	18.9	0.515
Antihyperglycemics, %	42.7	23.1	<0.001
Insulin therapy, %	16.4	7.7	0.022
Antihypertensives, %	71.8	60.4	0.049
Hypolipidemics, %	38.2	31.9	0.271

Data are presented as median (interquartile range) and compared with the Mann–Whitney U-test. $^{\#}$Normally distributed data are presented as arithmetic mean ± standard deviation and compared with Student's t-test. Categorical variables are presented as relative frequencies and compared by Chi-square test for contingency tables.

Table 2: Laboratory markers of the examined population according to gender.

	Men	Women	P
Glucose, mmol/L	6.1 (5.5-8.2)	5.7 (5.3-6.7)	0.002
HbA1c, %	5.9 (5.5-7.2)	5.6 (5.3-6.2)	<0.001
Total cholesterol, mmol/L	5.09 (4.57-6.03)	6.06 (5.13-6.88)	<0.001
HDL-c, mmol/L	1.20 (0.98-1.43)	1.44 (1.19-1.76)	<0.001
LDL-c, mmol/L	3.02 (2.36-3.84)	3.68 (2.78-4.40)	<0.001
TG, mmol/L	1.81 (1.36-2.44)	1.85 (1.20-2.54)	0.714
HsCRP, mg/L	1.05 (0.53-2.38)	1.18 (0.59-2.29)	0.804
GGT, U/L	22 (16-33)	15 (11-21)	<0.001
Uric acid, μmol/L	330 (277-383)	265 (215-318)	<0.001
VAI	2.20 (1.41-3.29)	1.77 (1.08-3.21)	0.137
LAP	73.40 (46.50-98.90)	65.22 (36.40-99.45)	0.254
tSHG, μmol/L	0.29 (0.24-0.35)	0.24 (0.19-0.31)	<0.001
PAB, HKU	95.85 (61.30-115.10)	116.05 (74.10-136.00)	<0.001
PAB/tSHG index	314 (213-439)	464 (304-644)	<0.001
siMS score	3.46 (2.78-3.99)	3.22 (2.49-3.86)	0.243

Data are presented as median (interquartile range) and compared with the Mann–Whitney U-test.

contingency tables and given as absolute and relative frequencies. Correlation coefficient (ρ) determination was performed by nonparametric bivariate Spearman's correlation analysis. To assess in-depth associations of clinical markers with tSHG, PAB levels and PAB/tSHG index (ordinal dependent variables given as tertiles) in univariate and multivariate ordinal regression analysis were applied. In univariate analysis, the independent variables were the indices VAI and LAP, and anthropometric (BMI and WC) or lipid markers (HDL-c and TG) were used for their calculations. They had the identical effect at each cumulative split of each ordinal dependent variable. In multivariate analysis, covariates were selected based on these criteria: firstly, continuous variables were in significant bivariate correlation with the dependent variable, and secondly, categorical variables had an unequal significant distribution between ordinal dependent variable tertiles. In multivariate ordinal regression analysis, none of the covariates showed multicollinearity. Data from ordinal regression analysis were presented as odds ratios (ORs) and 95% confidence intervals (CIs). The explained variations in tSHG, PAB levels, and PAB/tSHG index in the observed population were given by the Nagelkerke R^2 value. Principal component analysis (PCA) [26] with varimax–normalized rotation was used to reduce the number of variables (which were in significant

correlation with tSHG, PAB, and PAB/tSHG index) in several significant factors. Criterion for factor extraction was its >1, and factor loadings >0.5, and both were used for variable inclusion; the number of factors was fixed at 3. PCA produced scores for significant factors, which were used in the subsequent binary logistic regression analysis to estimate the predictive potency of the factors towards the highest PAB and tSHG values. The IBM® SPSS® Statistics version 22 software (USA) was used for statistical calculations. Significance level set at P value less than 0.05 was considered statistically significant.

4. Results

Demographic and clinical characteristics of the examined population were compared between men and women and were listed in Table 1. All participants were of similar ages. Although males and females did not differ in BMI and WHtR, females had lower WC than males. More patients with type 2 diabetes were among males than females, as well as more antihyperglycemic, insulin, and antihypertensive users were among males.

Males had higher glucose, HbA1c, GGT, uric acid levels, and tSHG levels than females (Table 2). However, females had higher lipid status markers (TC, HDL-c, and LDL-c), PAB levels, and PAB/tSHG index than males (Table 2). TG and hsCRP levels, VAI and LAP indices, and siMS score did not show significant differences between genders.

Since there were significant differences between oxidative stress markers (tSHG, PAB, and PAB/tSHG index) between males and females, we further wanted to examine whether or not anthropometric and/or lipid markers could serve as their potential determinants. Firstly, we performed Spearman's correlation analysis (Table 3). tSHG positively correlated with WC, WHtR, glucose, HbA1c, TG, GGT, uric acid, VAI, LAP, and siMS score. Significant negative correlation was only evident between tSHG and HDL-c. PAB levels correlated negatively with age, glucose, HbA1c, GGT, and uric acid and positively with SBP, HDL-c, LDL-c, and hsCRP. PAB/tSHG index demonstrated mostly negative correlations with age, WC, glucose, HbA1c, TG, GGT, uric acid, VAI, LAP, and siMS score. Positive correlation was observed between PAB/tSHG index and HDL-c.

Further investigations of the associations between tSHG, PAB levels, and PAB/tSHG index and anthropometric (BMI and WC), lipid (HDL-c and TG) markers and their indices (VAI and LAP), and siMS score were assessed by ordinal regression analysis (Table 4).

In univariate ordinal regression analysis, WC, TG, VAI, LAP, and siMS score positively and HDL-c negatively correlated with tSHG (Table 4). Examinees with higher WC, TG, VAI, LAP, and siMS score were 1.029, 2.337, 1.560, 1.015, and 2.020 times, respectively, more likely to exhibit higher tSHG levels. However, the odds of having higher tSHG was 72% greater in participants with lower HDL-c. Nagelkerke R^2 for WC, HDL-c, TG, VAI, LAP, and siMS score were 0.038, 0.086, 0.170, 0.158, 0.144, and 0.148, respectively, which means that 3.8%, 8.6%, 17%, 15.8%, 14.4%, 14.8%, of variation in tSHG could be explained by each marker. Before performing multivariate ordinal regression analysis, we tested categorical data distribution among tSHG tertiles to determine potential covariates. Unequal distributions were evident for gender ($P = 0.003$), diabetes presence ($P = 0.036$), antihyperglycemic ($P = 0.003$), insulin ($P = 0.003$), and antilipemic ($P = 0.035$) users between tSHG tertiles.

Independent continuous variables which correlated significantly with tSHG (Table 3) (HbA1c, GGT, and uric acid) and categorical variables (diabetes presence, antilipemic therapy, and gender) obtained by Chi-square analysis were included in the multivariate ordinal regression analysis as covariates (Table 4). TG, VAI, and LAP kept their positive and HDL-c negative independent associations and predictions of tSHG levels.

In univariate ordinal regression analysis, only HDL-c was positively associated with PAB levels (Table 4). Odds of having higher PAB levels were 1.976 times greater in participants with higher HDL-c concentration. Nagelkerke R^2 was 0.027, indicating that 2.7% variation in PAB levels could be explained by HDL-c (Table 4). When tested categorical data distribution among PAB levels tertiles, we determined unequal distributions for gender ($P < 0.001$), diabetes presence ($P = 0.001$), antihyperglycemic ($P = 0.004$), antihypertensive ($P = 0.006$) users between tertiles. Independent continuous variables which correlated significantly with

Table 3: The bivariate Spearman's correlation analysis between tSHG, PAB, and PAB/tSHG index and clinical markers.

	tSHG, μmol/L	PAB, HKU	PAB/tSHG index
Age, years	-0.037	-0.215∗∗∗	-0.121∗
BMI, kg/m^2	0.092	-0.059	-0.093
WC, cm	0.183∗∗	-0.084	-0.164∗∗
WHtR	0.158∗∗	0.036	0.017
SBP, mmHg	-0.005	0.116∗	0.072
DBP, mmHg	0.004	0.035	0.016
Glucose, mmol/L	0.243∗∗∗	-0.192∗∗	-0.294∗∗∗
HbA1c, %	0.271∗∗∗	-0.138∗	-0.237∗∗∗
Total cholesterol, mmol/L	-0.029	0.160∗∗	0.114∗
HDL-c, mmol/L	-0.355∗∗∗	0.116∗	0.308∗∗∗
LDL-c, mmol/L	-0.061	0.178∗∗	0.146∗
TG, mmol/L	0.397∗∗∗	-0.096	-0.318∗∗∗
HsCRP, mg/L	0.033	0.154∗∗	0.067
GGT, U/L	0.258∗∗∗	-0.150∗	-0.265∗∗∗
Uric acid, μmol/L	0.171∗∗	-0.206∗∗∗	-0.258∗∗∗
VAI	0.391∗∗∗	-0.104	-0.334∗∗∗
LAP	0.347∗∗∗	-0.094	-0.320∗∗∗
tSHG, μmol/L	—	-0.114	-0.742∗∗∗
PAB, HKU	-0.114	—	0.701∗∗∗
siMS score	0.377∗∗	-0.111	-0.321∗∗

Data are presented as the correlation coefficient Rho (ρ). $*P < 0.05$, $**P < 0.01$, $*** P < 0.001$.

Table 4: Estimated odds ratios after ordinal regression analysis for tSHG, PAB, and PAB/tSHG tertiles, respectively, as dependent variable.

	Unadjusted		
tSHG tertiles as dependent variable	*OR (95% CI)*	*P*	*Nagelkerke R^2*
BMI	1.046 (0.957-1.097)	0.072	0.013
WC	1.029 (1.011-1.049)	0.002	0.038
WHtR	2.27 (2.19-2.37)	0.022	0.037
HDL-c	0.281 (0.164-0.481)	<0.001	0.086
TG	2.337 (1.784-3.062)	<0.001	0.170
VAI	1.560 (1.339-1.820)	<0.001	0.158
LAP	1.015 (1.010-1.020)	<0.001	0.144
siMS score	2.020 (1.600-2.550)	<0.001	0.148
	Adjusted		
Model	*OR (95% CI)*	*P*	*Nagelkerke R^2*
WC	1.011 (0.989-1.033)	0.319	0.088
WHtR	0.128 (0.065-0.325)	0.069	0.121
HDL-c	0.359 (0.199-0.646)	0.001	0.126
TG	2.333 (1.754-3.102)	<0.001	0.220
VAI	1.540 (1.310-1.811)	<0.001	0.204
LAP	1.015 (1.009-1.021)	<0.001	0.192
	Unadjusted		
PAB tertiles as dependent variable	*OR (95% CI)*	*P*	*Nagelkerke R^2*
BMI	0.978 (0.932-1.026)	0.371	0.013
WC	0.985 (0.967-1.003)	0.104	0.010
HDL-c	1.976 (1.185-3.294)	0.009	0.027
TG	0.924 (0.768-1.112)	0.401	0.002
VAI	1.001 (0.924-1.083)	0.988	0
LAP	0.999 (0.996-1.003)	0.677	0.001
siMS score	0.840 (0.694-1.017)	0.075	0.012
	Adjusted		
Model	*OR (95% CI)*	*P*	*Nagelkerke R^2*
HDL-c	1.142 (0.640-2.056)	0.653	0.136
	Unadjusted		
PAB/tSHG tertiles as dependent variable	*OR (95% CI)*	*P*	*Nagelkerke R^2*
BMI	0.970 (0.924-1.019)	0.217	0.006
WC	0.978 (0.959-0.995)	0.014	0.024
HDL-c	3.699 (2.145-6.360)	<0.001	0.088
TG	0.742 (0.467-0.749)	<0.001	0.088
VAI	0.784 (0.691-1.124)	<0.001	0.075
LAP	0.992 (0.987-0.996)	<0.001	0.062
siMS score	0.603 (0.486-0.748)	<0.001	0.090
	Adjusted		
Model	*OR (95% CI)*	*P*	*Nagelkerke* R^2
WC	1.014 (0.991-1.039)	0.231	0.164
HDL-c	2.206 (1.214-4.011)	0.009	0.181
TG	0.602 (0.466-0.788)	<0.001	0.216
VAI	0.810 (0.709-0.925)	0.002	0.200
LAP	0.993 (0.988-0.998)	0.010	0.185

Data are given as OR (95% CI). Adjusted model for tSHG: Model included each marker and continuous (HbA1c, GGT, and uric acid) and categorical variables (diabetes presence, antilipemic therapy, and gender). Adjusted model for PAB: Model included continuous variables: age, HbA1c, hsCRP, GGT, uric acid, and categorical variables: diabetes presence, antihypertensive therapy, and gender. Adjusted model for PAB/tSHG: Model included continuous variables: age, HbA1c, GGT, uric acid, and categorical variables: diabetes presence, antihypertensive and antilipemic therapy, and gender.

PAB levels (Table 3) (age, HbA1c, hsCRP, GGT, and uric acid) and categorical variables (diabetes presence, antihypertensive therapy, and gender) obtained by Chi-square analysis were included in the multivariate ordinal regression analysis as covariates (Table 4). HDL-c lost significant independent association and prediction of PAB levels.

In univariate ordinal regression analysis, WC, TG, VAI, LAP, and siMS score were negatively and HDL-c positively associated with PAB/tSHG index (Table 4). Examinees with lower WC, TG, VAI, LAP, and siMS score were 2.2%, 25.8%, 21.6%, 0.8%, and 39.7%, respectively, more likely to exhibit higher PAB/tSHG index. However, the odds of having the

Table 5: Principal component analysis extracted factors connected with tSHG and PAB values.

Factors	Included variables with loadings	Factor variability
Obesity-dyslipidemia related factor	HDL-c (-0.628)	43%
	TG (0.956)	
	VAI (0.964)	
	LAP (0.959)	
Obesity-renal function-related factor	WHtR (0.581)	16%
	Urea (-0.652)	
	Creatinine (-0.666)	
Blood pressure-related factor	SBP (0.884)	13%
	DBP (0.903)	

higher PAB/tSHG index were 3.699 times greater in participants with higher HDL-c. Nagelkerke R^2 for WC, HDL-c, TG, VAI, LAP, and siMS score were 0.024, 0.088, 0.088, 0.075, 0.062, and 0.090, respectively, which means that 2.4%, 8.8%, 8.8%, 7.5%, 6.2%, and 9.0% of variation in PAB/tSHG index could be explained by each marker. When tested categorical data distribution among PAB/tSHG tertiles, we determined unequal distributions for gender ($P < 0.001$), diabetes presence ($P = 0.002$), antihyperglycemic ($P < 0.001$), antihypertensive ($P = 0.032$), and antilipemic ($P = 0.033$) users between tertiles.

Independent continuous variables which correlated significantly with PAB/tSHG index (Table 3) (age, HbA1c, GGT, and uric acid) and categorical variables (diabetes presence, antihypertensive and antilipemic therapy and gender) obtained by Chi-square analysis were included in the multivariate ordinal regression analysis as covariates (Table 4). TG, VAI, and LAP kept their negative and HDL-c positive independent associations and predictions of PAB/tSHG index.

PCA was implemented to get a smaller number of factors grouped according to the same level of variability, from the large number of parameters which significantly correlated with tSHG and PAB. This analysis emphasized 3 different factors explaining 72% of variance of the tested parameters (Table 5). The largest percent of variance (43%) showed the first, obesity-dyslipidemia-related factor with positive loadings of TG and lipid indices (VAI and LAP) and with negative loading of HDL-c. The second factor explained 16% of the variation and consisted of obesity-renal function parameters (obesity with positive and renal factors with negative loadings), and the third, blood pressure-related factor, explained 13% of the variation (both parameters with positive loadings).

Binary logistic regression analysis enabled us to estimate which factors, expressed as scores and given by PCA, could predict high PAB and tSHG values (Table 6). Our analysis showed that obesity-renal function-related factor predicts both high PAB and low tSHG, while obesity-dyslipidemia-related factor predicted significantly only high tSHG values. The third factor (i.e., blood pressure-related factor) did not predict either PAB or tSHG values.

5. Discussion

This study has shown several findings that merit to be emphasized. Firstly, tSHG and PAB/tSHG indices were independently correlated with lipid parameters (HDL-c and TG) and lipid indices (VAI and LAP), whereas no independent correlation between PAB and each examined parameter alone was found. Namely, multivariate ordinal regression analysis revealed that HDL-c showed negative and TG, VAI, and LAP positive independent associations and predictions of tSHG and vice versa of PAB/tSHG levels. Secondly, PCA analysis after grouping the variables into three factors (i.e., obesity-dyslipidemia related factor, obesity-renal function-related factor, and blood pressure-related factor) produced PCA scores for the mentioned factors. These scores were used in binary logistic regression analysis to estimate its predictive ability towards high PAB and tSHG values. Obesity-renal function-related factor (which included higher WHtR, but lower urea and creatinine) predicted high PAB values, but at the same time low tSHG values. The direction of this influence was opposite, i.e., higher values of this factor increase PAB, but a lower summary value of the same factor predicted higher tSHG. Obesity-dyslipidemia-related factor (which included lower HDL-c and higher TG, VAI, and LAP) predicted higher tSHG values, and this could be explained as a compensatory induction of available antioxidative potential. On the contrary, the third factor connected with blood pressure homeostasis did not predict any of these two redox status-related parameters. Such findings represent the novelty, since to the best of our knowledge, there are no studies that examined the joint effect of various cardiometabolic parameters on the circulating levels of prooxidants and antioxidants. Moreover, no previous studies examined lipid indices (VAI and LAP) in relation to oxidative stress indicators in the adult population. We have also shown for the first time positive association between siMS score and tSHG, and an inverse association between siMS and PAB/tSHG index, respectively. The siMS score represents a novel comprehensive score for quantification of metabolic status that included beside body height, several metabolic syndrome related parameters, i.e., WC, glucose, TG, and HDL-c, as well as SBP in its calculation) [24]. Furthermore, the relatively large sample size of our study (i.e., nearly 300 participants) is another strength of our research.

Previous reports suggested VAI and LAP as better determinants of cardiometabolic risk than anthropometric measures (i.e., BMI and WC) [27]. Indeed, although anthropometric indices correlated with oxidative stress determinants, these correlations lost their independence after further analysis in our study. Since both of these lipid indices are gender-specific and include a simple measure of central obesity as a principal indicator of increased cardiometabolic risk, it would be expected that with a greater extent of central obesity, prooxidants would be increased, whereas antioxidants would be lowered, as previous studies reported [3, 11]. However, results in the current study have shown the opposite, such as positive association between lipid indices and tSHG. Enhancement of antioxidant protection (in terms of higher tSHG) may be attributed to its compensation due to

Table 6: Binary logistic regression analysis of the highest PAB and the highest tSHG tertile values.

Predictors	PAB values (3rd tertile)	tSHG values (3rd tertile)
Obesity-dyslipidemia-related factor	1.069 (0.821-1.391)	2.433 (1.660-3.566)∗∗∗
Obesity-renal function-related factor	1.617 (1.204-2.171)∗∗	0.443 (0.317-0.618)∗∗∗
Blood pressure-related factor	1.184 (0.889-1.576)	1.013 (0.763-1.345)

Data are presented as OR (95% CI). Abbreviations: OR, odds ratio; CI, confidence interval. $**P < 0.01$, $*** P < 0.001$.

increased free radicals generation, since in the obese state prooxidant-antioxidant homeostasis is disturbed [3].

In such circumstances, lipids become very susceptible to oxidation. Enlarged visceral adipose tissue contributes to lipid accumulation and lipid peroxidation. The increased production of highly reactive free radicals (i.e., superoxide anions) through the mitochondrial electron transport chain can cause cellular damage in almost all organs if the antioxidant defence system fails to cope with them, as previously stated [1, 4, 28].

In a nutshell, proinflammatory adipokines (i.e., leptin, resistin, visfatin, apelin, etc.) and cytokines (interleukin-1, interleukin-6, tumor necrosis factor alpha, etc.), which are secreted by the enlarged visceral adipose tissue, affect insulin signalling pathways favouring the insulin resistant state. Therefore, antilipolytic effects of insulin and phosphatidylinositol 3-kinase (PI3K) pathways are compromised in favour of increased lipolysis of TG and increased release of free fatty acids (FFA) from adipose tissue. The latter reach the liver, enhancing oxidative phosphorylation, ROS production, and liver fat peroxidation [3], leading to increased synthesis of NADH/NAD+ ratio in mitochondria. All these processes favour an enhanced activation of protein kinase C (PKC), increased activity of nicotinamide adenine dinucleotide phosphate (NADPH) oxidase, and increased free radicals production. Consequently, inhibition of endothelial nitric oxide synthase (eNOS) and decreased nitric oxide (NO) synthesis, a potent vasodilatator, in vascular smooth muscle cells occur and precede vasoconstriction and endothelial dysfunction [3, 4].

The increased hepatic synthesis of lipotoxic TG-rich very-low-density lipoproteins (VLDL), small dense low-density lipoproteins (sdLDL), and shifted distribution of HDL particles to smaller proatherogenic HDL3 ones is another consequence of insulin resistant state [29]. The sdLDL and smaller HDL3 particles are susceptible to oxidative modifications and enable the onset and progression of atherosclerosis [30]. Moreover, cytotoxic effects of FFA and accumulated lipids lead to other organ impairments, such as tubulointerstitial and glomerular cells injury, thus promoting renal disease [31]. In line with this, the independent association between renal function markers and lipid parameters was reported earlier [32, 33].

Additionally, it was reported that sterol regulatory element-binding protein-1c (SREBP1-c), a sort of transcription factor, is involved in the regulation of gene expression responsible for the differentiation of adipocytes, lipogenesis, and FFA oxidation [3].

Since ROS/RNS are generated through various pathways, each prooxidant and antioxidant represent a different measure of oxidative stress [5]. This could explain in part the discrepancies in the results concerning antioxidative defence capacity in various cardiometabolic disorders. A study by Pande et al. [34] has shown higher levels of total thiol (i.e., tSHG) in both patients with prediabetes and diabetes as compared to control group. On the contrary, no difference in serum tSHG levels was reported between women with IR and noninsulin-resistant counterparts [18], as well as in patients with diabetes and prediabetes vs. control group [16]. Additionally, differences in ethnic background, sample sizes, and gender distribution in the examined cohorts and even different methods for measurement of prooxidant and antioxidant markers may also contribute to the inconclusive results. Moreover, the degree and duration of obesity and other comorbidities might be an important bias factor since antioxidative enzymes might be enhanced at the beginning of the process, but later depleted when the antioxidative pool becomes exhausted [3, 20]. Our unexpected results might also be explained by other environmental factors such as regular physical activity and nutritional habits (dietary factors) which may increase synthesis of antioxidant molecules and induce antioxidative enzymes activity [4, 35]. Namely, adequate intake of proteins and supplement N-acetylcysteine (which contains thiol compounds) may lead to the increase in tSHG [36]. Also, daily intake of antioxidant vitamins [4] may significantly contribute to cellular redox homeostasis. Unfortunately, this study is limited for such information. The other limitation of our study is its cross-sectional nature, and thus, the causality between the unfavorable cardiometabolic profile and higher tSHG and PAB could not be confirmed. At last, we were limited to examine thiol-disulphide homeostasis, which could provide better insight into the whole-body redox status [8].

6. Conclusion

Unfavorable cardiometabolic profile was associated with higher tSHG values. Longitudinal design of other studies is needed to further explore the underlying mechanisms of the relationship between prooxidants, antioxidants, and cardiometabolic disturbances and to enlighten the role of antioxidants in the fight against free radicals production and its negative side effects. These findings would enable us to find the most appropriate pharmaceutical target for treatment of population with increased cardiometabolic risk.

Data Availability

The data will be available upon reasonable request (contact person: aleksandranklisic@gmail.com).

Conflicts of Interest

The authors declare no conflict of interest.

Acknowledgments

This work was financially supported in part by a grant from the Ministry of Science, Montenegro and the Ministry of Education, Science and Technological Development, Republic of Serbia (project number 451-03-68/2020-14/200161).

References

[1] A. García-Sánchez, A. G. Miranda-Díaz, and E. G. Cardona-Muñoz, "The role of oxidative stress in physiopathology and pharmacological treatment with pro- and antioxidant properties in chronic diseases," *Oxidative Medicine and Cellular Longevity*, vol. 2020, Article ID 2082145, 16 pages, 2020.

[2] A. J. Lepedda and M. Formato, "Oxidative modifications in advanced atherosclerotic plaques: a focus on *in situ* protein sulfhydryl group oxidation," *Oxidative Medicine and Cellular Longevity*, vol. 2020, Article ID 6169825, 7 pages, 2020.

[3] E. Čolak and D. Pap, "The role of oxidative stress in the development of obesity and obesity-related metabolic disorders," *Journal of Medical Biochemistry*, 2020.

[4] C. Zanza, J. Thangathurai, A. Audo et al., "Oxidative stress in critical care and vitamins supplement therapy: "a beneficial care enhancing"," *European Review for Medical and Pharmacological Sciences*, vol. 23, no. 17, pp. 7703–7712, 2019.

[5] F. Ito, Y. Sono, and T. Ito, "Measurement and clinical significance of lipid peroxidation as a biomarker of oxidative stress: oxidative stress in diabetes, atherosclerosis, and chronic inflammation," *Antioxidants (Basel)*, vol. 8, no. 3, p. 72, 2019.

[6] D. H. Alamdari, K. Paletas, T. Pegiou, M. Sarigianni, C. Befani, and G. Koliakos, "A novel assay for the evaluation of the prooxidant-antioxidant balance, before and after antioxidant vitamin administration in type II diabetes patients," *Clinical Biochemistry*, vol. 40, no. 3-4, pp. 248–254, 2007.

[7] H. Ghazizadeh, M. Saberi-Karimian, M. Aghasizadeh et al., "Pro-oxidant-antioxidant balance (PAB) as a prognostic index in assessing the cardiovascular risk factors: A narrative review," *Obesity Medicine*, vol. 19, article 100272, 2020.

[8] O. Erel and S. Neselioglu, "A novel and automated assay for thiol/disulphide homeostasis," *Clinical Biochemistry*, vol. 47, no. 18, pp. 326–332, 2014.

[9] E. K. Çakıcı, F. K. Eroğlu, F. Yazılıtaş et al., "Evaluation of the level of dynamic thiol/disulphide homeostasis in adolescent patients with newly diagnosed primary hypertension," *Pediatric Nephrology*, vol. 33, no. 5, pp. 847–853, 2018.

[10] E. E. M. Schillern, A. Pasch, M. Feelisch et al., "Serum free thiols in type 2 diabetes mellitus: a prospective study," *Journal of Clinical & Translational Endocrinology*, vol. 16, p. 100182, 2019.

[11] A. Klisic, G. Kocic, N. Kavaric, M. Jovanovic, V. Stanisic, and A. Ninic, "Body mass index is independently associated with xanthine oxidase activity in overweight/obese population," *Eating and Weight Disorders - Studies on Anorexia, Bulimia and Obesity*, vol. 25, no. 1, pp. 9–15, 2020.

[12] A. Klisic, N. Kavaric, S. Vujcic, V. Spasojevic-Kalimanovska, A. Ninic, and J. Kotur-Stevuljevic, "Endocan and advanced oxidation protein products in adult population with hypertension," *European Review for Medical and Pharmacological Sciences*, vol. 24, no. 12, pp. 7131–7137, 2020.

[13] Y. I. Ragino, V. S. Shramko, E. M. Stakhneva et al., "Changes in the blood fatty-acid profile associated with oxidative-antioxidant disturbances in coronary atherosclerosis," *Journal of Medical Biochemistry*, vol. 39, no. 1, pp. 46–53, 2020.

[14] A. Klisic, N. Kavaric, and A. Ninic, "Serum uric acid, triglycerides and total bilirubin are associated with hepatic steatosis index in adolescent population," *Preventivna Pedijatrija*, vol. 6, pp. 71–76, 2020.

[15] A. Ninić, N. Bogavac-Stanojević, M. Sopić et al., "Superoxide dismutase Isoenzymes gene expression in peripheral blood mononuclear cells in patients with coronary artery disease," *Journal of Medical Biochemistry*, vol. 38, no. 3, pp. 284–291, 2019.

[16] A. Klisic, N. Kavaric, V. Stanisic et al., "Endocan and a novel score for dyslipidemia, oxidative stress and inflammation (DOI score) are independently correlated with glycated hemoglobin (HbA1c) in patients with prediabetes and type 2 diabetes," *Archives of Medical Science*, vol. 16, no. 1, pp. 42–50, 2020.

[17] A. Klisic, N. Kavaric, S. Vujcic, V. Spasojevic-Kalimanovska, J. Kotur-Stevuljevic, and A. Ninic, "Total oxidant status and oxidative stress index as indicators of increased Reynolds Risk Score in postmenopausal women," *European Review for Medical and Pharmacological Sciences*, vol. 24, no. 19, pp. 10126–10133, 2020.

[18] E. Ates, T. Set, S. C. Karahan, C. Biçer, and Ö. Erel, "Thiol/Disulphide homeostasis, ischemia modified albumin, and ferroxidase as oxidative stress markers in women with obesity with insulin resistance," *Journal of Medical Biochemistry*, vol. 38, no. 4, pp. 445–451, 2019.

[19] K. A. Or, M. Dağdeviren, T. Akkan et al., "Dynamic thiol/disulfide homeostasis and oxidant status in patients with hypoparathyroidism," *Journal of Medical Biochemistry*, vol. 39, no. 2, pp. 231–239, 2019.

[20] E. Čolak and D. Pap, "The impact of obesity to antioxidant defense parameters in adolescents with increased cardiovascular risk," *Journal of Medical Biochemistry*, vol. 39, no. 3, pp. 346–354, 2020.

[21] D. M. Adenan, Z. Jaafar, J. J. Jayapalan, and A. A. Abdul, "Plasma antioxidants and oxidative stress status in obese women: correlation with cardiopulmonary response," *PeerJ*, vol. 8, article e9230, 2020.

[22] A. Petelin, P. Tedeschi, A. Maietti, M. Jurdana, V. Brandolini, and Z. J. Pražnikar, "Total serum antioxidant capacity in healthy normal weight and asymptomatic overweight adults," *Experimental and Clinical Endocrinology & Diabetes*, vol. 125, no. 7, pp. 470–477, 2017.

[23] A. Klisic, N. Kavaric, V. Spasojevic-Kalimanovska, J. Kotur-Stevuljevic, and A. Ninic, "Serum endocan levels in relation to traditional and non-traditional anthropometric indices in adult population," *Journal of Medical Biochemistry*, 2020.

[24] I. Soldatovic, R. Vukovic, D. Culafic, M. Gajic, and V. Dimitrijevic-Sreckovic, "siMS Score: Simple method for quantifying metabolic syndrome," *PLoS One*, vol. 11, no. 1, article e0146143, 2016.

[25] G. I. Ellman, "Tissue sulfhydryl groups," *Archives of Biochemistry and Biophysics*, vol. 82, no. 1, pp. 70–77, 1959.

[26] H. Abdi and L. J. Williams, "Principal component analysis," *Wiley Interdisciplinary Reviews: Computational Statistics*, vol. 2, no. 4, pp. 433–459, 2010.

[27] Z. Biyik and I. Guney, "Lipid accumulation product and visceral adiposity index: two new indices to predict metabolic syndrome in chronic kidney disease," *European Review for Medical and Pharmacological Sciences*, vol. 23, no. 5, pp. 2167–2173, 2019.

[28] Q. Guo, F. Li, Y. Duan et al., "Oxidative stress, nutritional antioxidants and beyond," *Science China. Life Sciences*, vol. 63, no. 6, pp. 866–874, 2020.

[29] A. Klisic, N. Kavaric, S. Vujcic et al., "Inverse association between serum endocan levels and small LDL and HDL particles in patients with type 2 diabetes mellitus," *European Review for Medical and Pharmacological Sciences*, vol. 24, no. 15, pp. 8127–8135, 2020.

[30] J. Kotur-Stevuljević, J. Vekić, A. Stefanović et al., "Paraoxonase 1 and atherosclerosis-related diseases," *BioFactors*, vol. 46, no. 2, pp. 193–205, 2020.

[31] T. Jiang, Z. Wang, G. Proctor et al., "Diet-induced obesity in C57BL/6J mice causes increased renal lipid accumulation and glomerulosclerosis via a sterol regulatory element-binding protein-1c-dependent pathway," *The Journal of Biological Chemistry*, vol. 280, no. 37, pp. 32317–32325, 2005.

[32] Y. Wang, X. Qiu, L. Lv et al., "Correlation between serum lipid levels and measured glomerular filtration rate in Chinese patients with chronic kidney disease," *PLoS One*, vol. 11, no. 10, article e0163767, 2016.

[33] A. Klisic, N. Kavaric, and A. Ninic, "Serum cystatin C levels are associated with triglycerides/high-density lipoprotein cholesterol ratio in adolescent girls ages between 16-19 years old," *European Review for Medical and Pharmacological Sciences*, vol. 24, no. 20, pp. 10680–10686, 2020.

[34] A. P. Pande, B. Vijetha Shenoy, D. Datta, G. Nadeem Khan, and K. R. Ramya, "A correlative study of serum ischemia modified albumin and total thiol in prediabetes and diabetes mellitus," *International Journal of Clinical Biochemistry and Research*, vol. 6, no. 3, pp. 380–383, 2019.

[35] M. Gol, B. Özkaya, C. Yildirim, and R. Bal, "Regular exercise, overweight/obesity and sedentary lifestyle cause adaptive changes in thiol-disulfide homeostasis," *Anais da Academia Brasileira de Ciências*, vol. 91, no. 2, article e20180547, 2019.

[36] G. Cakirca, C. Nas, K. Yilmaz, A. Guzelcicek, and O. Erel, "Evaluation of dynamic thiol-disulfide balance in children with stage 3-5 chronic kidney disease," *Annals of Medical Research*, vol. 26, pp. 1–1568, 2019.

Hindawi
Oxidative Medicine and Cellular Longevity
Volume 2021, Article ID 6615787, 15 pages
https://doi.org/10.1155/2021/6615787

Research Article

Predicting Severity and Intrahospital Mortality in COVID-19: The Place and Role of Oxidative Stress

Ivan Cekerevac,[1,2] Tamara Nikolic Turnic,[3] Nevena Draginic,[3] Marijana Andjic,[3] Vladimir Zivkovic,[4] Stefan Simovic,[1,5] Romana Susa,[2] Ljiljana Novkovic,[1,2] Zeljko Mijailovic,[6,7] Marija Andjelkovic,[8,9] Vladimir Vukicevic,[10] Tatjana Vulovic,[10,11] and Vladimir Jakovljevic[4,12]

[1]*Department of Internal Medicine, Faculty of Medical Sciences, University of Kragujevac, Serbia*
[2]*Clinic for Pulmonology, Clinical Center Kragujevac, Kragujevac, Serbia*
[3]*Department of Pharmacy, Faculty of Medical Sciences, University of Kragujevac, Serbia*
[4]*Department of Physiology, Faculty of Medical Sciences, University of Kragujevac, Serbia*
[5]*Clinic for Cardiology, Clinical Center Kragujevac, Serbia*
[6]*Department of Infectious Diseases, Faculty of Medical Sciences, University of Kragujevac, Serbia*
[7]*Clinic for Infectious Diseases, Clinical Center Kragujevac, Serbia*
[8]*Department of Biochemistry, Faculty of Medical Sciences, University of Kragujevac, Serbia*
[9]*Center for Laboratory Diagnostics, Clinical Center Kragujevac, Serbia*
[10]*Center for Anesthesiology and Resuscitation, Clinical Center Kragujevac, Serbia*
[11]*Department of Surgery, Faculty of Medical Sciences, University of Kragujevac, Serbia*
[12]*Department of Hyman Pathology, IM Sechenov First Moscow State Medical University, Moscow, Russia*

Correspondence should be addressed to Vladimir Jakovljevic; drvladakgbg@yahoo.com

Received 28 December 2020; Revised 16 February 2021; Accepted 11 March 2021; Published 27 March 2021

Academic Editor: Gordana Kocic

Copyright © 2021 Ivan Cekerevac et al. This is an open access article distributed under the Creative Commons Attribution License, which permits unrestricted use, distribution, and reproduction in any medium, provided the original work is properly cited.

SARS-CoV-2 virus causes infection which led to a global pandemic in 2020 with the development of severe acute respiratory syndrome. Therefore, this study was aimed at examining its possible role in predicting severity and intrahospital mortality of COVID-19, alongside with other laboratory and biochemical procedures, clinical signs, symptoms, and comorbidity. This study, approved by the Ethical Committee of Clinical Center Kragujevac, was designed as an observational prospective cross-sectional clinical study which was conducted on 127 patients with diagnosed respiratory COVID-19 viral infection from April to August 2020. The primary goals were to determine the predictors of COVID-19 severity and to determine the predictors of the negative outcome of COVID-19 infection. All patients were divided into three categories: patients with a mild form, moderate form, and severe form of COVID-19 infection. All biochemical and laboratory procedures were done on the first day of the hospital admission. Respiratory ($p < 0.001$) and heart ($p = 0.002$) rates at admission were significantly higher in patients with a severe form of COVID-19. From all observed hematological and inflammatory markers, only white blood cell count (9.43 ± 4.62, $p = 0.001$) and LDH (643.13 ± 313.3, $p = 0.002$) were significantly higher in the severe COVID-19 group. We have observed that in the severe form of SARS-CoV-2, the levels of superoxide anion radicals were substantially higher than those in two other groups (11.3 ± 5.66, $p < 0.001$) and the nitric oxide level was significantly lower in patients with the severe disease (2.66 ± 0.45, $p < 0.001$). Using a linear regression model, TA, anosmia, ageusia, O_2^-, and the duration at the ICU are estimated as predictors of severity of SARS-CoV-2 disease. The presence of dyspnea and a higher heart rate were confirmed as predictors of a negative, fatal outcome. Results from our study show that presence of hypertension, anosmia, and ageusia, as well as the duration of ICU stay, and serum levels of O_2^- are predictors of COVID-19 severity, while the presence of dyspnea and an increased heart rate on admission were predictors of COVID-19 mortality.

1. Introduction

SARS-CoV-2, a new RNA virus, caused the worldwide pandemic in 2020 by developing severe acute respiratory syndrome [1]. Coronavirus disease 2019 (COVID-19) is induced by SARS-CoV-2 with varying symptomatology, from being asymptomatic to having pneumonia of different degrees of severity of acute respiratory distress syndrome (ARDS) or death [2]. Some reports from China estimated that the majority of cases were limited to a mild and moderate symptomatology, noticed in 81% of the infected population, 14% patients with progressive, severe pneumonia and 5% of the infected population developing ARDS [3]. And while the mortality rate still cannot be estimated, in most cases, it is related to multiple organ failure and ARDS. Direct or indirect lung injury results in the acute systemic inflammatory response and leads to ARDS, the same as acute myocardial injury and renal injury (7–17% and 3–15%, respectively) [2, 4–7]. However, the most important pathophysiological processes that lead to severe forms of the disease are not yet precisely known.

It has been postulated that marked elevation of proinflammatory cytokines and cytokine storm are significant contributors to the disease progress, as they significantly correlate to the severity and COVID-19 mortality [8]. Besides cytokine release and elevations in classic markers of acute inflammation, infiltration of immune cells, and progressive lymphopenia, the particularly ratio of neutrophil-to-lymphocyte is recognized as a prognostic marker [9]. It is hypothesized that in COVID-19, this infiltration of neutrophils leads to reactive oxygen species (ROS) secretion that boosts both hyperinflammation and further damage [10]. Alongside, the disturbed antioxidant-prooxidant balance that leads to oxidative stress (OS) is also contributed by the decreased antioxidant defense in viral infections, leading to lipid peroxidation and DNA oxidation [11].

However, besides several reviews hypothesizing the potential role of oxidative stress in COVID-19 and its possible implication in the disease severity, there is no data available on prooxidative and antioxidative parameters and their possible effects on prognosis in COVID-19 patients. Therefore, we aimed to explore their possible role in predicting severity and intrahospital mortality of COVID-19, alongside with other laboratory and biochemical procedures, symptoms, and admission arterial gas analysis parameters.

2. Patients and Methods

2.1. Ethical Concerns. The study was approved by the Ethical Committee of Clinical Center Kragujevac, number 01/20/485 from 24/04/2020. All researched procedures were done in Clinical Center Kragujevac, Serbia, and in the Laboratory for Cardiovascular Research, Faculty of Medical Science. In the study, all procedures were done according to the Declaration of Helsinki (Revision 2013) and Good Clinical Practice. Written informed consent for participation was obtained from all patients.

2.2. Protocol of the Study. This study was designed as an observational prospective cross-sectional clinical study which was conducted on 127 patients with diagnosed respiratory COVID-19 viral infection. All participants were included in the study during the second peak of the pandemic period from April to the end of August 2020. Inclusion criteria were written informed consent, older than 18 years, and PCR-confirmed (polymerase chain reaction test) SARS-CoV-2-etiology of disease. All patients were, after admission, followed-up for different periods, according to the course of the disease. From all patients, we collected anamnestic data, clinical symptom data, and biochemical data and oxidative stress parameters on the first day of hospitalization. We set two primary goals in our study:

(1) To determine the predictors of severity of COVID-19 and disease progression

(2) To determine the predictors of negative outcome (fatal) or positive outcome (complete or incomplete regression on chest roentgenogram at hospital discharge)

2.3. Clinical Management. All confirmed COVID-19 patients were hospitalized with precautions for airborne transmission. Patients were followed prospectively during hospital treatment. All predictors were determined on the first day of hospitalization: clinical symptoms and signs, comorbidities, and biochemical and oxidative stress parameters.

Patients with moderate to severe hypoxia (requiring of inspired oxygen ≥ 40%) were transferred during hospitalization to the intensive care unit (ICU) for high-flow oxygen via nasal cannula, noninvasive ventilation, or invasive mechanical ventilation. According to the World Health Organization (WHO), patients were assigned to one of the three categories/groups [12]:

(1) Patients with a mild form of COVID-19 (mild symptoms up to mild pneumonia) ($n = 17$)

(2) Patients with a moderate COVID-19 (dyspnea, hypoxia, or less than 50% lung involvement on imaging) ($n = 40$)

(3) Patients with a severe COVID-19 (patients with severe respiratory failure, need for high flow oxygen therapy, mechanical ventilation, sepsis, or multiorgan system dysfunction) ($n = 70$)

2.4. Biochemical Analysis. All biochemical procedures were done on the first day of hospital admission in a specialized biochemical laboratory of the Clinical Center Kragujevac, Serbia. Complete blood cell count (CBC) was measured using a hematology analyzer (DxH 800 Hematology Analyzer by Beckman Coulter). The biochemical parameters such as glucose, creatinine, urea, cholesterol, triglyceride (TG), aspartate aminotransferase (AST), alanine aminotransferase (ALT) gamma-glutamyl transferase (GGT), lactate dehydrogenase (LDH), total and direct bilirubin, C-reactive protein (CRP), sodium, and potassium were estimated from the serum samples by using standard kits in an automatic clinical chemistry analyzer (AU680 Clinical Chemistry Analyzer by Beckman Coulter). Measurement of the vitamin D level was performed

using an automated immunoassay analyzer—the Alinity i system (Abbott Laboratories, IL, USA) that utilizes the chemiluminescent microparticle immunoassay (CMIA) principle. The level of procalcitonin in the serum was determined by the method of electrochemiluminescence, on the immunochemistry analyzer (Cobas e 411 by Roche). D dimer concentration measurement was performed on coagulation analyzer ACL-TOP 300 (Instrumentation Laboratory, Bedford, USA) employing the automated latex-enhanced particle immunoturbidimetric method.

2.5. Determination of Markers of Oxidative Stress in Plasma and Lysate Samples. In plasma samples, on the first day of hospital treatment, we measured the concentration of prooxidative markers such as superoxide anion radical (O_2^-), hydrogen peroxide (H_2O_2), nitric oxide (NO^-), and the index of lipid peroxidation measured as TBARS (TBARS). The determination of the nonenzymatic antioxidant activity, such as the activity of the enzymatic defense system, by evaluating the catalase (CAT) and concentrations of superoxide dismutase (SOD) and reduced glutathione (GSH) was determined in the lysate.

Determination of the superoxide anion radical (O_2^-) was performed by measuring the concentration of the superoxide anion radical (O_2^-) after the reaction of nitro blue tetrazolium in Tris buffer with the plasma at 530 nm. Distilled water solution served as a blank probe [13]. An indirect method for monitoring nitric oxide (NO) by determining nitrate (NO_3^-) and nitrite (NO_2^-) was performed as previously described by Pick and Keisari [14]. The plasma volume of 0.5 ml was precipitated with 200 μl of 30% sulfosalicylic acid, then vortexed for 30 min, and centrifuged at $3000 \times g$. Supernatant and Griess reagent in the equal volumes containing 0.1% naphthalene ethylenediamine dihydrochloride/1% sulphanilamide in 5% phosphoric acid were added and then incubated for 10 min in the dark and measured at 543 nm [15]. The degree of lipid peroxidation in the plasma (TBARS) was estimated by measuring TBARS using 1% thiobarbituric acid in 0.05 NaOH, incubated with plasma at 100°C for 15 min, and measured at 530 nm. Distilled water served as a blank probe [16].

The level of reduced glutathione (GSH) was determined based on GSH oxidation with 5.5-dithio-bis-6.2-nitrobenzoic acid using the method of Beutler [17]. CAT activity was determined according to Aebi. Lysates were diluted with H_2O (1 : 7 *v*/*v*) and treated with chloroform-ethanol (0.6 : 1 *v*/*v*) in order to remove the hemoglobin. After that, 1 ml of 10 mM H_2O_2, 100 μl of the sample, and 50 μl of CAT buffer were added to the samples. Detection was performed at 360 nm [18]. In order to determine the SOD activity, the epinephrine method of Beutler was used. A total of 1 ml of carbonate buffer and 100 μl of lysate were mixed, after which100 μl of epinephrine was added. Detection was performed at 470 nm [19].

2.6. Statistical Analysis. Statistical analysis was conducted with the SPSS for Macintosh version 26.0 software. Data are presented as the mean values ± standard errors of the mean/-standard deviations with statistical significance. For the categorical variable, results are presented as the frequency from the total sample (in percent). The normality of the distribution of the parameters being analyzed was determined using the Shapiro-Wilk test. We used a parametric Friedman's ANOVA test or a nonparametric Kruskal-Wallis test or chi-squared test according to the data characteristics and distribution. Also, Pearson's correlation analysis and the linear regression model were used to test the association between variables and to find the significant predictors for general outcome and severity of SARS-CoV-2 infection. The accepted level of significance was defined as $p < 0.05$ for confidence interval of 95%.

3. Results

3.1. Demographic and Clinical Characteristics of Patients Infected with SARS-CoV-2. In Table 1, the basic demographic characteristics and presence of comorbidity in the study population according to the subgroups of patients are shown. Distribution of comorbidities and hypertension was significantly different in three groups of COVID-19 patients. Comorbidities were present in 66.7% of the patients with severe COVID-19 infection and in 20.5% of the patients with a moderate form of the disease. One of them, hypertension, was present in 70.1% of the patients with a severe form and in 16.4% of the patients with a moderate form of COVID-19 infection (Table 1). Other comorbidities were not significantly different in our three groups.

In Table 2, distribution of specific symptoms of COVID-19 infection in the study group is shown. It is observed that elevated body temperature, cough, and diarrhea were significantly different, distributed in these three groups: the elevated temperature was significantly present in the group with a severe form of the disease (58.6%) and in the group with a moderate form of the disease (28.8%); cough was present in 61.5% of the patients with a severe form and 23.1% of the patients with a moderate form of the disease; diarrhea was not present in 58.4% of the patients with a severe form and 31.9% in the group of patients with a moderate form of the disease (Table 2). Other specific symptoms such as anosmia, ageusia, and dyspnea were not significantly different, present in mild, moderate, and severe groups.

3.2. Respiratory and Cardiovascular Symptoms of COVID-19 in the Study Population. In our study, we evaluated the means of respiratory and cardiovascular symptoms in three groups of patients (Table 3). Patients with severe forms of infection were significantly older than other patients in groups. Also, respiratory and heart rates at admission were significantly higher in patients with severe and mild forms compared with respiratory and heart rates in patients with a moderate SARS-CoV-2 form of the disease. Also, SBP (systolic blood pressure) and DBP (diastolic blood pressure) were significantly higher in patients with the severe form of the disease. Other respiratory signs such as $SatO_2$ (oxygen saturation) did not significantly differ between these groups (Table 3).

Furthermore, from all observed hematological and inflammatory markers, only WBC (white blood cell) count

Table 1: Basic demographic characteristics and presence of comorbidity in the study population ($n = 127$). Data are presented as frequency (%) from the total number of participants.

Variables	Degree of COVID19 infection ($n = 127$)			p values
	Mild	Moderate	Severe	
Gender (M/F)	11/6 (12.6%/15%)	27/13 (31%/32.5%)	49/21 (56.3%/52.5%)	$p = 0.903$
Smoking (no/yes)	13/4 (11.8%/23.5%)	34/6 (30.9%/35.3%)	63/7 (57.3%/41.2%)	$p = 0.318$
Comorbidity (no/yes)	7/10 (14.3%/12.8%)	24/16 (49%/20.5%)	18/52 (36.7%/66.7%)	$p = 0.002^{a,b,c}$
Hypertension (no/yes)	8/9 (13.3%/13.4%)	29/11 (48.3%/16.4%)	23/47 (38.3%/70.1%)	$p \leq 0.001^{a,b,c}$
Diabetes mellitus (no/yes)	11/6 (11.5%/19.4%)	34/6 (35.4%/19.4%)	51/19 (53.1%/61.3%)	$p = 0.193$
Obesity (no/yes)	12/5 (11.3%/23.8%)	36/4 (34%/19%)	58/12 (54.7%/57.1%)	$p = 0.192$
COPD (no/yes)	16/1 (13.2%/16.7%)	38/2 (31.4%/33.3%)	67/3 (55.4%/50%)	$p = 0.957$
Malignant disease (no/yes)	16/1 (13%/25%)	39/1 (37.1%/25%)	68/2 (55.3%/50%)	$p = 0.782$

Statistical significance was established by chi square test (X^2 test) as follows: [a]mild vs. moderate; [b]mild vs. severe; [c]moderate vs. severe.

Table 2: Characteristic symptoms of SARS-CoV19 infection in the study population ($n = 127$). Data are presented as frequency (%) from the total number of participants.

Variables	Degree of COVID19 infection ($n = 127$)			p values
	Mild	Moderate	Severe	
Elevated body temperature (no/yes)	3/14 (18.8%/12.6%)	8/32 (50%/28.8%)	5/65 (31.3%/58.6%)	$p = 0.008^{a,b,c}$
Cough (no/yes)	3/14 (8.3%/15.4%)	19/21 (52.8%/23.1%)	14/56 (38.9%/61.5%)	$p = 0.005^{a,b,c}$
Anosmia (no/yes)	13/4 (12%/21.1%)	35/5 (32.4%/26.3%)	60/10 (55.6%/52.6%)	$p = 0.550$
Ageusia (no/yes)	14/3 (13%/16.7%)	35/5 (32.4%/27.8%)	59/10 (54.6%/55.6%)	$p = 0.887$
Dyspnea (no/yes)	10/7 (13.9%/12.7%)	26/14 (36.1%/25.5%)	36/34 (50%/61.8%)	$p = 0.378$
Diarrhea (no/yes)	11/6 (9.7%/42.9%)	36/4 (31.9%/28.6%)	66/4 (58.4%/28.6%)	$p = 0.002^{a,b,c}$

Statistical significance was established by chi square test (X^2 test) as follows: [a]mild vs. moderate; [b]mild vs. severe; [c]moderate vs. severe.

Table 3: Respiratory and cardiovascular symptoms of SARS-CoV19 infection in study population ($n = 127$). Data are presented as mean and standard deviation in all study groups.

Severity of COVID-19 infection		Respiratory symptoms								
		Age (years)	Resp rate (beats/min)	Heart rate (beats/min)	SBP (mmHg)	DBP (mmHg)	$SatO_2$ (%)	PaO_2 (mmHg)	$PaCO_2$ (mmHg)	pH
Mild	Mean	59.24	24.00	88.47	139.41	81.76	92.47	72.35	44.59	549.71
	Std. deviation	14.76	4.62	11.68	15.90	9.67	5.99	25.87	12.64	316.01
	n	17	17	17	17	17	11	17	17	17
Moderate	Mean	49.60	19.62	82.58	127.88	77.50	93.57	77.79	44.26	694.54
	Std. deviation	16.12	1.58	7.12	13.58	8.03	6.55	38.49	9.47	182.55
	n	40	26	26	26	26	7	28	27	26
Severe	Mean	61.39	24.02	90.67	142.81	83.76	92.33	74.31	41.07	683.98
	Std. deviation	12.87	3.83	8.30	12.62	7.24	4.19	32.78	15.18	197.59
	n	70	42	42	42	42	15	51	46	43
		$p \leq 0.001^{a,b}$	$p \leq 0.001^{a,c}$	$p \leq 0.001^{a,c}$	$p \leq 0.001^{a,b,c}$	$p = 0.010^{a,b,c}$	$p = 0.596$	$p = 0.852$	$p = 0.494$	$p = 0.075$

Statistical significance was established by ANOVA analysis with Tukey-B post hoc test as follows: [a]mild vs. moderate; [b]mild vs. severe; [c]moderate vs. severe.

Table 4: Hematological markers, cardiac enzymes, and inflammatory markers in all study groups. Data are presented as mean and standard deviation in all study groups.

		Parameters											
		WBCs	Lym	Lym%	HGB	PLT	Fe	Trop	CRP	FIB	CK	CK-MB	LDH
Mild	Mean	7.47	1.36	17.50	127.43	274.45	12.29	0.00	58.65	6.12	192.00	14.04	513.35
	Std. deviation	3.47	0.69	12.57	14.56	128.62	24.53	0.00	97.44	6.21	485.70	7.74	218.50
Moderate	Mean	8.14	1.39	19.26	131.51	259.92	5.38	0.00	51.10	4.79	114.57	12.48	501.80
	Std. deviation	4.43	0.84	10.62	18.91	103.79	4.50	0.00	61.76	1.78	102.47	5.72	314.78
Severe	Mean	9.43	1.65	17.38	130.54	281.94	5.92	0.86	76.19	5.26	128.19	12.62	643.13
	Std. deviation	4.62	1.81	12.79	17.09	125.19	5.62	9.06	87.28	1.96	148.96	6.76	313.30
		$p = 0.011^{b,c}$	$p = 0.306$	$p = 0.517$	$p = 0.453$	$p = 0.405$	$p = 0.063$	$p = 0.603$	$p = 0.076$	$p = 0.112$	$p = 0.252$	$p = 0.594$	$p = 0.003^{a,b,c}$

Statistical significance was established by ANOVA analysis with Tukey-B post hoc test as follows: [a]mild vs. moderate; [b]mild vs. severe; [c]moderate vs. severe. WBC: white blood cells ($10^3/\mu l$); Lym: lymphocytes ($10^3/\mu l$); HGB: hemoglobin (g/l); PLT: platelets ($10^3/\mu l$); Fe: iron levels (g/dl); D: dimer (mcg/ml); TropP: troponin T (ng/ml); CRP: C-reactive protein (mg/l); Fib: fibrinogen (g/l); CK and CK-MB: creatin kinase (U/l).

Table 5: Prooxidative and antioxidative parameters in the blood in all study groups. Data are presented as mean and standard deviation in all study groups.

Severity of COVID 19 infection		Prooxidants				Antioxidant enzymes		
		O_2^- (nmol/ml)	TBARS (μmol/ml)	H_2O_2 (nmol/ml)	NO^- (nmol/ml)	CAT (U/Hb × 10^3)	SOD (U/Hb × 10^3)	GSH (U/Hb × 10^3)
Mild	Mean	3.50	1.34	2.30	3.03	0.79	22.49	103394.79
	Std. deviation	1.83	0.48	0.68	0.62	0.38	9.27	17473.95
	n	33	35	35	35	35	35	35
Moderate	Mean	4.84	1.28	2.18	3.20	0.68	19.76	96202.84
	Std. deviation	3.29	0.64	0.65	0.68	0.36	9.53	21664.02
	n	48	50	50	50	50	48	50
Severe	Mean	11.30	1.20	2.07	2.66	1.15	22.39	95272.71
	Std. deviation	5.66	0.71	0.44	0.45	0.90	11.19	21315.30
	n	31	34	34	34	34	33	34
		$p \leq 0.001^{a,b,c}$	$p = 0.603$	$p = 0.287$	$p \leq 0.001^{b,c}$	$p = 0.001^{a,b,c}$	$p = 0.363$	$p = 0.184$

Statistical significance was established by ANOVA analysis with Tukey-B post hoc test as follows: [a]mild vs. moderate; [b]mild vs. severe; [c]moderate vs. severe.

and LDH activity were significantly different in patients with mild, moderate, and severe forms of the disease (Table 4).

3.3. Prooxidative and Antioxidative Parameters in Blood in SARS-CoA-2 Infection. In Table 5 are presented values of the main prooxidants and antioxidative enzymes measured in our study at hospital admission. We have observed that in the patients with a severe form of SARS-CoV-2, levels of superoxide anion radicals were significantly higher than those in the two other groups. On the other hand, the nitric oxide level was significantly lower in patients with severe COVID-19. Catalase activity was significantly lower in the patients with a moderate form of the disease compared with the group of patients with a severe form of the disease (Table 5).

3.4. Correlation and Linear Regression Analysis of Data. In correlation analysis (Table 6), we included all statistically significant variables from previous statistical research. We observed the positive correlation between age and most of the tested variables (Table 6). Also, HTA as a categorical variable was significantly associated with RR (respiration rate), SBP, DBP, WBC, and negative outcome (fatal outcome). In our study from total number of patients, fatal outcome was observed in 14.4% and positive outcome was in 85.6%. Furthermore, anosmia showed a strong positive correlation only with ageusia. Dyspnea was in positive moderate correlation with RR, negative outcome (fatal), and RTG outcome. On the other hand, RR was in inverse correlation with NO^- levels and in positive correlation with HR, SBP, DBP, negative outcome, and duration at the ICU. Also, the mean duration at the ICU was in correlation with the severity of the disease, so, the duration in the group with a severe form of the disease was 5.96 ± 4.2 days and that in the group of with mild COVID-19 was 3.06 ± 2.2 days. In general, the duration of hospital treatment was 14.4 ± 5.2 days in the mild group, 10.45 ± 5.6 in moderate, and 16.62 ± 9.2 in patients with a severe form. Interestingly, concentrations of NO^- were in moderate negative correlation with CAT activity, RTG outcome, duration at the ICU, and in-hospital death (Table 6).

the linear regression model for two separated dependent variables, such as the general outcome (positive or negative) and severity of COVID-19 infection, provided significant results (Tables 7 and 8 Figures 1(a)–1(e)). HTA, anosmia, ageusia, O_2^-, and duration at ICU are estimated as predictors of severity of COVID-19 (Table 7). Regression variable plots present the nature of association of two different variables (Figures 1(a)–1(e)). As it shows, HTA was in positive linear association with severity of COVID-19 infection, as well as the duration of stay in the ICU. Also, dyspnea was in positive linear association with positive outcome, while the anosmia was in negative linear association with severity of SARS-CoV-2 infection in patients. Very interestingly, HR was in positive linear association with outcome in patients and the higher heart rate was a good predictor of negative outcome in patients with confirmed COVID-19 disease (Figures 1(a)–1(e)). Definitely, the presence of dyspnea and the higher heart rate were confirmed as predictors of a negative outcome (fatal) (Table 8).

4. Discussion

The main purpose of this clinical prospective cross-sectional study was to provide novel information about potential molecular mechanisms during the different degree of COVID-19 in adult patients and in consequence to provide potential new preventive and therapeutical strategies.

Our population of 127 patients consisted predominantly of middle-aged, nonsmoker males, with hypertension as the most common comorbidity. Distribution of comorbidity

Table 6: Correlation matrix of significantly different parameters between groups of patients. Results of Pearson's correlation analysis are presented as statistical significance (p) and with Pearson correlation coefficient (R).

		Age	HTA	Anosmia	Ageusia	Dyspnea	RR	HR	SBP	DBP	PaO_2	$PaCO_2$	WBC	O_2	NO	CAT	RTG outcome	Outcome	ICU (days)	Hospital (days)
Age	R																			
	p																			
HTA	R	0.569**																		
	p	0.00																		
Anosmia	R	0.06	0.04																	
	p	0.49	0.63																	
Ageusia	R	0.05	0.03	0.969**																
	p	0.61	0.77	0.00																
Dyspnea	R	0.180*	0.13	0.12	0.10															
	p	0.04	0.16	0.17	0.24															
RR	R	0.402**	0.367**	0.02	0.02	0.434**														
	p	0.00	0.00	0.82	0.84	0.00														
HR	R	0.20	0.20	−0.04	0.07	0.18	0.452**													
	p	0.06	0.06	0.75	0.53	0.10	0.00													
SBP	R	0.646**	0.598**	0.21	0.235*	0.257*	0.493**	0.340**												
	p	0.00	0.00	0.05	0.03	0.02	0.00	0.00												
DBP	R	0.474**	0.480**	0.17	0.19	0.13	0.434**	0.261*	0.769**											
	p	0.00	0.00	0.12	0.09	0.25	0.00	0.02	0.00											
PaO_2	R	−0.02	−0.10	−0.11	−0.10	−0.16	−0.357**	−0.20	−0.261*	−0.257*										
	p	0.81	0.32	0.28	0.31	0.11	0.00	0.07	0.02	0.02										
$PaCO_2$	R	0.02	−0.09	−0.01	−0.03	−0.04	0.01	−0.15	0.06	0.00	0.08									
	p	0.87	0.41	0.93	0.80	0.74	0.91	0.17	0.62	0.98	0.48									
WBC	R	0.743**	0.616*	0.45	0.39	0.21	0.828*	0.04	0.41	0.17	−0.41	−0.34								
	p	0.01	0.04	0.00	0.00	0.54	0.04	0.94	0.41	0.74	0.37	0.51								
O_2	R	0.04	0.11	−0.10	−0.10	−0.04	0.00	0.05	0.06	−0.03	0.12	0.16	0.52							
	p	0.67	0.24	0.31	0.32	0.65	0.98	0.65	0.58	0.76	0.28	0.16	0.13							
NO	R	−0.226*	−0.06	0.05	0.07	−0.15	−0.278*	−0.10	−0.14	−0.02	0.229*	−0.08	−0.27	−0.17						
	p	0.02	0.50	0.62	0.45	0.10	0.01	0.37	0.21	0.82	0.03	0.48	0.43	0.07						
CAT	R	0.08	−0.05	−0.03	−0.04	−0.07	0.13	0.18	0.03	0.08	−0.234*	0.11	−0.30	0.15	−0.249**					
	p	0.40	0.60	0.71	0.71	0.47	0.25	0.11	0.77	0.47	0.02	0.30	0.37	0.12	0.01					
RTG_ outcome	R	0.349**	0.18	−0.02	−0.03	0.341**	0.354**	0.15	0.406**	0.267*	−.314**	−0.14	−0.39	−0.10	−0.265**	0.18				
	p	0.00	0.07	0.87	0.75	0.00	0.00	0.23	0.00	0.03	0.01	0.26	0.31	0.38	0.01	0.08				
Outcome	R	0.341**	0.255**	0.08	0.09	0.246**	0.432**	0.418**	0.415**	0.365**	−0.08	−0.06	0.65	−0.07	−0.09	0.05	0.32			

Table 6: Continued.

		Age	HTA	Anosmia	Ageusia	Dyspnea	RR	HR	SBP	DBP	PaO_2	$PaCO_2$	WBC	O_2	NO	CAT	RTG outcome	Outcome	ICU (days)	Hospital (days)
ICU (days)	*p*	0.00	0.00	0.38	0.33	0.01	0.00	0.00	0.00	0.00	0.44	0.60	0.00	0.47	0.37	0.62	0.00			
	R	0.231**	0.09	−0.10	−0.11	0.08	0.367**	0.274*	0.409**	0.21	−0.16	−0.04	−0.02	0.02	−.243**	0.13	0.17	0.439**		
Hospital (days)	*p*	0.01	0.30	0.25	0.23	0.38	0.00	0.01	0.00	0.06	0.13	0.73	0.96	0.83	0.01	0.15	0.08	0.00		
	R	0.287**	0.13	−0.14	−0.16	0.10	0.19	0.06	0.248*	0.06	0.06	−0.05	0.21	−0.08	−.185*	−0.02	0.336**	0.11	0.743**	
	p	0.00	0.17	0.12	0.07	0.28	0.08	0.61	0.02	0.58	0.59	0.64	0.53	0.42	0.05	0.82	0.00	0.22	0.00	

Pearson's correlation. RR: respiratory rate; HR: heart rate; SBP: systolic blood pressure; DBP: diastolic blood pressure; WBC: white blood cells; O2: superoxide anion radical; NO: nitric oxide; CAT: catalase; ICU: intensive care unit.

Table 7: Linear regression analysis of candidate predictors for dependent variable—severity of COVID-19 infection (mild, moderate, or severe form of SARS-CoV-2 infection).

	Dependent variable: severity of COVID-19 infection				
	Unstandardized coefficients (*B*)	Std. error	Standardized coefficients (beta)	*t*	*p*
Age	0.007	0.006	0.133	1.111	0.270
Male gender	−0.022	0.146	−0.014	−0.152	0.879
Present HTA	0.322	0.124	0.225	2.598	0.011
Elevated body temperature	0.310	0.186	0.144	1.662	0.099
Anosmia	−1.621	0.696	−0.811	−2.328	0.022
Ageusia	1.601	0.712	0.783	2.247	0.026
Cough	−0.015	0.160	−0.010	−0.096	0.924
Dyspnea	0.101	0.141	0.070	0.714	0.477
RR	0.005	0.026	0.023	0.178	0.859
HR	0.012	0.010	0.143	1.172	0.245
SBP	0.008	0.009	0.148	0.845	0.401
DBP	0.006	0.016	0.065	0.370	0.712
PaO_2	0.001	0.003	0.042	0.365	0.716
WBC	0.447	0.251	1.040	1.781	0.217
O_2-	0.087	0.012	0.565	7.330	≤0.001
H_2O_2	−0.069	0.098	−0.056	−0.700	0.485
TBARS	−0.055	0.118	−0.045	−0.464	0.644
NO-	−0.087	0.093	−0.074	−0.932	0.353
CAT	0.175	0.098	0.141	1.780	0.078
Hospital (days)	−0.098	0.084	−0.641	−1.163	0.365
ICU (days)	0.025	0.013	0.191	1.989	0.049

RR: respiratory rate; HR: heart rate; SBP: systolic blood pressure; DBP: diastolic blood pressure; WBC: white blood cells; O_2^-: superoxide anion radical; H_2O_2: hydrogen peroxide; CAT: catalase; ICU: intensive care unit.

and hypertension was significantly different in the mild, moderate, and severe groups. Also, hypertension was present in 70.1% of the patients with a severe form and in 16.4% of the patients with a moderate form of COVID-19 infection.

First reports from COVID-19 showed a higher incidence of hypertension in patients hospitalized with severe COVID-19 [7, 12, 20].

The link between COVID-19 and hypertension remains ambiguous, despite these observations. The severity of COVID-19 disease is amplified in aging members of the population with a higher prevalence of hypertension; on the other hand, it corresponds to a percentage in the general population. Still is unknown, whether this relationship is age-associated or causally linked to obesity and diabetes mellitus. We also found a higher incidence of diabetic and obese patients in the group of severe COVID-19 patients, but without statistical significance.

Despite the fact that it has been reported that current smokers show the expression of the ACE-2 gene which is higher comparing to nonsmokers and the possibility of a higher risk for COVID, all epidemiological data that have been published so far show low prevalence of smokers, as well as the lack of a link between current smoking status and severity of COVID-19 [13, 14]. Furthermore, there was no link between patients who never smoked and ex-smokers and severity of COVID-19. Also, the frequency of current smokers in our study did not differ considerably between groups with different severity of COVID-19. The number of active smokers in the study group was low 11/127 (8.6%), given that the prevalence of smoking in Serbia stands around 35%. Literature data suggests that smoking status, however, appears to correlate with ACE2 gene expression thus implicating differences in gender-specific behaviors. A previous study compared current smokers with never smokers and concluded that smokers have significantly upregulated ACE2 expression in the lung and oral epithelium [21].

We found that cough as a symptom of respiratory infection, was a significantly more common symptom in patients with severe COVID-19. In a study by Leung et al., fatigue, expectoration, and stuffed nose were prognostic symptoms of severe COVID-19. Fever existed in 92.1% of the COVID-19 patients but was not predictor of disease severity [22]. On other hand, in a study by Guan et al., fever was significantly correlated with the trend of intensification of COVID-19. In this study, despite that 43.8% of the patients have fever upon admission, 88.7% of the patients had a fever in the course of hospitalization [6]. Fever that developed as a result of critical pulmonary infection was regularly observed in patients with severe COVID-19; therefore, temperature monitoring should not be the only screening method for COVID-19.

Relevant studies have shown that elderly patients have an increasing risk of serious diseases, with 80% of deaths occurring in individuals over 60 years old [2]. This association is

Table 8: Linear regression analysis of candidate predictors for dependent variable—outcome of COVID-19 infection (positive or negative outcome).

Potential predictors	Dependent variable: outcome of COVID-19 infection				
	Unstandardized coefficients (*B*)	Std. error	Standardized coefficients (beta)	*t*	*p*
HTA	0.049	0.113	0.070	0.436	0.664
DM	0.007	0.085	0.008	0.078	0.938
Obesity	−0.006	0.092	−0.006	−0.060	0.953
Smoking	−0.052	0.091	−0.050	−0.568	0.571
Temp	0.062	0.100	0.059	0.621	0.536
Anosmia	0.074	0.089	0.076	0.836	0.405
Cough	0.105	0.074	0.134	1.422	0.158
Dyspnea	0.179	0.063	0.252	2.826	0.006
Diarrhea	0.022	0.099	0.020	0.224	0.823
RR	0.022	0.012	0.224	1.872	0.065
HR	0.011	0.005	0.262	2.432	0.017
SBP	0.005	0.004	0.190	1.207	0.231
DBP	0.004	0.007	0.079	0.518	0.606
PaO_2	0.001	0.001	0.115	1.115	0.268
O_2^-	−0.007	0.007	−0.096	−0.975	0.332
H_2O_2	−0.081	0.059	−0.139	−1.376	0.172
CAT	0.018	0.059	0.032	0.312	0.756

believed to be related to the weakened immune function in the elderly population [23]. However, the rate of the disease severity increased with age, suggesting variable susceptibility to the virus in different age groups, not only related to the weakened immune function of the elderly population. Our results also show that the mean age was highest in the severe COVID-19 group (61.39 ± 12.87). Despite this, age-related associations need further investigation. Also, several social, behavioral, and comorbid factors are implicated in the generally worse outcomes in men compared with women. Underlying biological sex differences and their effects on COVID-19 outcomes still are not clear [21].

Analyzing vital signs, we found in the group with severe COVID-19 a significantly higher respiratory rate, heart rate, and values of systolic and diastolic pressure at admission, while $SatO_2$ values did not significantly differ at admission. It has been shown that the increased respiratory rate and decreased oxygen saturation were associated with higher odds of mortality [24]. Also, the available data shows that COVID-19 patients who experienced the start of CPAP, NIV, admission to ICU, or death in the hospital at admission were increasingly tachypneic and required growing amounts of supplemental oxygen. On average, these patients suffered a minor increase in heart rate [25]. These results correspond to the results of Zhou et al., where tachycardia was a rare feature [7].

When lymphocyte and leukocyte counts were compared between the patients with severe versus mild cases of COVID-19, we found a significantly higher number of WBC in the group with severe COVID-19, while the number of lymphocytes did not vary significantly between groups. Overall, patients with severe COVID-19 tend to have lower lymphocyte counts and higher leukocyte counts. It is not yet known why lymphopenia is associated with a severe form of COVID-19. The possible association is explained by the consequences of direct infections with lymphocytes, apoptosis caused by inflammation, lactic acidosis that inhibits lymphocytes, and destruction of lymph tissue [26]. In our study baseline, LDH values were highest in the group with severe COVID 19. Li et al. analyzed the relationship between LDH and disease progression and in-hospital death. They showed that LDH levels in the group with fatal outcome were substantially higher. A cutoff LDH value of 353.5 U/l predicted the in-hospital mortality (sensitivity of 94.4% and a specificity of 89.2%) [27]. The high LDH level was a risk factor for the progression of diseases in mild COVID-19 patients [28]. It has been reported that LDH may be a predictor of respiratory failure in patients with COVID [29], as well as a predictive factor for early recognition of severe COVID-19 cases [30].

The onset of inflammation was considered to have a primordial role in the evolution of the disease. The group of severe COVID-19, in our study, had the highest mean value of CRP at admission although there was no statistical significance between the groups. During inflammatory disease phases of infection, CRP can activate the immune system classical complement cascade and modulate phagocytic cell activity [31]. In COVID-19, it has been reported that CRP levels can be used for early identification of pneumonia [27] and the assessment of severe pulmonary infectious diseases [32], even though the exact effect remains unclear. In addition, our findings show that CRP levels on admission were an early indicator for COVID-19 severity, which is consistent with recent publications [33]. Previous authors suggested that an early elevation in C-reactive protein (CRP) greater than 15 mg/l provides a marker of disease severity and levels greater than 200 mg/l on admission are independently associated with five times the odds of death [21].

In our study, anosmia was singled out as a predictor of a milder form of the disease by linear regression analysis (Table 6, Figure 1(e)). Patients with anosmia have been shown to have lower mortality (OR: 0.438) and less severe disease, with lower ICU admission as well. [34]. A potential explanation is a different inflammatory response in these patients and distinctive clinical presentation. Moreover, some of the studies even point that the persistence of severe chemosensitive dysfunction could be related to the need for hospitalization after 20 days. Up to this day, there are no studies which analyze other contributing risk factors for the outcomes [35].

We have a few concerns about our results, particularly those linked to arterial hypertension. In our study, these comorbidities significantly affected the severity of the disease during hospital treatment (Figure 1(a)). Guan et al. found that in the critical ill group (admission to ICU, the use of mechanical ventilation, or death) (35.8% versus 13.7%) with severe forms of the COVID-19 disease (23.7% versus 13.4%), hypertension was a more prevailing condition [6]. It has also been described that cardiovascular diseases and hypertension were more frequent in patients with fatal outcome than those who were discharged (43% versus 28%, *p*

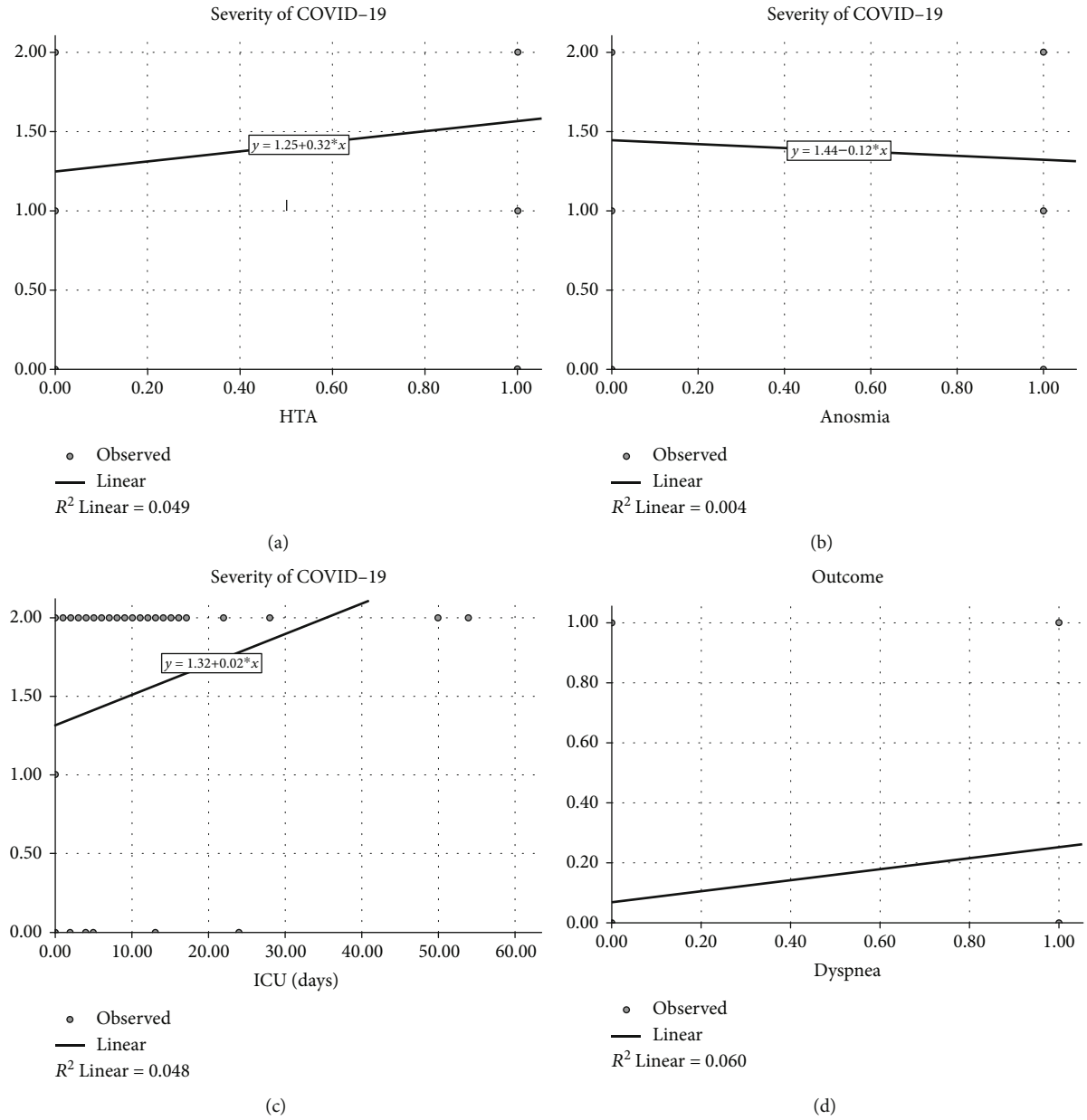

Figure 1: Continued.

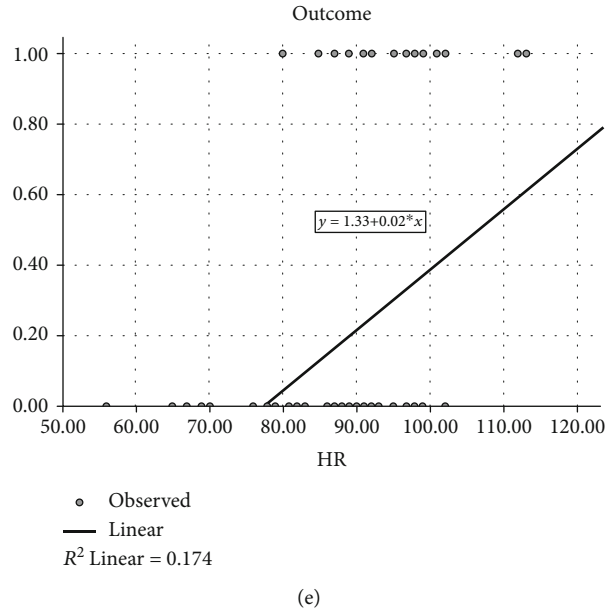

(e)

Figure 1: (a-e) Regression variable plots.

= 0.07) [36, 37]. All the evidence seem to be consistent. Contributing factors such as older age as well as associated cardiovascular disease, primarily coronary heart disease, can significantly affect the association between arterial hypertension and severity of COVID-19 and mortality rate.

The length of stay in the ICU significantly affected the severity of the disease in our study (Figure 1(c)). The mean value of days spent in the ICU in the group with severe COVID-19 was 5.96 ± 4.2 days, while the duration of hospital treatment was 14.4 ± 5.2 days in the mild group, 10.45 ± 5.6 in the moderate group, and 16.62 ± 9.2 in patients with a severe form. It has been reported that the majority of the patients (58%) were admitted to the ICU on the first day of hospital admission and in the following two days for most cases [38]. In severe pneumonia, late admission to ICU was associated with poor outcome [33]. The high extent of ICU stays and the duration of stay make challenges for hospital management. The main challenge is adequate initial assessment and treatment of patients to shorten their stay in the ICU and duration of hospitalization. On the other hand, it has been shown that a longer stay in the ICU leads to a better outcome. Reasons include slower patients weaning from the ventilator, longer follow-up of patients, prevention of relapse, and readmission in the ICU [39].

Although symptoms like dyspnea are subjective and tend to increase with reduced lung function or age, it often signifies serious underlying disease. We have shown that dyspnea on hospital admission represents an independent predictor of negative outcome (fatal). In the study of Xie et al., dyspnea was independently related with fatal outcome in COVID-19 (hazard ratio, 2.60, $p = 0.01$) [35]. Results of meta-analysis, based on 11 studies with 2091 COVID-19 patients, showed that dyspnea was frequently correlated with higher mortality (OR = 4.34, $p < 0.001$) [40].

Regarding the redox status, we evaluated the concentrations of reactive oxygen and nitrogen species, as well as the activity of enzymes of the antioxidative defense system in COVID-19 patients. As we know, the pathophysiology of pneumonia (bacterial or viral) includes activation of defense mechanisms, characterized by an immense influx of activated phagocytes [41]. Also, we know that the polymorphonuclear neutrophils and macrophages kill microorganisms by using ROS, increasing oxidative stress in the lung, which may cause a direct injury in the tissue and activate transcription factors. This leads to a local inflammatory response, which could progress to a systemic inflammatory response [42]. Definitely, oxidative stress could be an important factor in pneumonia and the crucial pathogenic mechanism underlying the development of this respiratory disease. In our study, we confirmed that in the severe form of SARS-CoA-2, levels of superoxide anion radicals were considerably higher than those in the two other groups. On the other hand, levels of nitric oxide were significantly lower in patients with the severe COVID-19. Catalase activity was significantly lower in the moderate form of the disease compared with the severe form (Table 5). A very interesting result was that the O_2^- as of the measured markers could be a sign of the severity of SARS-CoV-2 disease (Table 7). Also, the bioavailability of NO^- was in negative correlation with CAT activity, RTG outcome, duration at ICU, and in-hospital stay in general.

Today, there are very limited data about the role of oxidative stress in different degrees of viral pneumonia caused by SARS-CoV-2. Up to date, there are just a few studies which examined the redox status in COVID-19 patients. Laforge et al. examined the association of reactive oxygen species (ROS) with COVID-19 disease severity and concluded that ROS induce tissue damage, thrombosis, and red blood cell dysfunction, which contribute to COVID-19 disease severity [11]. Also, Ntyonga-Pono confirmed that oxidative stress is a strong contributor to COVID-19 infections [43]. Cecchini and Cecchini suggested that COVID-19 infection pathogenesis is a consequence of oxidative stress and after that,

cytokine storm and coagulopathy [44]. Also, they suggested that virus prompts oxidative stress but at the same time facilitates the nuclear translocation of Nrf2 with subsequent expression of HO-1, a protective enzyme against oxidative injury in the human alveolar epithelial cells. Our results, as well as results of previous studies, confirmed the connection between the severity of the disease; present comorbidities, such as elderly with diabetes, hypertension, and cardiovascular diseases; and elevated oxidative stress. In these patients, the viral infection will increase this stress, giving us one possible explanation of the severity of COVID-19 in these categories of patients [45]. With regard to the abovementioned, the oxidative stress is an important factor influencing the success or failure of the response to virus infection. The latest data about the role of oxidative stress in COVID-19 infection support the recommendation of antioxidant supplementation as a useful strategy against COVID-19. Several nutraceuticals have a proven ability of immune-boosting, antiviral, antioxidant, and anti-inflammatory effects. These include Zn, vitamin D, vitamin C, curcumin, cinnamaldehyde, probiotics, selenium, lactoferrin, quercetin, and other polyphenols. Grouping some of these phytonutrients in the right combination in the form of a food supplement may help to boost the immune system, prevent virus spread, preclude the disease progression to the severe stage, and further suppress the hyper inflammation providing both prophylactic support and therapeutic support against COVID-19 [46]. The literature clearly highlights the pharmacological activities of polyphenols from plants, that is, antioxidant, anti-inflammatory, anticancer, antibacterial, antifungal, and antiviral. Luteolin, daidzein, apigenin, amentoflavone, quercetin, epigallocatechin, epigallocatechin gallate, and gallocatechin gallate show antiviral activity through inhibition of the proteolytic activity of SARS-CoV 3C-like protease, which plays a key role for the viral replication [21].

The main limitations of our study are the presence of confounding factors (such as hypertension and obesity) that could influence the levels of oxidative stress parameters other than SARS-CoV2 infection. But given the fact that exclusion of all these factors could lead to bias regarding the predictive potential of each following parameter, we overcame this by using linear regression analysis. Also, the influence of different treatment and oxygenation types was not investigated and taken into consideration; also as one of confounding factors, however, most of the study population in our study was treated with the same type of treatment, differing just in oxygenation management.

We are sure that SARS-CoV2, probably like other RNA viruses, can trigger oxidative stress [44, 45] by disturbing the main reactive oxygen and nitrogen species such as superoxide anion radical and nitric oxide. Based on these results, we propose a reduction of patient's level of oxidative stress by supplying them with substances that improve their antioxidant system.

5. Conclusion

This is the first study to investigate the circulating oxidative stress parameters in COVID-19 patients, as well as their predictive role in the disease severity and mortality. Definitely, oxidative stress could be an important factor in this viral pneumonia and the crucial pathogenic mechanism underlying the development of this respiratory disease. We confirmed that in the different severity of SARS-CoA-2 infection are differently changed levels of superoxide anion radical, nitric oxide, and catalase activity.

Furthermore, hypertension, anosmia, and ageusia, as well as the duration of ICU stay, were identified as predictors of COVID-19 severity, while the presence of dyspnea and increased heart rate on admission were predictors of COVID-19 mortality.

Data Availability

All data are available upon request.

Conflicts of Interest

The authors declare that there is no conflict of interest.

References

[1] N. Zhu, D. Zhang, W. Wang et al., "A novel coronavirus from patients with pneumonia in China, 2019," *New England Journal of Medicine*, vol. 382, no. 8, pp. 727–733, 2020.

[2] C. Huang, Y. Wang, X. Li et al., "Clinical features of patients infected with 2019 novel coronavirus in Wuhan, China," *Lancet*, vol. 395, no. 10223, pp. 497–506, 2020.

[3] Z. Wu and J. M. McGoogan, "Characteristics of and important lessons from the coronavirus disease 2019 (COVID-19) outbreak in China," *JAMA*, vol. 323, no. 13, pp. 1239–1242, 2020.

[4] N. Chen, M. Zhou, X. Dong et al., "Epidemiological and clinical characteristics of 99 cases of 2019 novel coronavirus pneumonia in Wuhan, China: a descriptive study," *Lancet*, vol. 395, no. 10223, pp. 507–513, 2020.

[5] D. Wang, B. Hu, C. Hu et al., "Clinical characteristics of 138 hospitalized patients with 2019 novel coronavirus-infected pneumonia in Wuhan, China," *JAMA*, vol. 323, no. 11, pp. 1061–1069, 2020.

[6] W. J. Guan, Z. Y. Ni, Y. Hu et al., "Clinical characteristics of coronavirus disease 2019 in China," *New England Journal of Medicine*, vol. 382, no. 18, pp. 1708–1720, 2020.

[7] F. Zhou, T. Yu, R. Du et al., "Clinical course and risk factors for mortality of adult inpatients with COVID-19 in Wuhan, China: a retrospective cohort study," *Lancet*, vol. 395, no. 10229, pp. 1054–1062, 2020.

[8] M. K. Bohn, A. Hall, L. Sepiashvili, B. Jung, S. Steele, and K. Adeli, "Pathophysiology of COVID-19: Mechanisms underlying disease severity and progression," *Physiology*, vol. 35, no. 5, pp. 288–301, 2020.

[9] Y. Liu, X. du, J. Chen et al., "Neutrophil-to-lymphocyte ratio as an independent risk factor for mortality in hospitalized patients with COVID-19," *The Journal of Infection*, vol. 81, no. 1, pp. e6–e12, 2020.

[10] M. Z. Tay, C. M. Poh, L. Rénia, P. A. MacAry, and L. F. Ng, "The trinity of COVID-19: immunity, inflammation and intervention," *Nature Reviews Immunology*, vol. 20, no. 6, pp. 363–374, 2020.

[11] M. Laforge, C. Elbim, C. Frère et al., "Tissue damage from neutrophil-induced oxidative stress in COVID-19," *Nature Reviews Immunology*, vol. 20, no. 9, pp. 515-516, 2020.

[12] G. Onder, G. Rezza, and S. Brusaferro, "Case-fatality rate and characteristics of patients dying in relation to COVID-19 in Italy," *JAMA*, vol. 323, no. 18, pp. 1775-1776, 2020.

[13] C. Auclair and E. Voisin, *Nitroblue tetrazolium reduction*, CRC Handbook of Methods for Oxygen Radical Research, R. A. Greenvvald, Ed., CRC Press, Boca Raton, 1985.

[14] E. Pick and Y. Keisari, "A simple colorimetric method for the measurement of hydrogen peroxide produced by cells in culture," *Journal of immunological methods*, vol. 38, no. 1-2, pp. 161–170, 1980.

[15] L. C. Green, D. A. Wagner, J. Glogowski, P. L. Skipper, J. S. Wishnok, and S. R. Tannenbaum, "Analysis of nitrate, nitrite, and [^{15}N]nitrate in biological fluids," *Analytical Biochemistry*, vol. 126, no. 1, pp. 131–138, 1982.

[16] H. Ohkawa, N. Ohishi, and K. Yagi, "Assay for lipid peroxides in animal tissues by thiobarbituric acid reaction," *Analytical Biochemistry*, vol. 95, no. 2, pp. 351–358, 1979.

[17] E. Beutler, "Superoxide dismutase," in *Red Cell Metabolism, a Manual of Biochemical Methods*, E. Beutler, Ed., Grune & Stratton, New York, 1984.

[18] E. Beutler, O. Duron, and B. M. Kelly, "Improved method for the determination of blood glutathione," *The Journal of Laboratory and Clinical Medicine*, vol. 61, no. 8, pp. 882–888, 1963.

[19] H. Aebi, "Catalase in vitro," *Methods in Enzymology*, vol. 105, no. 1, pp. 121–126, 1984.

[20] S. Richardson, J. S. Hirsch, M. Narasimhan et al., "Presenting characteristics, comorbidities, and outcomes among 5700 patients hospitalized with COVID-19 in the New York City area," *JAMA*, vol. 323, no. 20, pp. 2052–2059, 2020.

[21] T. Haitao, J. V. Vermunt, J. Abeykoon et al., "COVID-19 and sex differences: mechanisms and biomarkers," *Mayo Clinic Proceedings*, vol. 95, no. 10, pp. 2189–2203, 2020.

[22] J. M. Leung, C. X. Yang, A. Tam et al., "ACE-2 expression in the small airway epithelia of smokers and COPD patients: implications for COVID-19," *European Respiratory Journal*, vol. 55, no. 5, p. 2000688, 2020.

[23] P. Goyal, J. J. Choi, L. C. Pinheiro et al., "Clinical characteristics of Covid-19 in New York City," *England Journal of Medicine*, vol. 382, no. 24, pp. 2372–2374, 2020.

[24] J. Li, Z. Chen, Y. Nie, Y. Ma, Q. Guo, and X. Dai, "Identification of symptoms prognostic of COVID-19 severity: multivariate data analysis of a case series in Henan province," *Journal of Medical Internet Research*, vol. 22, no. 6, p. 19636, 2020.

[25] J. Wu, W. Li, X. Shi et al., "Early antiviral treatment contributes to alleviate the severity and improve the prognosis of patients with novel coronavirus disease (COVID-19)," *Journal of Internal Medicine*, vol. 288, no. 1, pp. 128–138, 2020.

[26] K. E. Sands, R. P. Wenzel, L. E. McLean et al., "Patient characteristics and admitting vital signs associated with coronavirus disease 2019 (COVID-19)–related mortality among patients admitted with noncritical illness," *Infection Control & Hospital Epidemiology*, vol. 1, pp. 1–7, 2020.

[27] M. Pimentel, O. C. Redfern, R. Hatch, J. D. Young, L. Tarassenko, and P. J. Watkinson, "Trajectories of vital signs in patients with COVID-19," *Resuscitation*, vol. 156, pp. 99–106, 2020.

[28] L. Tan, Q. Wang, D. Zhang et al., "Lymphopenia predicts disease severity of COVID-19: a descriptive and predictive study," *Signal Transduction and Targeted Therapy*, vol. 5, no. 1, p. 33, 2020.

[29] X. Dong, L. Sun, and Y. Li, "Prognostic value of lactate dehydrogenase for in-hospital mortality in severe and critically ill patients with COVID-19," *International Journal of Medical Sciences*, vol. 17, no. 14, pp. 2225–2231, 2020.

[30] J. Shi, Y. Li, X. Zhou et al., "Lactate dehydrogenase and susceptibility to deterioration of mild COVID-19 patients: a multicenter nested case-control study," *BMC Medicine*, vol. 18, no. 1, p. 168, 2020.

[31] E. Poggiali, D. Zaino, P. Immovilli et al., "Lactate dehydrogenase and C-reactive protein as predictors of respiratory failure in CoVID-19 patients," *Clinica Chimica Acta*, vol. 509, pp. 135–138, 2020.

[32] Y. Han, H. Zhang, S. Mu et al., "Lactate dehydrogenase, an independent risk factor of severe COVID-19 patients: a retrospective and observational study," *Aging*, vol. 12, no. 12, pp. 11245–11258, 2020.

[33] S. P. Ballou and I. Kushner, "C-reactive protein and the acute phase response," *Advances in Internal Medicine*, vol. 37, pp. 313–336, 1992.

[34] A. Warusevitane, D. Karunatilake, J. Sim, C. Smith, and C. Roffe, "Early diagnosis of pneumonia in severe stroke: clinical features and the diagnostic role of C-reactive protein," *PloS One*, vol. 11, no. 3, article e0150269, 2016.

[35] R. Muñoz-Bermúdez, E. Abella, F. Zuccarino, J. R. Masclans, and J. Nolla-Salas, "Diagnosis and treatment of acute pulmonary inflammation in critically ill patients: the role of inflammatory biomarkers," *World Journal of Critical Care Medicine*, vol. 8, no. 5, pp. 59–63, 2019.

[36] W. Chen, K. I. Zheng, S. Liu, Z. Yan, C. Xu, and Z. Qiao, "Plasma CRP level is positively associated with the severity of COVID-19," *Annals of Clinical Microbiology and Antimicrobials*, vol. 19, no. 1, p. 18, 2018.

[37] B. Talavera, et al.D. García-Azorín, E. Martínez-Pías et al., "Anosmia is associated with lower in-hospital mortality in COVID-19," *Journal of the Neurological Sciences*, vol. 419, p. 117163, 2020.

[38] L. A. Vaira, C. Hopkins, M. Petrocelli et al., "Do olfactory and gustatory psychophysical scores have prognostic value in COVID-19 patients? A prospective study of 106 patients," *Journal of Otolaryngology-Head & Neck Surgery*, vol. 49, no. 1, p. 56, 2020.

[39] Q. Ruan, K. Yang, W. Wang, L. Jiang, and J. Song, "Clinical predictors of mortality due to COVID-19 based on an analysis of data of 150 patients from Wuhan, China," *Intensive Care Medicine*, vol. 46, no. 5, pp. 846–848, 2020.

[40] P. Boëlle, T. Delory, X. Maynadier et al., "Trajectories of hospitalization in COVID-19 patients: an observational study in France," *Journal of Clinical Medicine*, vol. 9, no. 10, p. 3148, 2020.

[41] P. K. Bhatraju, B. J. Ghassemieh, M. Nichols et al., "Covid-19 in critically ill patients in the Seattle region — case series," *The Lancet Respiratory Medicine*, vol. 382, no. 21, pp. 2012–2022, 2020.

[42] J. Xie, N. Covassin, Z. Fan et al., "Association between hypoxemia and mortality in patients with COVID-19," *Mayo Clinic Proceedings*, vol. 95, no. 6, pp. 1138–1147, 2020.

[43] M.-P. Ntyonga-Pono, "COVID-19 infection and oxidative stress: an underexplored approach for prevention and treatment?," *Pan Africa Medical Journal*, vol. 35, no. Supp 2, 2020.

[44] R. Cecchini and A. L. Cecchini, "SARS-CoV-2 infection pathogenesis is related to oxidative stress as a response to aggression," *Medical Hypotheses*, vol. 143, p. 110102, 2020.

[45] P. Mehta, D. F. McAuley, M. Brown et al., "COVID-19: consider cytokine storm syndromes and immunosuppression," *Lancet*, vol. 395, no. 10229, pp. 1033-1034, 2020.

[46] C. Lammi and A. Arnoldi, "Food-derived antioxidants and COVID-19," *Journal of Food Biochemistry*, vol. 45, no. 1, p. e13557, 2021.

Hindawi
Oxidative Medicine and Cellular Longevity
Volume 2021, Article ID 6676057, 7 pages
https://doi.org/10.1155/2021/6676057

Research Article

The Impact of Hepatitis C Virus Genotypes on Oxidative Stress Markers and Catalase Activity

Vukica Đorđević,[1] Dobrila Stanković Đorđević,[1] Branislava Kocić,[1] Marina Dinić,[1] Danka Sokolović,[2] and Jana Pešić Stanković[3]

[1]*Faculty of Medicine University of Niš, Serbia*
[2]*Clinical Centre of Niš, Serbia*
[3]*Institute of Public Health Niš, Serbia*

Correspondence should be addressed to Vukica Đorđević; vukica.djordjevic@medfak.ni.ac.rs

Received 4 December 2020; Accepted 27 January 2021; Published 25 February 2021

Academic Editor: Daniele Vergara

Copyright © 2021 Vukica Đorđević et al. This is an open access article distributed under the Creative Commons Attribution License, which permits unrestricted use, distribution, and reproduction in any medium, provided the original work is properly cited.

Hepatitis C virus (HCV) is a major cause of liver disease worldwide. Chronic HCV infections are usually associated with increased oxidative stress in the liver tissue. The intensity of oxidative stress may be a detrimental factor in liver injury and may determine the severity of the disease. The aim of the present case-control study was to determine the level of lipid peroxidation (TBARS), protein oxidative modification (AOPP), and catalase activity in sera of patients infected with HCV, in relation to different HCV genotypes and viral load. Considering the HCV patients with chronic hepatitis C (52) and control subject (50) recruitment, the study was designed as a case–control-type. The HCV RNA isolation, viral load, and HCV genotyping were performed according to the standard protocols. A significant difference compared to control healthy subjects was reported for TBAR ($p < 0.001$), AOPP ($p = 0.001$), and catalase activity ($p = 0.007$). In a gender-based comparison, a significantly higher level of AOPP for females was reported ($p < 0.001$). As stratified by HCV genotype, the most common was HCV-1 (HCV-1a and HCV 1b), with the overall participation of more than 60%, followed by genotype 3, while the least represented was genotype 2. No significant difference was documented among genotypes in regard to oxidative stress markers, although somewhat higher TBARS level, but not significant, was registered in patients infected with genotype 1b. A statistically significant positive correlation was found between the concentration of HCV genome copies and AOPP ($r = 0.344$; $p = 0.012$). A high level of HCV viral load was more likely to have a higher TBARS, but still without statistical significance ($p = 0.072$). In conclusion, the results obtained confirmed an imbalance between the ROS production and antioxidative defense system in HCV-infected patients. Since oxidative stress may have a profound influence on disease progression, fibrosis, and carcinogenesis, our results may meet the aspirations of mandatory introduction of antioxidants as early HCV therapy to counteract ROS consequences.

1. Introduction

Hepatitis C virus (HCV) is a major cause of liver disease worldwide. According to the World Health Organization (WHO) report, the estimated prevalence of 0.5%-3% is registered worldwide. In Europe, it is estimated that there are about 14 million people infected [1]. Hepatitis C virus (HCV) belongs to the *Flaviviridae* family, genus *Hepacivirus*. HCV is a small (55-65 nm in diameter), enveloped, icosahedral particle. The genome of the virus is positive single-stranded RNA with approximately 9600 nucleotides in length. It is composed of two conserved untranslated terminal regions at the 5′ and 3′ ends and the open reading frame (ORF) in the middle. ORF is divided into structural genes (C, E1, and E2) and nonstructural genes (NS2, NS3, NS4a, NS4b, NS5a, and NS5b). The C gene encodes nucleocapsid protein; E1 and E2 genes encode glycosylated proteins of the envelope membrane; nonstructural genes encode nonstructural proteins, which participate in the processes of virus replication [2]. According to the level of nucleotide sequence homology, HCV isolates are divided into seven genotypes. The isolates, which belong to the same genotype, are further divided into

subtypes (a, b, c, *etc*.) [3]. The degree of homology of nucleotide sequences between different genotypes is about 65% [4]. The region 5′, the core and nonstructural genes are highly conserved sequences of the viral genome, while E1 and E2 genes show a high nucleotide sequence heterogeneity among isolates of different genotypes [4]. In addition, a very important biological characteristic of HCV is the variability of its E2 gene domains HVR1 and HVR2. Mutations in the E2 gene lead to the appearance of HCV mutants (quasispecies). Since the E2 protein is a target for neutralizing antibodies, mutations of this HCV region enable the virus to escape the elimination by the humoral immune response. This is explained as the mechanism of establishing a persistent infection [5].

The HCV infection is a serious health problem, because of a persistent infection in most infected individuals. It may be clinically manifested by chronic liver disease, often with a progressive course, from chronic hepatitis, through liver cirrhosis, to primary hepatocellular carcinoma. About 20 to 30% of patients with chronic hepatitis develop cirrhosis after 10 to 30 years. In these patients, the risk of death from cirrhosis-related complications is 4% per year, and the risk of developing a hepatocellular carcinoma (HCC) in cirrhotic patients is 1% to 5% per year. Thirty-three percent of patients with HCC die within one year after diagnosis [6, 7]. The pathogenetic mechanisms responsible for hepatocyte damage include cytotoxic T cell immune response and oxidative stress [8].

Chronic hepatitis C virus (HCV) infections are usually associated with increased oxidative stress in the liver tissue. The intensity of oxidative stress may be a detrimental factor in liver injury and may determine the severity of the disease [9, 10]. The cells responsible for ROS production and liberation are hepatocytes, nonparenchymal liver cells, such as Kupffer cells (resident macrophages), inflammatory cells, hepatic stellate cells (HSCs), and other immune effector cells [11]. They interact with each other, and a vicious cycle arises. Following liver injury, a set of reactive oxygen species (ROS) is released throughout the disturbance of mitochondrial electron transfer chain and oxidase activity [12]. Among the increased rate of ROS, species are the superoxide anions (O_2^-), hydrogen peroxide (H_2O_2), and the most hazardous hydroxyl radical (HO•). It may lead to a serious disintegration of cell lipid components (phospholipid membranes), the oxidative modification of proteins, and oxidative modification of DNA. They may induce cell damage, protein functional deficiency, and genome instability, associated with the increased incidence of cell death and/or hepatocellular carcinoma. Hepatic fibrosis is a complex process, which involves the death of hepatocytes and activation of hepatic stellate cells [13].

Liver cells possess a specialized system of defense against oxidative stress, which comprises enzymes and nonenzymatic system of vitamin and nonvitamin origin. Among the enzymatic systems in the liver tissue, the most pronounced are catalase, superoxide dismutase (SOD), glutathione reductase (GSR), and glutathione transferase (GST). Consequent cell damage may lead to a short-term adaptation via induced liver regeneration, but very quickly, the adaptive mechanisms are reduced and the two possible pathways may arise, i.e., genomic instability, which may lead to carcinogenesis or to cell death. As a consequence of altered protein synthesis and consequent protein oxidative modification, the antioxidative defense enzymatic system becomes relatively insufficient to protect against the enormous attack of liberated ROS [14, 15]. Cell death induces the replacement of functional liver tissue by fibroblasts and in consequence functional liver failure and cirrhosis begin. ROS may play an important role as signal molecules responsible for the activation of stress-surviving signaling pathways and the redox-sensitive transcriptional factors. It may further induce inflammation and consequent free radical release from the next actor-inflammatory cells. Among them are Kupffer cells, which secrete interleukin- (IL-) 1?, tumor necrosis factor-α (TNF-α), TGF-beta, and release ROS by activation of NADPH oxidase. ROS production induces the activation of redox-sensitive proinflammatory transcription factor NF-?B. Released free radicals activate hepatic stellate cells further, which become the next player and important source of ROS responsible for further hepatocyte damage and induction of the fibrosis process [16, 17].

The aim of the present case-control study was to determine the level of lipid peroxidation (TBARS), protein oxidative modification (AOPP), and catalase activity in serum of patients infected with HCV, in relation to different HCV genotypes and viral load.

2. Patients and Methods

Considering the patients with chronic hepatitis C (52) and control subject (50) recruitment, the study was designed as a case–control-type. The study was approved by the Ethical Committee of Faculty of Medicine (Decision no. 12-6972-2/6). All subjects recruited for the study signed the informed consent. The investigation was performed at the Institute for Public Health and Faculty of Medicine University of Niš (Serbia).

The enrolled patients, besides being HCV positive, were recruited by specific eligibility criteria, including the absence of HBV infection, HIV infection, other chronic liver diseases, any acute or chronic systemic immunologic conditions and inflammatory diseases, cancer, cardiovascular, or kidney diseases. The control group comprised 50 healthy volunteers, who met the same eligibility criteria, i.e., they were HCV negative, and were age- and gender-matched.

The diagnosis of HCV was performed according to the standard diagnostic protocols. The HCV RNA isolation was performed by kit Ribo-virus Sacace. Plasma HCV RNA was detected using HCV REAL-TM QUAL new version Sacace. For the detection of HCV RNA concentration (IU/mL of plasma)-viral load, HCV REAL-TM QUANT new version Sacace was used. HCV genotyping was performed using HCV Genotype PLUS REAL-TN, Sacace. All the diagnostic procedures were performed according to the recommendations of the manufacturer.

For the analysis, morning blood samples from HCV patients and control subjects were taken and centrifuged at 3.000 rpm; serum samples were kept at −80°C.

The concentration of TBARS-reactive compounds (MDA level) was performed according to the method described by Sahreen et al. [18], based on the determination

of malondialdehyde (MDA), which reacts with the thiobarbituric acid, forming a pink complex. The reaction mixture contained 0.2 mL of serum, 0.2 mL of the ascorbic acid (100 mM), 0.58 mL of the potassium phosphate buffer (0.1 M; pH = 7.4), 0.02 mL of the Ferric chloride-FeCl3 (100 mM), 1 mL of the CCl3COOH (10%), and 1 mL of the TBA (0.67% dissolved in 0.1 M NaOH) and heated for 30 min in a boiling water bath (100°C). After the centrifugation at 4000 rpm for 10 min, the absorbance of pink color was read at 535 nm. The concentration of the TBARS was expressed in μmol/L MDA.

The concentration of AOPP was determined by spectrophotometric method according to the method of Witko-Sarsat et al. [19]. The quantity of 200 μL of serum, diluted as 1 : 5 in PBS, and chloramine-T standard solutions were placed in a 96-well microtiter plate, followed by 20 μL of acetic acid. Ten microliters of 1.16 M KJ was added, followed by 20 μL of the glacial CH3COOH. The yellow color was read at 340 nm in a microplate reader against a blank. The concentration of the AOPP was expressed in μmol/L chloramine T.

Catalase activity in serum was determined using a spectrophotometric method of Nabavi et al. [20]. Briefly, a reaction mixture contained 0.5 mL of 50 mM phosphate buffer (pH 5.0), 1.5 mL of 5.9 mM H_2O_2, and 0.1 mL of serum. It was incubated for 5 min; afterward, the reaction was stopped by adding 0.1 mL of 20% TCA and 1 mL of 4% ammonium molybdate. The samples were centrifuged and, the change in absorbance was calculated at 240 nm, by subtracting from the standard sample, where 0.1 mL of distilled water was added instead of serum. CAT activity was defined as Kat/L, meaning an absorbance change of 0.01 as unit/min.

Statistical data analysis was performed in the SPSS program, version 20. The normality of data distribution was tested by the Kolmogorov-Smirnov test. The comparison between groups was performed by the Student's t-test and ANOVA in the case of normally distributed data. In the case when the data distribution was not normal, Mann–Whitney U test or Kruskal-Wallis test was used. The correlation between the variables was performed by the Pearson coefficient of the linear correlation. Statistical significance is considered for $p < 0.05$.

3. Results

Table 1 shows the HCV genotype distribution among patients. As stratified by HCV genotype, the distribution of the study population was as follows: the most common was HCV-1 (HCV-1a and HCV 1b), with the overall participation of HCV-1 more than 60%, followed by genotype 3, while the least represented was genotype 2.

Table 2 shows the level of oxidative stress parameters (TBARS, AOPP) and catalase activity in HCV patients and control healthy subjects. All parameters examined showed a significant difference compared to control healthy subjects, which for TBAR was as $p < 0.001$, for AOPP as $p = 0.001$, and for catalase as $p = 0.007$.

Table 3 shows a gender-based comparison of oxidative stress parameters (TBARS and AOPP) and catalase activity in the HCV patient group. A significantly higher level of AOPP for females was reported, which was as $p < 0.001$. Additionally, a gender distribution showed that males were more likely to have a higher TBARS level and catalase activity, but without any statistical significance.

Table 1: Genotype distribution among HCV patients.

	n	%
1a	17	33.3
1b	14	27.5
2	4	7.8
3	16	31.4

HCV genotyping was performed using HCV Genotype PLUS REAL-TN.

The values of oxidative stress parameters (TBARS and AOPP) and catalase activity in patients infected with different HCV genotypes are summarized in Table 4. Genotype distribution revealed that HCV1b patients were more likely to have a higher TBARS compared to others, HCV 3 patients were more likely to have a higher AOPP level, while patients infected with HCV1a were more likely to have a low catalase activity, but without statistical significance.

Table 5 shows the correlation of HCV viral load and oxidative stress parameters (TBARS and AOPP) and catalase activity. A statistically significant positive correlation was found between virus genome copies concentration and AOPP ($r = 0.344$; $p = 0.012$), which means that with the increase in the concentration of gene copies the level of AOPP increases significantly. Correlation analysis showed that the high level of HCV viral load was more likely to have a higher TBARS, but without statistical significance ($p = 0.072$).

4. Discussion

Our study documented that among all HCV genotypes detected, genotype 1 (a and b) represents the most prevalent genotype with the distribution of over 60%, followed by genotype 3 (Table 1). This frequency distribution is reported worldwide [4].

The present study further involved the evaluation of oxidative stress markers (TBARS and AOPP) and catalase activity in patients infected with HCV genotypes 1a, 1b, 2, and 3. The results obtained indicated that patients infected with different genotypes were under altered equilibrium between the ROS production and antioxidant defense system, due to overproduction of ROS and a decreased antioxidative defense. The level of TBAR-reacting substances, expressed as MDA level, was almost twice as that of the uninfected, healthy controls (Table 2). A gender-based comparison of oxidative stress parameters (TBARS and AOPP) and catalase activity in the HCV patients group revealed a significantly higher level of AOPP for females, while males were more likely to have a higher TBARS level, but without statistical significance (Table 3).

No significant difference was documented among genotypes, although somewhat higher TBARS level, but not significant, was registered in patients infected with genotype 1b (Table 4). Our results are in accordance with Ansari et al.

Table 2: Oxidative stress parameters (TBARS and AOPP) and catalase activity between HCV patients and control healthy group.

	HCV patients	Control group	t/Z	p
TBARS	6.99 ± 4.02	4.38 ± 1.38	3.712	<0.001
AOPP	122.40 ± 43.12	97.92 ± 30.90	3.285	0.001
Catalase	183.41 ± 134.08	260.60 ± 132.04	2.677	0.007

Data are expressed as mean ± SD.TBARS were expressed as (μmol/LMDA), AOPP as μmol/L chloramine T, and catalase as (Kat/L). Statistical analysis was performed by using Z- Mann–Whitney U test.

Table 3: Gender-based comparison of oxidative stress parameters (TBARS and AOPP) and catalase activity in the HCV patient group.

	Man	Women	t/Z	p
TBARS	7.72 ± 5.00	6.55 ± 3.26	3.712	0.522
AOPP	107.42 ± 40.38	131.74 ± 42.72	2.034	0.047
Catalase	195.84 ± 118.33	174.67 ± 145.69	2.677	0.409

Data are expressed as mean ± SD. TBARS were expressed as (μmol/LMDA), AOPP as μmol/L chloramine T, and catalase as (Kat/L). Statistical analysis was performed by using Z- Mann–Whitney U test.

Table 4: Oxidative stress parameters (TBARS and AOPP) and catalase activity in regard to HCV genotype.

	TBARS	AOPP	Catalase
1a	6.73 ± 3.11	117.27 ± 33.84	172.17 ± 149.34
1b	7.45 ± 5.86	122.46 ± 48.53	190.92 ± 137.66
2	6.93 ± 4.47	124.14 ± 43.41	192.00 ± 180.68
3	6.73 ± 3.15	125.87 ± 50.98	182.38 ± 125.25
F/χ_{KW}^2	0.180	0.107	0.420
p	0.981	0.955	0.936

Data are expressed as mean ± SD. TBARS were expressed as (μmol/LMDA), AOPP as μmol/L chloramine T, and catalase as (Kat/L). Statistical analysis was performed by using F-ANOVA and χ_{KW}^2 –Kruskal-Wallis test.

Table 5: Correlations between HCV viral load and oxidative stress parameters.

		Viral load	TBARS	AOPP	Catalase
Viral load	r		0.251	0.344	0.020
	p	1	0.072	0.012	0.897
TBARS	r			0.098	0.189
	p		1	0.489	0.209
AOPP	r				0.101
	p			1	0504
Catalase	r				
	p				1

HCV RNA concentration (IU/mL of plasma)-viral load was correlated with TBARS, AOPP, and catalase by using r-Pearson correlation coefficient.

[21] and Limongi et al. [22], in which only subtle changes in MDA level in groups of 1a and 1b genotype have been documented [21].

The HCV genotype studies have been mainly oriented toward the evaluation of their correlation with the severity of the disease, the appearance of fibrosis, carcinogenesis, and resistance to therapy. The increase in ROS production and their consequences on lipid peroxidation and protein oxidative modification are among the mechanisms which have been implicated in the end-stage cirrhosis following the HCV infection [23–25]. As our study suggests, the correlation of viral load and oxidative stress parameter AOPP revealed a statistically significant positive correlation (Table 5). This result suggests that viral load can be directly responsible for ROS production and liberation and consequent cell damage. Since the correlation analysis showed that the high level of HCV viral load was more likely to have a higher TBARS, it may suggest that viral load can also have an impact on membrane damage and lipid peroxidation.

It is possible that HCV genome-encoded nonstructural proteins have a role in pathogenetic mechanisms responsible for excessive ROS release in hepatocytes. Among them, the best explained is a NS5A, which is a multifunctional protein and it contributes to the HCV replication. Besides the central role of NS5A in HCV replication, it is capable of inducing IFN resistance, through the repression of PKR function. The mechanisms of triggering the liberation of ROS by NS5A are complex, finally leading to consequent activation of inflammatory, redox-sensitive NF-κ B, and AP-1 transcription factors. Proinflammatory transcription factor NF-κB has been declared the central mediator of cell immune and inflammatory response. Its active subunits, comprising the NF-κB1 (p50, p105), NF-κB2 (p52, p100), RelA (p65), RelB, and c-Rel, induce the expression of many genes, with consequent synthesis of a number of inflammatory cytokines, such as tumor necrosis factor-α (TNF-α), IL-1, IL-6, IL-18, lymphotoxin CXCL4, IFN-γ, chemokines, and TGF-β [26, 27]. It is very interesting to note that generated ROS although HCV NS protein reaction products, in turn, may suppress HCV replication [23]. A recent publication documented that HCV core protein may induce inflammasome activation and IL-1β release from hepatic macrophages [28]. The precise mechanisms for this have been documented by using an *in vitro* model of Huh-7 cell culture, transfected with NS5A, where untransfected tissue served as control. By studying the existing NS5A three domains involvement in ROS production, it was reported that besides full-length NS5A protein, its domain I may exclusively induce ROS production [29]. As a possible mechanism of NS5A-induced release of ROS is a direct NS5A-induced damage of intracellular membrane components, including ER, peroxisomes, and mitochondria. After the association with membrane components, it induces ER stress, followed by a simultaneous efflux of Ca^{2+} ions from the ER. They can be taken up by mitochondria, altering in that way a transmembrane potential, followed by a reduction of molecular oxygen, which induces the accumulation of unstable superoxide anion radical (O^{2-}) in mitochondria. In this pathway, the mitochondrial oxidative phosphorylation chain located on the inner mitochondrial membrane is the main source of free radical generation [30–32].

Besides the abovementioned mitochondrial mechanism of NS5A-induced release of ROS, the expression of NADPH oxidase family (NOX1 and NOX4) and cyclooxygenase 2 (COX-2) have been shown to occur simultaneously. As in the case of the mitochondrial pathway, it was reported that the domain I can induce NOX1. Specific cascade of their effect lead to the conclusion that all systems can act in accord with a specific order, which includes TGFβ1, NOX1, COX-2, and NOX4. In that context, the next player involved in active ROS generation seems to be a Cytochrome P450 2E1 (CYP2E1) which has a typical localisation in the ER membrane. Besides NS5A, the effect on NOX4 may exert HCV structural proteins as well [29]. The importance of NADPH oxidase and CYP2E1 was documented in the development of chronic inflammation and hepatocyte death. Since the activation of fibroblasts migration and excessive collagen deposition overcome liver regenerative capacity, consequent liver fibrosis seems to be a necessary harm [29, 33, 34].

Released ROS may damage susceptible cell biomolecules and related cell structures, such as unsaturated free fatty acids of membrane phospholipids, proteins of structural and functional cellular components, such as enzymes and receptors, and DNA. As concerns the cell membranes, generated ROS can alter the structure and function of cell organelles and outer cell membrane, leading to peroxidative breakdown of membrane phospholipids. The release of lysosomal hydrolytic enzymes can further aggravate liver cell damage. The released damaged particles may further act as the DAMP molecules (damage-associated molecular patterns), activating HSCs, which proliferate and belong to the transformation into myofibroblast-like cells. Following the transformation, they exert fibrogenic potential, by secreting collagen type I, III, and IV, fibronectin, laminin, proteoglycans, and transforming growth factor-β (TGF-β). In this way, they fill irreversibly the empty spaces of dead hepatocytes. Inflammatory cytokines, released from the surrounding inflammatory cells, may further produce ROS [35, 36]. ROS has the potential to decrease tumor-suppressor p53 protein expression [14, 15], stimulating a possible carcinogenesis. The values of oxidative stress parameters (TBARS and AOPP) and catalase activity in diverse to HCV genotypes (Table 4) may suggest that among the genotype distribution, the HCV1b patients were more likely to have a higher TBARS compared to others, HCV 3 patients were more likely to have a higher AOPP level, while patients infected with HCV1a were more likely to have a low catalase activity, but without statistical significance. The absence of a statistically significant difference in the production of ROS between the genotypes can be explained by the fact that nonstructural viral proteins have a high level of homogeneity between different genotypes.

Considering the activity of catalase in relation to the single genotypes, a trend of significantly decreased catalase activity was observed in each of the presented genotypes. Liver cells develop different protective mechanisms to prevent ROS effects. It is well-documented that among the antioxidative enzymes, the activity of catalase is very high in liver tissue. In this way, it provides the first line of antioxidative defense enzymatic system. In the case of chronic hepatitis C, a number of results documented decreased antioxidative defense system, expressed as total antioxidative capacity or the low level of reduced glutathione. Decreased antioxidative capacity in view of catalase activity brings about the inability of liver tissues to counteract oxidative stress or persistent and chronic tissue damage [21, 23].

In this way, both increased ROS production and decreased antioxidative defense are working in accord with inflammation to produce cell damage and hepatic genome instability. Our results are consistent with the results of other studies, concerning the level of nonenzymatic antioxidative defense level (GSH) [33]. The activity of antioxidative enzymes may vary, depending on preserved compensatory mechanisms. Some reports discussed the increased activity of antioxidant enzymes MnSOD and catalase in HCV infections [37–39].

In conclusion, the results obtained confirmed an imbalance between the ROS production and antioxidative defense system in HCV infected patients, with a markedly enhanced lipid peroxidation and protein oxidative modification, followed by the reduction of catalase activity. Since oxidative stress may have a profound influence on disease progression, fibrosis, and carcinogenesis, our results may meet the aspirations of mandatory introduction of antioxidants as early HCV therapy to counteract ROS consequences.

Data Availability

The data that support the findings of this study are available from the corresponding author, [VD], upon request.

Conflicts of Interest

The authors declare that there is no conflict of interest regarding the publication of this paper.

Acknowledgments

This research was funded by the Serbian Ministry of Education, Science and Technological development of Serbia, grant for Medical Faculty University of Nis; Internal project of Medical Faculty University of Nis No 7.

References

[1] World Health Organization, "Hepatitis C fact sheet," 2019, https://www.who.int/news-room/fact-sheets/detail/hepatitis-c.

[2] L. Du and H. Tang, "An insight into the molecular characteristics of hepatitis C virus for clinicians," *Saudi Medical Journal*, vol. 37, no. 5, pp. 483–491, 2016.

[3] V. A. Morozov and S. Lagaye, "Hepatitis C virus: morphogenesis, infection and therapy," *World Journal of Hepatology*, vol. 10, no. 2, pp. 186–212, 2018.

[4] G. L. Davis, "Hepatitis C virus genotypes and quasispecies," *The American Journal of Medicine*, vol. 107, no. 6B, pp. 21S–26S, 1999.

[5] K. Sandres, M. Dubois, C. Pasquier et al., "Genetic heterogeneity of hypervariable region 1 of the hepatitis C virus (HCV)

genome and sensitivity of HCV to alpha interferon therapy," *Journal of Virology*, vol. 74, no. 2, pp. 661–668, 2000.

[6] D. L. Thomas and L. B. Seeff, "Natural history of hepatitis C," *Clinics in Liver Disease*, vol. 9, no. 3, pp. 383–398, 2005.

[7] J. D. Scott and D. R. Gretch, "Molecular diagnostics of hepatitis C virus infection: a systematic review," *JAMA*, vol. 297, no. 7, pp. 724–732, 2007.

[8] L. G. Guidotti and F. V. Chisari, "Immunobiology and pathogenesis of viral hepatitis," *Annual Review of Pathology*, vol. 1, no. 1, pp. 23–61, 2006.

[9] G. Vendemiale, I. Grattagliano, P. Portincasa, G. Serviddio, G. Palasciamo, and E. Altomare, "Oxidative stress in symptom-free HCV carriers: relation with ALT flare-up," *European Journal of Clinical Investigation*, vol. 31, no. 1, pp. 54–63, 2001.

[10] M. L. Reshi, Y. C. Su, and J. R. Hong, "RNA viruses: ROS-mediated cell death," *International Journal of Cell Biology*, vol. 2014, Article ID 467452, 16 pages, 2014.

[11] C. Fierbinţeanu-Braticevici, M. Mohora, D. Creţoiu et al., "Role of oxidative stress in the pathogenesis of chronic hepatitis C (CHC)," *Romanian Journal of Morphology and Embryology*, vol. 50, no. 3, pp. 407–412, 2009.

[12] A. V. Ivanov, B. Bartosch, O. A. Smirnova, M. G. Isaguliants, and S. N. Kochetkov, "HCV and oxidative stress in the liver," *Viruses*, vol. 5, no. 2, pp. 439–469, 2013.

[13] K. Rebbani and K. Tsukiyama-Kohara, "HCV-induced oxidative stress: battlefield-winning strategy," *Oxidative Medicine and Cellular Longevity*, vol. 2016, Article ID 7425628, 7 pages, 2016.

[14] N. Fu, H. Yao, Y. Nan, and L. Qiao, "Role of oxidative stress in hepatitis C virus induced hepatocellular carcinoma," *Current Cancer Drug Targets*, vol. 17, no. 6, pp. 498–504, 2017.

[15] R. Cardin, M. Piciocchi, M. Bortolami et al., "Oxidative damage in the progression of chronic liver disease to hepatocellular carcinoma: an intricate pathway," *World Journal of Gastroenterology*, vol. 20, no. 12, pp. 3078–3086, 2014.

[16] R. Zampino, A. Marrone, L. Restivo et al., "Chronic HCV infection and inflammation: clinical impact on hepatic and extra-hepatic manifestations," *World Journal of Hepatology*, vol. 5, no. 10, pp. 528–540, 2013.

[17] T. Luedde and R. F. Schwabe, "NF-κB in the liver–linking injury, fibrosis and hepatocellular carcinoma," *Nature Reviews. Gastroenterology & Hepatology*, vol. 8, no. 2, pp. 108–118, 2011.

[18] S. Sahreen, M. R. Khan, and R. A. Khan, "Hepatoprotective effects of methanol extract of Carissa opaca leaves on CCl4-induced damage in rat," *BMC Complementary and Alternative Medicine*, vol. 11, no. 1, p. 48, 2011.

[19] V. Witko-Sarsat, M. Friedlander, C. Capeillere-Blandin et al., "Advanced oxidation protein products as a novel marker of oxidative stress in uremia," *Kidney International*, vol. 49, no. 5, pp. 1304–1313, 1996.

[20] S. F. Nabavi, S. M. Nabavi, F. Abolhasani, and A. H. Moghaddam, "Cytoprotective effects of curcumin on sodium fluoride-induced intoxication in rat erythrocytes," *Bulletin of Environmental Contamination and Toxicology*, vol. 88, no. 3, pp. 486–490, 2012.

[21] M. H. Khadem Ansari, M. D. Omrani, and F. Kheradmand, "Oxidative stress response in patients infected by diverse hepatitis C virus genotypes," *Hepatitis Monthly*, vol. 15, no. 2, article e22069, 2015.

[22] D. Limongi, S. Baldelli, F. Santi et al., "Redox alteration in patients infected by different HCV genotypes," *Le Infezioni in Medicina*, vol. 26, no. 3, pp. 249–254, 2018.

[23] Z. Razzaq and A. Malik, "Viral load is associated with abnormal serum levels of micronutrients and glutathione and glutathione-dependent enzymes in genotype 3 HCV patients," *BBA Clinical*, vol. 2, pp. 72–78, 2014.

[24] A. Ploss, M. J. Evans, V. A. Gaysinskaya et al., "Human occludin is a hepatitis C virus entry factor required for infection of mouse cells," *Nature*, vol. 457, no. 7231, pp. 882–886, 2009.

[25] P. Andre, F. Komurian-Pradel, S. Deforges et al., "Characterization of low- and very-low-density hepatitis C virus RNA-containing particles," *Journal of Virology*, vol. 76, no. 14, pp. 6919–6928, 2002.

[26] Q. Li and I. M. Verma, "NF-κB regulation in the immune system," *Nature Reviews Immunology*, vol. 2, no. 10, pp. 725–734, 2002.

[27] M. Yue, T. Tian, C. Wang et al., "Genetic mutations in NF-κB pathway genes were associated with the protection from hepatitis C virus infection among Chinese Han population," *Scientific Reports*, vol. 9, no. 1, p. 10830, 2019.

[28] A. A. Negash, R. M. Olson, S. Griffin, and M. Gale Jr., "Modulation of calcium signaling pathway by hepatitis C virus core protein stimulates NLRP3 inflammasome activation," *PLoS Pathogens*, vol. 15, no. 2, article e1007593, 2019.

[29] O. A. Smirnova, O. N. Ivanova, B. Bartosch et al., "Hepatitis C virus NS5A protein triggers oxidative stress by inducing NADPH oxidases 1 and 4 and cytochrome P450 2E1," *Oxidative Medicine and Cellular Longevity*, vol. 2016, Article ID 8341937, 10 pages, 2016.

[30] M. Gale Jr., C. M. Blakely, B. Kwieciszewski et al., "Control of PKR protein kinase by hepatitis C virus nonstructural 5A protein: molecular mechanisms of kinase regulation," *Molecular and Cellular Biology*, vol. 18, no. 9, pp. 5208–5218, 1998.

[31] G. Gong, G. Waris, R. Tanveer, and A. Siddiqui, "Human hepatitis C virus NS5A protein alters intracellular calcium levels, induces oxidative stress, and activates STAT-3 and NF-kappa B," *Proceedings of the National Academy of Sciences of the United States of America*, vol. 98, no. 17, pp. 9599–9604, 2001.

[32] N. Kato, K. H. Lan, S. K. Ono-Nita, Y. Shiratori, and M. Omata, "Hepatitis C virus nonstructural region 5A protein is a potent transcriptional activator," *Journal of Virology*, vol. 71, no. 11, pp. 8856–8859, 1997.

[33] N. Nieto, S. L. Friedman, and A. I. Cederbaum, "Stimulation and proliferation of primary rat hepatic stellate cells by cytochrome P450 2E1-derived reactive oxygen species," *Hepatology*, vol. 35, no. 1, pp. 62–73, 2002.

[34] P. Sancho, J. Mainez, E. Crosas-Molist et al., "NADPH oxidase NOX4 mediates stellate cell activation and hepatocyte cell death during liver fibrosis development," *PLoS One*, vol. 7, no. 9, p. e45285, 2012.

[35] K. Wake, "Cell-cell organization and functions of 'sinusoids' in liver microcirculation system," *Journal of Electron Microscopy*, vol. 48, no. 2, pp. 89–98, 1999.

[36] I. Shimizu, "Antifibrogenic therapies in chronic HCV infection," *Current Drug Targets. Infectious Disorders*, vol. 1, no. 2, pp. 227–240, 2001.

[37] M. Y. Abdalla, I. M. Ahmad, D. R. Spitz, W. N. Schmidt, and B. E. Britigan, "Hepatitis C virus-core and non structural proteins lead to different effects on cellular antioxidant defenses," *Journal of Medical Virology*, vol. 76, no. 4, pp. 489–497, 2005.

[38] F. Farinati, R. Cardin, M. Bortolami et al., "Hepatitis C virus: from oxygen free radicals to hepatocellular carcinoma," *Journal of Viral Hepatitis*, vol. 14, no. 12, pp. 821–829, 2007.

[39] M. E. H. Kayesh, S. Ezzikouri, T. Sanada et al., "Oxidative stress and immune responses during hepatitis C virus infection in Tupaia belangeri," *Scientific Reports*, vol. 7, no. 1, p. 9848, 2017.

Hindawi
Oxidative Medicine and Cellular Longevity
Volume 2021, Article ID 6678924, 12 pages
https://doi.org/10.1155/2021/6678924

Research Article

GSTM1 Modulates Expression of Endothelial Adhesion Molecules in Uremic Milieu

Djurdja Jerotic,[1,2] **Sonja Suvakov**,[1,2,3] **Marija Matic**,[1,2] **Abdelrahim Alqudah**,[4,5] **David J. Grieve**,[5] **Marija Pljesa-Ercegovac**,[1,2] **Ana Savic-Radojevic**,[1,2] **Tatjana Damjanovic**,[6] **Nada Dimkovic**,[2,6] **Lana McClements**,[5,7] **and Tatjana Simic**[1,2,8]

[1]*Institute of Medical and Clinical Biochemistry, Faculty of Medicine, University of Belgrade, 11000 Belgrade, Serbia*
[2]*Faculty of Medicine, University of Belgrade, 11000 Belgrade, Serbia*
[3]*Division of Nephrology and Hypertension, Mayo Clinic, Rochester, MN, USA*
[4]*Department of Clinical Pharmacy and Pharmacy Practice, Faculty of Pharmaceutical Sciences, The Hashemite University, P.O. Box 330127 Zarqa 13133, Jordan*
[5]*The Wellcome-Wolfson Institute for Experimental Medicine, School of Medicine, Dentistry and Biomedical Sciences, Queen's University Belfast, Belfast, UK*
[6]*Clinical Department for Renal Diseases, Zvezdara University Medical Center, 11000 Belgrade, Serbia*
[7]*School of Life Sciences, Faculty of Science, University of Technology Sydney, 2007, NSW, Australia*
[8]*Serbian Academy of Sciences and Arts, 11000 Belgrade, Serbia*

Correspondence should be addressed to Lana McClements; lana.mcclements@uts.edu.au and Tatjana Simic; tatjana.simic@med.bg.ac.rs

Received 20 November 2020; Revised 22 December 2020; Accepted 26 December 2020; Published 27 January 2021

Academic Editor: Gordana Kocic

Copyright © 2021 Djurdja Jerotic et al. This is an open access article distributed under the Creative Commons Attribution License, which permits unrestricted use, distribution, and reproduction in any medium, provided the original work is properly cited.

Deletion polymorphism of glutathione S-transferase M1 (GSTM1), a phase II detoxification and antioxidant enzyme, increases susceptibility to end-stage renal disease (ESRD) as well as the development of cardiovascular diseases (CVD) among ESRD patients and leads to their shorter cardiovascular survival. The mechanisms by which GSTM1 downregulation contributes to oxidative stress and inflammation in endothelial cells in uremic conditions have not been investigated so far. Therefore, the aim of the present study was to elucidate the effects of GSTM1 knockdown on oxidative stress and expression of a panel of inflammatory markers in human umbilical vein endothelial cells (HUVECs) exposed to uremic serum. Additionally, we aimed to discern whether *GSTM1-null* genotype is associated with serum levels of adhesion molecules in ESRD patients. HUVECs treated with uremic serum exhibited impaired redox balance characterized by enhanced lipid peroxidation and decreased antioxidant enzyme activities, independently of the GSTM1 knockdown. In response to uremic injury, HUVECs exhibited alteration in the expression of a series of inflammatory cytokines including retinol-binding protein 4 (RBP4), regulated on activation, normal T cell expressed and secreted (RANTES), C-reactive protein (CRP), angiogenin, dickkopf-1 (Dkk-1), and platelet factor 4 (PF4). GSTM1 knockdown in HUVECs showed upregulation of monocyte chemoattractant protein-1 (MCP-1), a cytokine involved in the regulation of monocyte migration and adhesion. These cells also have shown upregulated intracellular and vascular cell adhesion molecules (ICAM-1 and VCAM-1). In accordance with these findings, the levels of serum ICAM-1 and VCAM-1 (sICAM-1 and sVCAM-1) were increased in ESRD patients lacking GSTM1, in comparison with patients with the *GSTM1-active* genotype. Based on these results, it may be concluded that incubation of endothelial cells in uremic serum induces redox imbalance accompanied with altered expression of a series of cytokines involved in arteriosclerosis and atherosclerosis. The association of GSTM1 downregulation with the altered expression of adhesion molecules might be at least partly responsible for the increased susceptibility of ESRD patients to CVD.

1. Introduction

Endothelial dysfunction is an underlying mechanism of cardiovascular diseases (CVD) which are the leading cause of death among patients with end-stage renal disease (ESRD) [1–4]. The vascular endothelium is likely the primary target of uremic toxins generated in ESRD. In these conditions, the endothelium is continuously exposed to accumulated uremic toxins hence inducing oxidative stress and inflammation, which can lead to endothelial impairment [2, 5–7].

Homozygous deletion of glutathione S-transferase M1 (GSTM1), which is a phase II detoxification enzyme, leads to accumulation of oxidative stress byproducts which indicates its role in antioxidant protection as well [8]. Between 30 to 50 percent of different human population are homozygous for GSTM1 deletion (usually denoted as *GSTM1-null* genotype), thus completely lacking the GSTM1 enzyme [9]. The GSTM1 deficiency is linked to higher susceptibility to CVD as individuals with *GSTM1-null* genotype were shown to have significantly increased risk for developing resistant hypertension [10], coronary artery disease/atherosclerosis [11, 12], and stroke [13, 14]. In addition, the *GSTM1-null* genotype increases susceptibility to ESRD and leads to shorter overall and cardiovascular survival of the patients on haemodialysis [8, 15–17]. The association between GSTM1 deletion and oxidative stress in ESRD patients was supported by our previous results that demonstrated elevated levels of several byproducts of protein and lipid oxidative damage in ESRD patients with *GSTM1-null* genotype compared to those with *GSTM1-active* genotype [8]. It has been suggested that in inflammatory and prooxidant environment observed in patients with ESRD, the endothelium responds by expressing intracellular and vascular cell adhesion molecules (ICAM-1 and VCAM-1) that facilitate migration and adhesion of leukocytes to the endothelial cells [18]. We have recently shown that soluble ICAM-1 and VCAM-1 (sICAM-1 and sVCAM-1) levels have a strong predictive role in terms of overall and cardiovascular survival in ESRD patients on haemodialysis [17]. Nevertheless, the potential influence of GSTM1 deletion on the aforementioned inflammatory markers has not been elucidated before in dialyzed patients or in endothelial cells exposed to uremic toxins commonly present in ESRD.

Despite the convincing findings in human cohorts showing the importance of GSTM1 deletion on susceptibility and development of CVD among dialyzed patients [15, 16, 19, 20], its role in the vascular pathophysiology has not been established yet. A functional role of GSTM1 was investigated in vascular smooth muscle cells (VSMC), showing that the reduction in GSTM1 expression in these cells caused increased cell proliferation, oxidative stress, and migration [21]. However, the mechanisms associated with GSTM1 downregulation in endothelial cells in uremic conditions have not been investigated so far.

Therefore, the aim of the present study was to elucidate the effects of GSTM1 knockdown on oxidative stress and expression of a panel of inflammatory markers in human umbilical vein endothelial cells (HUVECs) exposed to uremic serum. Additionally, we aimed to discern whether the *GSTM1-null* genotype is associated with serum levels of adhesion molecules in ESRD patients.

2. Materials and Methods

2.1. Cell Cultures. HUVECs (*ATCC Manassas*, *Virginia*, *USA*) were seeded on 0.2% gelatine-coated culture plates and grown in a MV2 growth medium (*Endothelial Cell Growth Medium MV2*, *PromoCell*, *Germany*) under standard cell culture conditions (humidified atmosphere, 5% CO_2, 37°C). Cells were seeded in gelatine-coated plates for viability assays, Western blot analyses, oxidative stress measurements, and assessment of cytokine expression. HUVECs were incubated in a pool of human serums obtained from either healthy volunteers (control serum, $n = 10$) or ESRD patients on haemodialysis (uremic serum, $n = 30$). All patients underwent haemodialysis 3 times a week for at least 3 months before the study onset using polysulfone dialysis membranes and conventional bicarbonate-buffered dialysate. Participants with any form of malignancy, autoimmune disease, or infectious comorbidities (HIV, HBV, or HCV infections) were excluded. The blood was taken from patients prior to a haemodialysis session at the Center for the Renal Diseases, Zvezdara University Medical Center, Belgrade. All patients signed informed consent agreeing to participate in the study. This study was approved by the Ethical Committee of the Faculty of Medicine, University of Belgrade (No. 1550/V-30), and conducted in accordance with the Helsinki Declaration from 2013.

2.2. Cell Viability Assay. Cell viability was assessed by a colorimetric method based on measuring mitochondrial dehydrogenase activity, using the *MTS Cell Proliferation Assay Kit* (*Abcam, UK*), according to the manufacturer's protocol. 5000 cells/well were cultured in a 96-well plate. After 24 h, growth media were discarded and cells were treated with media, 10%, 20%, or 30% control or uremic serum for 4 h and 6 h. The formazan salt produced by viable cells was quantified by measuring the absorbance at 490 nm on the *FLUOstar® Omega plate reader* (*BMG Labtech*, *Germany*). The viability of cells incubated in pooled human sera for 6 h did not change significantly compared to the cells incubated in the normal growth medium (Figure 1S A&B, Supplement). Therefore, all further HUVEC treatments were performed using 30% control or uremic serum-containing media for 6 h, before cytokine expression and oxidative stress measurements were performed.

2.3. GSTM1 Knockdown Using siRNA in HUVECs. To silence GSTM1 protein expression, HUVECs were seeded at a density of 1.5×10^5 cells per well in 6-well plates and grown in a MV2 growth medium. The following day, cells were transfected with 100 nM GSTM1 small interfering RNA (siRNA) (*Thermo Fisher Scientific*, *UK*) using the DharmaFECT transfection reagent (*GE Healthcare*, *USA*) or treated with DharmaFECT as a control. Ninety-six hours posttransfection, the silencing effect was confirmed by Western blot.

2.4. Western Blot Analysis. HUVECs were lysed in a RIPA buffer (50 mM Tris-HCL pH 8.0, 150 mM NaCl, 1% IGEPAL, 0.5% sodium deoxycholate, and 10% SDS) supplemented with protease inhibitor cocktail (*Roche*, *UK*). After extraction, protein concentrations were determined by the *Bicinchoninic*

Acid Protein Assay kit (*BCA*, *Thermo Fisher Scientific*, *UK*). An equal amount of proteins was loaded on 10% polyacrylamide gel, and electrophoresis was performed at 80 V for 10 min, then 100 V for 90 min. After wet transfer, nitrocellulose membranes were blocked in 5% nonfat milk (*Bio-Rad*, *UK*) for 1 h at room temperature and then incubated overnight at 4°C with primary antibodies: monoclonal mouse anti-GSTM1 (1 : 1000, *R&D Systems*, *USA*), monoclonal mouse anti-ICAM1 (1 : 200, *Santa Cruz*, *USA*), polyclonal goat anti-VCAM1 (1 : 200, *Santa Cruz*, *USA*), and monoclonal mouse anti-β actin (1 : 10 000, *Thermo Fisher Scientific*, *UK*). The following day, membranes were incubated with appropriate HRP-conjugated secondary antibodies: anti-mouse 1 : 5000 (*Abcam*, *UK*) and anti-goat 1 : 1000 (*RayBiotech*, *USA*) for 1 h at room temperature. Chemiluminescent bands were detected using the *West Femto Maximum sensitivity substrate* (*Thermo Fisher Scientific*, *UK*) on the *G-box* (*Kodak*, *UK*) *or ChemiDoc* (*BioRad*, *USA*). Densitometry analysis was performed using *ImageJ* software (*National Institutes of Health*, *Bethesda*, *USA*).

2.5. Measurement of the Activity of Antioxidant Enzymes in HUVECs. The activity of antioxidant enzymes, superoxide dismutase (SOD) and glutathione peroxidase (GPX), in cell lysates was determined by spectrophotometric methods. SOD activity was assessed as previously described by Misra and Fridovich [22]. This method is based on the ability of SOD to inhibit the autoxidation of adrenaline at pH 10.2. The production of colored adrenochrome in reaction mixtures with cell protein extracts (sample) or without them (control) was followed at 480 nm. Activity of SOD was expressed as the percentage of inhibition of adrenaline autoxidation. GPX activity was assessed as reported by Günzler et al. [23]. GPX activity was assayed by the subsequent oxidation of NADPH at 340 nm with t-butyl-hydroperoxide as the substrate. One unit of enzyme activity was expressed as nmol NADPH oxidized per minute, assuming 6.22×10^3/l/mol/cm to be the molar absorbance of NADPH at 340 nm.

2.6. Measurement of Malondialdehyde Levels in HUVECs. Malondialdehyde (MDA) levels in cell lysates were measured using the competitive ELISA kit (*Elabscience*, *Wuhan*, *China*) in accordance with the manufacturer's instructions. In brief, 50 μl of standards, samples, and blanks was added to each well of the MDA precoated ELISA plate with consecutive addition of 50 μl biotinylated antibody. After the 45 min of incubation, wells were washed in order to eliminate excess conjugate and unbound sample or standard, and HRP-conjugated antibody was added. The color change was measured spectrophotometrically at a wavelength of 450 nm.

2.7. Measurement of Total Reactive Oxygen Species in HUVECs. The total reactive oxygen species (ROS) production was assessed by flow cytometry (FACS) using 2′,7′-dichlorodihydrofluorescein diacetate (H_2DCFDA; *Invitrogen*, *California*, *USA*) stain. HUVECs were seeded in 6-well plates (1.5×10^5 cells/well) and transfected with GSTM1 siRNA as described above. After 90 h incubation, the transfection solution was discarded, and cells were incubated for the next 6 h with the 30% control or uremic serum-containing media. Treatments were removed, and cells were trypsinised. Cell pellets were resuspended in 5 ml flow cytometry buffer (1% FBS in PBS) and incubated with 5 μl H_2DCFDA stain for 30 min at 37°C. FACS tubes were centrifuged at 400 g for 8 min, supernatants were removed, and cells were allowed to recover for 15 min at 37°C in 1 ml of MV2 growth media. In the final step, cells were resuspended in 500 μl FACS buffer, and 5 μl *7-AAD-viability staining solution* (*eBioscience*, *San Diego*, *USA*) was added prior to performing measurements on the *Attune NxT Acoustic Focusing Flow Cytometer* (*Invitrogen*, *California*, *USA*). The results were analysed using *FlowJo*, *ver. 10.4* (*Stanford Jr. University*, *USA*).

2.8. Analysis of Cytokine Expression in HUVECs. To explore the effect of uremic serum and GSTM1 silencing on endothelial cell inflammation, the relative expression of 105 cytokines was assessed simultaneously in cell protein extracts using the *Proteome Profiler™ Human XL Cytokine Array Kit* (*R&D Systems*, *UK*) according to the manufacturer's instruction. HUVECs were seeded in 6-well Petri dishes at a density of 1.5×10^5 cells per well. Following the transfection, GSTM1$^{+/+}$ and GSTM1$^{+/-}$ cells were incubated in 30% control or uremic serum-containing media for 6 h. After the incubation time expired, treatments were removed and cells were rinsed with PBS. Cells were then scraped in a *lysis buffer 17* (*R&D Systems*, *UK*), supplemented with 10 μg/ml aprotinin, 10 μg/ml leupeptin, and 10 μg/ml pepstatin. Cell lysates were obtained after centrifugation at 14 000 g for 5 min. Pooled cell lysates ($n = 3$/group) were probed on four separate nitrocellulose membranes. Each membrane contained capture and control antibodies spotted in duplicate, which allowed simultaneous measuring of 105 cytokine expressions. Chemiluminescent spots were visualised on the *G-box* (*Kodak*, *UK*). Results were quantified using *HLimage++ software* and normalized to the reference spots positioned at three of the corners of each blot (*Western Vision Software*, *US*).

2.9. Analysis of Circulating Adhesion Molecules in Plasma of ESRD Patients. Circulating adhesion molecules were determined in plasma of ESRD patients by enzyme immunoassays, according to the manufacturer's protocols. The description of a cohort of 199 ESRD patients involved in this study has been described in details previously [17]. sICAM-1 was assayed by commercial solid-phase sandwich ELISA (*Thermo Fisher Scientific*, *Waltham*, *Massachusetts*, *USA*). sVCAM-1 was determined by a solid-phase sandwich ELISA kit (*Novex, Life Technologies*). Absorbances were read at 450 nm on the *LKB 5060-006 Micro Plate Reader* (*Vienna*, *Austria*). sICAM concentrations were expressed as pg/ml, and sVCAM levels were expressed as ng/ml.

3. Statistical Analysis

Statistical analysis was performed using the SPSS version 17.0 statistical package (*IBM SPSS Statistics*). All analysed parameters were tested for normality of the data using the Shapiro-Wilk test. For normally distributed data, differences between the groups were evaluated by the independent sample t-test

or one-way ANOVA with Fisher's least significant difference (LSD) post hoc. For non-normally distributed data, the Mann-Whitney or Kruskal-Wallis test was used. The results were considered statistically significant if $p < 0.05$.

4. Results

To determine the effects of GSTM1 expression on oxidative stress and expression of a panel of inflammatory markers, we used specific siRNA to silence GSTM1 gene in HUVECs. Following 96 h of transfection, diminished GSTM1 expression was confirmed by immunoblotting which showed around ~90% reduction in GSTM1 protein levels in HUVECs treated with GSTM1 siRNA ($GSTM1^{+/-}$) compared to the control ($GSTM1^{+/+}$) ($p < 0.001$; Figure 2S, Supplement).

4.1. The Influence of Uremic Serum and GSTM1 Knockdown on Biomarkers of Oxidative Stress (SOD, GPX, MDA, and ROS) in HUVECs. Antioxidant enzyme activity and byproducts of oxidative stress were assessed in $GSTM1^{+/+}$ and $GSTM1^{+/-}$ HUVECs incubated in control or uremic serum-containing media. The incubation of HUVECs with uremic serum led to a significant decrease in the activity of SOD and GPX antioxidant enzymes in $GSTM^{+/+}$ HUVECs compared to control serum conditions ($p < 0.05$; Figures 1(a) and 1(b)). To determine the extent of GSTM1 activity loss on redox status of HUVECs, we silenced the GSTM1 gene by corresponding siRNA. Silencing of the GSTM1 gene did not affect antioxidant enzyme activity in any of the observed settings (Figures 1(a) and 1(b)). With respect to oxidative stress byproducts, the exposure to the uremic serum led to the significantly higher MDA concentrations ($p < 0.05$) in $GSTM1^{+/+}$ HUVECs compared to their counterparts incubated in control serum (Figures 1(c) and 1(d)). However, the GSTM1 knockdown did not have statistically significant impact on total oxidative stress byproducts in HUVECs in either control or uremic serum (Figures 1(c) and 1(d)). Only a trend towards increased MDA levels was observed in $GSTM1^{+/-}$ HUVECs compared to $GSTM1^{+/+}$ HUVECs in control serum ($p = 0.053$).

4.2. The Influence of Uremic Serum and GSTM1 Knockdown on Cytokine Expression in HUVECs. In order to explore the effects of uremic serum and GSTM1 knockdown on endothelial cell inflammation, we assessed the relative expression of over 100 inflammatory markers with the proteome array. Pooled protein lysates ($n = 3$/group) from four different groups of treated cells ($GSTM1^{+/+}$ control serum, $GSTM1^{+/-}$ control serum, $GSTM1^{+/+}$ uremic serum, and $GSTM1^{+/-}$ uremic serum) were probed on four separate nitrocellulose membranes to measure cytokine expression. The array key and original blots are presented in Table 1 and Figure 2, respectively.

The relative expression of 103 cytokines is also presented as a graded heatmap (Figure 3S, Supplement) where the lowest expressions of proteins are showed in green, and the highest expression in black. The most highly expressed proteins in HUVECs, according to our results, are shown in Figure 3 in the manuscript. In addition, the proteins whose expression was changed 2-fold in response to GSTM1 knockdown or uremic serum treatment are presented as bars (Figure 4).

According to our analysis, the most highly expressed proteins in HUVECs were serpin, endoglin (data not shown due to their impact on the heatmap legend), and CD31. CD31 is well-established as one of the markers of HUVECs, which confirms the technical validity of the performed assay. The most prominent changes in cytokine expression were exerted by uremic serum treatment (Figures 2–4). Notably, incubation in uremic serum resulted in markedly higher expression of retinol-binding protein 4 (RBP4), regulated on activation, normal T cell expressed and secreted (RANTES), C-reactive protein (CRP), and angiogenin (Figure 4). Besides, the uremic serum treatment suppressed the expression of dickkopf-1 (Dkk-1) and platelet factor 4 (PF4). Interestingly, among numerous cytokines determined, the expression of only one protein was above the set threshold in response to GSTM1 knockdown. Namely, the monocyte chemoattractant protein-1 (MCP-1) expression increased 2-fold in $GSTM1^{+/-}$ HUVECs incubated in control serum and 3.8-fold in $GSTM1^{+/-}$ HUVECs incubated in uremic serum in comparison to corresponding $GSTM1^{+/+}$ HUVECs.

4.3. The Influence of GSTM1 Deletion on ICAM-1 and VCAM-1 Expression in ESRD Patients and Endothelial Cells Exposed to Uremic Serum. According to proteome array analysis, ICAM-1 and VCAM-1 expression was elevated in HUVECs silenced for the GSTM1 gene, although these did not achieve the set 2-fold threshold limit. Given that we previously demonstrated ICAM-1 and VCAM-1 as key biomarkers of cardiovascular survival in ESRD patients [17], we investigated the changes in these proteins separately using Western blotting (Figures 5(a) and 5(b)). The incubation of HUVECs with uremic serum led to a significant increase in ICAM-1 expression in $GSTM^{+/-}$ HUVECs compared to control serum conditions ($p < 0.05$). GSTM1 knockdown led to the increase in ICAM-1 expression in HUVECs incubated in control serum, which was more pronounced in HUVECs incubated in uremic serum ($p < 0.05$). Similarly, HUVECs silenced for the GSTM1 gene had higher expression of VCAM-1 when incubated in control serum, as well as in uremic serum treatment when compared to HUVECs with normal levels of GSTM1; however, this was not statistically significant.

Using clinical plasma samples from patients with ESRD, we compared the concentrations of soluble adhesion molecules, sICAM-1 and sVCAM-1, between patients with *GTSM1-null* and *GSTM1-active* genotypes (Figures 6(a) and 6(b), respectively). These results present refined analyses of the recent findings on oxidative stress and endothelial dysfunction biomarkers that can predict survival in ESRD patients [17]. As hypothesized, sICAM-1 levels were 24% higher in patients with *GSTM1-null* genotype compared to the *GSTM1-active* genotype (93.28 (78.34-108.16) pg/ml and 75.34 (68.32-95.4) pg/ml, respectively, $p < 0.05$). Similarly, patients with *GSTM1-null* genotype had 24% higher levels of sVCAM-1 levels (662.38 (637.98-704.38) ng/ml), in comparison to ESRD patients with *GSTM1-active* genotype (532.51 (420.78-653.24) ng/ml, $p < 0.001$).

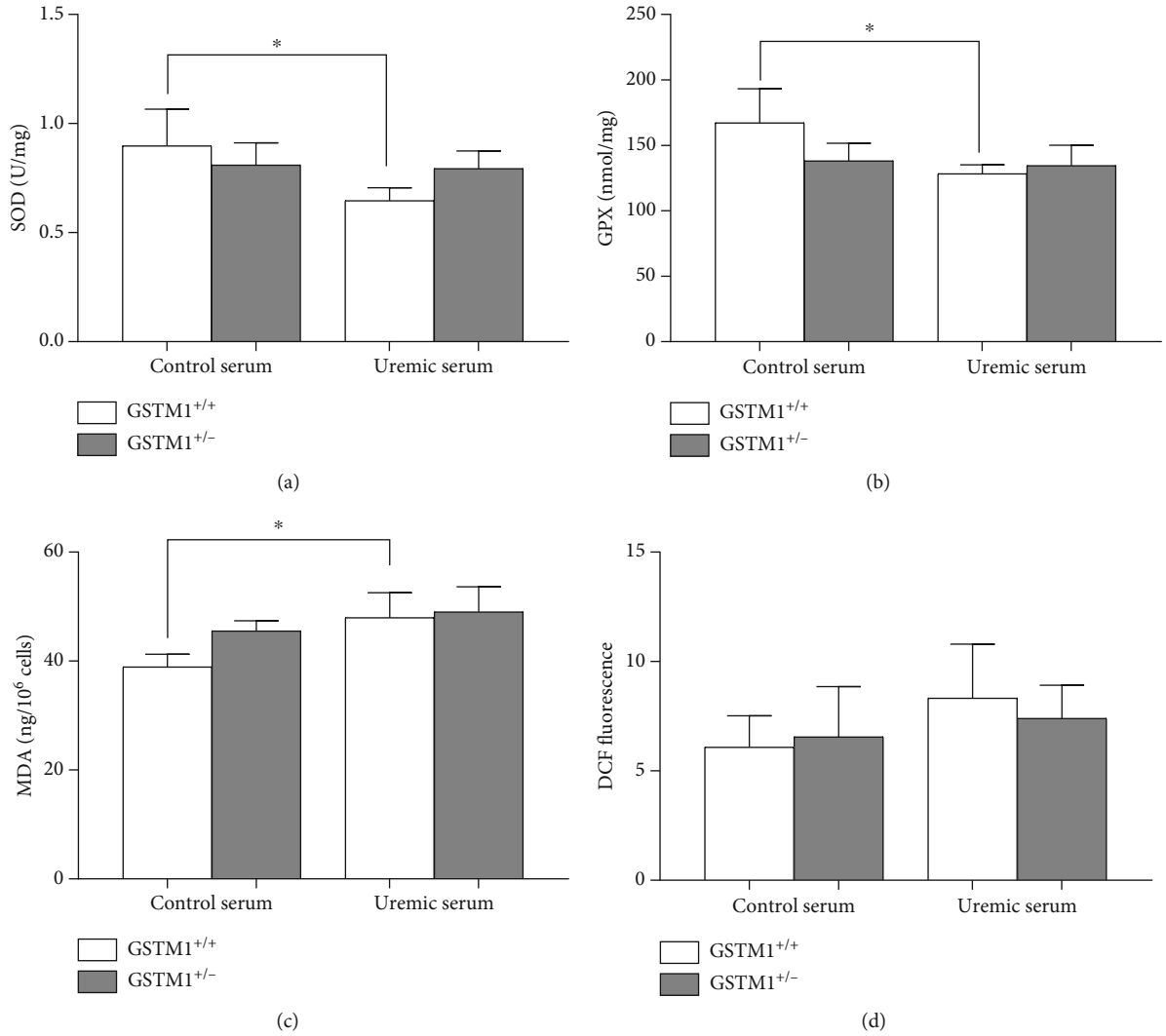

Figure 1: The influence of uremic serum and GSTM1 knockdown on oxidative stress parameters in HUVECs. GSTM1$^{+/+}$ and GSTM1$^{+/-}$ HUVECs were incubated in 30% control and 30% uremic serum-containing media for 6 h. (a) SOD activity and (b) GPX activity were determined by spectrophotometry. (c) The total ROS were determined by flow cytometry after DCF staining. (d) MDA levels were determined by ELISA. Results are presented as the mean ± SD, $n = 3$. $^{*}p < 0.05$.

Table 1: Array key.

	1	2	3	4	5	6	7	8	9	10	11	12	13	14	15	16	17	18	19	20	21	22	23	24
A	Reference		Adiponectin		Apo A-I		Angiogenin		ANGPT1		ANGPT2		BAFF		BDNF		C5/C5a		CD14		CD30		Reference	
B			CD40 L		CHI3L1		Compl.F D		CRP		Cripto-1		Cystatin C		Dkk-1		DPPIV		EGF		EMMPRIN			
C			ENA-78		Endoglin		Fas Ligand		FGF basic		FGF-7		FGF-19		Flt-3 L		G-CSF		GDF-15		GM-CSF			
D	GRO-α		Somatotropin		HGF		ICAM-1		IFN-γ		IGFBP-2		IGFBP-3		IL-1α		IL-1β		IL-1ra		IL-2		IL-3	
E	IL-4		IL-5		IL-6		IL-8		IL-10		IL-11		IL-12 p70		IL-13		IL-15		IL-16		IL-17A		IL-18 BPa	
F	IL-19		IL-22		IL-23		IL-24		IL-27		IL-31		IL-32		IL-33		IL-34		IP-10		I-TAC		Kallikrein 3	
G	Leptin		LIF		Lipocalin-2		MCP-1		MCP-3		M-CSF		MIF		MIG		MIP-1α/1β		MIP-3 α		MIP-3 β		MMP-9	
H	MPO		Osteopontin		PDGF-AA		PDGF-AB/BB		Pentraxin-3		PF4		RAGE		RANTES		RBP-4		Relaxin-2		Resistin		SDF-1α	
I	Serpin E1		SHBG		ST2		TARC		TFF3		TfR		TGF-α		THBS1		TNF-α		uPAR		VEGF			
J	Reference				Vit D BP		CD31		TIM-3		VCAM-1												NC	

5. Discussion

In this study, we showed that uremic serum caused redox imbalance independently of the GSTM1 knockdown, as well as an alteration in the expression of a series of inflammatory cytokines. Moreover, the reduction in GSTM1 in HUVECs led to an increase in MCP-1 expression. In addition, GSTM1 knockdown induced *in vitro* upregulation of cell adhesion molecules and markers of endothelial dysfunction, ICAM-1 and VCAM-1, which

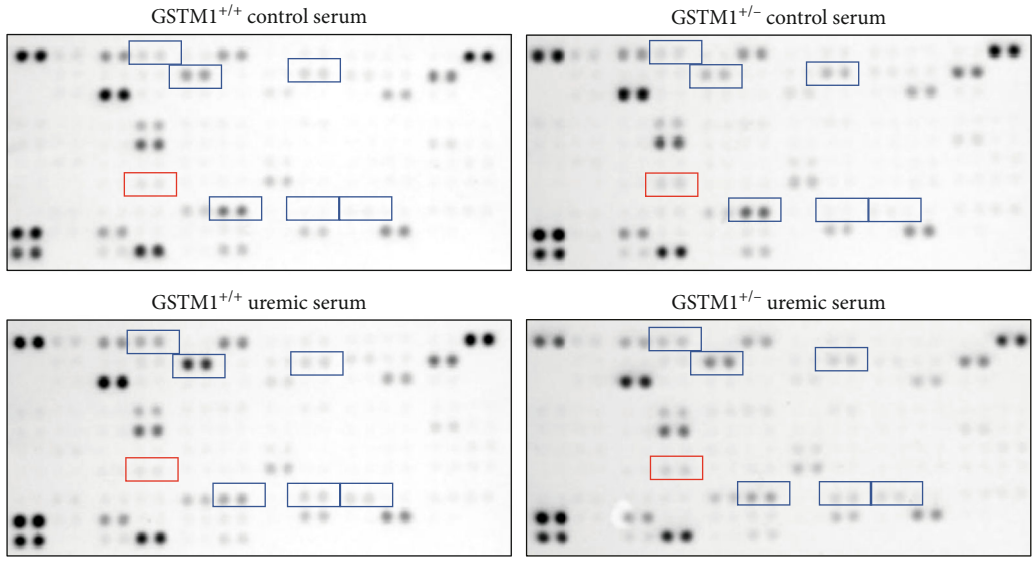

Figure 2: Proteome Profiler Human XL Cytokine Array and original blots. Cytokines that exhibited ≥2-fold change in uremic serum when compared to control serum treatment are marked blue (vertical comparison between images). Cytokines that exhibited ≥2-fold change in GSTM1$^{+/-}$ cells when compared to GSTM1$^{+/+}$ are marked red (horizontal comparison between images).

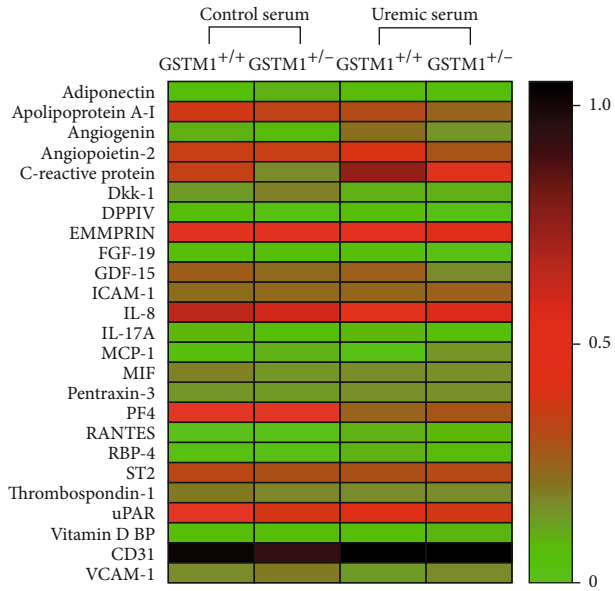

Figure 3: Expression of 25 cytokines determined by Proteome Profiler Human XL Cytokine Array. HUVECs ($n = 3$/group, pooled) transfected with GSTM1 siRNA and GSTM1$^{+/+}$ HUVECs were incubated in 30% control or uremic serum-containing media for 6 h. Heatmap represents pixel densities of spots normalized by respective reference spots.

has also been confirmed in the clinical settings using plasma samples from patients with ESRD.

GSTM1 belongs to the detoxifying group of enzymes able to remove numerous reactive compounds from the body [24, 25]. Patients on haemodialysis homozygous for GSTM1 deletion are at higher overall and cardiovascular mortality risk [16, 17], most likely due to higher oxidative burden [8]. Given the pivotal role that oxidative stress plays in the development of endothelial dysfunction, we postulated that the lack of GSTM1 activity contributes to the formation of ROS and oxidative damage. To further elucidate the effects of the GSTM1 reduction on oxidative stress in uremic conditions, in this study, we performed a series of HUVEC-based *in vitro* experiments following GSTM1 knockdown. The results presented herewith show that uremic serum caused a decrease in both SOD and GPX antioxidant enzyme activities, which was accompanied by an increase of MDA levels. These results are in line with the *in vitro* study of Chen et al., as well as well-documented increase of MDA levels and downregulated extracellular antioxidant capacity in the clinical settings [26–28]. Taken together, our results provide further evidence that endothelial cells contribute to systemic oxidative stress in uremia. This effect on oxidative stress in HUVECs exposed to uremic conditions appears independent of GSTM1 levels.

Regarding the expression of cytokines, incubation in uremic serum resulted in markedly higher expression of RBP4, RANTES, CRP, and angiogenin, while the expression of Dkk-1 and PF4 was suppressed. These changes should be interpreted in the context of complex pathophysiology of ESRD patients' vasculature, often leading to arteriosclerosis and atherosclerosis. Disturbance of calcium and phosphate homeostasis together with uremic toxins plays a key role in arteriosclerosis and contributes to accelerated calcifications of arteries in CKD patients. One of the proteins involved in mineralization or calcification of arterial walls is Dkk-1 [29]. Dkk-1 is a well-established protein associated with impaired osteoblast activation and bone loss. Up to date, several approaches to study Dkk-1 suggest its protective role in arterial calcifications. Interestingly, negative association between circulating Dkk-1 and arterial stiffness was found in predialysis CKD patients [30]. In the present study, we have shown, for the first time, that components of the uremic serum alter the expression of Dkk-1 in HUVECs. Our results

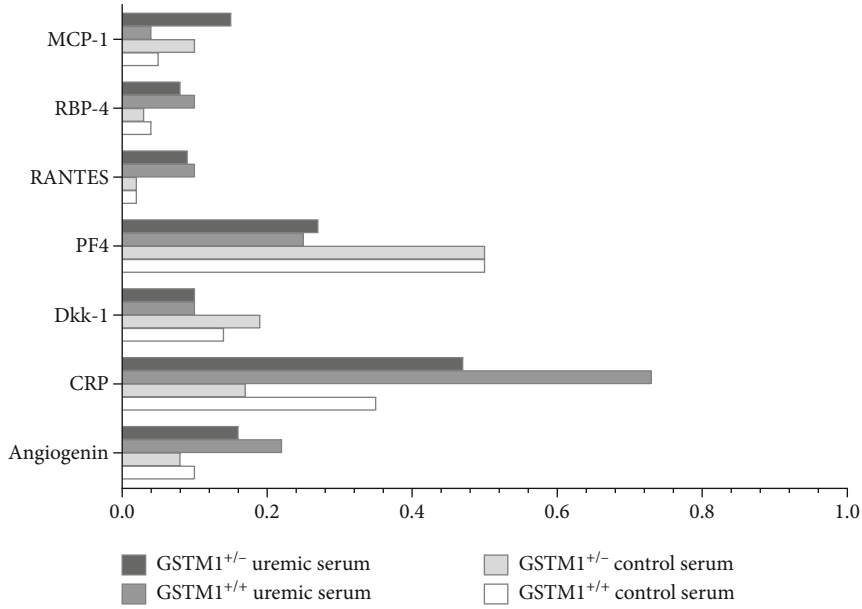

Figure 4: The relative expression of cytokines that exhibited at least 2-fold change in response to GSTM1 knockdown or uremic serum treatment.

are in line with those of other authors that report a negative association between circulating Dkk-1 and arterial calcified plaques in type 2 diabetes mellitus [31]. Although our findings should be confirmed in larger clinical studies, these results likely suggest that Dkk-1 could be a potential therapeutic target in ESRD.

Atherosclerosis is primarily a disorder of the intima of medium diameter arteries, characterized by plaque formation, narrowing, and occlusion of the blood vessels. It is likely that the mechanism of atherosclerosis in ESRD patients includes the same events as in the rest of the population without CKD. However, the rate of progression of atherosclerosis as well as the degree of oxidative modifications, expression of adhesion molecules, formation of foam cells, and proliferation of smooth muscle cells is more pronounced in CKD patients. Results of our study showed that uremic serum exerted changes in the expression of several molecules involved in the atherosclerotic processes in HUVECs. These proteins have been shown to stimulate either cell proliferation (angiogenin) or monocyte adhesion (ICAM-1, RANTES, and PF4). Angiogenin induces angiogenesis by activating endothelial and vascular smooth muscle cells [32]. According to our results, uremic serum led to an increase in endothelial angiogenin expression. It has been shown before that angiogenin levels increase significantly with CKD progression [33]. Moreover, high angiogenin levels have been linked with peripheral occlusive arterial disease and acute coronary syndrome [34, 35]. Therefore, our results indicate that the endothelium might contribute to accelerated atherosclerosis in uremic conditions by upregulating angiogenin expression. During the early stages of atherosclerosis, stimulation of endothelial cells results in the secretion of adhesion molecules, leading to the recruitment of leukocytes to the vascular wall. ICAM-1 is constitutively expressed, whereas VCAM-1 is weakly expressed by resting endothelium [36]. Both molecules are upregulated by inflammatory stimuli. Our western blot analysis showed increased expression of ICAM-1, but not VCAM-1, in HUVECs incubated in uremic serum. Our results are in line with the study of Tumur et al. who found that one of the uremic toxins, indoxyl sulfate, significantly increased ICAM-1 expression in HUVECs, while this effect on VCAM-1 was slower [36]. In our experimental design, the incubation in uremic serum lasted only 6 h, which may not be a sufficient time for endothelial response in terms of VCAM-1 expression. Previous reports showed that CKD patients have elevated levels of ICAM-1 and VCAM-1 adhesion molecules [37]. The possible explanation might be that elevated levels of VCAM-1 in patients with CKD are influenced not only by the endothelium but also by the other sources such as monocytes and macrophages. An additional adhesion molecule, whose expression was increased upon incubation in uremic serum in our study, was RANTES. RANTES mediates transmigration and arrest of monocytes onto activated endothelium. To our knowledge, this is the first report on upregulated RANTES expression in uremic conditions *in vitro*. RANTES is a well-established mediator of atherogenic processes [38]. Moreover, the importance of RANTES in renal disease was established in a study of renal transplants undergoing rejection [39], since rejecting grafts exhibited large amounts of RANTES bound to the vascular endothelium. In our study, RANTES was expressed in HUVECs exposed to uremic serum, while the HUVECs incubated in control serum did not have visually detectable expression of this protein. In our study, the only adhesion molecule with reduced expression in uremic serum was PF4. Given the fact that PF4 inhibits progenitor cell proliferation and angiogenesis [40], its decreased expression in HUVECs might result in atherosclerosis promotion and therefore seems biologically plausible.

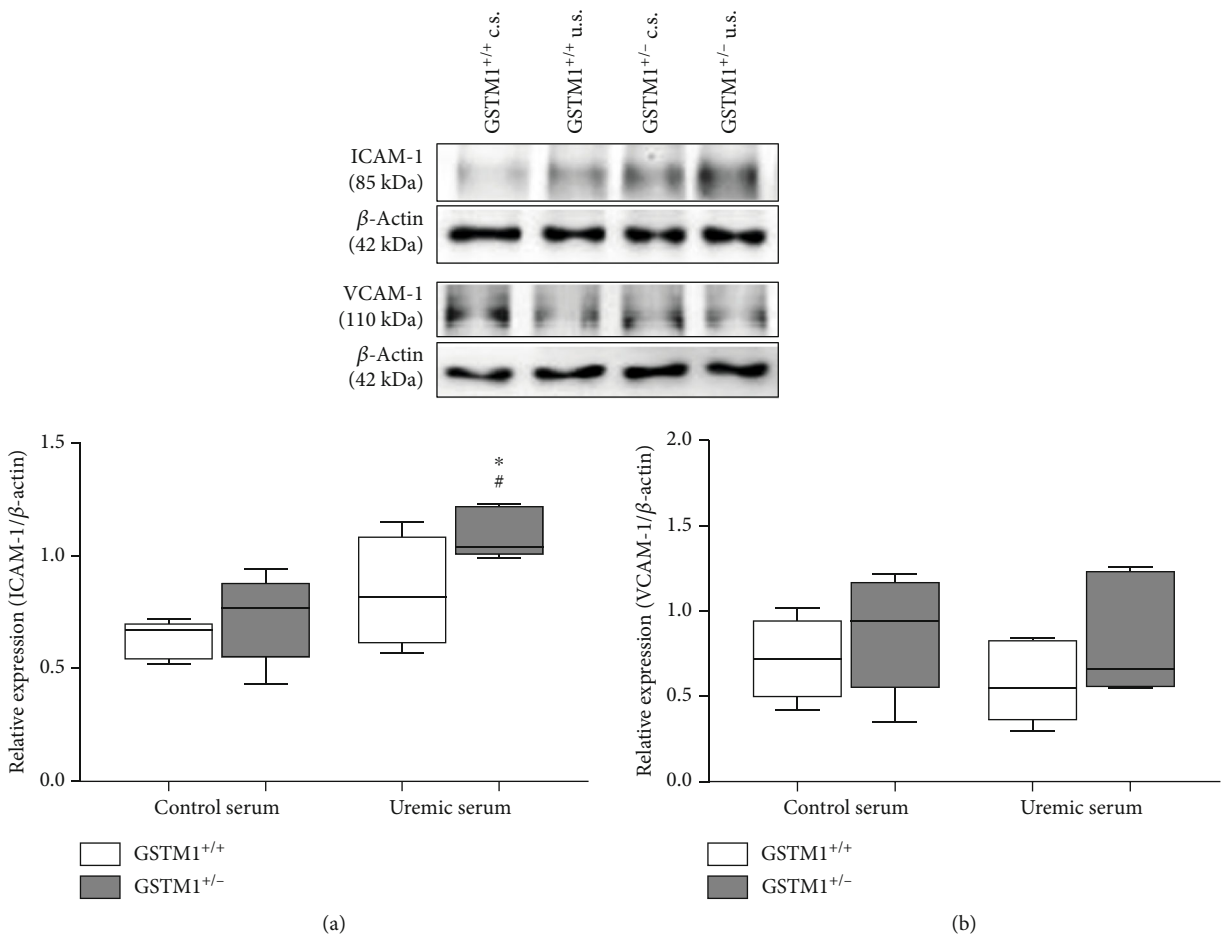

Figure 5: The influence of uremic serum and GSTM1 knockdown on ICAM-1 and VCAM-1 expression in HUVECs. $GSTM1^{+/+}$ and $GSTM1^{+/-}$ HUVECs were incubated in 30% control- (c.s.-) or 30% uremic serum- (u.s.-) containing media for 6 h. ICAM-1 and VCAM-1 expression was determined by Western blot. Results are presented as the median with interquartile range, $n = 5$. $^{*}p < 0.05$ $GSTM1^{+/-}$ HUVECs compared to $GSTM1^{+/+}$ HUVECs; $^{\#}p < 0.05$ $GSTM1^{+/-}$ HUVECs in uremic serum compared to $GSTM^{+/-}$ HUVECs in control serum.

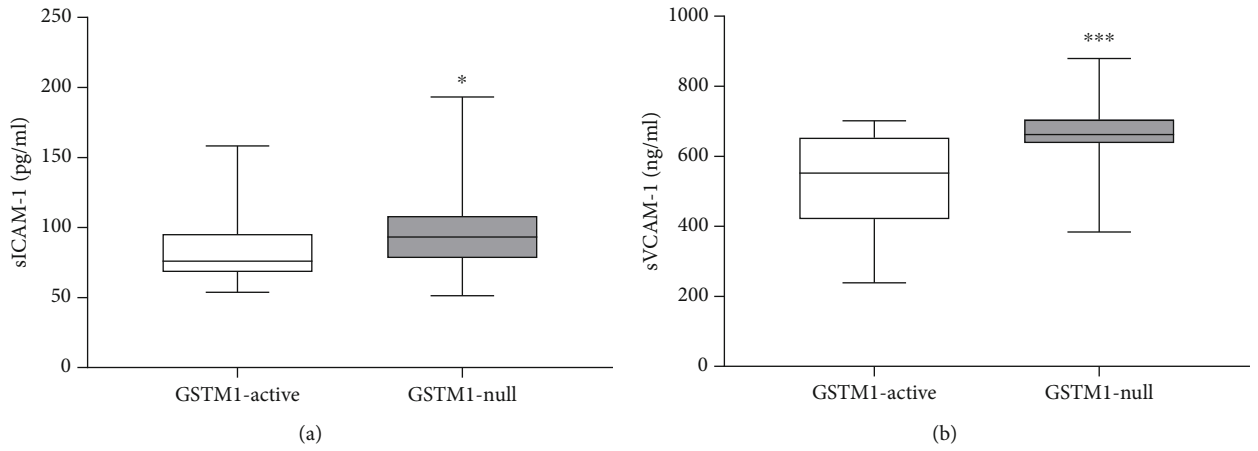

Figure 6: The influence of GSTM1 deletion on sICAM and sVCAM plasma concentration in ESRD patients. A cohort of ESRD patients was genotyped for GSTM1 gene by multiplex PCR. sICAM-1 and sVCAM concentrations were determined in plasma of ESRD patients by ELISA. Results are presented as the median with interquartile range. $^{*}p < 0.05$, $^{***}p < 0.001$.

Additionally, in our study, HUVECs incubated in uremic serum showed increased expression of two acute-phase reactants, RBP4 and CRP. RBP4 is a plasma protein, which is mainly secreted by the liver and adipose tissue, and is known to transport retinol in the blood [41]. It has been shown that RBP4 elevation induces inflammation in primary human retinal microvascular endothelial cells (HRECs) and HUVECs by increasing the expression of proinflammatory cytokines, chemokines, and adhesion molecules [42]. RBP4 levels have also demonstrated positive association with the degree of carotid intima media thickness [43]. Moreover, RBP4 levels have been reported to be elevated in kidney disorders in late stages [44]. Notably, Frey et al. showed that the relative amount of RBP4 isoforms was increased in CKD patients in comparison to controls [45]. In relation to other well-established marker of inflammation, CRP was over 2-fold overexpressed in HUVECs incubated in uremic serum compared to control serum. HUVECs express CRP mRNA and protein constitutively, revealing that vascular cells are another source of CRP production [46]. In addition to being a marker of inflammation, a growing body of evidence suggests that CRP may directly participate in the development of atherosclerotic vascular disease. Therefore, elevated CRP levels have emerged as one of the most powerful independent predictors of cardiovascular disease. Our study showed for the first time that CRP expression might increase in endothelial cells upon exposure to uremic serum.

It is tempting to speculate that regulatory and executive adhesion molecule response to uremic serum could be a consequence of activation of the overlapping signaling pathway. Namely, the promoters of ICAM-1, RANTES, RBP4, and CRP genes contain binding sites for the transcription factor NF-κB [36, 47–49]. It is well established that uremic toxins promote oxidative stress which activates the NF-κB signaling pathway in HUVECs [50–53]. Given that uremic serum led to redox imbalance in HUVECs in our study, induction of the NF-κB signaling pathway might be one of the possible mechanisms potentially explaining the upregulation of aforementioned adhesion molecules in HUVECs.

Silencing of GSTM1 in HUVECs led to an increased expression of endothelial adhesion molecules including MCP-1 and ICAM-1 and a possible trend in VCAM-1 overexpression. Notably, the MCP-1 expression increased over 2-fold in response to GSTM1 knockdown in HUVECs incubated in both control and uremic serum. With respect to the role of MCP-1 in attracting monocytes to the site of vascular injury, our results provide one of the mechanistic clues for higher risk of cardiovascular diseases in subjects lacking GSTM1 (*GSTM1-null* genotype), which is even more pronounced in uremic milieu in ESRD patients. Our results are in line with the very recent report of Gigliotti et al., which showed that GSTM1 knockout mice had a significant increase in renal expression of MCP-1 [54]. MCP-1 is also an important factor in the pathogenesis and progression of renal failure [55]. Higher urinary MCP-1 concentrations were found in CKD patients and correlated with kidney damage. Although the precise mechanism of GSTM1-mediated regulation of MCP-1 remains elusive, it is important to note that GSTM1 has a functional noncatalytic domain that inhibits activation of the apoptosis signaling-regulating kinase 1 (ASK1)-p38 signaling pathway [56]. Terada et al. reported that ASK1 directly regulates MCP-1 expression [57]. Moreover, p38 MAPK-mediated regulation of MCP-1 expression has also been confirmed in HUVECs [58]. Therefore, it is reasonable to assume that the lack of GSTM1 protein in GSTM1$^{+/-}$ HUVECs results in higher expression of MCP-1 due to the lack of ASK1 inhibition. Similarly, it is likely that another two upregulated proteins, ICAM-1 and VCAM-1, in response to GSTM1 knockdown might be associated with the ASK1 signaling pathway [59]. This should be explored in future studies.

6. Conclusions

The results of the present study show that uremic serum caused redox imbalance characterized by enhanced lipid peroxidation and decreased antioxidant enzyme activities, independently of the GSTM1 knockdown. In response to uremic injury, HUVECs exhibited changes in the expression of a series of cytokines involved in either arteriosclerosis and/or atherosclerosis, some of which might be relevant as therapy targets. Markers of endothelial dysfunction, ICAM-1 and VCAM-1, were both increased in ESRD patients lacking GSTM1, while ICAM-1 was upregulated in endothelial cells with a low level of GSTM1 exposed to uremic serum, further strengthening their potential biomarker role as predictors of CVD in ESRD patients. Interestingly, our study describes a novel function of endothelial GSTM1 in the regulation of monocyte migration and adhesion, through its role in the upregulation of MCP-1. Future studies confirming and expanding on these findings with the inclusion of functional assays of cell adhesion migration, and invasion would strengthen of our results.

Based on these results, it may be concluded that incubation of endothelial cells in uremic serum induces redox imbalance accompanied with altered expression in a series of cytokines involved in arteriosclerosis and atherosclerosis pathogenesis. The association of GSTM1 downregulation with the altered expression of adhesion molecules might be at least partly responsible for increased susceptibility of ESRD patients to CVD.

Data Availability

The data used to support the findings of this study are available from the corresponding authors upon request.

Conflicts of Interest

The authors declare that they have no conflict of interest.

Authors' Contributions

Djurdja Jerotic and Sonja Suvakov contributed equally as first authors of the manuscript.

Acknowledgments

We are grateful to the participants for donating blood for this study. We thank Prof. Andriana Margariti (Queen's University Belfast) for kindly donating HUVECs to us. We wish to thank Sanja Sekulic and Eleanor Gill for technical support. This work was supported by the Ministry of Education, Science and Technological Development of the Republic of Serbia, grant number 175052, and grant of the Federation of European Biochemical Societies (*FEBS*).

Supplementary Materials

Supplementary 1. Figure 1S: the viability of HUVECs. HUVECs ($n = 6$) were incubated in growth medium; 10%, 20%, and 30% control and uremic serum-containing media for 4 h and 6 h. Cell viability was determined by the MTS test.

Supplementary 2. Figure 2S: GSTM1 knockdown in HUVECs. GSTM1 siRNA successfully knocked down GSTM1 expression in HUVECs by ~90% when compared to the control. HUVECs were treated with 100 nM siRNA. 96 h posttransfection, the GSTM1 reduction was confirmed by Western blot (representative pictures inset). Results are presented as the mean ± SD, $n = 3$, $^{***}p < 0.001$.

Supplementary 3. Figure 3S: expression of a panel of cytokines determined by Proteome Profiler Human XL Cytokine Array. HUVECs ($n = 3$/group, pooled), transfected with GSTM1 siRNA and GSTM1$^{+/+}$ HUVECs were incubated in 30% control or uremic serum-containing media for 6 h. Heatmap represents pixel densities of spots normalized by respective reference spots.

References

[1] A. Lindner, B. Charra, D. J. Sherrard, and B. H. Scribner, "Accelerated atherosclerosis in prolonged maintenance hemodialysis," *The New England Journal of Medicine*, vol. 290, no. 13, pp. 697–701, 1974.

[2] K. Zafeiropoulou, T. Bita, A. Polykratis, S. Karabina, J. Vlachojannis, and P. Katsoris, "Hemodialysis removes uremic toxins that alter the biological actions of endothelial cells," *PLoS One*, vol. 7, no. 2, article e30975, 2012.

[3] K. Kunz, P. Petitjean, M. Lisri et al., "Cardiovascular morbidity and endothelial dysfunction in chronic haemodialysis patients: is homocyst (e) ine the missing link?," *Nephrology, Dialysis, Transplantation*, vol. 14, no. 8, pp. 1934–1942, 1999.

[4] C. Zoccali, R. Maio, G. Tripepi, F. Mallamaci, and F. Perticone, "Inflammation as a mediator of the link between mild to moderate renal insufficiency and endothelial dysfunction in essential hypertension," *Journal of the American Society of Nephrology*, vol. 17, 4 supplement 2, pp. S64–S68, 2006.

[5] F. Stam, C. van Guldener, A. Becker et al., "Endothelial dysfunction contributes to renal function–associated cardiovascular mortality in a population with mild renal insufficiency: the Hoorn study," *Journal of the American Society of Nephrology*, vol. 17, no. 2, pp. 537–545, 2006.

[6] U. Schwarz, M. Buzello, E. Ritz et al., "Morphology of coronary atherosclerotic lesions in patients with end-stage renal failure," *Nephrology, Dialysis, Transplantation*, vol. 15, no. 2, pp. 218–223, 2000.

[7] J. G. Dickhout, G. S. Hossain, L. M. Pozza, J. Zhou, Ś. Lhoták, and R. C. Austin, "Peroxynitrite causes endoplasmic reticulum stress and apoptosis in human vascular endothelium," *Arteriosclerosis, Thrombosis, and Vascular Biology*, vol. 25, no. 12, pp. 2623–2629, 2005.

[8] S. Suvakov, T. Damjanovic, A. Stefanovic et al., "*Glutathione S-transferase A1, M1, P1* and *T1* null or low-activity genotypes are associated with enhanced oxidative damage among haemodialysis patients," *Nephrology, Dialysis, Transplantation*, vol. 28, no. 1, pp. 202–212, 2013.

[9] S. Garte, L. Gaspari, A. K. Alexandrie et al., "Metabolic gene polymorphism frequencies in control populations," *Cancer Epidemiology and Prevention Biomarkers*, vol. 10, no. 12, pp. 1239–1248, 2001.

[10] I. Cruz-Gonzalez, E. Corral, M. Sanchez-Ledesma, A. Sanchez-Rodriguez, C. Martin-Luengo, and R. Gonzalez-Sarmiento, "An association between resistant hypertension and the null GSTM1 genotype," *Journal of Human Hypertension*, vol. 23, no. 8, pp. 556–558, 2009.

[11] X. L. Wang, M. Greco, A. S. Sim, N. Duarte, J. Wang, and D. E. L. Wilcken, "Glutathione S-transferase mu1 deficiency, cigarette smoking and coronary artery disease," *Journal of Cardiovascular Risk*, vol. 9, no. 1, pp. 25–31, 2002.

[12] S. Manfredi, C. Federici, E. Picano, N. Botto, A. Rizza, and M. G. Andreassi, "GSTM1, GSTT1 and CYP1A1 detoxification gene polymorphisms and susceptibility to smoking-related coronary artery disease: a case-only study," *Mutation Research/Fundamental and Molecular Mechanisms of Mutagenesis*, vol. 621, no. 1–2, pp. 106–112, 2007.

[13] K.-S. Moon, H.-J. Lee, S.-H. Hong, H.-M. Kim, and J.-Y. Um, "CYP1A1 and GSTM1/T1 genetic variation in predicting risk for cerebral infarction," *Journal of Molecular Neuroscience*, vol. 32, no. 2, pp. 155–159, 2007.

[14] A. Türkanoğlu, B. Can Demirdöğen, Ş. Demirkaya, S. Bek, and O. Adali, "Association analysis of GSTT1, GSTM1 genotype polymorphisms and serum total GST activity with ischemic stroke risk," *Neurological Sciences*, vol. 31, no. 6, pp. 727–734, 2010.

[15] D. Jerotic, M. Matic, S. Suvakov et al., "Association of Nrf2, SOD2 and GPX1 polymorphisms with biomarkers of oxidative distress and survival in end-stage renal disease patients," *Toxins*, vol. 11, no. 7, 2019.

[16] S. Suvakov, T. Damjanovic, T. Pekmezovic et al., "Associations of *GSTM1 ∗ 0* and *GSTA1* ∗Agenotypes with the risk of cardiovascular death among hemodialyses patients," *BMC Nephrology*, vol. 15, no. 1, 2014.

[17] S. Suvakov, D. Jerotic, T. Damjanovic et al., "Markers of oxidative stress and endothelial dysfunction predict haemodialysis patients survival," *American Journal of Nephrology*, vol. 50, no. 2, pp. 115–125, 2019.

[18] Z. J. Guo, H. X. Niu, F. F. Hou et al., "Advanced oxidation protein products activate vascular endothelial cellsviaa RAGE-mediated signaling pathway," *Antioxidants & Redox Signaling*, vol. 10, no. 10, pp. 1699–1712, 2008.

[19] J. Chang, J. Z. Ma, Q. Zeng et al., "Loss of *GSTM1*, a *NRF2* target, is associated with accelerated progression of hypertensive kidney disease in the African American Study of Kidney Disease (AASK)," *American Journal of Physiology-Renal Physiology*, vol. 304, no. 4, pp. F348–F355, 2013.

[20] A. Tin, R. Scharpf, M. M. Estrella et al., "The loss of *GSTM1* associates with kidney failure and heart failure," *Journal of*

the American Society of Nephrology, vol. 28, no. 11, pp. 3345–3352, 2017.

[21] Y. Yang, K. K. Parsons, L. Chi, S. M. Malakauskas, and T. H. Le, "GlutathioneS-transferase-μ1 regulates vascular smooth muscle cell proliferation, migration, and oxidative stress," *Hypertension*, vol. 54, no. 6, pp. 1360–1368, 2009.

[22] H. P. Misra and I. Fridovich, "The role of superoxide anion in the autoxidation of epinephrine and a simple assay for superoxide dismutase," *The Journal of Biological Chemistry*, vol. 247, no. 10, pp. 3170–3175, 1972.

[23] W. A. Günzler, H. Kremers, and L. Flohe, "An improved coupled test procedure for glutathione peroxidase (EC 1.11. 1.9.) in blood," *Clinical Chemistry and Laboratory Medicine*, vol. 12, no. 10, pp. 444–448, 1974.

[24] J. J. P. Bogaards, J. C. Venekamp, F. G. C. Salmon, and P. J. van Bladeren, "Conjugation of isoprene monoepoxides with glutathione, catalyzed by α, μ, π and θ-class glutathione S-transferases of rat and man," *Chemico-Biological Interactions*, vol. 117, no. 1, pp. 1–14, 1999.

[25] S. S. Singhal, P. Zimniak, S. Awasthi et al., "Several closely related glutathione S-transferase isozymes catalyzing conjugation of 4-hydroxynonenal are differentially expressed in human tissues," *Archives of Biochemistry and Biophysics*, vol. 311, no. 2, pp. 242–250, 1994.

[26] Z.-W. Chen, H.-F. Miu, H.-P. Wang et al., "Pterostilbene protects against uraemia serum-induced endothelial cell damage via activation of Keap1/Nrf2/HO-1 signaling," *International Urology and Nephrology*, vol. 50, no. 3, article 1734, pp. 559–570, 2018.

[27] J. Mimić-Oka, T. Simić, L. Djukanović, Z. Reljić, and Z. Davicević, "Alteration in plasma antioxidant capacity in various degrees of chronic renal failure," *Clinical Nephrology*, vol. 51, no. 4, pp. 233–241, 1999.

[28] J. Mimic-Oka, T. Simic, V. Ekmescic, and P. Dragicevic, "Erythrocyte glutathione peroxidase and superoxide dismutase activities in different stages of chronic renal failure," *Clinical Nephrology*, vol. 44, no. 1, pp. 44–48, 1995.

[29] P. Evenepoel, P. D'Haese, and V. Brandenburg, "Sclerostin and DKK1: new players in renal bone and vascular disease," *Kidney International*, vol. 88, no. 2, pp. 235–240, 2015.

[30] S. Thambiah, R. Roplekar, P. Manghat et al., "Circulating sclerostin and Dickkopf-1 (DKK1) in predialysis chronic kidney disease (CKD): relationship with bone density and arterial stiffness," *Calcified Tissue International*, vol. 90, no. 6, article 9595, pp. 473–480, 2012.

[31] T. C. Register, K. A. Hruska, J. Divers et al., "Plasma Dickkopf1 (DKK1) concentrations negatively associate with atherosclerotic calcified plaque in African-Americans with type 2 diabetes," *The Journal of Clinical Endocrinology and Metabolism*, vol. 98, no. 1, pp. E60–E65, 2013.

[32] X. Gao and Z. Xu, "Mechanisms of action of angiogenin," *Acta biochimica et biophysica Sinica*, vol. 40, no. 7, pp. 619–624, 2008.

[33] H.-M. Choi, Y.-E. Kwon, S. Kim, and D.-J. Oh, "Changes in FGF-23, neutrophil/platelet activation markers, and angiogenin in advanced chronic kidney disease and their effect on arterial stiffness," *Kidney & Blood Pressure Research*, vol. 44, no. 5, pp. 1166–1178, 2019.

[34] H. Burgmann, U. Hollenstein, T. Maca et al., "Increased serum laminin and angiogenin concentrations in patients with peripheral arterial occlusive disease," *Journal of Clinical Pathology*, vol. 49, no. 6, pp. 508–510, 1996.

[35] A. Tello-Montoliu, F. Marin, J. Patel et al., "Plasma angiogenin levels in acute coronary syndromes: implications for prognosis," *European Heart Journal*, vol. 28, no. 24, pp. 3006–3011, 2007.

[36] Z. Tumur, H. Shimizu, A. Enomoto, H. Miyazaki, and T. Niwa, "Indoxyl sulfate upregulates expression of ICAM-1 and MCP-1 by oxidative stress-induced NF-κB activation," *American Journal of Nephrology*, vol. 31, no. 5, pp. 435–441, 2010.

[37] S. S. Bessa, S. M. Hamdy, and R. G. El-Sheikh, "Serum visfatin as a non-traditional biomarker of endothelial dysfunction in chronic kidney disease: an Egyptian study," *European Journal of Internal Medicine*, vol. 21, no. 6, pp. 530–535, 2010.

[38] H. Sano, N. Nakagawa, R. Chiba, K. Kurasawa, Y. Saito, and I. Iwamoto, "Cross-linking of intercellular adhesion molecule-1 induces interleukin-8 and RANTES production through the activation of MAP kinases in human vascular endothelial cells," *Biochemical and Biophysical Research Communications*, vol. 250, no. 3, pp. 694–698, 1998.

[39] J. Pattison, P. J. Nelson, I. von Leuttichau et al., "RANTES chemokine expression in cell-mediated transplant rejection of the kidney," *Lancet (London, England)*, vol. 343, no. 8891, pp. 209–211, 1994.

[40] A. Bikfalvi, "Platelet factor 4: an inhibitor of angiogenesis," *Seminars in thrombosis and hemostasis*, vol. 30, no. 3, pp. 379–385, 2004.

[41] R. Blomhoff, "Transport and metabolism of vitamin A," *Nutrition Reviews*, vol. 52, no. 2, pp. S13–S23, 1994.

[42] K. M. Farjo, R. A. Farjo, S. Halsey, G. Moiseyev, and J. Ma, "Retinol-binding protein 4 induces inflammation in human endothelial cells by an NADPH oxidase-and nuclear factor kappa B-dependent and retinol-independent mechanism," *Molecular and Cellular Biology*, vol. 32, no. 24, pp. 5103–5115, 2012.

[43] T. Bobbert, J. Raila, F. Schwarz et al., "Relation between retinol, retinol-binding protein 4, transthyretin and carotid intima media thickness," *Atherosclerosis*, vol. 213, no. 2, pp. 549–551, 2010.

[44] K. Thawnashom, R. Tungtrongchitr, S. Chanchay et al., "Association between retinol-binding protein and renal function among Asian subjects with type 2 diabetes mellitus: a cross-sectional study," *Southeast Asian Journal of Tropical Medicineand Public Health*, vol. 42, no. 4, pp. 936–945, 2011.

[45] S. K. Frey, B. Nagl, A. Henze et al., "Isoforms of retinol binding protein 4 (RBP4) are increased in chronic diseases of the kidney but not of the liver," *Lipids in Health and Disease*, vol. 7, no. 1, pp. 29–29, 2008.

[46] D.-H. Kang, S.-K. Park, I.-K. Lee, and R. J. Johnson, "Uric acid–induced C-reactive protein expression: implication on cell proliferation and nitric oxide production of human vascular cells," *Journal of the American Society of Nephrology*, vol. 16, no. 12, pp. 3553–3562, 2005.

[47] C. Dai, X. Wen, W. He, and Y. Liu, "Inhibition of proinflammatory RANTES expression by TGF-β1 is mediated by glycogen synthase kinase-3β-dependent β-catenin signaling," *The Journal of Biological Chemistry*, vol. 286, no. 9, pp. 7052–7059, 2011.

[48] Rainer de Martin, M. Hoeth, R. Hofer-Warbinek, and J. A. Schmid, "The transcription factor NF-κB and the regulation of vascular cell function," *Arteriosclerosis, Thrombosis, and Vascular Biology*, vol. 20, no. 11, pp. e83–e88, 2000.

[49] V. García-Mediavilla, I. Crespo, P. S. Collado et al., "The anti-inflammatory flavones quercetin and kaempferol cause

inhibition of inducible nitric oxide synthase, cyclooxygenase-2 and reactive C-protein, and down-regulation of the nuclear factor kappaB pathway in Chang liver cells," *European Journal of Pharmacology*, vol. 557, no. 2–3, pp. 221–229, 2007.

[50] L. Dou, M. Sallée, C. Cerini et al., "The cardiovascular effect of the uremic solute indole-3 acetic acid," *Journal of the American society of nephrology*, vol. 26, no. 4, pp. 876–887, 2015.

[51] S. Ito, M. Osaka, Y. Higuchi, F. Nishijima, H. Ishii, and M. Yoshida, "Indoxyl sulfate induces leukocyte-endothelial interactions through up-regulation of E-selectin," *The Journal of Biological Chemistry*, vol. 285, no. 50, pp. 38869–38875, 2010.

[52] W. Zeng, Y.-H. Guo, W. Qi et al., "4-Phenylbutyric acid suppresses inflammation through regulation of endoplasmic reticulum stress of endothelial cells stimulated by uremic serum," *Life Sciences*, vol. 103, no. 1, pp. 15–24, 2014.

[53] K. Saum, B. Campos, D. Celdran-Bonafonte et al., "Uremic advanced glycation end products and protein-bound solutes induce endothelial dysfunction through suppression of Krüppel-like factor 2," *Journal of the American Heart Association*, vol. 7, no. 1, article e007566, 2018.

[54] J. C. Gigliotti, A. Tin, S. Pourafshar et al., "GSTM1deletion exaggerates kidney injury in experimental mouse models and confers the protective effect of cruciferous vegetables in mice and humans," *Journal of the American Society of Nephrology*, vol. 31, no. 1, pp. 102–116, 2020.

[55] C. Viedt and S. R. Orth, "Monocyte chemoattractant protein-1 (MCP-1) in the kidney: does it more than simply attract monocytes?," *Nephrology, Dialysis, Transplantation*, vol. 17, no. 12, pp. 2043–2047, 2002.

[56] S.-G. Cho, Y. H. Lee, H.-S. Park et al., "GlutathioneS-transferase mu modulates the stress-activated signals by suppressing apoptosis signal-regulating kinase 1," *The Journal of Biological Chemistry*, vol. 276, no. 16, pp. 12749–12755, 2001.

[57] Y. Terada, S. Inoshita, H. Kuwana et al., "Important role of apoptosis signal-regulating kinase 1 in ischemic acute kidney injury," *Biochemical and Biophysical Research Communications*, vol. 364, no. 4, pp. 1043–1049, 2007.

[58] H. Takaishi, T. Taniguchi, A. Takahashi, Y. Ishikawa, and M. Yokoyama, "High glucose accelerates MCP-1 production via p38 MAPK in vascular endothelial cells," *Biochemical and Biophysical Research Communications*, vol. 305, no. 1, pp. 122–128, 2003.

[59] N. Wongeakin, P. Bhattarakosol, and S. Patumraj, "Molecular mechanisms of curcumin on diabetes-induced endothelial dysfunctions: Txnip, ICAM-1, and NOX2 expressions," *BioMed Research International*, vol. 2014, Article ID 161346, 10 pages, 2014.